REGULATION OF DYNAMIC CHANGES AND REMODELING EVENTS DURING THE FORMATION, RESCUE AND REGRESSION OF THE CORPUS LUTEUM

EDITED BY: Jens Vanselow, Lane K. Christenson and Joy L. Pate
PUBLISHED IN: Frontiers in Endocrinology

frontiers Research Topics

ISSN 1664-8714
ISBN 978-2-88963-785-0
DOI 10.3389/978-2-88963-785-0

About Frontiers

Frontiers is more than just an open-access publisher of scholarly articles: it is a pioneering approach to the world of academia, radically improving the way scholarly research is managed. The grand vision of Frontiers is a world where all people have an equal opportunity to seek, share and generate knowledge. Frontiers provides immediate and permanent online open access to all its publications, but this alone is not enough to realize our grand goals.

Frontiers Journal Series

The Frontiers Journal Series is a multi-tier and interdisciplinary set of open-access, online journals, promising a paradigm shift from the current review, selection and dissemination processes in academic publishing. All Frontiers journals are driven by researchers for researchers; therefore, they constitute a service to the scholarly community. At the same time, the Frontiers Journal Series operates on a revolutionary invention, the tiered publishing system, initially addressing specific communities of scholars, and gradually climbing up to broader public understanding, thus serving the interests of the lay society, too.

Dedication to Quality

Each Frontiers article is a landmark of the highest quality, thanks to genuinely collaborative interactions between authors and review editors, who include some of the world's best academicians. Research must be certified by peers before entering a stream of knowledge that may eventually reach the public - and shape society; therefore, Frontiers only applies the most rigorous and unbiased reviews.
Frontiers revolutionizes research publishing by freely delivering the most outstanding research, evaluated with no bias from both the academic and social point of view. By applying the most advanced information technologies, Frontiers is catapulting scholarly publishing into a new generation.

What are Frontiers Research Topics?

Frontiers Research Topics are very popular trademarks of the Frontiers Journals Series: they are collections of at least ten articles, all centered on a particular subject. With their unique mix of varied contributions from Original Research to Review Articles, Frontiers Research Topics unify the most influential researchers, the latest key findings and historical advances in a hot research area! Find out more on how to host your own Frontiers Research Topic or contribute to one as an author by contacting the Frontiers Editorial Office: researchtopics@frontiersin.org

REGULATION OF DYNAMIC CHANGES AND REMODELING EVENTS DURING THE FORMATION, RESCUE AND REGRESSION OF THE CORPUS LUTEUM

Topic Editors:
Jens Vanselow, Leibniz Institute for Farm Animal Biology, Germany
Lane K. Christenson, University of Kansas Medical Center, United States
Joy L. Pate, Pennsylvania State University (PSU), United States

Citation: Vanselow, J., Christenson, L. K., Pate, J. L., eds. (2020). Regulation of Dynamic Changes and Remodeling Events During the Formation, Rescue and Regression of the Corpus Luteum. Lausanne: Frontiers Media SA. doi: 10.3389/978-2-88963-785-0

Table of Contents

frontiers in Endocrinology

EDITORIAL
published: 24 April 2020
doi: 10.3389/fendo.2020.00244

Editorial: Regulation of Dynamic Changes and Remodeling Events During the Formation, Rescue and Regression of the Corpus Luteum

Jens Vanselow[1]*, *Lane K. Christenson*[2] and *Joy L. Pate*[3]

[1] Reproductive Biology, Leibniz Institute for Farm Animal Biology (FBN), Dummerstorf, Germany, [2] Department of Molecular and Integrative Physiology, University of Kansas Medical Center, Kansas City, MO, United States, [3] Department of Animal Science, Pennsylvania State University (PSU), University Park, PA, United States

Keywords: folliculo-luteal transition, granulosa cells, luteal cells, theca cells, apoptosis, necroptosis, autophagy, progesterone

Editorial on the Research Topic

Regulation of Dynamic Changes and Remodeling Events During the Formation, Rescue and Regression of the Corpus Luteum

Hormonal communication among the hypothalamus, pituitary, ovary, and uterus regulates the female reproductive cycle to provide fertilizable oocytes and a favorable environment for embryo implantation and fetal growth. In the ovary, a recurring sequence of cellular development, differentiation, cell survival and cell death, better known as folliculogenesis, ovulation, luteinization, and luteolysis occurs throughout the female's fertile lifespan. This Research Topic is mainly focused on the fascinating transformation of the hormone-producing theca (TC) and granulosa cells (GC) of the ovarian follicle during the formation, rescue or regression of the corpus luteum (CL). Articles of this Research Topic cover different mammalian species, novel cell culture models and approaches, and present data on a variety of specific factors and molecular mechanisms occurring within this dynamic tissue during its limited lifespan and the regulation of its primary hormonal product progesterone, which is critically important for female fertility. Bagnjuk and Mayerhofer review an interesting cell culture model of luteinized human GC derived from IVF patients. The authors emphasize how this model of a primate CL can be used to study two different forms of cell death, apoptosis, and necroptosis, which occur during luteolysis *in situ*. Future studies with these cells may identify novel molecular targets (e.g., blockers of necroptosis), which may provide insights into the regulation of luteal life and function. To study the biology of the feline CL, Hryciuk et al. established an approach to isolate small (SLC) and large (LLC) steroidogenic luteal cells from domestic cats. Using this cell culture model the authors studied the morphology and physiology of these individual cells; ultimately these studies may also provide insights into luteal biology of endangered feline species. In their review article, Abedel-Majed et al. discuss the lineage of the four most important hormone-producing cells of the bovine ovary, GC and TC before, and SLC and LLC after the preovulatory luteinizing hormone (LH) surge. Growth factors, androgen excess and inflammatory cytokines and their molecular mechanisms affecting ovulation and formation of the CL are also discussed. Better understanding of the profound transformation processes these cells undergo will improve our knowledge on causes of anovulation induced infertility. Interesting insight into the unique transitional gonadotropin independence of the canine CL and in particular prostaglandin actions are provided by Tavares Pereira et al. By inhibiting cyclooxygenase-2 (COX-2) activity *in situ* these authors examined the effects that loss of prostaglandins had on luteal transcriptomes at different post-ovulatory stages.

OPEN ACCESS

Edited and reviewed by:
Richard Ivell,
University of Nottingham,
United Kingdom

***Correspondence:**
Jens Vanselow
vanselow@fbn-dummerstorf.de

Specialty section:
This article was submitted to Reproduction, a section of the journal Frontiers in Endocrinology

Received: *27 March 2020*
Accepted: *02 April 2020*
Published: *24 April 2020*

Citation:
Vanselow J, Christenson LK and Pate JL (2020) Editorial: Regulation of Dynamic Changes and Remodeling Events During the Formation, Rescue and Regression of the Corpus Luteum. Front. Endocrinol. 11:244. doi: 10.3389/fendo.2020.00244

With luteal maturation and emerging gonadotropin dependence, the canine CL transcriptome became more sensitive to COX-2 inhibition. These studies set the stage for more in depth functional examination of the mechanisms of prostaglandin-regulated cellular proliferation, immune cell infiltration and steroidogenesis. Likszo et al. examined the changing proteome during the folliculo-luteal transition in pigs. Proteins expressed in pre-ovulatory follicles were associated with cellular infiltration, endoplasmic stress responses and the protein ubiquitination pathway, whereas early luteal stage proteins were associated with steroid metabolism, cell death and survival, free radical scavenging, and protein ubiquitination pathways. Novel mechanisms of luteal cell differentiation, survival, and pathways regulating steroidogenesis in the newly formed CL were advanced by these authors. Lipid regulation of bovine luteal function was studied by Hughes et al.. In a targeted metabolomic analysis using ultra performance liquid chromatography-tandem mass spectrometry, several lipid mediators were identified as potential regulators of leukocyte activation, cell migration, and proliferation during early, mid and late luteal stages. Cultured luteal cells demonstrated a role of select lipid mediators in regulating luteal progesterone production and suggest a role for lipid mediators as regulators of steroidogenesis, immune cell activation and function, intracellular signaling, and cell survival and death. Two studies, Bender et al. and Walewska et al., demonstrate novel roles for thrombospondin 1 (THBS1) in follicular angiogenesis, luteinization, and ovulation in the primate CL, and in luteolysis of the equine CL, respectively. In the cynomologus macaque, Bender et al. block ovulation and follicular angiogenesis with an intrafollicular injection of anti-THBS1 antibody. Additionally, THBS1 treatment stimulated migration, proliferation, and sprout formation in cultured monkey ovarian microvascular endothelial cells. These groundbreaking studies clearly implicate THBS1 as an important regulator of ovulation and corpus luteum formation. Walewska et al. studied the interaction of THBS1 with hypoxia-inducible factor 1 alpha (HIF1α) and Nodal, a member of the transforming growth factor-beta superfamily in equine luteal tissue explants and demonstrated *in vitro* interactions between these factors. This study sheds light on the interactions between two novel regulators of luteal function. Berisha et al. examined bovine follicular fluid hormones and GC transcriptomics collected at different times following induced superovulation. The authors focus on prostaglandin family members and posit involvement in the local mechanisms regulating final follicle maturation and ovulation during the folliculo-luteal transition and formation of the CL. In their review, Teeli et al. describe the role of the proteasome/autophagy axis in the context of luteal formation and regression, respectively. The authors propose that CL regression may be governed by the ubiquitin-proteasome and autophagy pathways and consider the potential role of specific transcription factors involved in these events.

Taken together the articles in this Research Topic present novel data, approaches and ideas on the development of the corpus luteum, and its subsequent function and demise. However, in spite of these new perspectives and insights, which will provide useful stimuli for future approaches, our understanding of this essential female hormonal gland remains incomplete. Further efforts are necessary to further elucidate its most important key feature, its ephemeral nature.

AUTHOR CONTRIBUTIONS

JV, LC, and JP have written this editorial.

Conflict of Interest: The authors declare that the research was conducted in the absence of any commercial or financial relationships that could be construed as a potential conflict of interest.

frontiers in Endocrinology

MINI REVIEW
published: 09 July 2019
doi: 10.3389/fendo.2019.00452

Human Luteinized Granulosa Cells—A Cellular Model for the Human Corpus Luteum

*Konstantin Bagnjuk and Artur Mayerhofer**

Biomedical Center Munich (BMC), Cell Biology, Anatomy III, Ludwig-Maximilians-University (LMU), Planegg, Germany

In the ovary, the corpus luteum (CL) forms a temporal structure. Luteinized mural granulosa cells (GCs), which stem from the ruptured follicle, are the main cells of the CL. They can be isolated from follicular fluid of woman undergoing *in vitro* fertilization. In culture, human GCs are viable for several days and produce progesterone, yet eventually steroid production stops and GCs with increasing time in culture undergo changes reminiscent of the ones observed during the demise of the CL *in vivo*. This short review summarizes the general use of human GCs as a model for the primate CL and some of the data from our lab, which indicate that viability, functionality, survival and death of GCs can be regulated by local signal molecules (e.g., oxytocin and PEDF) and the extracellular matrix (e.g., via the proteoglycan decorin). We further summarize studies, which identified autophagocytotic events in human GCs linked to the activation of an ion channel. More recent studies identified a form of regulated cell death, namely necroptosis. This form of cell death may, in addition to apoptosis, contribute to the demise of the human CL. We believe that human GCs are a unique window into the human CL. Studies employing these cells may lead to the identification of molecular events and novel targets, which may allow to interfere with CL functions.

Keywords: cell death, human ovary, paracrine action, extracellular matrix, hormone, proteomic, necroptosis

OPEN ACCESS

Edited by:
Lane K. Christenson, University of Kansas Medical Center, United States

Reviewed by:
Jürgen Michael Weiss, Lucerne Cantonal Hospital, University of Lucerne, Switzerland
Hao Chen, Guangdong University of Technology, China
Misung Jo, University of Kentucky, United States

****Correspondence:***
Artur Mayerhofer
Mayerhofer@lrz.uni-muenchen.de

Specialty section:
This article was submitted to Reproduction, a section of the journal Frontiers in Endocrinology

Received: *25 March 2019*
Accepted: *21 June 2019*
Published: *09 July 2019*

Citation:
Bagnjuk K and Mayerhofer A (2019) Human Luteinized Granulosa Cells—A Cellular Model for the Human Corpus Luteum. Front. Endocrinol. 10:452. doi: 10.3389/fendo.2019.00452

INTRODUCTION AND SCOPE

To better understand the biology of human reproduction, studies addressing the human situation are required. This is due to distinct differences between humans and other mammalian species regarding structure and function of reproductive organs. The central organs of the female reproductive tract are the ovaries, which cannot be readily studied in the human.

The ovary is a highly dynamic organ that contains resting, growing, and dying follicles, as well as the corpus luteum (CL). During a menstrual cycle this temporal structure comes into existence upon ovulation and develops into an active, but short-lived (about 2 weeks) endocrine structure. It exists longer (months) if a pregnancy occurs, but in any case eventually it will shut down functionally and structurally. These events are termed functional and structural luteolysis.

Ovarian functions are frequently studied in animal models. In typical laboratory animals, such as mice and rats, the life time of the CL is restricted to only a couple of days, i.e., it is much shorter than in women. Domestic animals, while more similar to primates (1) with respect to the lifespan of the CL, differ in e.g., luteolytic signaling and the cellular events responsible for luteolysis (2). Therefore, non-human primates appear to be the best suited translational model for the human (3).

Due to the development of ART, a further possibility for the study of human ovary has opened. While connective tissue and newly formed blood vessel (4) are parts of the CL, its main cellular components are cells, which stem from the ovulatory follicle, in particular, mural

luteinizing granulosa cells (GCs). These cells are by-products of follicular aspiration performed during IVF-procedures in women. They can be isolated, cultured, and studied.

As true for all cellular studies, cell culture phenomena must be considered and verification studies, involving human and/or non-human primate tissue are therefore required. If combined with such studies, we believe that cell cultures of human GCs are a unique window into the human ovary, and allow one to identify and study specifically events of relevance to the human CL.

This short review will briefly describe the cell culture model of human GCs, and will then summarize data mainly from our studies, in which we observed apoptosis and autophagocytotic events. We will then present recent data, which implicate necroptotic cell death in GCs and in human CL regression. We will here not discuss studies, which identified further factors of potential relevance to ovarian follicular fate, e.g., handling of catecholamines and generation of H_2O_2 (5–9).

HUMAN GC CULTURE—A SPECIFIC WINDOW TO THE HUMAN CORPUS LUTEUM

As mentioned, human mural GC can be gathered during IVF procedures. Different methods have been developed to separate contaminating cells, namely leukocytes or erythrocytes, from granulosa cells. This can be achieved either by employing e.g., fluorescent activated cell sorting (FACS) and magnetic activated cell sorting (MACS, Dynabeads) or by physical properties (aggregation of GCs, density, selective adherence speed or size) (10). All methods except the so-called cell strainer technique involve a density gradient centrifugation step or a red blood cell lysis buffer (11) to eliminate specifically erythrocytes (12, 13). A comparison study came to the conclusion that the cell strainer method, developed by Kossowska-Tomaszczuk et al. (12), offers the best balance between purity, yield, speed, and simplicity (10, 12). We therefore employed this isolation method during the last years.

GCs stem from individual IVF-patients. While we have focused on cells derived from patients with male factor as the reason for IVF, the women undergoing this procedure are not a homogeneous population with respect of age, life style and medication. As well-known for all human subjects, heterogeneity between the derived GC samples is typically large. A usual consequence is that large number of repetitions are needed to obtain statistically valid results.

Most IVF patients undergo a controlled ovarian stimulation protocol (COS) before oocyte retrieval. Various COS have been established over time (14) and have distinct effects on the patients, their gonads and the outcome (birth rates) (15, 16). Most protocols include three main steps. First, drugs that interfere with gonadotropin releasing hormone (GnRH) are administered to shut down the natural pituitary-ovary axis. In a second step follicular stimulating hormone (FSH) is given. Prior to ovulation, oocyte maturation is forced by exogenously administered human chorionic gonadotropin (hCG), a luteinizing hormone (LH) analog. In primates the midcycle LH surge paves the way for *in vivo* luteinization of GCs (17, 18). Therefore, typical IVF-derived human GCs are most likely luteinizing or luteinized GCs and indeed they produce progesterone (19) like their *in situ*-counterparts. In case of pregnancy, hCG from the syncytiotrophoblast stimulates progesterone production and acts as a luteotrophic factor. Without hCG support the CL shuts down functionally and then, at least in some cases, it will regress to form a scar-like structure, the corpus albicans (20). How this is brought about in women is one of the many questions that remain to be studied.

To examine to what extend IVF-derived cultured GCs resemble their *in vivo*-counterparts, and are an appropriate model for the study of the CL (21), we combined a number of techniques, e.g., live cell imaging, cell death measurements, immunocytochemistry, and mass spectrometry analysis. We specifically studied GCs cultured from day 2 up to day 5 after retrieval from patients. The results were validated by comparison to *in vivo* generated non-human primate CL and immunohistochemical examinations of human and non-human primate ovary tissues.

In vivo follicular GCs differentiate upon ovulation to form large luteal cells (22). *In vitro*, the increase in size accompanying this differentiation is recapitulated and became likewise apparent over culture time. Large luteal cells express CYP11A1, a protein known to be crucial for progesterone production. Mass spectrometry revealed that it is highly expressed in IVF-derived human GCs (21, 23). Also low density lipoprotein receptor (LDL-R), 3β-hydroxysteroid dehydrogenase and steroidogenic acute regulatory protein (StAR) were found by mass spectrometry in cultured GCs. Next to CYP11A1 these proteins are indispensable for progesterone synthesis (24). In GCs, StAR, and LDL-R protein expression massively declined over culture time, which indicates a loss of steroidogenic function (21). *In situ,* the human corpus luteum only produces progesterone during a specific period of its lifetime (25). StAR expression is practically absent before the LH peak and the subsequent ovulation, is elevated during mid-phase CL and then is reduced in the regressing CL (26). Therefore, from an endocrine point of view, it appears that human, IVF-derived GCs are an apt model, especially for the study of the corpus luteum lifecycle from the mid-phase onwards.

Interestingly, Bildik et al. (15) recently showed that in comparison to naturally matured luteinized GCs, GCs from routine IVF-patients, who underwent COS, are more steroidogenic, express less anti-apoptotic but more pro-apoptotic factors and show a diminished viability under culture conditions. However, these characteristics vary and depend on the stimulation protocol (15). Thus, human, IVF-derived GCs may be specifically useful to study luteal phase defects, which sometimes occur during IVF procedures (27).

A SODIUM CHANNEL, OXYTOCIN, PEDF, AND DECORIN ARE INVOLVED IN GC DEATH

Over the years our studies with human GCs, isolated from follicular fluid of IVF patients, in combination with studies in

human and non-human primate ovaries, led to the identification of a number of factors with the potential to influence the functions and the fate of these ovarian cells. Our studies addressed among others the role of a sodium ion channel, expressed by GCs, and the roles of oxytocin, PEDF, and decorin, i.e., secreted molecules, which may act in a paracrine fashion. We found that these molecules are intrinsically linked to different forms of cell death.

Human GCs, but also non-human primate luteal cells, express a sodium ion channel (*SCN9A*), which is regulated by the luteotrophic hormone hCG (28). Upon hCG-stimulation, *SCN9A* mRNA levels and ion channel activity were suppressed in GCs. The pharmacologically induced channel opening resulted in strikingly increased lysosomal activation and autophagocytic events. Autophagocytic events in the large granulosa luteal cells of the non-human primate CL were also deducted from results of electron microscopical examination and were later confirmed by further studies to occur in human CL (29). For instance, expression of the autophagy related protein Beclin-1 is elevated in the young CL, compared to old (regressing) CL, which may indicate that autophagy, in contrast to other cell death forms, may even be involved in maintaining the CL. This point requires further investigation, however. Recently, interconnectivity of different cell death forms was reviewed by Chen et al. (30). Although each cell death form has a distinct pathway some of the involved proteins act as molecular switches between different cell death pathways. Therefore, more than one cell death form can be activated simultaneously. In this context autophagy plays a special role as it can be seen as a mechanism with high potency to results in cell survival.

Apoptosis of luteal cells is known to be the main cause for the demise of the CL in rodents, but in humans it has been shown that only a small fraction of luteal cells undergoes apoptosis (20). Several factors may be involved in its initiation. Oxytocin (OT), a small peptide hormone was found in the human and non-human primate CL, as well as in the bovine ovary. It was hypothesized to act locally, e.g., as a luteolytic factor (31–33), because local production was accompanied by expression of the OT receptor (OTR) (34–36). Two studies in human mural GCs built on these results (37, 38) and confirmed expression of the receptor in GCs and CL. Exogenously applied to human GCs, OT acutely within seconds elevated the levels of intracellular Ca^{2+} and within hours, changed progesterone production (37). A further downstream role of OT in the induction of apoptosis of GCs became apparent in a follow-up study, also employing IVF-derived GCs. OT reduced viability by increasing caspase 3/7 activity, resulting in typical apoptosis, confirmed by electron microscopy (38). As OTR were found in the CL of humans and non-human primates, we concluded that the OT/OTR system may contribute to luteolysis.

Another factor identified more recently, is pigment-epithelium derived factor (PEDF). It is produced by GCs and was linked to anti-angiogenesis and apoptosis (39). We found that exogenously applied PEDF elevated reactive oxygen species (ROS) in human GCs, yet the exact mode of action of the multifunctional PEDF molecule and specifically the PEDF-receptor(s) involved, remain to be identified. PEDF and its ovarian roles are evolving. It has recently been shown to be involved in counteracting the activity of the hCG/vascular endothelial growth factor pathway and therefore may also attenuate ovarian hyperstimulation syndrome (OHSS) symptoms (40).

The CL is composed of the genuine follicle-derived cells (large and small luteal cells), blood vessels, connective tissue cells, and extracellular matrix. Extracellular matrix of the CL contains decorin (DCN), a proteogylcan, which was identified as a product of luteinized GCs (41). It is absent from the GC compartment of growing follicles in human and a non-human primate, but is present in the ovarian interstitial and theca compartments. It may leak from there to the follicular fluid, where it was observed in higher concentrations as in the blood serum (42). Interestingly it was recently suggested that its concentrations may be correlated with oocyte quality (42). DCN, besides its role in the "decoration" (hence the name decorin) and thereby the stabilization of collagen fibrils, also interferes with growth factor signaling (e.g., epidermal growth factor receptor; EGFR). DCN is also known to play a role in autophagocytotic events (43, 44), a possibility which however has not been examined in the ovary yet. Taken together, it is possible that DCN may be involved in the regulation of the life span of the CL via interactions with various ovarian and luteal growth factor systems. This assumption is based on the changing expression levels of DCN in the aging CL on one side, and the ability of DCN to reduce apoptosis (evidenced by caspase 3/7 activity) in GCs on the other side. This mode of action was, however, only found when GCs were studied that were cultured for 5 days, but not in "younger" cells. The results indicate that GCs *in vitro* i.e., during the time of culture change their behavior, an observation, which fostered the idea that studying such changes may be useful to identify events related to the fate of the CL.

IDENTIFICATION OF NECROPTOSIS IN GC AND LUTEAL CELLS

When we followed GC changes during culture time, we found that in addition to apoptosis, necroptosis takes place (45). Necroptosis is a form of regulated cell death, which involves a cascade of events and the formation of the necrosome, i.e., receptor interacting protein kinase 1, 3 (RIP1, RIP3) and phosphorylation and oligomerization of mixed lineage kinase domain like pseudokinase (MLKL), which is the executioner and unique marker for necroptosis (46, 47). Of note, blockers Of note, blockers of necroptosis [e.g., necrostatin 1 (Nec1) and necrosulfonamide (NSA)] have been developed, which prevent cell death. Necroptotic cells exhibit typical morphological signs of necrosis including ballooning and cell burst (21). In contrast to apoptosis, necro(pto)sis leads to porous cell membranes and, in the body, eventually to an immune reaction (48). Hence, necroptosis could be important for immune cell attraction to the CL, which appear to be crucial in its demise (20, 29, 49). Necroptosis in humans was until recently (21),

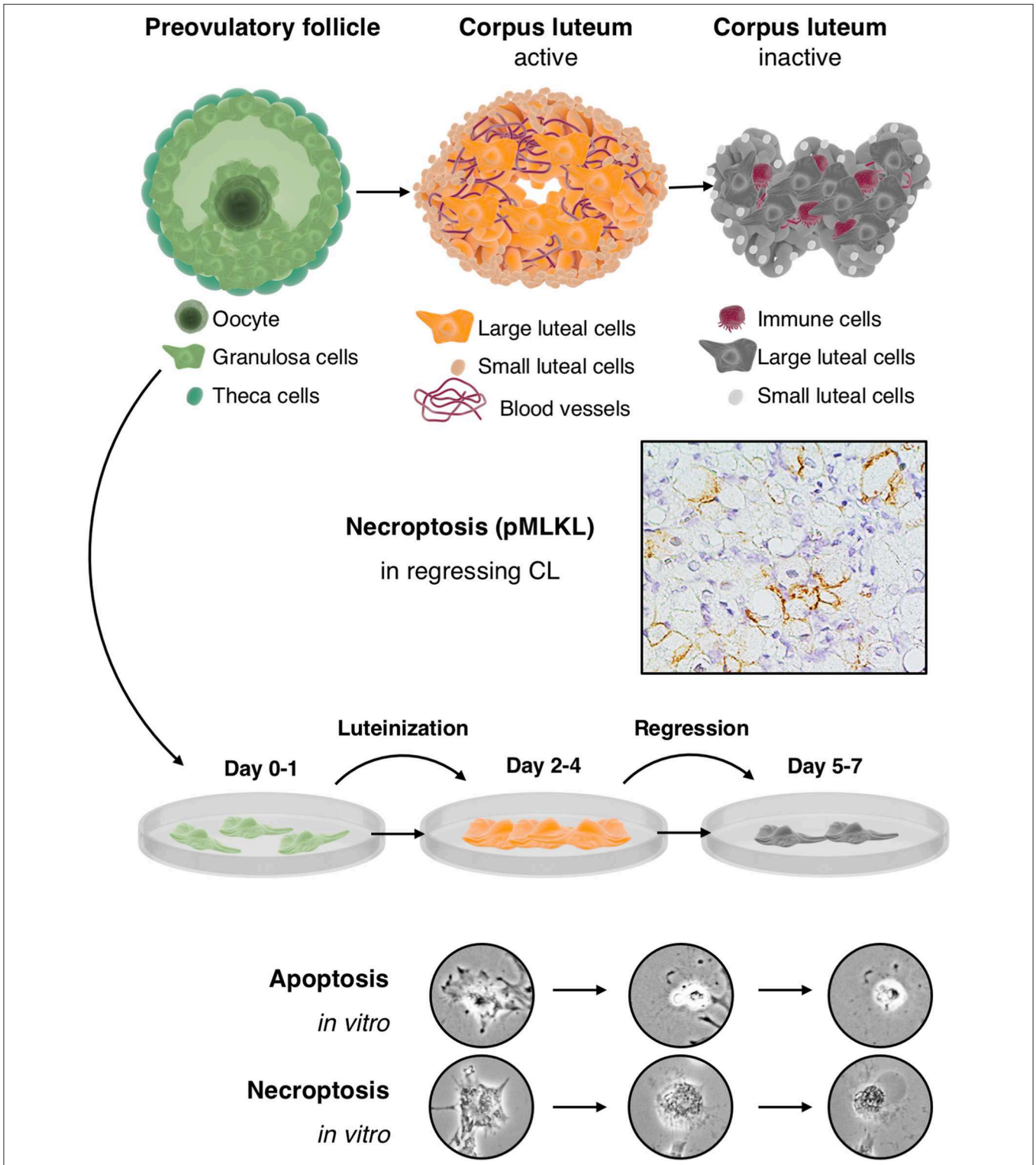

FIGURE 1 | Cultured human GCs represent a model for the human CL, which comes into existence after ovulation and contains the GC-derived large luteal cells and other cell types: The upper part depicts the preovulatory follicle with its main cellular components, i.e., granulosa cells, the oocyte and theca cells (left), an active corpus luteum (middle), and a regressing corpus luteum (right). Mural GCs of the preovulatory follicle can be isolated and cultured from aspirated follicular fluid, which also contains cumulus cells and the oocyte. The active corpus luteum is a temporal organ, which is highly vascularized and produces progesterone. The inactive and regressing corpus luteum also contains immune cells. As shown in the second row, there is evidence for necroptosis in this structure, indicated by immunohistochemical

(Continued)

FIGURE 1 | detection of the necroptosis marker pMLKL in large luteal cells of a regressing corpus luteum (*M. mulatta*) (21). The third row schematically depicts isolated and cultured human GCs. This culture system recapitulates in a short period some of the main events occurring in the corpus luteum. In brief, isolated GCs luteinize in culture and produce progesterone but eventually die by apoptosis and necroptosis. These two cell death forms can be distinguished, albeit only if accompanied by other modes of detection (21), by morphological signs (two bottom rows). Apoptosis of GCs is typically characterized e.g., by a condensed cytoplasm and nucleus, whereas necroptotic cells show cellular ballooning.

described only in various pathologies, e.g., neurodegenerative disease, heart attack or brain injury (50). Our studies (21, 45, 51) and one in regressing bovine CL (52) extend this to physiological situations.

The reasons leading to necroptosis were described to vary significantly between different cells (47). In human cultured GCs necroptosis was observed under basal culture condition and like apoptosis progressed during culture time of GCs. It is possible that a small peptide (ARP), derived from a special splice form of acetylcholinesterase (AChE), namely AChE-R is involved. AChE-R and likely also ARP are formed by GCs and exogenous ARP, if added to cultured GCs, enhanced necroptosis.

The roles of acetylcholine (ACh) and AChE in the determination of life and death may go beyond the CL and include the GCs in the follicle, as concluded from studies in 3D cultured primate follicles (51). We found that elevation of ACh (induced by a blocker of AChE), as well as inhibition of necroptosis (using Nec-1) improved follicular growth. The results might be of translational relevance and may help to improve primate follicular growth *in vitro* and thus may allow to develop better strategies to preserve fertility in oncological patients.

In an attempt to examine underlying causes for basal cell death events in cultured GCs, we monitored cellular changes by employing mass spectrometry (21). The cellular proteins, which increased during a culture period of 5 days, belonged to distinct pathways, and results indicated that among others the ceramide salvage pathway is involved. It consists of enzymes including sphingomyelin phosphodiesterase 1 (SMPD1), acid ceramidase (ASAH1), galactosylceramidase (GALC), and glucosylceramidase beta (GBA) (53), all of which metabolize sphingolipids to generate ceramide and its metabolite sphingosine.

Sphingolipids consist of a sphingosine backbone linked to a fatty acid via an amide bond. Two metabolites, namely ceramide (CER) and sphingosine-1-phosphate (S1P) have excited researchers over many decades (54, 55). These two molecules are described to exert opposite actions on cell viability. For example, S1P blocks hydrogen peroxide induced apoptosis in primary GCs (56). In mice it was found that ceramide, on the other hand, induced cell cycle arrest and cell death in proliferating GCs (57). Further, this molecule was shown to induce apoptosis in human GCs, which could be rescued by prolactin (58). At the time of the mentioned study, Annexin-V staining was used as an apoptotic marker, however this kind of staining does not reliably distinguish between apoptosis and necroptosis, which was identified as a distinct form of cells death later. Of note, in the published pictures of the mentioned study, morphological signs for necrotic cell death are evident (e.g., ballooning).

Cell death of GCs in culture goes along with elevated LDH levels measured in the culture supernatant. This indicates that necro(pto)sis occurs. That necroptosis in GCs is linked to ceramides is based on the following experiments. We blocked endogenous ceramide production by fumonisin B1 (FB1) (59) and observed improved overall GC-viability. We also added exogenous ceramide and observed a reduction of viability. Results of blocker experiments using blockers of apoptosis (Z-VAD-FMK) or necroptosis (NSA, Nec-1s) finally identified that necroptosis is the principal form of cell death induced by endogenous ceramide. The presence of phosphorylated MLKL (pMLKL) in CL samples from different primate species and the appearance of pMLKL only in the regressing CL of non-human primate CL samples, support *in vivo* relevance, as do results of transcriptomic analysis of *in vivo* developed non-human primate CL (21).

SUMMARY

IVF-derived cultured human GCs resemble luteinized large granulosa cells of the CL. They are a highly relevant *in vitro* model for the human CL, yet parallel studies in human or non-human primate tissues remain crucial because the CL also contains further cell types, which must be taken into consideration as players in the concert of luteal activity and regression. The data summarized in this review imply that during the first days of culture, GCs resemble the active CL, while at later time points they resemble the regressing CL (**Figure 1**). Studies employing these cells may lead to the identification of pathways, involved in the regulation of the CL. They may then pave the way for novel treatment strategies. For example, the recent identification of necroptosis suggest that blockers of necroptosis may be employed to possibly prevent luteolysis and may help to prevent luteal phase defects in ART patients.

AUTHOR CONTRIBUTIONS

AM conceived of the studies mentioned in the review. KB performed one of the most recent studies mentioned. KB and AM wrote the minireview and the figure. For generation of the figure, tools provided at https://www.somersault1824.com were used. This is gratefully acknowledged.

FUNDING

This work was performed in partial fulfillment of the requirements of a Dr. rer. nat. thesis (KB) at LMU. Grant support: Deutsche Forschungsgemeinschaft (DFG) MA1080/19-2.

ACKNOWLEDGMENTS

We thank all our collaborators, especially Dres. Ulrike Berg, Dieter Berg, and Jing Xu, and all former and present lab members, who contributed over the years to the establishment of GC cultures and the discovery studies. We apologize to all colleagues, whose work could not be mentioned due to the brief nature of this mini review.

REFERENCES

1. Stouffer RL, Hennebold JD. Chapter 23: structure, function, and regulation of the corpus luteum. 4 edn. In: Plant TM, Zeleznik AJ, editors. *In Knobil and Neill's Physiology of Reproduction.* Academic Press (2015). p. 1023–76. doi: 10.1016/B978-0-12-397175-3.00023-5
2. Knickerbocker JJ, Wiltbank MC, Niswender GD. Mechanisms of luteolysis in domestic livestock. *Domest Anim Endocrinol.* (1988) 5:91–107. doi: 10.1016/0739-7240(88)90011-2
3. Phillips KA, Bales KL, Capitanio JP, Conley A, Czoty PW, 't Hart BA, et al. Why primate models matter. *Am J Primatol.* (2014) 76:801–27. doi: 10.1002/ajp.22281
4. Smith MF, McIntush EW, Smith GW. Mechanisms associated with corpus luteum development. *J Anim Sci.* (1994) 72:1857–72. doi: 10.2527/1994.7271857x
5. Buck T, Hack CT, Berg D, Berg U, Kunz L, Mayerhofer A. The NADPH oxidase 4 is a major source of hydrogen peroxide in human granulosa-lutein and granulosa tumor cells. *Sci Rep.* (2019) 9:3585. doi: 10.1038/s41598-019-40329-8
6. Blohberger J, Buck T, Berg D, Berg U, Kunz L, Mayerhofer A. L-DOPA in the hu man ovarian follicular fluid acts as an antioxidant factor on granulosa cells. *J Ovarian Res.* (2016) 9:62. doi: 10.1186/s13048-016-0269-0
7. Saller S, Kunz L, Berg D, Berg U, Lara H, Urra J, et al. Dopamine in human follicular fluid is associated with cellular uptake and metabolism-dependent generation of reactive oxygen species in granulosa cells: implications for physiology and pathology. *Human Reprod.* (2014) 29:555–67. doi: 10.1093/humrep/det422
8. Saller S, Merz-Lange J, Raffael S, Hecht S, Pavlik R, Thaler C, et al. Norepinephrine, active norepinephrine transporter, and norepinephrine-metabolism are involved in the generation of reactive oxygen species in human ovarian granulosa cells. *Endocrinology.* (2012) 153:1472–83. doi: 10.1210/en.2011-1769
9. Meinel S, Blohberger J, Berg D, Berg U, Dissen GA, Ojeda SR, et al. Pro-nerve growth factor in the ovary and human granulosa cells. *Hormone Mol Biol Clin Investig.* (2015) 24:91–9. doi: 10.1515/hmbci-2015-0028
10. Ferrero H, Delgado-Rosas F, Garcia-Pascual CM, Monterde M, Zimmermann RC, Simón C, et al. Efficiency and purity provided by the existing methods for the isolation of luteinized granulosa cells: a comparative study. *Human Reprod.* (2012) 27:1781–9. doi: 10.1093/humrep/des096
11. Aghadavod E, Zarghami N, Farzadi L, Zare M, Barzegari A, Movassaghpour AA, et al. Isolation of granulosa cells from follicular fluid; applications in biomedical and molecular biology experiments. *Adv Biomed Res.* (2015) 4:250. doi: 10.4103/2277-9175.170675
12. Kossowska-Tomaszczuk K, De Geyter C, De Geyter M, Martin I, Holzgreve W, Scherberich A, et al. The multipotency of luteinizing granulosa cells collected from mature ovarian follicles. *Stem Cells.* (2009) 27:210–9. doi: 10.1634/stemcells.2008-0233
13. Richardson MC, Ingamells S, Simonis CD, Cameron IT, Sreekumar R, Vijendren A, et al. Stimulation of lactate production in human granulosa cells by metformin and potential involvement of adenosine 5′ monophosphate-activated protein kinase. *J Clin Endocrinol Metab.* (2009) 94:670–7. doi: 10.1210/jc.2008-2025
14. Tarlatzis BC, Fauser BC, Kolibianakis EM, Diedrich K, Rombauts L, Devroey P. GnRH antagonists in ovarian stimulation for IVF. *Human Reprod Update.* (2006) 12:333–40. doi: 10.1093/humupd/dml001
15. Bildik G, Akin N, Seyhan A, Esmaeilian Y, Yakin K, Keles I, et al. Luteal granulosa cells from natural cycles are more capable of maintaining their viability, steroidogenic activity and LH receptor expression than those of stimulated IVF cycles. *Human Reprod.* (2018) 34:345–55. doi: 10.1093/humrep/dey353
16. Macklon NS, Stouffer RL, Giudice LC, Fauser BC. The Science behind 25 years of ovarian stimulation for *in vitro* fertilization. *Endocrine Rev.* (2006) 27:170–207. doi: 10.1210/er.2005-0015
17. Zeleznik A, Benyo DF. Control of follicular development, corpus luteum function, and the recognition of pregnancy in higher primates. *Physiol Reprod.* (1994) 2:751–82.
18. Stouffer RL, Bishop CV, Bogan RL, Xu F, Hennebold JD. Endocrine and local control of the primate corpus luteum. *Reprod Biol.* (2013) 13:259–71. doi: 10.1016/j.repbio.2013.08.002
19. Kunz L, Thalhammer A, Berg FD, Berg U, Duffy DM, Stouffer RL, et al. $Ca2^{+}$-activated, large conductance K^{+} channel in the ovary: identification, characterization, and functional involvement in steroidogenesis. *J Clin Endocrinol Metab.* (2002) 87:5566–74. doi: 10.1210/jc.2002-020841
20. Morales C, García-Pardo L, Reymundo C, Bellido C, Sánchez-Criado JE, Gaytán F. Different patterns of structural luteolysis in the human corpus luteum of menstruation. *Human Reprod.* (2000) 15:2119–28. doi: 10.1093/humrep/15.10.2119
21. Bagnjuk K, Stöckl JB, Fröhlich T, Arnold GJ, Behr R, Berg U, et al. Necroptosis in primate luteolysis: a role for ceramide. *Cell Death Disc.* (2019) 5:67. doi: 10.1038/s41420-019-0149-7
22. Webley GE, Richardson MC, Smith CA, Masson GM, Hearn JP. Size distribution of luteal cells from pregnant and non-pregnant marmoset monkeys and a comparison of the morphology of marmoset luteal cells with those from the human corpus luteum. *Reproduction.* (1990) 90:427–37. doi: 10.1530/jrf.0.0900427
23. Devoto L, Fuentes A, Kohen P, Céspedes P, Palomino A, Pommer R, et al. The human corpus luteum: life cycle and function in natural cycles. *Fertil Steril.* (2009) 92:1067–79. doi: 10.1016/j.fertnstert.2008.07.1745
24. Chaffin CL, Dissen GA, Stouffer RL. Hormonal regulation of steroidogenic enzyme expression in granulosa cells during the peri-ovulatory interval in monkeys. *Mol Hum Reprod.* (2000) 6:11–8. doi: 10.1093/molehr/6.1.11
25. Christenson LK, Devoto L. Cholesterol transport and steroidogenesis by the corpus luteum. *Reprod Biol Endocrinol.* (2003) 1:90. doi: 10.1186/1477-7827-1-90
26. Devoto L, Kohen P, Gonzalez RR, Castro O, Retamales I, Vega M, et al. Expression of steroidogenic acute regulatory protein in the human corpus luteum throughout the luteal phase. *J Clin Endocrinol Metab.* (2001) 86:5633–9. doi: 10.1210/jcem.86.11.7982
27. Humaidan P, Kol S, Papanikolaou EG, Copenhagen GnRH Agonist Triggering Workshop Group. GnRH agonist for triggering of final oocyte maturation: time for a change of practice? *Human Reprod Update.* (2011) 17:510–24. doi: 10.1093/humupd/dmr008
28. Bulling A, Berg FD, Berg U, Duffy DM, Stouffer RL, Ojeda SR, et al. Identification of an ovarian voltage-activated Na^{+}-channel type: hints to involvement in luteolysis. *Mol Endocrinol.* (2000) 14:1064–74. doi: 10.1210/mend.14.7.0481
29. Gaytán M, Morales C, Sánchez-Criado JE, Gaytán F. Immunolocalization of beclin 1, a bcl-2-binding, autophagy-related protein, in the human ovary: possible relation to life span of corpus luteum. *Cell Tissue Res.* (2008) 331:509–17. doi: 10.1007/s00441-007-0531-2
30. Chen Q, Kang J, Fu C. The independence of and associations among apoptosis, autophagy, and necrosis. *Signal Transd Targeted Ther.* (2018) 3:18. doi: 10.1038/s41392-018-0018-5
31. Wathes DC, Swann RW, Pickering BT, Porter DG, Hull MG, Drife JO. Neurohypophysial hormones in the human ovary. *Lancet.* (1982) 320:410–2. doi: 10.1016/S0140-6736(82)90441-X

32. Khan-Dawood FS, Dawood MY. Human ovaries contain immunoreactive oxytocin. *J Clin Endocrinol Metab*. (1983) 57:1129–32. doi: 10.1210/jcem-57-6-1129
33. Khan-Dawood FS, Huang JC, Dawood MY. Baboon corpus luteum oxytocin: an intragonadal peptide modulator of luteal function. *Am J Obstetr Gynecol*. (1988) 158:882–91. doi: 10.1016/0002-9378(88)90089-0
34. Furuya K, Mizumoto Y, Makimura N, Mitsui C, Murakami M, Tokuoka S, et al. Gene expressions of oxytocin and oxytocin receptor in cumulus cells of human ovary. *Hormone Res*. (1995) 44(Suppl. 2):47–9. doi: 10.1159/000184661
35. McArdle CA, Holtorf AP. Oxytocin and progesterone release from bovine corpus luteal cells in culture: effects of insulin-like growth factor I, insulin, and prostaglandins. *Endocrinology*. (1989) 124:1278–86. doi: 10.1210/endo-124-3-1278
36. Ivell R, Furuya K, Brackmann B, Dawood Y, Khan-Dawood F. Expression of the oxytocin and vasopressin genes in human and baboon gonadal tissues. *Endocrinology*. (1990) 127:2990–6. doi: 10.1210/endo-127-6-2990
37. Mayerhofer A, Sterzik K, Link H, Wiemann M, Gratzl M. Effect of oxytocin on free intracellular $Ca2^{+}$ levels and progesterone release by human granulosa-lutein cells. *J Clin Endocrinol Metab*. (1993) 77:1209–14. doi: 10.1210/jcem.77.5.8077313
38. Saller S, Kunz L, Dissen GA, Stouffer R, Ojeda SR, Berg D, et al. Oxytocin receptors in the primate ovary: molecular identity and link to apoptosis in human granulosa cells. *Human Reprod*. (2010) 25:969–76. doi: 10.1093/humrep/dep467
39. Kampfer C, Saller S, Windschüttl S, Berg D, Berg U, Mayerhofer A. Pigment-Epithelium Derived Factor (PEDF) and the human ovary: a role in the generation of ROS in granulosa cells. *Life Sci*. (2014) 97:129–36. doi: 10.1016/j.lfs.2013.12.007
40. Miller I, Chuderland D, Grossman H, Ron-El R, Ben-Ami I, Shalgi R. The dual role of PEDF in the pathogenesis of OHSS: negating both angiogenic and inflammatory pathways. *J Clin Endocrinol Metab*. (2016) 101:4699–709. doi: 10.1210/jc.2016-1744
41. Adam M, Saller S, Ströbl S, Hennebold JD, Dissen GA, Ojeda SR, et al. Decorin is a part of the ovarian extracellular matrix in primates and may act as a signaling molecule. *Human Reprod*. (2012) 27:3249–58. doi: 10.1093/humrep/des297
42. Sawada Y, Sato T, Saito C, Ozawa F, Ozaki Y, Sugiura-Ogasawara M. Clinical utility of decorin in follicular fluid as a biomarker of oocyte potential. *Reprod Biol*. (2018) 18:33–9. doi: 10.1016/j.repbio.2017.12.001
43. Buraschi S, Neill T, Iozzo RV. Decorin is a devouring proteoglycan: Remodeling of intracellular catabolism via autophagy and mitophagy *Matrix Biol*. (2017) 75–6:260–70. doi: 10.1016/j.matbio.2017.10.005
44. Gubbiotti MA, Vallet SD, Ricard-Blum S, Iozzo RV. Decorin interacting network: a comprehensive analysis of decorin-binding partners and their versatile functions. *Matrix Biol*. (2016) 55:7–21. doi: 10.1016/j.matbio.2016.09.009
45. Blohberger J, Kunz L, Einwang D, Berg U, Berg D, Ojeda SR, et al. Readthrough acetylcholinesterase (AChE-R) and regulated necrosis: pharmacological targets for the regulation of ovarian functions? *Cell Death Dis*. (2015) 6:e1685. doi: 10.1038/cddis.2015.51
46. Huang D, Zheng X, Wang ZA, Chen X, He WT, Zhang Y, et al. The MLKL channel in necroptosis is an octamer formed by tetramers in a dyadic process. *Mol Cell Biol*. (2017) 37:e00497-16. doi: 10.1128/MCB.00497-16
47. Galluzzi L, Vitale I, Aaronson SA, Abrams JM, Adam D, Agostinis P, et al. Molecular mechanisms of cell death: recommendations of the nomenclature committee on cell death 2018. *Cell Death Diff*. (2018) 25:486–541. doi: 10.1038/s41418-017-0012-4
48. Pasparakis M, Vandenabeele P. Necroptosis and its role in inflammation. *Nature*. (2015) 517:311–20. doi: 10.1038/nature14191
49. Gaytán F, Morales C, García-Pardo L, Reymundo C, Bellido C, Sánchez-Criado JE. Macrophages, cell proliferation, and cell death in the human menstrual corpus luteum. *Biol Reprod*. (1998) 59:417–25. doi: 10.1095/biolreprod59.2.417
50. Dunai Z, Bauer PI, Mihalik R. Necroptosis: biochemical, physiological and pathological aspects. *Pathol Oncol Res*. (2011) 17:791. doi: 10.1007/s12253-011-9433-4
51. Du Y, Bagnjuk K, Lawson MS, Xu J, Mayerhofer A. Acetylcholine and necroptosis are players in follicular development in primates. *Sci Rep*. (2018) 8:6166. doi: 10.1038/s41598-018-24661-z
52. Hojo T, Siemieniuch MJ, Lukasik K, Piotrowska-Tomala KK, Jonczyk AW, Okuda K, et al. Programmed necrosis - a new mechanism of steroidogenic luteal cell death and elimination during luteolysis in cows. *Sci Rep*. (2016) 6:38211. doi: 10.1038/srep38211
53. Kitatani K, Idkowiak-Baldys J, Hannun YA. The sphingolipid salvage pathway in ceramide metabolism and signaling. *Cell Signal*. (2008) 20:1010–8. doi: 10.1016/j.cellsig.2007.12.006
54. Ye X. Lysophospholipid signaling in the function and pathology of the reproductive system. *Human Reprod Update*. (2008) 14:519–36. doi: 10.1093/humupd/dmn023
55. Vázquez-Nin GH, Escobar ML, De Felici M, Echeverría OM, Klinger FG. *Cell Death Mamm Ovary*. (2011). Luxembourg: Springer Science and Business Media.
56. Nakahara T, Iwase A, Nakamura T, Kondo M, Bayasula, Kobayashi H, et al. Sphingosine-1-phosphate inhibits H_2O_2-induced granulosa cell apoptosis via the PI3K/Akt signaling pathway. *Fertil Steril*. (2012) 98:1001–8.e1001. doi: 10.1016/j.fertnstert.2012.06.008
57. Kim JH, Han JS, Yoon YD. Biochemical and morphological identification of ceramide-induced cell cycle arrest and apoptosis in cultured granulosa cells. *Tissue Cell*. (1999) 31:531–9. doi: 10.1054/tice.1999.0061
58. Perks CM, Newcomb PV, Grohmann M, Wright RJ, Mason HD, Holly JM. Prolactin acts as a potent survival factor against C2-ceramide-induced apoptosis in human granulosa cells. *Human Reprod*. (2003) 18:2672–7. doi: 10.1093/humrep/deg496
59. Wang E, Norred WP, Bacon CW, Riley RT, Merrill AH. Inhibition of sphingolipid biosynthesis by fumonisins. Implications for diseases associated with *Fusarium moniliforme*. *J Biol Chem*. (1991) 266: 14486–90.

Conflict of Interest Statement: The authors declare that the research was conducted in the absence of any commercial or financial relationships that could be construed as a potential conflict of interest.

frontiers in Endocrinology

ORIGINAL RESEARCH
published: 10 July 2019
doi: 10.3389/fendo.2019.00467

Prostaglandins in Superovulation Induced Bovine Follicles During the Preovulatory Period and Early Corpus Luteum

Bajram Berisha[1,2]*, *Daniela Rodler*[3], *Dieter Schams*[2], *Fred Sinowatz*[2] and *Michael W. Pfaffl*[2]

[1] Department of Animal Biotechnology, Faculty of Agriculture and Veterinary, University of Prishtina, Pristina, Kosovo, [2] Animal Physiology and Immunology Weihenstephan, Technical University of Munich, Munich, Germany, [3] Department of Veterinary Sciences, Ludwig Maximilian University of Munich, Munich, Germany

The aim of this study was to characterize the regulation pattern of prostaglandin family members namely prostaglandin F2alpha (PTGF), prostaglandin E2 (PTGE), their receptors (PTGFR, PTGER2, PTGER4), cyclooxygenase 2 (COX-2), PTGF synthase (PTGFS), and PTGE synthase (PTGES) in the bovine follicles during preovulatory period and early corpus luteum (CL). Ovaries containing preovulatory follicles or CL were collected by transvaginal ovariectomy ($n = 5$ cows/group), and the follicles were classified: (I) before GnRH treatment; (II) 4 h after GnRH; (III) 10 h after GnRH; (IV) 20 h after GnRH; (V) 25 h after GnRH, and (VI) 60 h after GnRH (early CL). In these samples, the concentrations of progesterone (P4), estradiol (E2), PTGF and PTGE were investigated in the follicular fluid (FF) by validated EIA. Relative mRNA abundance of genes encoding for prostaglandin receptors (PTGFR, PTGER2, PTGER4), COX-2, PTGFS and PTGES were quantified by RT-qPCR. The localization of COX-2 and PTGES were investigated by established immunohistochemistry in fixed follicular and CL tissue samples. The high E2 concentration in the FF of the follicle group before GnRH treatment (495.8 ng/ml) and during luteinizing hormone (LH) surge (4 h after GnRH, 574.36 ng/ml), is followed by a significant ($P<0.05$) downregulation afterwards with the lowest level during ovulation (25 h after GnRH, 53.11 ng/ml). In contrast the concentration of P4 was very low before LH surge (50.64 mg/ml) followed by a significant upregulation ($P < 0.05$) during ovulation (537.18 ng/ml). The mRNA expression of COX-2 increased significantly ($P < 0.05$) 4 h after GnRH and again 20 h after GnRH, followed by a significant decrease ($P < 0.05$) after ovulation (early CL). The mRNA of PTGFS in follicles before GnRH was high followed by a continuous and significant downregulation ($P < 0.05$) afterwards. In contrast, PTGES mRNA abundance increased significantly ($P < 0.05$) in follicles 20 h after GnRH treatment and remained high afterwards. The mRNA abundance of PTGFR, PTGER2, and PTGER4 in follicles before GnRH was high, followed by a continuous and significant down regulation afterwards and significant increase ($P < 0.05$) only after ovulation (early CL). The low concentration of PTGF (0.04 ng/ml) and PTGE (0.15 ng/ml) in FF before GnRH, increased continuously in follicle groups before ovulation and displayed a further significant and dramatic increase ($P < 0.05$) around ovulation (101.01 ng/ml, respectively,

OPEN ACCESS

Edited by:
Jens Vanselow, Leibniz Institute for Farm Animal Biology, Germany

Reviewed by:
Dariusz Jan Skarzynski, Institute of Animal Reproduction and Food Research (PAN), Poland
Rubina Kumari Baithalu, National Dairy Research Institute (ICAR), India

***Correspondence:**
Bajram Berisha
bajram.berisha@uni-pr.edu

Specialty section:
This article was submitted to Reproduction, a section of the journal Frontiers in Endocrinology

Received: *21 March 2019*
Accepted: *27 June 2019*
Published: *10 July 2019*

Citation:
Berisha B, Rodler D, Schams D, Sinowatz F and Pfaffl MW (2019) Prostaglandins in Superovulation Induced Bovine Follicles During the Preovulatory Period and Early Corpus Luteum. Front. Endocrinol. 10:467. doi: 10.3389/fendo.2019.00467

484.21 ng/ml). Immunohistochemically, the granulosa cells showed an intensive signal for COX-2 and PTGES in follicles during preovulation and in granulosa-luteal cells of the early CL. In conclusion, our results indicate that the examined bovine prostaglandin family members are involved in the local mechanisms regulating final follicle maturation and ovulation during the folliculo-luteal transition and CL formation.

Keywords: prostaglandins, steroids, gene regulation, ovarian function, follicle, ovulation, cow

INTRODUCTION

The ovarian cycle in bovine is characterized by regularly repeating patterns of cellular proliferation, differentiation and transformation that accompanies follicular maturation and ovulation during the folliculo-luteal transition and corpus lutem (CL) formation and function (1–5). It is well-known that the ruminant reproductive function and especially the ovarian cycle is regulated through endocrine, as well as intraluteal (autocrine/paracrine) actions (6–9). The LH surge triggers a biochemical cascade that leads to the ovulation, resulting in development of the CL (10–12). Ovulation occurs as a result of a dynamic interaction between the luteinising hormone (LH) surge and local follicular factors including steroid hormones, extracellular matrix (ECM) proteases, prostaglandins, vasoactive peptides and growth factors in a time-dependent manner (1, 13–15). During these developments in the bovine ovary, steroid hormones and prostaglandins seem to be highly important regulatory mediators playing a central role in the regulation of the estrous cycle (16–22). Progesterone (P4) and estradiol (E2) steroid production of ovulatory follicles change dramatically during the preovulatory period, suggesting them to have an important role during ovulation (19, 23–25). The later stage of follicular development, ovulation and CL formation depends upon growth of new blood vessels (angiogenesis) and the establishment of a functional blood supply (12, 26, 27).

A recent finding demonstrates that steroid hormones and prostaglandins in addition to different angiogenic factors are required for angiogenesis and folliculo-luteal transition (28–33). The prostaglandins are of particular interest because of their endocrine as well as local effects within the ovarian tissue during different physiological stages (20, 34, 35). Intraluteal prostaglandin production is regulated by a variety of endocrine and autocrine/paracrine factors secreted by different immune cells, namely, macrophages, eosinophils, lymphocytes and monocytes (5, 8, 36). The production of prostaglandins from arachidonic acid is primarily governed by the rate-limiting enzymes cyclooxygenase (COX)-1 and COX-2 (16, 34). The downstream enzymes, PTGF synthase (PTGFS) and PTGE synthase (PTGES), catalyze the conversion of prostaglandin H2 precursors to prostaglandin F2alpha (PTGF) and prostaglandin E2 (PTGE) respectively, (14, 20). PTGF has the highest affinity for the specific receptor (PTGFR), and PTGE may interact with at least four receptor subtypes (PTGER1—PTGER4) and initiate biological signaling pathways (21, 37–39).

The steroid hormones and prostaglandins were shown to regulate ovarian cycle in cattle, but the examination of these factors during final follicle regulation, ovulation and CL formation, has not been thoroughly elucidated to date. Therefore, we tested the hypothesis if the preovulatory LH surge may affect COX-2, prostaglandin synathases (PTGFS and PTGES), prostaglandin ligands (PTGF and PTGE) and their receptors (PTGFR, PTGER2, and PTGER4), which may have further effects to the folliculo-luteal transition and CL formation in the cow. With the present study, we aim to evaluate the expression pattern and localization of earlier mentioned prostaglandin family members in time-defined follicle classes before (control) and after the application of GnRH and after ovulation (early CL) in the cow.

MATERIALS AND METHODS

Animals, Procedure of Superovulation and Collection of Ovaries

The animal trail was approved by the animal ethics committee located at the government of Upper Bavaria (reference number 211-2531.3-33/96). The study was conducted on 30 German Fleckvieh cows and the superovulation procedure was conducted as described by Berisha et al. (40). For confirmation of LH surge, blood samples were collected from the jugular vein at −24 h, −12 h, −1 h, and 0 h before and 3 h and 12 h after GnRH application (27). The bovine ovaries (containing preovulatory follicles or early CL) were collected at (I) 0 h, (II) 4 h, (III) 10 h, (IV) 20 h, (V) 25 h (for follicle collection) and (VI) 60 h (for early CL collection) relative to injection of GnRH (n=5 cow/group) as described by Berisha et al. (27). The schematic time schedule of the superovulatory treatment and ovary collection is shown in **Figure 1**.

Collection, Classification and Preparation of Preovulatory Follicles and Early CL

Only follicles which appeared healthy (i.e., well-vascularised and having transparent follicular wall and fluid) and whose diameter were >10 mm were collected. The number of follicles per ovary varied between 8 and 20. Follicular fluid (FF) was aspirated from single follicles, and then the follicles tissue (theca interna and granulose cells) aliquots were stored at −80°C until extraction for RNA. The FF (1.0–1.5 ml) was stored from single follicles at −20°C until determination of P4, E2, PTGF, and PTGE (40). The follicles, after aspiration of FF and injection of fixative (27) and pieces of CL tissue were fixed for immunohistochemical analysis of COX-2 and PTGES (22).

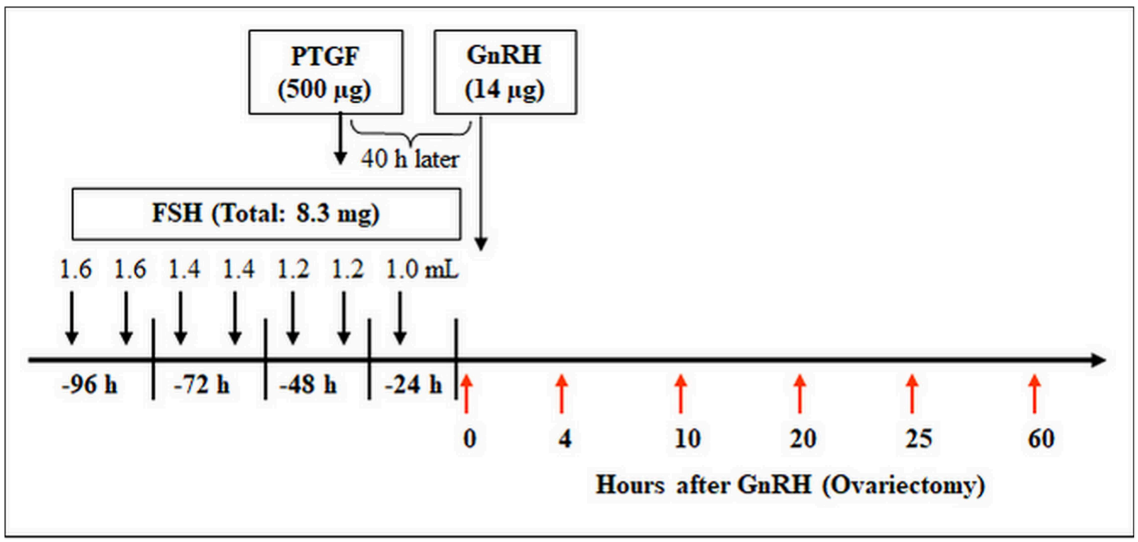

FIGURE 1 | Time schedule of the treatment for multiple ovulation and ovary collection in cows. Ovaries containing preovulatory follicles or new CL were collected at (I) 0 h, (II) 4 h, (III) 10 h, (IV) 20 h, (V) 25 h (follicles), and (VI) 60 h (early CL, Day 2–3) relative to injection of GnRH to induce an luteinizing hormone (LH) surge ($n = 5$ cows/group).

Hormone Determinations

The concentrations of P4, E2, PTGF, and PTGE were determined in the FF with an enzyme immunoassay (EIA) using the second antibody technique as described by our lab and reviewed by Berisha et al. (40). The concentration of progesterone in blood plasma was measured using EIA technique as described by Berisha et al. (41).

Total RNA Extraction and Quality Determination

Total RNA from 200 mg follicles and CL (deep frozen by −80°C) were extracted with peqGOLD TriFAst (PeqLab, Erlangen, Germany) according to the manufacturer's instructions and described by Berisha et al. (40). For DNA digestion the DNA-free kit (Ambion, Austin, USA) was used. Total RNA was dissolved in RNAse-free water and spectroscopically quantified at 260 nm. The purity of isolated RNA was verified by optical density (OD) absorption ratio OD260 nm/OD280 nm between 1.8 and 2.0.

The RNA integrity was measured with the Agilent 2100 bioanalyzer (Agilent Technologies, Deutschland Gmbh, Waldbronn, Germany) in conjunction with the RNA 6000 Nano Assay according to the manufacturer's instructions. The Bioanalyzer 2100 enables the standardization of total RNA quality control for quantitative downstream applications (42). The automatically calculated RNA Integrity Number (RIN) allows classification of total RNA based on a numbering system from 1 to 10, with 1 being the most degraded profile and 10 being the most intact (43). Herein integer total RNA with RIN values of 7–8 were achieved over all tissue extractions.

RNA Reverse Transcription and Real-Time PCR

Constant amounts of 1 µg of total RNA were reverse-transcribed to cDNA using the following master mix: 26 µl RNAse-free water, 12 µl 5 × Buffer (Promega, Mannheim, Germany), 3 µl Random Primers (50 µM) (Invitrogen, Carlsbad, Germany), 3 µl dNTPs (10 mM) (Fermentas, St. Leon-Rot, Germany) and 200 U of M-MLV Reverse Transcriptase (Promega, Mannheim, Germany) according to the manufacturer's instructions. A master mix of the reaction components was prepared according to Berisha et al. (22). The following Real-Time PCR protocol was employed for all investigated factors: denaturation for 10 min at 95°C, 40 cycles of a three segmented amplification and quantification program (denaturation for 10 s at 95°C, annealing for 10 s at 60°C, elongation for 15 s at 72°C), a melting step by slow heating from 60 to 99°C with a rate of 0.5°C/s and continuous fluorescence measurement, and a final cooling down to 40°C. Data were analyzed using Rotor-Gene 3000 software (Corbett Research version 5.03). The relative mRNA abundance of each target gene were calculated using the "comparative quantification" method (Corbett Reasearch). The changes in mRNA expression of examined target genes were assayed by normalization to the stable expressed and internal UBQ control gene. In order to obtain the CT (cycle threshold) difference the data were analyzed using the well-established ΔΔCT method described by Livak and Schmittgen (44). Thereby ΔCT was not subtracted from a non-treated control group, which does not exist in this study, but from the constant number 40, so that a high "40-ΔCT" value indicated a high-gene expression level and vice versa. This results in directly comparable relative expression values between the examined follicle classes before and after the application of GnRH and after ovulation (early CL) in the cow.

Immunohistochemistry of COX-2 and PTGES

Paraffin-embedded mature follicles and CL tissue (fixed in Bouin's fluid for 24 h) were cut into 5-µm serial sections and collected on amino-propyltriethoxysilane coated slides

TABLE 1 | Concentration of Prostaglandin F2alpha (PTGF), Prostaglandin E2 (PTGE), Estradiol (E2), and Progesterone (P4) in follicular fluid (FF) of preovulatory follicles collected at (I) 0 h, (II) 4 h, (III) 10 h, (IV) 20 h, and (V) 25 h relative to injection of GnRH to induce an LH surge.

	Follicle groups (hours after GnRH administration)				
Hormones in FF (ng/ml)	**Group I (0 h)**	**Group II (4 h)**	**Group III (10 h)**	**Group IV (20 h)**	**Group V (25 h)**
PTGF	0.04 ± 0.1^{b}	1.50 ± 0.5^{b}	1.18 ± 0.26^{b}	36.25 ± 7.13^{ab}	101.01 ± 33.42^{a}
PTGE	0.15 ± 0.03^{c}	1.21 ± 0.26^{c}	3.60 ± 0.63^{bc}	15.16 ± 6.07^{b}	484.21 ± 109.27^{a}
E2	495.8 ± 80.09^{a}	574.36 ± 109.7^{a}	178.96 ± 29.06^{b}	59.25 ± 8.4^{b}	53.11 ± 7.28^{b}
P4	50.64 ± 11.49^{b}	186.41 ± 45.60^{b}	130.63 ± 20.17^{b}	203.78 ± 32.82^{b}	537.18 ± 81.26^{a}

Results are presented as the mean ± SEM (ng/ml FF, n = 8–12 follicle/group from 5 animals). Different superscripts denote significantly different values (P < 0.05).

(SupraFrost Ultra Plus; Menzel-Gläser, Braunschweig, Germany). Paraffin sections were dewaxed and then washed three times for 5 min with PBS at pH 7.4. The sections were incubated with polyclonal primary antibodies to PTGES (ab62050; diluted 1:300, host rabbit; Abcam, Cambridge, UK; secondary antibody: pig anti-rabbit IgG (F(ab′)2), diluted 1:300) and with polyclonal primary antibodies to COX-2 (ab2367; diluted 1:400, host goat; Abcam; secondary antibody: rabbit-anti-goat IgG (F(ab′)2), diluted 1:300) at 6°C overnight. Endogenous peroxidase activity was blocked with 7.5% H_2O_2 (diluted in distilled water) at room temperature for 10 min.

Nonspecific antibody binding was blocked with Dako protein block serum-free (Dako Deutschland GmbH; Hamburg, Germany) for 10 min. The sections were incubated with the primary antibodies at 6°C overnight. Localization of the antigen was achieved using the avidin–biotin-complex technique. The appropriate biotinylated secondary antibodies were incubated with the sections for 16 h at room temperature. Subsequently, treatment with Strept-ABComplex-HRP (Dako Deutschland GmbH) was performed for 30 min at room temperature, and treatment with 1 mg/ml 3,3-diaminobenzidinetetrahydrochloride (BIOTREND Chemikalien GmbH; Cologne, Germany) was performed for 5 min. All incubations were performed in a humidified chamber.

Sections were slightly counterstained with haematoxylin (20 s), dehydrated and mounted with the Eukitt quick hardening mounting medium for microscopy (Fluka Analytical©; Sigma-Aldrich Laborchemikalien GmbH, Seelze, Germany). Negative controls were performed by incubating with the 3,3-diaminobenzidine reagent alone to exclude the possibility of detecting the non-suppressed endogenous peroxidase activity. A lack of detectable staining in the negative controls demonstrated that the reactions were specific. The images were captured with a Leica Labo-Lux microscope equipped with a Zeiss Axiocam camera (Zeiss, Munich, Germany). As positive controls, ovarian tissues from quails (Coturnix japonica) and cats (Felis silvestris) of proven immunoreactivity were used (45). The reaction intensities were marked as weak (+), distinct (++), and strong (+++).

Statistical Analysis

The statistical significance of differences in hormone concentration in FF and mRNA expressions in follicle and CL tissue of the examined factors was assessed by one way ANOVA followed by the Holm Sidak as a multiple comparison test. Data, which failed the normality or equal variance test, were tested by one way ANOVA on ranks followed by the Kruskal-Wallis test (Sigma Stat 3.0). All experimental data are shown as means±SEM ($n = 8$–12). The differences were considered significant if $P < 0.05$.

RESULTS

Concentration of E2, P4 and PTGE and PTGF in FF During Preovulation

We analyzed the concentration of E2, P4, PTGF, and PTGE in FF for a better characterization of follicle groups before and after GnRH application and during ovulation (**Table 1**).

The high E2 concentration in the FF of the follicle group before GnRH treatment (495.8 ng/ml) and during luteinizing hormone (LH) surge (4 h after GnRH, 574.36 ng/ml), is followed by a significant ($P < 0.05$) downregulation afterwards with the lowest level during ovulation (25 h after GnRH, 53.11 ng/ml). In contrast the concentration of P4 was very low before LH surge (50.64 mg/ml) followed by a significant upregulation ($P < 0.05$) during ovulation (537.18 ng/ml).

The low concentration of PTGF (0.04 ng/ml) and PTGE (0.15 ng/ml) in FF before GnRH, increased continuously in follicle groups before ovulation and displayed a further significant and dramatic increase ($P<0.05$) around ovulation (101.01 ng/ml respectively 484.21 ng/ml).

Confirmation of Primer Specificity and Sequence Analysis

The mRNA expression was quantified by the reverse transcription quantitative polymerase chain reaction (RT-qPCR), as described in detail in our previous study (46). Amplified RT-qPCR products were separated on agarose gel electrophoresis for length verification, and for sequence confirmation additionally sequenced by a commercial provider (TopLab, Munich, Germany). All amplified RT-qPCR products showed 100% homology to the known bovine gene sequence published in NCBI GenBank (complete sequences are not shown herein). The primer sequences and expected PCR product length are shown in **Table 2**.

TABLE 2 | Primer sequences for investigates genes, respective RT-qPCR product length, and appropriate reference.

Target	Sequence of nucleotide fragment*	Size (bp)	References
UBQ	For 5′-AGATCCAGGATAAGGAAGGCAT-3′ Rev 5′-GCTCCACCTCCAGGGTGATT-3′	189	(30)
GAPDH	For 5′-GTCTTCACTACCATGGAGAAGG-3′ Rev 5′-TCATGGATGACCTTGGCCAG-3′	197	(30)
COX-2	For 5′-CTCTTCCTCCTGTGCCTGAT-3′ Rev 5′-GACTCATAGAAACTGACACCCTC-3′	359	(30)
PTGFS	For 5′-ACCTGGACCTCTACCTCATCCA-3′ Rev 5′-TCCTCATCCAATGGGAAGAAGT-3′	100	(22)
PTGES	For 5′-GCGCGCTGCTGGTCATCAAA-3′ Rev 5′-GTGTAGGCCAGGGAGCGGGT-3′	334	(22)
PTGFR	For 5′-TCAGCCCTCACCCAGATAGT-3′ Rev 5′-GGCCATTTCACTGTTCAGGT-3′	167	(22)
PTGER2	For 5′-CTACTTTGCCTTTTCCATGACC-3′ Rev 5′-GATGAAGCACCACGTCCC-3′	210	(22)
PTGER4	For 5′-CGATGAGTATTGAGCGCTACC-3′ Rev 5′-AGCCCGCATACATGTAGGAG-3′	220	(22)

For, forwards; Rev, reverse.

Relative mRNA Abundance

To evaluate equal quantity and quality of the preceding RT reaction in each sample, the housekeeping genes ubiquitin (UBQ) and glyceraldehyde-3-phosphate dehydrogenase (GAPDH) were examined in all samples. As both housekeeping genes were constantly expressed in all samples we choose UBQ as normalizer. The results of mRNA expression of examined factors (**Figures 2**, **3**) are presented as changes (40-ΔCT $\pm$ SEM from 6 follicles or CL per group) in the target gene expression, normalized to UBQ as described by Berisha et al. (22).

Relative mRNA Expression of COX-2, PTGES and PTGFS in Preovulatory Follicles and Early CL

The mRNA expression of COX-2 (**Figure 2A**) increased significantly ($P < 0.05$) 4 h after GnRH and again 20 h after GnRH, followed by a significant decrease ($P < 0.05$) after ovulation (early CL). The mRNA of PTGFS (**Figure 2B**) in follicles before GnRH was high followed by a continuous and significant downregulation ($P < 0.05$) afterwards. In contrast, PTGES mRNA abundance increased significantly ($P < 0.05$) in follicles 20 h after GnRH treatment and remained high afterwards (**Figure 2C**).

Relative mRNA Expression of PTGFR, PTGER2 and PTGER4 in Preovulatory Follicles and Early CL

The mRNA abundance of PTGFR (**Figure 3A**), PTGER2 (**Figure 3B**), and PTGER4 (**Figure 3C**) in follicles before GnRH was high, followed by a continuous and significant down regulation afterwards and significant ($P < 0.05$) increase only after ovulation (early CL).

Immunohistochemical Localization of COX-2 in Preovulatory Follicles and Early CL

The multilayered epithelium of follicles at the time of ovulation (follicle diameter 18- 25 mm) displayed a clear signal for COX-2 (**Figure 4A**). COX-2 was expressed in the cytoplasm of more than 90% of the high prismatic basal cells located at the top of the basal membrane (BM). A slight staining was also seen in the theca interna surrounding the follicular epithelium. On days 1–2 after ovulation a strong signal for COX-2 could be noted in a subpopulation of cells located in the apical half of the folded membrana granulosa around the former antrum (**Figure 4C**). They were surrounded by other granulosa cells (GC), which showed only a weak signal. On days 3–4 scattered and distinctly COX-2-positive progesterone producing granulosa-luteal cells (LC) occurred in the developing corpus luteum (**Figure 4E**).

Immunohistochemical Localization of PTGES in Preovulatory Follicles and Early CL

A distinct to strong immunoreactivity for PTGES was found throughout the follicular epithelium before ovulation (**Figure 4B**). Most cells of the theca interna (TI) displayed only weak immunoreactivity for this enzyme and the stromal cells of the theca were almost negative. On days 1–2 after ovulation, granulosa cells (GC) of the developing CL showed distinct signal with the PTGES antibody ($\pm$). The signal intensity of the granulosa-luteal cells (LC) increased in the CL at days 3–4 (**Figure 4F**).

DISCUSSION

Recent studies have demonstrated the important role of steroid hormones and prostaglandins during follicle development, ovulation and CL formation in different species and various study models (8, 22, 31, 47, 48). Our present study demonstrates the expression pattern of steroid hormones (E2 and P4) and prostaglandin family members (COX-2, PTGFS, PTGES, PTGF, PTGE, and their receptors) in different timely defined follicle classes before and after GnRH application and after ovulation (early CL) in the cow. We have shown in our previous studies (40, 49) that superovulated follicles after GnRH application are comparable to natural ovulation in the cow. We demonstrated in addition that also the time interval between the LH surge and ovulation is quite comparable between induced ovulation (40) and spontaneous ovulation in cows (49).

The LH surge initiates a series of biochemical events in ovary, such as upregulation of steroids, prostaglandins, ECM proteases and many locally produced growth and angiogenic factors to complement gonadotropins action in process of ovulation and CL formation (8, 13, 27, 50–52).

It is well-known that P4 and E2 steroid production of preovulatory follicles change dramatically during the periovulatory period, suggesting them to play an important role during final follicle development and ovulation (11, 14, 23–25, 53, 54). In addition our previous studies demonstrated

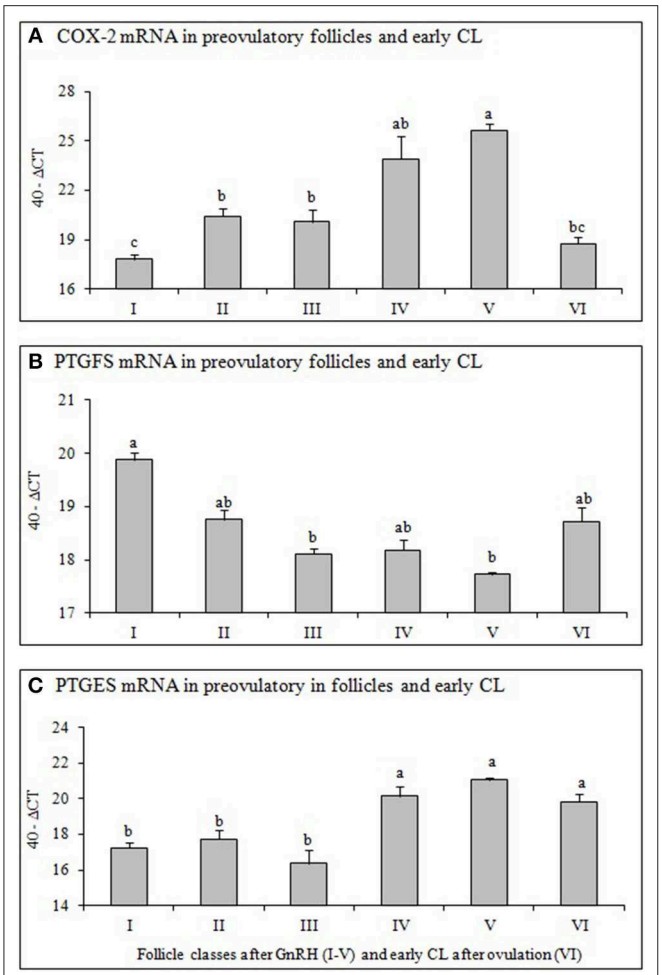

FIGURE 2 | Changes of mRNA for **(A)** Cyclooxygenase 2 (COX-2), **(B)** Prostaglandin F2alpha synthase (PTGFS) and **(C)** Prostaglandin E2 synthase (PTGFS) in preovulatory follicles collected at (I) 0 h, (II) 4 h, (III) 10 h, (IV) 20 h, (V) 25 h (follicles), and (VI) 60 h (new CL, Day 2–3) relative to injection of GnRH to induce an LH surge (5 follicles or CL per group from 5 animals). Different superscripts denote statistically different values ($P < 0.05$).

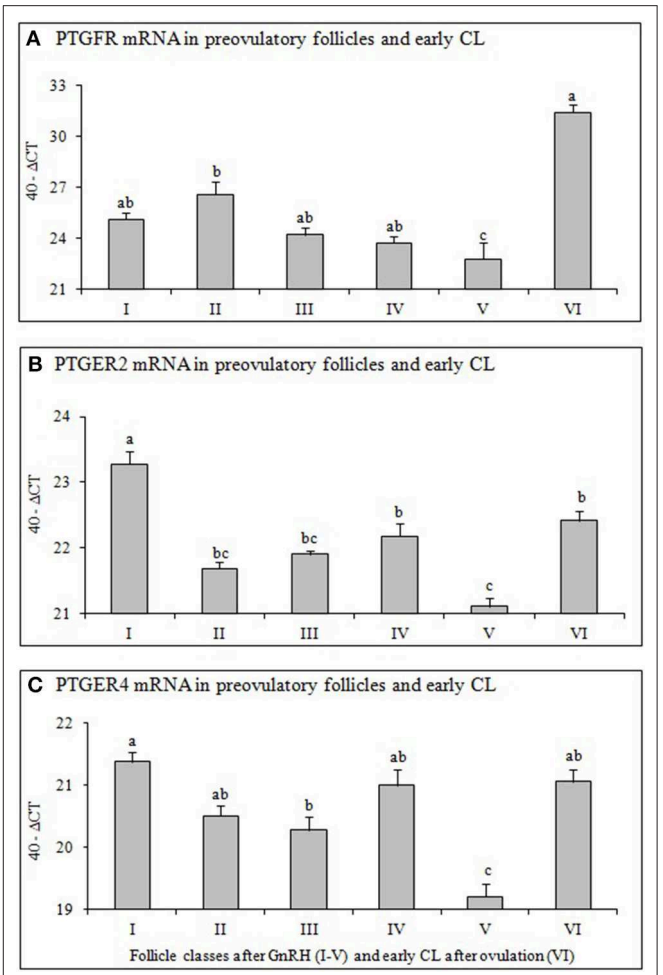

FIGURE 3 | Expression of mRNA for **(A)** Prostaglandin F2alpha receptor (PTGFR), **(B)** Prostaglandin E2 receptor 2 (PTGER2), and **(C)** Prostaglandin E2 receptor 4 (PTGER4) in preovulatory follicles collected at (I) 0 h, (II) 4 h, (III) 10 h, (IV) 20 h, (V) 25 h (follicles), and (VI) 60 h (new CL, Day 2–3) relative to injection of GnRH to induce an LH surge (5 follicles or CL/group from 5 animals). Different superscripts denote statistically different values ($P < 0.05$).

clear evidence for steroids as local regulators of follicular and luteal activity (4, 19). *In vivo* and *in vitro* studies demonstrated production and localization of P4 and E2 and their specific receptors in both granulosa and theca cells of perovulatory follicles (11, 14, 23–25). The E2 concentration in the FF of our study (**Table 2**) was high in the follicle group before and during LH surge, followed by a significant downregulation afterwards. In contrast the concentration of P4 was very low before LH surge followed by a significant upregulation during LH surge, with maximal level during ovulation (**Table 2**). Our present data agree with results of Fortune et al. (11) suggesting that increase in follicular P4 production and associated decreases in E2 concentration in FF prior ovulation, reflect transition from a follicular to a luteal steroidogenic profile of cells.

The results of our present study clearly demonstrate the expression pattern of examined prostaglandin family members, which depends on the developmental stage of the follicles before and after LH surge and after ovulation (early CL) in the bovine ovary. The multilayered epithelium of mature follicles shows a distinct to strong signal for COX-2 and PTGES, whereas the theca interna is only weakly positive (**Figure 4**). At day 1–2 after ovulation, a subpopulation of GC of the former follicle epithelium is distinctly immunopositive for COX-2 and PTGES. According to Fortune et al. (11), the major source of prostaglandins is believed to be GC of the preovulatory follicle. At day 3–4 large (granulosa luteal cells) and small (theca luteal cells) can be discerned. A subpopulation of the large luteal cells is distinctly immunopositive for both enzymes. As COX-2 and PTGES are key enzymes for the synthesis of prostaglandins, their similar expression pattern makes sense.

It is well-known that LH surge and ovulation process influence production of COX, prostaglandin synthases (PTGFS and PTGES), prostaglandin ligands (PTGF and PTGE) but also regulates expression of prostaglandin receptors (PTGFR,

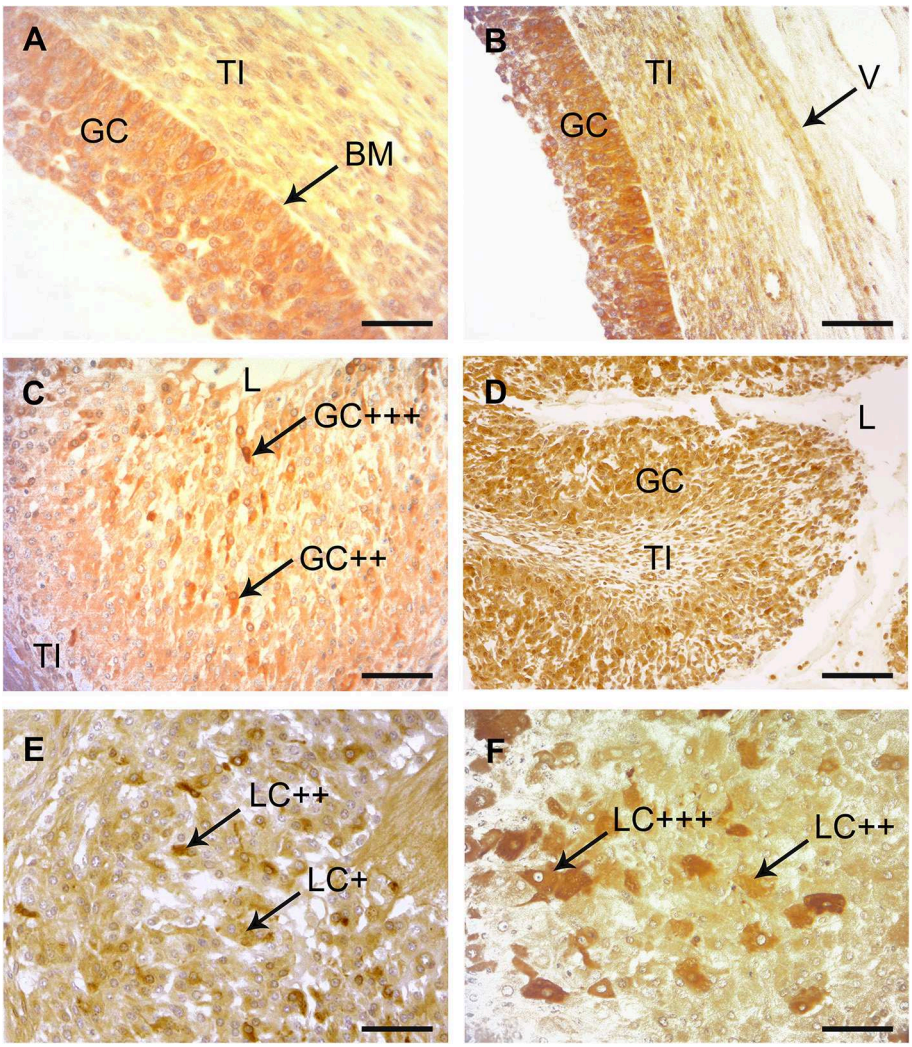

FIGURE 4 | Immunohistochemical localization of COX-2 and PTGES in bovine preovulatory follicles and early corpus lutem (CL). **(A)** Immunohistochemical localization of COX-2 in a mature preovulatory follicle. A distinct to strong immunostaining was found throughout the granulosa cells (GC) with increaded intensity adjacent to the basement membrane (BM). The theca interna (TI) was also weakly stained. SB = 75 μm. **(B)** Immunohistochemical localization of PTGES in a mature preovulatory follicle. A distinct to strong immunostaining is found in the cytoplasma of the GC. Similar to the result with COX-2, the basal cells show stronger reactions than the luminal cells. The TI and the endothelium of this longitudinal cut vessel (V) show slight positive reactions. SB = 150 μm. **(C)** Immunohistochemical localization of COX-2 in the CL at days 1–2. A subpopulation of the folded membrana granulosa (GC) surrounding the remaining lumen (L) of the former antrum of the ovulated follicle display distinct (++) to strong (+ + +) positive immunostaining with the COX-2 antibody. TI = theca interna; SB = 100 μm. **(D)** Immunohistochemical localization of PTGES in the CL at days 1–2. Many of the former GC display distinct immunostaining. L = lumen, TI = theca interna; SB = 200 μm. **(E)** Immunohistochemical localization of COX-2 in the CL at days 3–4. At this magnification many granulosa-luteal cells (LC) with distinct (++) immunostaining alternate with negative or only weakly stained cells (+). SB = 150 μm. **(F)** Immunohistochemical localization of PTGES in the CL at days 3–4. Several of the granulosa-luteal cells (LC) show strong immunostaining (+ + +) with PTGES antibodies, whereas the rest of this cell population display only distinct to moderate immunopositivity (++). SB = 75 μm.

PTGER2, and PTGE4). In our present study the concentration of PTGF and PTGE in FF (**Table 2**) was low prior to LH surge (before GnRH application), increased continuously and significantly 20h after GnRH and further increase around ovulation (25 h after GnRH). The rapid increase of PTGF and especially PTGE in preovulatory follicles close to ovulation is in accordance with previous studies in bovine and other mammals (55–57). The data of Fortune et al. (11) supported the hypothesis that prostaglandins, especially PTGE, can stimulate P4 secretion by both follicular cell types and suggest a positive feedback relationship between P4 and the prostaglandins. In addition, Bridges and Fortune (21) demonstrated that both theca and GC of preovulatory follicles are targets for both the PTGF and the PTGE produced by the GC. The results of some earlier studies showed clearly that ovulation process is dependent from follicular prostaglandin production also in cows (23, 47, 53–59). LH surge has been reported to induce enzymes modulating prostaglandin production and specific prostaglandin receptors in the preovulatory follicles (21, 33, 39, 60).

The upregulation of COX-2 and PTGES expression in our study was followed by a dramatic increase of PTGF and PTGE in the FF starting 20 h after GnRH application (**Table 2**). The preovulatory increases of prostaglandin concentration in FF have shown to be necessary component of the ovulation in several species (11, 33, 57, 59–61). Some earliest studies in different species suggested both PTGF and PTGE to be important to the ovulatory process (59, 62). However, the recent studies in different mammalian species clearly demonstrated that PTGE is more essential for ovulation and CL formation (14, 39, 47). Based on these findings, it is widely accepted that PGE2 is an essential paracrine mediator of the LH surge in mammalian (39, 57). The concentration of PTGE during ovulation in our study (**Table 2**) was much higher (484.21 ng/ml) than PTGF concentration (101.01 ng/ml). The marked increase of PTGF and especially PTGE in response to LH surge agrees with observation of other authors made in cow (23, 33, 59, 63).

The final follicle growth and ovulation process involves intense interactions between endothelial, steroidogenic and migrating immune cells, leading to the folliculo-luteal cell transition, ECM remodeling and further angiogenesis in the developing CL (9). Previous studies demonstrated the effects of LH surge in remodeling of ECM by regulation of diverse proteases of the plasminogen activators (PA) and the matrix metalloproteinase (MMP) enzyme systems in follicles during ovulation process and CL formation in cow (64–69). In addition Fortune et al. (11) demonstrated the effect of LH, P4 and prostaglandins in regulation of ADAMTS proteases (A Disintegrin And Metalloproteinase with Thrombo Spondin motifs), suggesting an important role of these factors in remodeling the preovulatory follicle during ovulation and angiogenesis. This study as well as others demonstrated that prostaglandins act via multiple receptors to regulate follicle-luteal transition and CL formation (22, 37–39, 57).

Not just the upregulation, but also the shift in the localization of different factors after LH surge suggests them to have an important role during the follicle-luteal transition. In our previous study in the same samples we have shown a distinct change in localization of FGF2 in the bovine follicles from the theca cell compartments (cytoplasm of endothelial cells) to the GC initiated by the LH surge. We suggested that nuclear FGF2 localization may be important for GC survival until ovulation and for a transition of GC to luteal cells in early CL (40). Examples of spatial differences are obvious for FGF2 (28) and, in particular, FGF7, for which the ligand is localized in the theca tissue and its receptor is localized mainly in GC (70). However, the aim of the present study was to analyze the regulation of the factors examined in whole follicle tissue (without GC and TI separation) in order to compare the expression between whole follicles tissue (GC and TI) and CL during follicle–luteal transition.

The significant upregulation of all prostaglandin receptors just after ovulation (early CL) in our study (**Figure 3**) demonstrates the important role of prostaglandins they play in the ovulation process, luteinisation and CL formation. Our previous study (22) demonstrated that PTGF and PTGE are involved in the local (autocrine/paracrine) mechanisms regulating CL formation and function. In early CL, the PTGE is known as a luteotropic factor, as it stimulates *in vitro* P4 production by bovine luteal steroidogenic cells (71, 72). In addition, PTGF stimulates P4 production, as well as PTGE, by cultured luteal cells (16, 73–75). Furthermore, PTGF and PTGE can suppress the apoptosis of steroidogenic and endothelial cells in bovine CL (72). In addition, our previous *in vivo* studies demonstrated that PTGF stimulates itself and PTGE in bovine CL (76, 77).

Moreover, in the early CL, prostaglandins regulate the expression of angiogenic factors in a luteal stage-dependent manner (9, 12, 35, 78). High expression and tissue levels of angiogenic factors during the early luteal stage (PTGF-refractory days) suggest a survival function for both endothelial cells of the capillaries and steroidogenic cells of the CL (12, 79). In our recent study we assume that LH modulates prostaglandin production in the bovine CL by stimulating the expressions of COX-2, prostaglandin synthases and angiogenic factors and that these actions help to maintain CL function during the early luteal phase (22). Moreover, intraluteal prostaglandins in the early CL may have different other functions, such as cellular transition and differentiation, blood flow regulation and intercellular communication (34, 80).

In conclusion, our results indicate that the LH surge upregulated prostaglandin family members in the follicle before ovulation, support the potential role of these system components in GC and TI tissue remodeling during ovulation process. The further upregulation of prostaglandin family members after ovulation (early CL) suggests that they play an important role in follicle-luteal transition and CL formation in the cow.

DATA AVAILABILITY

All datasets generated for this study are included in the manuscript and/or the supplementary files.

ETHICS STATEMENT

The experimental protocol was approved by the institutional care and use committee (AZ 211-2531.3-33/96).

AUTHOR CONTRIBUTIONS

BB and DS: designed and executed all the experiments. BB: wrote the manuscript. MP: qRT-PCR and data analysis. FS and DR: immunohistochemistry and data analysis. All the authors edited the manuscript.

FUNDING

This study was supported by the German Research Foundation (DFG BE 3189/2-2).

REFERENCES

1. Fortune JE. Ovarian follicular growth and development in mammals. *Biol Reprod*. (1994) 50:225–32. doi: 10.1095/biolreprod50.2.225
2. Fraser HM, Lunn SF. Angiogenesis and its control in the female reproductive system. *Br Med Bull*. (2000) 56:787–97. doi: 10.1258/0007142001903364
3. Berisha B, Schams D, Kosmann M, Amselgruber W, Einspanier R. Expression and tissue concentration of vascular endothelial growth factor, its receptors, and localization in the bovine corpus luteum during estrous cycle and pregnancy. *Biol Reprod*. (2000) 63:1106–14. doi: 10.1095/biolreprod63.4.1106
4. Berisha B, Schams D. Ovarian function in ruminants. *Domest Anim Endocrinol*. (2005) 29:305–17. doi: 10.1016/j.domaniend.2005.02.035
5. Meidan R, Levy N. The ovarian endothelin network: an evolving story. *Trends Endocrinol Metab*. (2007) 18:379–85. doi: 10.1016/j.tem.2007.09.002
6. Berisha B, Schams D, Miyamoto A. The expression of angiotensin and endothelin system members in bovine corpus luteum during estrous cycle and pregnancy. *Endocrine*. (2002) 19:305–12. doi: 10.1385/ENDO:19:3:305
7. Robinson RS, Nicklin LT, Hammond AJ, Schams D, Hunter MG, Mann GE. Fibroblast growth factor 2 is more dynamic than vascular endothelial growth factor A during niswenthe follicle-luteal transition in the cow. *Biol Reprod*. (2007) 77:28–36. doi: 10.1095/biolreprod.106.055434
8. Skarzynski DJ, Piotrowska-Tomala KK, Lukasik K, Galvão A, Farberov S, Zalman Y, et al. Growth and regression in bovine corpora lutea: regulation by local survival and death pathways. *Reprod Domest Anim*. (2013) 48(Suppl. 1):25–37. doi: 10.1111/rda.12203
9. Berisha B, Schams D, Rodler D, Pfaffl MW. Angiogenesis in The Ovary - the most important regulatory event for follicle and corpus luteum development and function in cow - an overview. *Anat Histol Embryol*. (2016) 45:124–30. doi: 10.1111/ahe.12180
10. Schams D, Berisha B. Regulation of corpus luteum function in cattle-an overview. *Reprod Domest Anim*. (2004) 39:241–51. doi: 10.1111/j.1439-0531.2004.00509.x
11. Fortune JE, Willis EL, Bridges PJ, Yang CS. The periovulatory period in cattle: progesterone, prostaglandins, oxytocin and ADAMTS proteases. *Anim Reprod*. (2009) 6:60–71.
12. Zalman Y, Klipper E, Farberov S, Mondal M, Wee G, Folger JK, et al. Regulation of angiogenesis-related prostaglandin f2alpha-induced genes in the bovine corpus luteum. *Biol Reprod*. (2012) 30:92. doi: 10.1095/biolreprod.111.095067
13. Tsafriri A, Lindner HR, Zor U, Lamprecht SA. Physiological role of prostaglandins in the induction of ovulation. *Prostaglandins*. (1972) 2:1–10. doi: 10.1016/0090-6980(72)90024-X
14. Bridges PJ, Komar CM, Fortune JE. Gonadotropin-induced expression of messenger ribonucleic acid for cyclooxygenase-2 and production of prostaglandins E and F2alpha in bovine preovulatory follicles are regulated by the progesterone receptor. *Endocrinology*. (2006) 147:4713–22. doi: 10.1210/en.2005-1575
15. Berisha B, Schams D, Rodler D, Sinowatz F, Pfaffl MW. Expression pattern of HIF1alpha and vasohibins during follicle maturation and corpus luteum function in the bovine ovary. *Reprod Domest Anim*. (2017) 52:130–9. doi: 10.1111/rda.12867
16. Milvae RA, Hansel W. Prostacyclin, prostaglandin F2α and progesterone production by bovine luteal cells during the estrous cycle. *Biol Reprod*. (1983) 29:1063–8. doi: 10.1095/biolreprod29.5.1063
17. Okuda K, Uenoyama Y, Berisha B, Lange IG, Taniguchi H, Kobayashi S, et al. Estradiol-17beta is produced in bovine corpus luteum. *Biol Reprod*. (2001) 65:1634–9. doi: 10.1095/biolreprod65.6.1634
18. Kobayashi S, Acosta TJ, Ozawa T, Hayashi K, Berisha B, Ohtani M, et al. Intraluteal release of angiotensin II and progesterone *in vivo* during corpora lutea development in the cow: effect of vasoactive peptides. *Biol Reprod*. (2002) 66:174–9. doi: 10.1095/biolreprod66.1.174
19. Schams D, Berisha B. Steroids as local regulators of ovarian activity in domestic animals. *Domest Anim Endocrinol*. (2002) 23:53–65. doi: 10.1016/S0739-7240(02)00145-5
20. Arosh JA, Banu SK, Chapdelaine P, Madore E, Sirois J, Fortier MA. Prostaglandin biosynthesis, transport, and signaling in corpus luteum: a basis for auto-regulation of luteal function. *Endocrinology*. (2004) 145:2551–60. doi: 10.1210/en.2003-1607
21. Bridges PJ, Fortune JE. Regulation, action and transport of prostaglandins during the periovulatory period in cattle. *Mol Cell Endocrinol*. (2007) 15:1–9. doi: 10.1016/j.mce.2006.08.002
22. Berisha B, Schams D, Rodler D, Sinowatz F, Pfaffl MW. Changes in the expression of prostaglandin family members in bovine corpus luteum during the estrous cycle and pregnancy. *Mol Reprod Dev*. (2018) 85:622–34. doi: 10.1002/mrd.22999
23. Wise T, Vernon MW, Maurer RR. Oxytocin, prostaglandins E and F, estradiol, progesterone, sodium and potassium in preovulatory bovine follicles, either developed normally or stimulated by FSH. *Theriogenology*. (1986) 26:757–78. doi: 10.1016/0093-691X(86)90006-3
24. Suchanek E, Simunic V, Macas E, Kopjar B, Grizelj V. Prostaglandin F2 alpha, progesterone and estradiol concentrations in human follicular fluid and their relation to success of *in vitro* fertilization. *Eur J Obstet Gynecol Reprod Biol*. (1988) 28:331–9. doi: 10.1016/0028-2243(88)90019-6
25. Komar CM, Berndtson AK, Evans AC, Fortune JE. Decline in circulating estradiol during the periovulatory period is correlated with decreases in estradiol and androgen, and in messenger RNA for p450 aromatase and p450 17alpha-hydroxylase, in bovine preovulatory follicles. *Biol Reprod*. (2001) 64:1797–805. doi: 10.1095/biolreprod64.6.1797
26. Hayashi KG, Berisha B, Matsui M, Schams D, Miyamoto A. Expression of mRNA for the angiopoietin-tie system in granulosa cells during follicular development in cows. *J Reprod Dev*. (2004) 50:477–80. doi: 10.1262/jrd.50.477
27. Berisha B, Steffl M, Welter H, Kliem H, Meyer HH, Schams D, et al. Effect of the luteinising hormone surge on regulation of vascular endothelial growth factor and extracellular matrix-degrading proteinases and their inhibitors in bovine follicles. *Reprod Fertil Dev*. (2008) 20:258–68. doi: 10.1071/RD07125
28. Berisha B, Schams D, Kosmann M, Amselgruber W, Einspanier R. Expression and localisation of vascular endothelial growth factor and basic fibroblast growth factor during the final growth of bovine ovarian follicles. *J Endocrinol*. (2000) 167:371–82. doi: 10.1677/joe.0.1670371
29. Schams D, Kosmann M, Berisha B, Amselgruber WM, Miyamoto A. Stimulatory and synergistic effects of luteinising hormone and insulin like growth factor 1 on the secretion of vascular endothelial growth factor and progesterone of cultured bovine granulosa cells. *Exp Clin Endocrinol Diabetes*. (2001) 109:155–62. doi: 10.1055/s-2001-14839
30. Hayashi KG, Acosta TJ, Tetsuka M, Berisha B, Matsui M, Schams D, et al. Involvement of angiopoietin-tie system in bovine follicular development and atresia: messenger RNA expression in theca interna and effect on steroid secretion. *Biol Reprod*. (2003) 69:2078–84. doi: 10.1095/biolreprod.103.017152
31. Trau HA, Brannstrom M, Curry TE Jr, Duffy DM. Prostaglandin E2 and vascular endothelial growth factor A mediate angiogenesis of human ovarian follicular endothelial cells. *Hum Reprod*. (2016) 31:436–44. doi: 10.1093/humrep/dev320
32. Bender HR, Trau HA, Duffy DM. Placental growth factor is required for ovulation, luteinization, and angiogenesis in primate ovulatory follicles. *Endocrinology*. (2018) 159:710–22. doi: 10.1210/en.2017-00739
33. Shrestha K, Meidan R. The cAMP-EPAC pathway mediates PGE2-induced FGF2 in bovine granulosa cells. *Endocrinology*. (2018) 159:3482–91. doi: 10.1210/en.2018-00527
34. Wiltbank MC, Ottobre JS. Regulation of intraluteal production of prostaglandins. *Reprod Biol Endocrinol*. (2003) 1:91. doi: 10.1186/1477-7827-1-91
35. Weems YS, Ma Y, Ford SP, Nett TM, Vann RC, Lewis AW, et al. Effects of intraluteal implants of prostaglandin E1 or E2 on angiogenic growth factors in luteal tissue of Angus and Brahman cows. *Theriogenology*. (2014) 82:1224–30. doi: 10.1016/j.theriogenology.2014.07.039
36. Pate JL, Toyokawa K, Walusimbi S, Brzezicka E. The interface of the immune and reproductive systems in the ovary: lessons learned from the corpus luteum of domestic animal models. *Am J Reprod Immunol*. (2010) 64:275–86. doi: 10.1111/j.1600-0897.2010.00906.x
37. Markosyan N, Duffy DM. Prostaglandin E2 acts via multiple receptors to regulate plasminogen-dependent proteolysis in the primate periovulatory follicle. *Endocrinology*. (2009) 150:435–44. doi: 10.1210/en.2008-0591
38. Harris SM, Aschenbach LC, Skinner SM, Dozier BL, Duffy DM. Prostaglandin E2 receptors are differentially expressed in subpopulations of granulosa cells from primate periovulatory follicles. *Biol Reprod*. (2011) 85:916–23. doi: 10.1095/biolreprod.111.091306

39. Kim SO, Duffy DM. Mapping PTGERs to the ovulatory follicle: regional responses to the ovulatory PGE2 Signal. *Biol Reprod*. (2016) 95:33. doi: 10.1095/biolreprod.116.140574
40. Berisha B, Steffl M, Amselgruber W, Schams D. Changes in fibroblast growth factor 2 and its receptors in bovine follicles before and after GnRH application and after ovulation. *Reproduction*. (2006) 131:319–29. doi: 10.1530/rep.1.00798
41. Kliem H, Welter H, Kraetzl WD, Steffl M, Meyer HH, Schams D, et al. Expression and localisation of extracellular matrix degrading proteases and their inhibitors during the oestrous cycle and after induced luteolysis in the bovine corpus luteum. *Reproduction*. (2007) 134:535–47. doi: 10.1530/REP-06-0172
42. Kirchner B, Paul V, Riedmaier I, Pfaffl MW. mRNA and microRNA purity and integrity: the key to success in expression profiling. *Methods Mol Biol*. (2014) 1160:43–53. doi: 10.1007/978-1-4939-0733-5_5
43. Mueller O, Lightfoot S, Schroeder A. *RNA Integrity Number (RIN) – Standardization of RNA Quality Control*. Agilent Application Notes Publication Number-5989-1165EN: 1-8. (2004). Available online at: https://www.agilent.com/cs/library/applications/5989-1165EN.pdf
44. Livak KJ, Schmittgen TD. Analysis of relative gene expression data using real-time quantitative PCR and the 2(-Delta Delta C(T)) Method. *Methods*. (2001) 25:402–8. doi: 10.1006/meth.2001.1262
45. Rodler D, Sinowatz F. Expression of prostaglandin-synthesizing enzymes (cyclooxygenase 1, cyclooxygenase 2) in the ovary of the quail (Coturnix japonica). *Folia Biol*. (2015) 61:125–33. doi: 10.1016/j.acthis.2014.11.005
46. Berisha B, Meyer HH, Schams D. Effect of prostaglandin F2 alpha on local luteotropic and angiogenic factors during induced functional luteolysis in the bovine corpus luteum. *Biol Reprod*. (2010) 82:940–7. doi: 10.1095/biolreprod.109.076752
47. Peters MW, Pursley JR, Smith GW. Inhibition of intrafollicular PGE2 synthesis and ovulation following ultrasound-mediated intrafollicular injection of the selective cyclooxygenase-2 inhibitor NS-398 in cattle. *J Anim Sci*. (2004) 82:1656–62. doi: 10.2527/2004.8261656x
48. Trau HA, Davis JS, Duffy DM. Angiogenesis in the primate ovulatory follicle is stimulated by luteinizing hormone via prostaglandin E2. *Biol Reprod*. (2015) 92:15. doi: 10.1095/biolreprod.114.123711
49. Schams D, Schallenberger E, Hoffmann B, Karg H. The oestrous cycle of the cow: hormonal parameters and time relationships concerning oestrus, ovulation, and electrical resistance of the vaginal mucus. *Acta Endocrinol*. (1977) 86:180–92. doi: 10.1530/acta.0.0860180
50. Curry TE Jr, Osteen KG. The matrix metalloproteinase system: changes, regulation, and impact throughout the ovarian and uterine reproductive cycle. *Endocr Rev*. (2003) 24:428–65. doi: 10.1210/er.2002-0005
51. Schams D, Steinberg V, Steffl M, Meyer HH, Berisha B. Expression and possible role of fibroblast growth factor family members in porcine antral follicles during final maturation. *Reproduction*. (2009) 138:141–9. doi: 10.1530/REP-09-0033
52. Schilffarth S, Antoni B, Schams D, Meyer HH, Berisha B. The expression of apelin and its receptor APJ during different physiological stages in the bovine ovary. *Int J Biol Sci*. (2009) 13:344–50. doi: 10.7150/ijbs.5.344
53. Shemesh M. Inhibitory action of follicular fluid on progesterone and prostaglandin synthesis in bovine follicles. *J Endocrinol*. (1979) 82:27–31. doi: 10.1677/joe.0.0820027
54. Murdoch WJ, Peterson TA, Van Kirk EA, Vincent DL, Inskeep EK. Interactive roles of progesterone, prostaglandins, and collagenase in the ovulatory mechanism of the ewe. *Biol Reprod*. (1986) 35:1187–94. doi: 10.1095/biolreprod35.5.1187
55. Armstrong DT. Prostaglandins and follicular functions. *J Reprod Fertil*. (1981) 62:283–91. doi: 10.1530/jrf.0.0620283
56. Murdoch WJ, Hansen TR, McPherson LA. A review: role of eicosanoids in vertebrate ovulation. *Prostaglandins*. (1993) 46:85–115. doi: 10.1016/0090-6980(93)90037-8
57. Markosyan N, Dozier BL, Lattanzio FA, Duffy DM. Primate granulosa cell response via prostaglandin E2 receptors increases late in the periovulatory interval. *Biol Reprod*. (2006) 75:868–76. doi: 10.1095/biolreprod.106.053769
58. De Silva M, Reeves JJ. Indomethacin inhibition of ovulation in the cow. *J Reprod Fertil*. (1985) 75:547–9. doi: 10.1530/jrf.0.0750547
59. Algire JE, Srikandakumar A, Guilbault LA, Downey BR. Preovulatory changes in follicular prostaglandins and their role in ovulation in cattle. *Can J Vet Res*. (1992) 56:67–9.
60. Sirois J. Induction of prostaglandin endoperoxide synthase-2 by human chorionic gonadotropin in bovine preovulatory follicles *in vivo*. *Endocrinology*. (1994) 135:841–8. doi: 10.1210/endo.135.3.8070377
61. Duffy DM, Dozier BL, Seachord CL. Prostaglandin dehydrogenase and prostaglandin levels in periovulatory follicles: implications for control of primate ovulation by prostaglandin E2. *J Clin Endocrinol Metab*. (2005) 90:1021–7. doi: 10.1210/jc.2004-1229
62. Duffy DM, Stouffer RL. The ovulatory gonadotrophin surge stimulates cyclooxygenase expression and prostaglandin production by the monkey follicle. *Mol Hum Reprod*. (2001) 7:731–9. doi: 10.1093/molehr/7.8.731
63. Shemesh M, Hansel W. Stimulation of prostaglandin synthesis in bovine ovarian tissue by arachidonic acid and luteinizing hormone. *Biol Reprod*. (1975) 13:448–52. doi: 10.1095/biolreprod13.4.448
64. Smith MF, McIntush EW, Ricke WA, Kojima FN, Smith GW. Regulation of ovarian extracellular matrix remodelling by metalloproteinases and their tissue inhibitors: effects on follicular development, ovulation and luteal function. *J Reprod Fertil Suppl*. (1999) 54:367–81.
65. Dow MP, Bakke LJ, Cassar CA, Peters MW, Pursley JR, Smith GW. Gonadotropin surge-induced upregulation of the plasminogen activators (tissue plasminogen activator and urokinase plasminogen activator) and the urokinase plasminogen activator receptor within bovine periovulatory follicular and luteal tissue. *Biol Reprod*. (2002) 66:1413–21. doi: 10.1095/biolreprod66.5.1413
66. Bakke LJ, Li Q, Cassar CA, Dow MP, Pursley JR, Smith GW. Gonadotropin surge-induced differential upregulation of collagenase-1 (MMP-1) and collagenase-3 (MMP-13) mRNA and protein in bovine preovulatory follicles. *Biol Reprod*. (2004) 71:605–12. doi: 10.1095/biolreprod.104.027185
67. Li Q, Bakke LJ, Pursley JR, Smith GW. Localization and temporal regulation of tissue inhibitors of metalloproteinases 3 and 4 in bovine preovulatory follicles. *Reproduction*. (2004) 128:555–64. doi: 10.1530/rep.1.00282
68. Curry TE Jr, Smith MF. Impact of extracellular matrix remodeling on ovulation and the folliculo-luteal transition. *Semin Reprod Med*. (2006) 24:228–41. doi: 10.1055/s-2006-948552
69. Duffy DM, Ko C, Jo M, Brannstrom M, Curry TE Jr. Ovulation: parallels with inflammatory processes. *Endocr Rev*. (2018). 40:369–416. doi: 10.1210/er.2018-00075
70. Berisha B, Welter H, Shimizu T, Miyamoto A, Meyer HH, Schams D. Expression of fibroblast growth factor 1 (FGF1) and FGF7 in mature follicles during the periovulatory period after GnRH in the cow. *J Reprod Dev*. (2006) 52:307–13. doi: 10.1262/jrd.17077
71. Kotwica J, Skarzynski D, Mlynarczuk J, Rekawiecki R. Role of prostaglandin E2 in basal and noradrenaline-induced progesterone secretion by the bovine corpus luteum. *Prostaglandins Other Lipid Mediat*. (2003) 70:351–9. doi: 10.1016/S0090-6980(02)00149-1
72. Bowolaksono A, Nishimura R, Hojo T, Sakumoto R, Acosta TJ, Okuda K. Anti-apoptotic roles of prostaglandin E2 and F2alpha in bovine luteal steroidogenic cells. *Biol Reprod*. (2008) 79:310–7. doi: 10.1095/biolreprod.107.066084
73. Miyamoto A, von Lützow H, Schams D. Acute actions of prostaglandin F2 alpha, E2, and I2 in microdialyzed bovine corpus luteum *in vitro*. *Biol Reprod*. (1993) 49:423–30. doi: 10.1095/biolreprod49.2.423
74. Okuda K, Uenoyama Y, Lee KW, Sakumoto R, Skarzynski DJ. Progesterone stimulation by prostaglandin F2alpha involves protein kinase C pathway in cultured bovine luteal cells. *J Reprod Dev*. (1998) 44:79–84. doi: 10.1262/jrd.44.79
75. Kawaguchi S, Bowolaksono A, Yoshioka S, Sakumoto R, Okuda K. Luteoprotective mechanisms of prostaglandin F2α stimulated by luteinizing hormone in the bovine corpus luteum. *J Reprod Dev*. (2013) 59:225–30. doi: 10.1262/jrd.2012-187
76. Kobayashi S, Miyamoto A, Berisha B, Schams D. Growth hormone, but not luteinizing hormone, acts with luteal peptides on prostaglandin F2alpha and progesterone secretion by bovine corpora lutea *in vitro*. *Prostaglandins Other Lipid Mediat*. (2001) 63:79–92. doi: 10.1016/S0090-6980(00)00099-X

77. Kobayashi S, Acosta TJ, Hayashi K, Berisha B, Ozawa T, Ohtani M, et al. Intraluteal release of prostaglandin F2α and E2 during corpora lutea development in the cow. *J Reprod Dev*. (2002) 48:583–90. doi: 10.1262/jrd.48.583
78. Kobayashi S, Berisha B, Amselgruber WM, Schams D, Miyamoto A. Production and localisation of angiotensin II in the bovine early corpus luteum: a possible interaction with luteal angiogenic factors and prostaglandin F2 alpha. *J Endocrinol*. (2001) 170:369–80. doi: 10.1677/joe.0.1700369
79. Gabler C, Plath-Gabler A, Killian GJ, Berisha B, Schams D. Expression pattern of fibroblast growth factor (FGF) and vascular endothelial growth factor (VEGF) system members in bovine corpus luteum endothelial cells during treatment with FGF-2, VEGF or oestradiol. *Reprod Domest Anim*. (2004) 39:321–7. doi: 10.1111/j.1439-0531.2004.00517.x
80. Grazul AT, Kirsch JD, Slanger WD, Marchello MJ, Redmer DA. Prostaglandin F2 alpha, oxytocin and progesterone secretion by bovine luteal cells at several stages of luteal development: effects of oxytocin, luteinizing hormone, prostaglandin F2 alpha and estradiol-17 beta. *Prostaglandins*. (1989) 38:307–18. doi: 10.1016/0090-6980(89)90135-4

Conflict of Interest Statement: The authors declare that the research was conducted in the absence of any commercial or financial relationships that could be construed as a potential conflict of interest.

frontiers in Endocrinology

ORIGINAL RESEARCH
published: 01 October 2019
doi: 10.3389/fendo.2019.00667

The Interaction Between Nodal, Hypoxia-Inducible Factor 1 Alpha, and Thrombospondin 1 Promotes Luteolysis in Equine Corpus Luteum

Edyta Walewska[1†], Karolina Wołodko[1†], Dariusz Skarzynski[1], Graça Ferreira-Dias[2] and António Galvão[1]*

[1] Department of Reproductive Immunology and Pathology, Institute of Animal Reproduction and Food Research, Polish Academy of Sciences, Olsztyn, Poland, [2] The Centre for Interdisciplinary Research in Animal Health, Faculty of Veterinary Medicine, University of Lisbon, Lisbon, Portugal

The regulation of corpus luteus (CL) luteolysis is a complex process involving a myriad of factors. Previously, we have shown the involvement of Nodal in functional luteolysis in mares. Presently, we ask the extent of which Nodal mediation of luteolysis is done through regulation of angioregression. We demonstrated the interaction between Nodal and hypoxia-inducible factor 1 α (HIF1α) and thrombospondin 1/thrombospondin receptor (TSP1/CD36) systems, could mediate angioregression during luteolysis. First, we demonstrated the inhibitory effect of Nodal on the vascular marker platelet/endothelial cell adhesion molecule 1 (CD31). Also, treatment of mid CL explants with vascular endothelial growth factor A (VEGFA) showed a trend on activin-like kinase 7 (Alk7) protein inhibition. Next, Nodal was also shown to activate HIF1α and *in vitro* culture of mid CL explants under decreased oxygen level promoted Nodal expression and SMAD family member 3 (Smad3) phosphorylation. In another experiment, the crosstalk between Nodal and TSP1/CD36 was investigated. Indeed, Nodal increased the expression of the anti-angiogenic TSP1 and its receptor CD36 in mid CL explants. Finally, the supportive effect of prostaglandin F2α (PGF2α) on TSP1/CD36 was blocked by SB431542 (SB), a pharmacological inhibitor of Nodal signaling. Thus, we evidenced for the first time the *in vitro* interaction between Nodal and both HIF1α and TSP1 systems, two conserved pathways previously shown to be involved in vascular regression during luteolysis. Considering the given increased expression of Nodal in mid CL and its role on functional luteolysis, the current results suggest the additional involvement of Nodal in angioregression during luteolysis in the mare, particularly in the activation of HIF1α and TSP1/CD36.

Keywords: Nodal, hypoxia inducible factor 1 alpha, thrombospondin 1, prostaglandin F2 alpha, corpus luteum, luteolysis

OPEN ACCESS

Edited by:
Lane K. Christenson, University of Kansas Medical Center, United States

Reviewed by:
Devoto Luigi, University of Chile, Chile
Mohamed Ayoub Abedal-Majed, University of Jordan, Jordan

***Correspondence:**
António Galvão
a.galvao@pan.olsztyn.pl

[†]These authors have contributed equally to this work

Specialty section:
This article was submitted to Reproduction, a section of the journal Frontiers in Endocrinology

Received: *29 May 2019*
Accepted: *16 September 2019*
Published: *01 October 2019*

Citation:
Walewska E, Wołodko K, Skarzynski D, Ferreira-Dias G and Galvão A (2019) The Interaction Between Nodal, Hypoxia-Inducible Factor 1 Alpha, and Thrombospondin 1 Promotes Luteolysis in Equine Corpus Luteum. Front. Endocrinol. 10:667. doi: 10.3389/fendo.2019.00667

INTRODUCTION

Molecular regulation of luteolysis is a very intricate process (1). Following the trigger of the uterine prostaglandin (PG) $F_{2\alpha}$, various local auto-, paracrine interactions are initiated (1, 2). Amongst others, the morphogens from transforming growth factor-β (TGF β) superfamily Nodal and TGFβ1 appear to be key for luteolysis in the mare (3).

Particularly Nodal, after binding to its type II receptor, the activin-A receptor 2B (ACVR2B), phosphorylates either activin-like kinase 4 (Alk4) or activin-like kinase 7 (Alk7), and subsequently mediates the phosphorylation of a SMAD family member 2 (Smad2) or Smad3, which finally translocates to the nucleus and regulates transcription (4). We have recently shown that Nodal enters a close feed-forward loop with $PGF_{2\alpha}$ toward progesterone (P4) downregulation and intraluteal $PGF_{2\alpha}$ amplification at the time of luteolysis initiation (2). Importantly, when we blocked Nodal and TGFβ1 signaling in $PGF_{2\alpha}$ treated cells we abolished its functional and structural luteolytic role (3). Furthermore, the regression of the corpus luteum (CL) is also associated with decreased blood flow (5, 6), which originates low oxygen (O_2) tension in the organ, an event named hypoxia (7). In response to hypoxic conditions, cells develop different strategies such as the transcription of hypoxia-inducible factor 1 (HIF1). Indeed, HIF1 consists of two subunits: (i) HIF1β, which is constitutively expressed in the nucleus; and (ii) HIF1α, which responds to different factors like cellular O_2 tension or other cytokines (7). Importantly, HIF1α has been linked to both functional and structural luteolysis (8, 9).

Additionally, a well-characterized anti-angiogenic factor is the thrombospondin 1 (TSP1) (10). Previous studies revealed the reciprocal inhibitory action between TSP1 and the proangiogenic fibroblast growth factor 2 (FGF) (11). Thrombospondin 1 belongs to a family of five conserved glycoproteins that are associated with cell-to-cell and cell-matrix interactions (11, 12). The ligand TSP1 and its receptor cluster of differentiation 36 (CD36) were shown to be widely expressed in the ovary, mainly in granulosa cells, large steroidogenic cells, and endothelial cells (13). Indeed, TSP1/CD36 system was shown to promote luteal endothelial cells apoptosis and in this way inhibit angiogenesis (14).

The present study investigates the putative involvement of Nodal in vascular regression in the mare. Taking advantage of an *in vitro* model with mid CL explants, presenting cell-to-cell interactions that are absent in luteal cell systems, we studied the crosstalk between Nodal signaling various vasoactive mediators. Thus, it was assessed: (i) the effect of Nodal on the marker cluster of differentiation 31 (CD31) protein, and, conversely, Nodal signaling protein components regulation by vascular endothelial factor A (VEGFA) and FGF; (ii) HIF1α profile in early, mid, and late CL and the effect of Nodal treatment on HIF1α expression in mid CL explants; (iii) the extent of which hypoxia activates Nodal signaling in mid CL explants; (iv) if the putative crosstalk between Nodal and HIF1α includes VEGFA activity; and (v) Nodal regulation of TSP1/CD36 system, as well as Nodal supportive role on $PGF_{2\alpha}$-mediated amplification of TSP1 and CD36 proteins.

MATERIALS AND METHODS

Equine Corpus Luteum Collection

All procedures for animal handling and tissue collection were approved by the Local Animal Care and Use Committee in Olsztyn, Poland (Agreement No. 51/2011). The mares used in this study (aged 3–8 years) were declared clinically healthy by the official government veterinary inspector and by individual historical records of animal health. After stunning, mares were euthanized, according to European Legislation concerning welfare aspects of animal stunning and euthanasia methods (EFSA, AHAW/04-027). Genitalia were collected *post-mortem* at the abattoir. As previously described, mare luteal samples were collected from April until the end of July and classified based on the morphological appearance of the CL, the presence of follicles in the ovary and plasma P4 concentration as: early luteal phase CL (early CL; presence of corpus hemorrhagicum, P4 < 1 ng/mL), mid luteal phase CL (mid CL; CL associated with follicles 15–20 mm in diameter, P4 > 6 ng/mL), and late luteal phase CL (late CL; CL associated with preovulatory follicle 30–35 mm in diameter, P4 between 1 and 2 ng/mL) (15). Immediately after collection, luteal samples were placed in specific solutions: (i) RNAlater (AM7020; Ambion, Carlsbad, USA) for gene ($n = 6$) and protein ($n = 6$) expression quantification; (ii) transport media M199 (M2154; Sigma-Aldrich, Saint Louis, USA) with 20 μg/mL gentamicin (G1397; Sigma-Aldrich) for *in vitro* studies.

An *in vitro* Culture for Mid CL Explants

Corpora lutea from mid luteal phase ($n = 6$) were washed in phosphate buffered saline (PBS) 0.1 M (pH = 7.4) supplemented with 20 μg/mL gentamicin and minced into small pieces of ∼1 mm^3 and 30 mg weight. Luteal explants (30 mg) were then cultured in 1 mL of Dulbecco's modified eagle's medium (DMEM) and F-12 Ham medium (D/F medium; D-8900; Sigma-Aldrich) containing 10% fetal bovine serum (FBS) (26140-079, ThermoFisher-Scientific, Waltham, USA), 20 μg/mL gentamicin and 250 μg/mL amphotericin (A2942, Sigma-Aldrich), in 24 well-culture plates, at 37°C in humidified atmosphere (5% CO_2, 95% air). After stabilization for 1 hour (h), culture media was changed with fresh one and mid CL explants cultured for 24 h and treated differently.

To assess the effect of Nodal treatment on proangiogenic factor (CD31), mid CL explants were treated as (i) no factor (negative control); (ii) Nodal (10 ng/mL, 3218-ND-025, R&D Systems, Minneapolis, USA); (iii) $PGF_{2\alpha}$ (10^{-7} M, P0424-1MG, Sigma Aldrich); and (iv) luteinizing hormone (LH) (10 ng/mL, L9773; Sigma). Next, in order to examine Nodal signaling responsiveness to proangiogenic factors, mid CL explants were exposed to (i) no factor (negative control); (ii) VEGFA (selected dose 25 ng/mL—doses tested 1, 10, and 25 ng/mL, V7259, Sigma); (iii) FGF (selected dose 10 ng/mL—doses tested 1, 10, and 25 ng/mL, SRP3040, Sigma); and (iv) LH (10 ng/mL). Subsequently, in order to study the crosstalk between Nodal and HIF1α, mid CL explants were treated with (i) no factor (negative control); (ii) Nodal (0.1, 1, and 10 ng/mL); (iii) $PGF_{2\alpha}$ (10^{-7} M); and (iv) LH (10 ng/mL). Additionally, we assessed VEGFA mRNA and protein levels. In another experiment, the crosstalk between Nodal and TSP1 system was studied, and TSP1 and CD36 expression analyzed after treating mid CL explants with (i) no factor (negative control); (ii) Nodal (10 ng/mL); (iii) $PGF_{2\alpha}$ (10^{-7} M); and (iv) LH (10 ng/mL). Finally, we confirmed the requirement of Nodal signaling during the $PGF_{2\alpha}$ upregulation of TSP1/CD36, as mid CL explants were treated with (i) no factor (negative control); (ii) SB431542

(SB) (10 μM, 1614/1, R&D Systems); (iii) $PGF_{2\alpha}$ (10^{-7} M); and (iv) simultaneously SB (10 μM) and $PGF_{2\alpha}$ (10^{-7} M). Both $PGF_{2\alpha}$ and LH treatments of mid CL explants represented internal controls. Mid CL explants after treatment were stored in RNAlater or Radioimmunoprecipitation Assay buffer (RIPA) buffer (89901, Life-Technologies, Carlsbad, USA) at −80°C until mRNA and protein expression analysis was performed.

An *in vitro* Culture for Mid CL Explants Under Hypoxia

In order to characterize Nodal signaling activation under hypoxic conditions, mid CL explants were cultured in normoxia (20% O_2) or hypoxia (5% O_2). After 12 h of tissue culture in normoxia, the medium was replaced and cultures were subjected for 24 h to either: (i) 20% O_2; (ii) or 5% O_2 at 37.5°C in a N_2-O_2-CO_2-regulated incubator (ESPEC Corp., Osaka, Japan; no. BNP- 110) as described before (8). Subsequently, mid CL explants were stored in RNAlater or RIPA at −80°C for mRNA and protein expression analysis.

The Assessment of Mid CL Explants Viability

Tissue viability was assessed with Alamar-Blue Assay (Alamar-Blue, Serotec, UK) (n = 4–6) (16). After *in vitro* culture, the Alamar-Blue reagent was added to 24 well-plates and incubated for 4 h in 37°C. Plates were read at 560 nm wavelength. Cell viability in control wells (without any reagent) was considered 100%.

Real-Time PCR

Total RNA was extracted from either fresh CL tissues (early CL, n = 6; mid CL, n = 6; late CL, n = 6) or after *in vitro* culture of mid CL explants (mid CL, n = 6) using Trizol (T9424, Sigma-Aldrich) (16). Briefly, the tissue was minced with homogenizer in Trizol, incubated for 5 min in room temperature (RT) followed by centrifugation at 9,400 g, 4°C for 15 min and collection of supernatant to the new tube. Then, solution was thoroughly mixed with 1-Bromo-3-chloropropan (BCP, BP151, Molecular Research Centre, Cincinnati, Ohio, USA), incubated in RT for 10 min and centrifuged (13,500 g, 15 min, 4°C). The aqueous phase was mixed with isopropanol (190764, Sigma Aldrich), incubated in −80°C for 60 min, centrifuged (20,000 g, 15 min, 4°C) followed by multiple washes with 75% ethanol. On the next day samples concentrations and purity were measured on NanoDrop and the ratio between absorbance at 230, 260, and 280 nm was calculated and confirmed good quality and quantity of extracted RNA. Reverse transcription was performed with 1.5 μg RNA according to the manufacturer's instructions (A15299; Applied-Biosystems, Warrington, UK). The cDNA was stored in −20°C until real-time Polymerase Chain Reaction (PCR) was performed. Then real-time PCR was performed in a 7900 Real-Time PCR System (Applied Biosystems) (primers in **Table 1**) as described before (16), using Maxima SYBR Green/ROX qPCR Master Mix (K0223, ThermoScientific). The primers were designed using Primer 3.0 v.0.4.0. software (17, 18), based on gene sequences in GeneBank (NCBI). All primers were synthesized by Sigma Aldrich and validated before running experimental samples. Two different primers concentration were tested (80 or 160 nM). The melting curves after each run were obtained by stepwise increases from 60 to 95°C, in order to ensure a single product amplification. Primer concentration was chosen based on the lowest cycle threshold value and the highest melting temperature (Tm) for the product. Primers were also tested for dimers formation. Target gene and a reference gene *β2 microglobulin (B2MG)* were run simultaneously. The total reaction volume was 12 μL, containing 4 μL cDNA (10 μg), 1 μL each forward and reverse primers (80 or 160 nM), and 6 μL SYBR Green PCR master mix. Real-time PCR was carried out as follows: initial denaturation (10 min at 95°C), followed by 45 cycles of denaturation (15 s at 95°C) and annealing (1 min at 60°C). After each PCR reaction, melting curves were obtained by stepwise increases in temperature from 60 to 95°C to ensure single product amplification. Real-time PCR results were analyzed with the Real-time PCR Miner algorithm (19).

Western Blot

Fresh CL tissue (early CL, n = 6; mid CL, n = 6; late CL, n = 6) and *in vitro* tissue explants (mid CL, n = 6) were disrupted by homogenization in RIPA (250 μL) containing protease inhibitor (P8340, Sigma-Aldrich), phospho-stop solution

TABLE 1 | Specific primers sequences used for quantitative real-time PCR.

Gene name	Gene symbol	GeneBank accession no.	Sequences 5′–3′	Length (base pair)
Cluster of differentiation 36	*CD36*	XM_001487907.1	For: AACCACACCGTCTCCTTCGT	107
			Rev: GCCGCTACAGCCAGATTGAG	
Hypoxia inducible factor 1α	*HIF1α*	XM_023627857.1	For: CCAAAAGCCGAAATCCCTTC	80
			Rev: CCAGCCCACGTCTTCTCCTA	
Thrombospondin 1	*TSP1*	XM_001503599.2	For: GCTCCAGCTCTACCAATGTCCT	91
			Rev: TTGTGGCCGATGTAGTTAGTGC	
Vascular endothelial growth factor A	*VEGFA*	NM_001081821	For: ATGCGGATCAAACCTCACCA	117
			Rev: AGGCCCACAGGGATTTTCTT	
β-2 microglobulin	*B2mg*	X69083	For: CGGGCTACTCTCCCTGACTG	92
			Rev: AACCGAAAGGTAAGAGACGAC	
			Rev: GGGACGAGGTTGTCCTGGTA	

TABLE 2 | Specification of antibodies used for western blot.

Antibody name and specificity	Cat no, company	RRID no.	Antibody dilution
Mouse monoclonal against HIF1α	ab16066, Abcam, UK	RRID:AB_302234	1:200
Mouse monoclonal against Nodal	ab55676, Abcam	RRID:AB_2151660	1:400
Mouse monoclonal against TSP1	ab1823, Abcam	RRID:AB_2201948	1:100
Rabbit polyclonal against Smad3	ab73942, Abcam	RRID:AB_1566742	1:500
Rabbit polyclonal against Smad3 Phosphorylated	ab51451, Abcam	RRID:AB_882595	1:1000
Rabbit polyclonal against CD31	ab28364, Abcam	RRID:AB_726362	1:200
Rabbit polyclonal against Alk7	ab71539, Abcam	RRID:AB_1267623	1:100
Rabbit polyclonal against VEGFAA	sc-152, Santa Cruz Biotechnology, Dallas, USA	RRID:AB_2212984	1:200
Goat polyclonal against CD36	sc-5522, Santa Cruz Bioetchnology	RRID:AB_638143	1:200
Mouse monoclonal against β-actin	A2228, Sigma Aldrich	RRID:AB_476697	1:10000

(88667, ThermoFisher) and phenylmethylsulfonyl fluoride (PMSF) (P7626, Sigma-Aldrich) at 4°C. Protein concentration was determined with bicinchoninic acid assay (BCA) (BCA1-1KT, Sigma-Aldrich). A total of 10–80 μg of protein was run on 6–12% (varying accordingly to each protein) polyacrylamide gel followed by transfer to nitrocellulose membranes. Then, membranes were incubated with primary antibodies (**Table 2**) at 4°C, overnight. Goat anti-mouse alkaline phosphatase conjugated antibodies (1:30,000, 31321, ThermoFisher), goat anti-rabbit alkaline phosphatase-conjugated antibodies (1:30,000, A3687, Sigma-Aldrich), and rabbit anti-goat alkaline phosphatase-conjugated antibodies (1:30,000, A4187, Sigma-Aldrich) were used as a secondary antibody. Immune complexes were visualized using alkaline phosphatase substrate. Blots were scanned in Molecular Imager VersaDoc MP 4000 System (BioRad, Hercules, California, USA) and specific bands quantified using ImageLab Software (BioRad). At last, band density for each of the target protein was normalized against β-actin.

Plasma Progesterone Analysis

Progesterone levels were determined as before (15). The antiserum was used at the final dilution of 1:100 000, and HRP-labeled P4 was used at the concentration of 1:75 000. The standard curve ranged from 0.39 to 100 ng/mL, and the concentration of P4 at 50% binding (ED50) was 4.3 ng/mL. Finally, intra- and interassay coefficients of variation were 5.8 and 8.5%, respectively.

Statistical Analysis

The data are shown as mean ± SEM of values obtained in separate experiments, each performed in triplicate. Statistical analysis was performed using GraphPad Prism 7.0. In all experiments, samples were tested for normality with the D'Agostino-Pearson omnibus normality test. The real-time PCR and western blot results obtained from studies on fresh CL tissue were analyzed using non-parametric one-way ANOVA Kruskal-Wallis followed by Dunn's multiple comparison test. The analysis of mRNA and protein expression from *in vitro* experiments was performed using non-parametric Friedman test with Dunn's multiple comparison test. The tissue viability was analyzed using Wilcoxon test (Graph Pad Software version7, San Diego, USA). Significance was defined as $p < 0.05$.

RESULTS

Nodal Downregulates the Vascular Marker CD31

We first asked if Nodal was able to modulate angiogenic factors expression, and confirmed the level of CD31 protein was significantly downregulated in *in vitro* culture of mid CL explants treated with Nodal ($n = 6$) (**Figure 1A**; $p < 0.05$). Conversely, when we treated mid CL explants with VEGFA, we found no changes in Nodal (**Figure 1B**) and Alk4 (**Figure 1C**), but a trend was visible on Alk7 expression inhibition (**Figure 1D**; $p = 0.06$). Finally, FGF did not affect Nodal or the receptors Alk4, Alk7 (**Figures 1B–D**).

Nodal Stimulates HIF1α and Responds to Oxygen Levels

In order to confirm the expression of HIF1α in equine CL, we performed real-time PCR and western blot in fresh CL samples from early, mid and late CL samples ($n = 6$ for each stage of luteal phase) isolated from cyclic animals. We found that transcription of *HIF1α* peaked in early and mid CL and decreased in late CL, whereas protein did not change significantly (**Figures 2A,B**; $p < 0.05$). Next, we investigated the direct interaction between Nodal and HIF1α *in vitro* and verified that Nodal (10 ng/mL) stimulated *HIF1α* mRNA and protein expression (**Figures 2C,D**; $p < 0.05$). Moreover, we plotted the protein levels of Nodal and its receptor Alk7 against HIF1α and found a similar signature throughout luteal phase, with a sharp raise from early CL to mid CL, and a slight drop in late CL (**Figure 2E**; $p < 0.01$, $p < 0.05$, respectively). We than tested these results manipulating the availability of O_2, and exposed the mid CL explants to different O_2 levels. We discovered that Nodal was actively upregulated and Smad3 was phosphorylated when the O_2 level decreased from 20 to 5% (**Figures 3A,B**; $p < 0.05$). Neither Nodal treatment nor O_2 level affected the viability of CL tissues (**Supplementary Figures 1A–C**). In the last part of the experiment we questioned if the stimulatory effect of Nodal on HIF1α affected its main target, the VEGFA. We found that

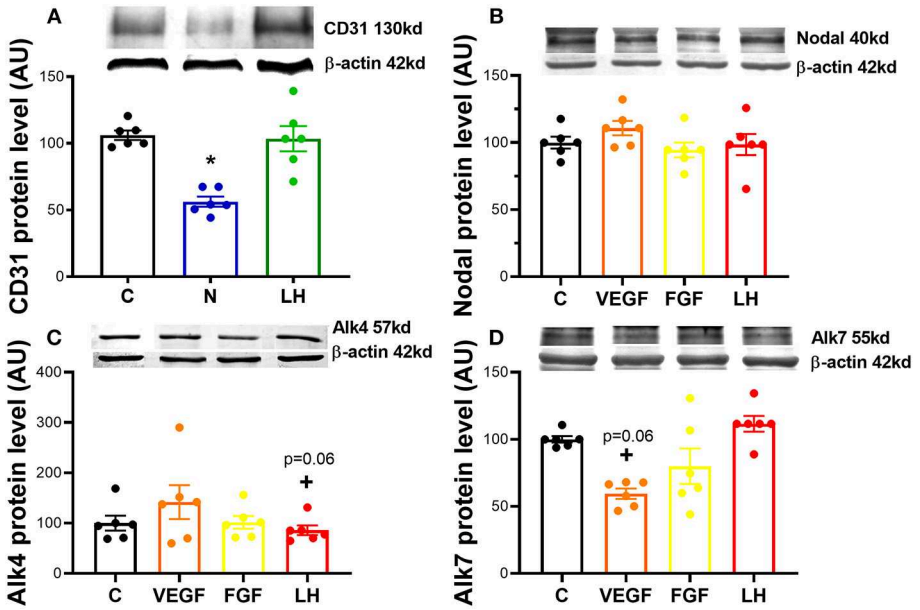

FIGURE 1 | Nodal interaction with proangiogenic factors. **(A)** Expression of proangiogenic cluster of differentiation 31 (CD31) protein after 24 h culture: (i) no factor (C, negative control); (ii) Nodal (10 ng/mL); and (iii) luteinizing hormone (LH, 10 ng/mL). Expression of angiogenic factors on **(B)** Nodal, **(C)** activin receptor (Alk) type 1B (Alk4) and **(D)** type 1C (Alk7) after 24 h culture with: (i) C (negative control); (ii) vascular endothelial growth factor A (VEGFA, 25 ng/mL); (iii) fibroblast growth factor (FGF, 10 ng/mL); (iv) luteinizing hormone (LH, 10 ng/mL). Protein expression determined by western blot, upper panel: representative immunoblot; lower panel: densitometry of protein expression relative to β-actin expression. ($n = 6$). Values are expressed as means ± SEM in arbitrary units (AU). Statistical differences marked with an asterisk (*$p < 0.05$).

lower doses of Nodal (0.1 ng/mL) were able to amplify *VEGFA* mRNA (**Figure 4A**; $p < 0.05$) and VEGFA protein was slightly increased ($p = 0.06$) for the treatments 0.1 and 1 ng/mL, but no effect after Nodal 10 ng/mL treatment (**Figure 4B**).

Nodal Crosstalk With TSP1 and CD36 in Mid CL Explants

In the last experiment we tested the extent of which TSP1 and CD36 are modulated by Nodal. We confirmed that mRNA and protein levels of TSP1 and CD36 were increased after Nodal treatment (**Figure 5A**, $p < 0.05$, **Figure 5B**, $p < 0.01$; **Figures 5C,D**, $p < 0.05$). Also, $PGF_{2\alpha}$ treatment upregulated mRNA and protein of TSP1 (**Figure 5A**, $p < 0.001$, **Figure 5B**, $p < 0.01$), and exclusively augmented CD36 protein (**Figure 5D**, $p < 0.05$). Furthermore, we tested the effect of loss of Nodal and TGFβ1 activity in $PGF_{2\alpha}$ action. When we blocked Nodal and TGFβ1 signaling pathway with SB, $PGF_{2\alpha}$ upregulation of TSP1 and CD36 was abolished (**Figures 5E,F**, $p < 0.05$).

DISCUSSION

In the present report we investigate the putative involvement of Nodal in angioregression during luteolysis in the mare. Facing the inexistence of a reliable *in vitro* system with equine luteal endothelial cells, we decided to use mid CL explants in order to instigate the extent of which Nodal luteolytic role involves the activation of vasoactive mediators. Indeed, our previous studies on luteal steroidogenic cells revealed that a great number of the endothelial cells are lost during cell isolation (15, 16). Overall, with mid CL explants we lose cell specificity on the response to our treatments, but we benefit from the contribution of the microvasculature to the response obtained. Thus, we studied the interaction between Nodal and HIF1α and TSP1/CD36 in mid CL explants, two vasoactive systems previously shown to play a role in CL luteolysis (9, 10).

We started the study assessing the effect of Nodal treatment on the endothelial cell marker CD31 and, vice-versa, testing the action of conventional proangiogenic factors like VEGFA and FGF on Nodal signaling regulation in mid CL explants. Members of TGFβ family can play either proangiogenic or antiangiogenic roles (20, 21). For instance, Geng and co-workers evidenced that TGFβ1 decreased VEGFA expression via Smad3P activation in colon cancer cells (22). Presently, we found that Nodal played an inhibitory role on CD31 protein, revealing for the first time the antiangiogenic properties of Nodal in the CL. Indeed, the interaction between TGFβ family and CD31 has been previously reported, particularly under the regulation of endothelial-to-mesenchymal transformation (23). Similar events appear to take place in the CL undergoing luteolysis, as the consistent proliferation of luteal fibroblast was shown to be mediated by TGFβ1 in bovine CL (24). Importantly, our recent studies also revealed the effect of TGFβ1 on equine functional and structural luteolysis (3, 25), reiterating the importance of the TGFβ ligands Nodal and TGFβ1 for equine CL regression. Next, we treated the mid CL explants with the proangiogenic factors VEGFA and

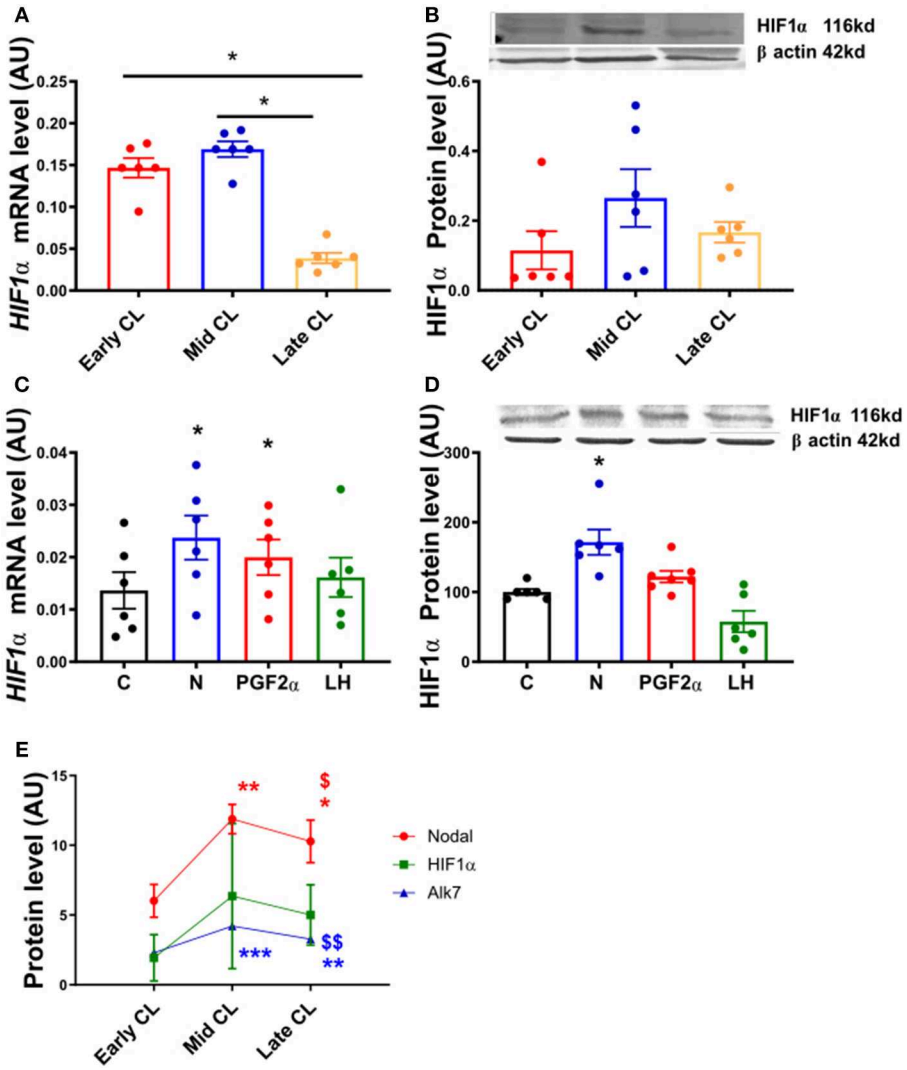

FIGURE 2 | HIF1α mRNA and protein expression in fresh CL explants and after *in vitro* culture of mid CL explants. **(A)** *Hypoxia inducible factor 1 α (HIF1α)* mRNA and **(B)** HIF1α protein expression in early, mid and late CL explants ($n = 6$). Expression of **(C)** *HIF1α* mRNA and **(D)** HIF1α protein after 24 h culture: (i) no factor (C, negative control); (ii) Nodal (10 ng/mL); (iii) prostaglandin F2α ($PGF_{2\alpha}$, 10^{-7} M); and (iv) luteinizing hormone (LH, 10 ng/mL) ($n = 6$). **(E)** Nodal, HIF1α, and Alk7 protein level in early, mid and late CL explants. mRNA expression determined by real-time PCR, expression relative to *β-2-microglobulin (B2MG)* expression. Protein expression determined by western blot, upper panel: representative immunoblot; lower panel: densitometry of protein expression relative to β-actin expression. Values are expressed as means ± SEM in arbitrary units (AU). Statistical differences are marked with asterisks (*$p < 0.05$). **(E)** *Significant differences with regard to early CL; $^{\$}$significant differences with regard to mid CL (one symbol, $p < 0.05$; two symbols $p < 0.01$).

FGF, and found that only VEGFA treatment showed a trend on Alk7 downregulation. Interestingly, Alk7 can be seen as an important intracellular mediator of Nodal signaling, once its protein expression profile mimics the one of Nodal throughout the luteal phase [(2); **Figure 2E**]. Overall, these results suggested the involvement of Nodal in angioregression and encouraged us to further instigate alleged antiangiogenic properties of Nodal during luteolysis in the mare.

Vascular regression is one of the main features of luteolysis and was primarily linked to $PGF_{2\alpha}$ activity (26). Consequently, O_2 supply in the CL is decreased both physiological luteolysis or after *in vivo* $PGF_{2\alpha}$ treatment (8, 27, 28). Indeed, it was shown that low O_2 concentration promoted functional luteolysis through inhibition of P4 synthesis, and induced apoptosis and structural regression (8, 9). Therefore, we interrogated if Nodal mediates HIF1α activity, and conversely if O_2 tension in the CL is able to modulate Nodal signaling expression. First, we characterized the expression of HIF1α in fresh cyclic CL. Despite increased *HIF1α* mRNA levels in early, and mid CL, no changes were found in HIF1α protein. Nonetheless, HIF1α was clearly expressed in mid CL, and a similar expression pattern was found for both Nodal and Alk7. This suggested the availability of these three proteins in mid CL, the time of luteolysis initiation (2, 6, 29). Furthermore, other studies reported Nodal responsiveness

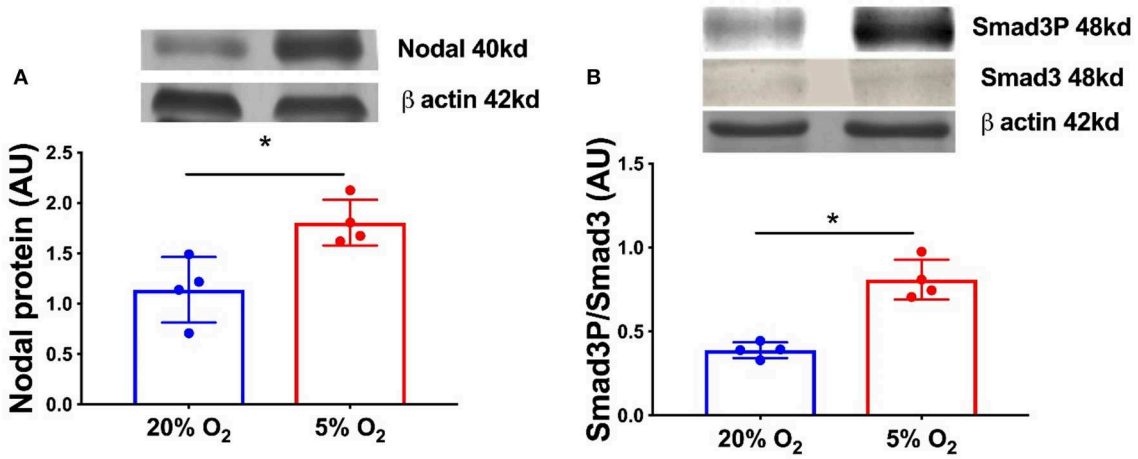

FIGURE 3 | Nodal signaling in mid CL explants cultured *in vitro* under hypoxia. Effect of hypoxia on **(A)** Nodal protein expression and **(B)** phosphorylation of Smad3 in mid CL explants cultured under 20% O_2 or 5% O_2 for 24 h ($n = 4$). Protein expression determined by western blot, upper panel: representative immunoblot; lower panel: densitometry of protein expression relative to β-actin expression. Values are expressed as means ± SEM in arbitrary units (AU). Statistical differences are marked with asterisks (*$p < 0.05$).

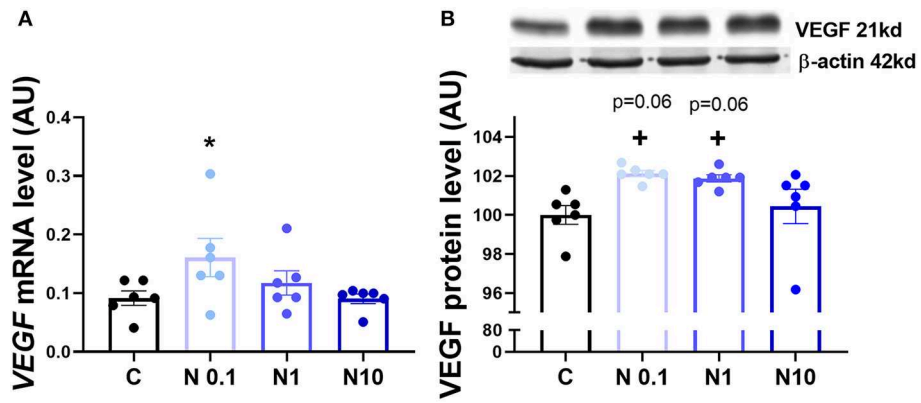

FIGURE 4 | VEGFA mRNA and protein expression after *in vitro* culture of mid CL explants. Expression of **(A)** *vascular endothelial growth factor A (VEGFA)* mRNA, **(B)** VEGFA protein after 24 h culture: (i) no factor (C, negative control); (ii) Nodal (0.1 ng/mL); (iii) Nodal (1 ng/mL); (iv) Nodal (10 ng/mL) ($n = 6$). mRNA expression determined by real-time PCR, expression relative to *β-2-microglobulin (B2MG)* expression. Protein expression determined by western blot, upper panel: representative immunoblot; lower panel: densitometry of protein expression relative to β-actin expression. Values are expressed as means ± SEM in arbitrary units (AU). Statistical differences are marked with asterisks (*$p < 0.05$).

to hypoxia, like in melanoma cancer cells (30) and breast cancer cells (31). Also, in glioma cells Nodal was shown to increase HIF1α activity (32). Accordingly, the incubation of our explants in hypoxia (5% O_2) significantly increased Nodal protein, as well as Smad3P levels. Additionally, after the *in vitro* treatment of mid CL explants with Nodal we verified the amplification of HIF1α protein. Taken together, these results suggested that Nodal not only activated HIF1α, but also was amplified in equine mid CL under low O_2 tension, which itself represents a feature of luteolysis (8, 27, 28).

A major target of HIF1α is the VEGFA (33), a proangiogenic protein which expression is downregulated in equine regressing CL (34). We challenged our hypothesis, and analyzed the expression of VEGFA in mid CL explants treated with Nodal. Indeed, we found a dose-dependent response to Nodal treatment, in which the lowest dose of Nodal (0.1 ng/mL) increased *VEGFA* mRNA and Nodal 0.1 and 1 ng/mL showed a tendency to upregulate VEGFA protein ($p = 0.06$). However, no effect was seen for Nodal 10 ng/mL, the luteolytic dose, on both mRNA and protein of VEGFA. Despite out of the scope of the present study, one should not exclude a putative proangiogenic action of Nodal in early CL. As mentioned above, TGFβ family members can play either angiogenic or anti-angiogenic roles (21, 22, 24), regarding the physiological context. In fact, Nodal was shown to promote vascularization in breast cancer cells (31), despite its role in CL establishment being unknown. Importantly, it remains clear that the activation of HIF1α by Nodal was done exclusively at 10 ng/mL (**Supplementary Figure 2**), the

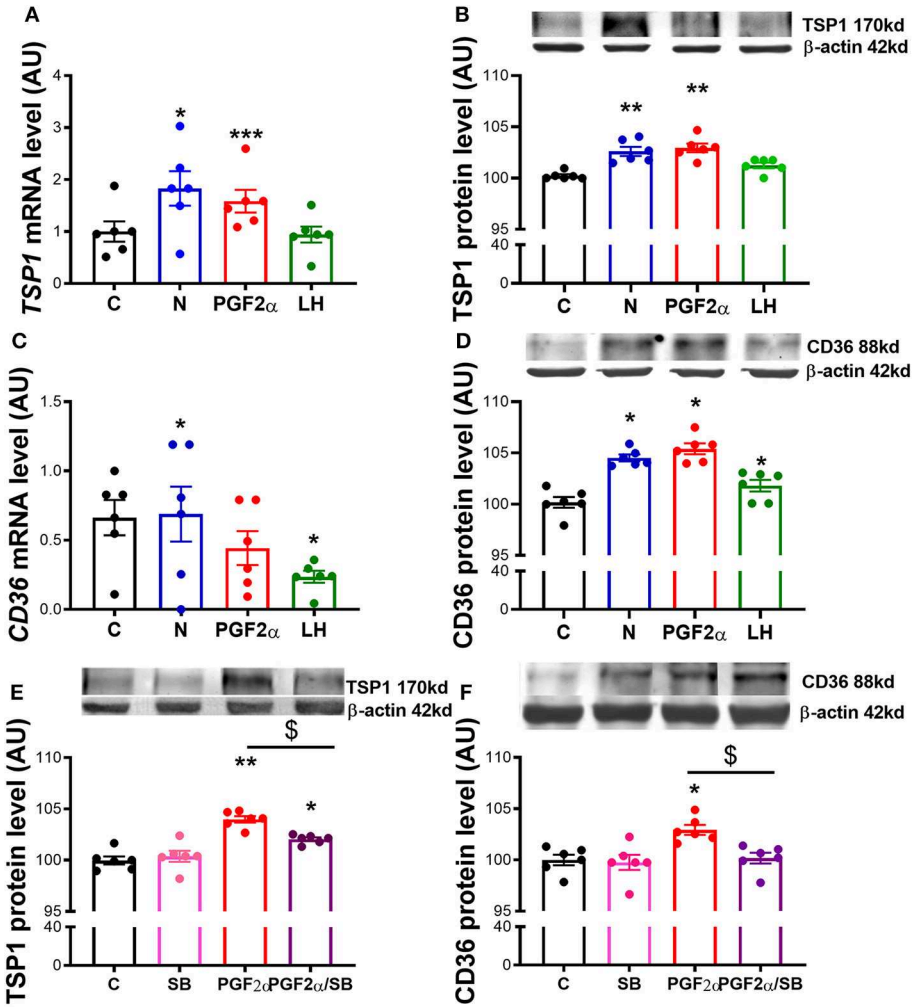

FIGURE 5 | Nodal crosstalk with TSP1 and CD36 in mid CL explants cultured *in vitro*. Expression of **(A)** *thrombospondin 1 (TSP1)* mRNA, **(B)** TSP1 protein, **(C)** *cluster of differentiation 36 (CD36)* mRNA and **(D)** CD36 protein after 24 h culture: (i) no factor (C, negative control); (ii) Nodal (10 ng/mL); (iii) prostaglandin F2α ($PGF_{2\alpha}$ 10^{-7} M); and (iv) luteinizing hormone (LH, 10 ng/mL) ($n = 6$). Expression of **(E)** TSP1 protein and **(F)** CD36 protein after 24 h culture: (i) no factor (C, negative control); (ii) SB (10 μM); (iii) $PGF_{2\alpha}$ (10^{-7} M); and (iv) simultaneously SB (10 μM) and $PGF_{2\alpha}$ (10^{-7} M) ($n = 6$). mRNA expression determined by real-time PCR, expression relative to *b-2-microglobulin (B2MG)* expression. Protein expression determined by western blot, upper panel: representative immunoblot; lower panel: densitometry of protein expression relative to β-actin expression. Values are expressed as means ± SEM in arbitrary units (AU). Statistical differences with regard to control are marked with asterisks (*$p < 0.05$; **$p < 0.01$; ***$p < 0.001$); Statistical differences with regard to $PGF_{2\alpha}$ are marked with dollars ($^{\$}p < 0.05$).

treatment dose previously shown to induce functional luteolysis (2). Also, Nodal protein expression profile in cycling CL denotes a sharp rise in mid CL, which supports the idea of higher levels of Nodal being required for mediation of its luteolytic actions. Thus, one may conclude the crosstalk between Nodal and HIF1α in mid CL during luteolysis activation does not imply VEGFA activity.

In the last experiment we explored the interaction between Nodal and another anti-angiogenic system, the TSP1/CD36 pathway (11). Importantly, TSP1 has been shown to be a downstream factor upregulated by HIF1α during hypoxia (35). Furthermore, the luteolytic role of TSP1 has been well-documented before (10). Indeed, we have previously demonstrated that tumor necrosis factor-α anti-angiogenic role comprised TSP1 and its receptor CD36 activation in equine luteal cells (16). Furthermore, in bovine CL, $PGF_{2\alpha}$ induced-luteolysis mediated the upregulation of TSP1 and CD36 (10, 13, 36, 37), a finding which is in agreement with our former results. In the present study, we reported the upregulation of TSP1 and CD36 by Nodal in *in vitro* explants of equine mid CL. These findings further uncovered the intricacies of molecular regulation of luteolysis. We can now consider the interactions in mid CL between O_2 levels, HIF1α activity, and Nodal signaling as a relevant step for luteolysis activation, which in turn supports the TSP1/CD36 anti-angiogenic activity.

Our last observation made evident the importance of Nodal and TGFβ1 signaling components on $PGF_{2\alpha}$ upregulation of TSP1 and CD36 proteins. In the present study, we used both $PGF_{2\alpha}$ and LH treatments as a positive controls for our culture

system. Expectedly, $PGF_{2\alpha}$ amplified both TSP1 mRNA and protein and CD36 protein, as seen before in bovine CL (10, 13, 36, 37). However, no changes were seen on *CD36* mRNA. The absence of agreement between CD36 mRNA and protein level can be eventually linked to mRNA half-life, which can be shorter than 24 h, or post-translational processing of the RNA (38, 39). Conversely, when we pharmacologically blocked Nodal and TGFβ1 receptor Alk4, Alk5, and Alk7 with SB, the effect of $PGF_{2\alpha}$ was abolished. Our previous studies on functional luteolysis and P4 inhibition have made clear the supportive role of Nodal on $PGF_{2\alpha}$-induced functional luteolysis (2). Presently, we confirmed also that $PGF_{2\alpha}$ luteolytic amplification of TSP1/CD36 requires Nodal and TGFβ1 active signaling. This definitely highlights the prominent role of Nodal in the luteolytic cascade.

During luteolysis, $PGF_{2\alpha}$ orchestrates the interactions between TSP1 and TGFβ1 (10). Our previous results demonstrated the importance of the crosstalk between $PGF_{2\alpha}$ and Nodal/ TGFβ1 (2, 3). Furthermore, the link between the main luteolysin and HIF1α was also shown to mediate functional and structural regression of the CL (8). Thus, our present findings invite us to propose a luteolytic network, in which under the regulatory action of $PGF_{2\alpha}$, Nodal acts on two important anti-angiogenic systems, the HIF1α and TSP1/CD36, to support vascular regression during CL regression. Furthermore, taking into consideration the previously documented involvement in functional luteolysis (2), we may now consider too the involvement of Nodal in the modulation of anti-angiogenic factors during luteolysis in mares. To conclude, we made an evidence for the possible interaction between Nodal and HIF1α, as well as Nodal signaling sensitivity to hypoxia in the CL. Additionally, Nodal not only upregulated TSP1/CD36 system, but was also shown to be required for $PGF_{2\alpha}$-induced upregulation of TSP1 and CD36 in equine CL. These results suggest the involvement of Nodal in angioregression during luteolysis in the mare and deserve being further studied.

DATA AVAILABILITY STATEMENT

The datasets generated for this study are available on request to the corresponding author.

ETHICS STATEMENT

The animal study was reviewed and approved by Local Animal Care and Use Committee in Olsztyn, Poland (Agreement No. 51/2011).

AUTHOR CONTRIBUTIONS

EW and KW: conception and design, acquisition of data, analysis and interpretation of data, and drafting and revising the article. DS and GF-D: analysis and interpretation of data and drafting or revising the article. AG: conception and design, analysis and interpretation of data, and drafting and revising the article.

FUNDING

Work supported by Program Iuwentus Plus (IP2014011373)—Polish Ministry of Science and Higher Education awarded to AG. Processing charge covered by the KNOW Consortium: Healthy Animal—Safe Food (Ministry of Sciences and Higher Education; Dec: 05-1/KNOW2/2015).

SUPPLEMENTARY MATERIAL

The Supplementary Material for this article can be found online at: https://www.frontiersin.org/articles/10.3389/fendo.2019.00667/full#supplementary-material

REFERENCES

1. Galvão AM, Ferreira-Dias G, Skarzynski DJ. Cytokines and angiogenesis in the corpus luteum. *Mediators Inflamm.* (2013) 2013:420186. doi: 10.1155/2013/420186
2. Galvão A, Skarzynski D, Ferreira-Dias G. Nodal promotes functional luteolysis via down-regulation of progesterone and prostaglandins E2 and promotion of PGF2α synthetic pathways in mare corpus luteum. *Endocrinology.* (2016) 157:858–71. doi: 10.1210/en.2015-1362
3. Galvão A, Wolodko K, Rosa M, Skarzynski D. Cytokine TGFB1 modulates *in vitro* secretory activity and viability of equine luteal cells. *Cytokine.* (2018) 110:316–27. doi: 10.1016/j.cyto.2018.03.038
4. Schier AF. Nodal signaling in vertebrate development. *Annu Rev Cell Dev Biol.* (2003) 19:589–621. doi: 10.1146/annurev.cellbio.19.041603.094522
5. Ginther OJ, Gastal EL, Gastal MO, Utt MD, Beg MA. Luteal blood flow and progesterone production in mares. *Anim Reprod Sci.* (2007) 99:213–20. doi: 10.1016/j.anireprosci.2006.05.018
6. Meidan R, Girsh E, Mamluk R, Farberov S. Chapter 9: Luteolysis in ruminants: past concepts, new insights, and persisting challenges. In: *The Life Cycle of the Corpus Luteum*. Jerusalem: Springer Nture Inc. (2017). p. 159–83. doi: 10.1007/978-3-319-43238-0_9
7. Wang GL, Semenza GL. Purification and characterization of Hypoxia-inducible Factor 1. *J Biol Chem.* (1995) 270:1230–7. doi: 10.1074/jbc.270.3.1230
8. Nishimura R, Sakumoto R, Tatsukawa Y, Acosta TJ, Okuda K. Oxygen concentration is an important factor for modulating progesterone synthesis in bovine corpus luteum. *Endocrinology.* (2006) 147:4273–80. doi: 10.1210/en.2005-1611
9. Nishimura R, Komiyama J, Tasaki Y, Acosta TJ, Okuda K. Hypoxia promotes luteal cell death in bovine corpus luteum. *Biol Reprod.* (2008) 78:529–36. doi: 10.1095/biolreprod.107.063370
10. Meidan R, Farberov S, Basavaraja R. Thrombospondin-1 at the crossroads of corpus luteum fate decision. *Reproduction.* (2018) 157:R73–83. doi: 10.1530/REP-18-0530
11. Bornstein P. Thrombospondins function as regulators of angiogenesis. *J Cell Commun Signal.* (2009) 189–200. doi: 10.1007/s12079-009-0060-8
12. Bornstein P. Matricellular proteins Thrombospondins as matricellular modulators of cell function. *J Clin Invest.* (2001) 107:929–34. doi: 10.1172/JCI12749
13. Berisha B, Schams D, Rodler D, Sinowatz F, Pfaffl MW. Expression and localization of members of the thrombospondin family during final follicle maturation and corpus luteum formation and function in the bovine ovary. *J Reprod Dev.* (2016) 62:20–2. doi: 10.1262/jrd.2016-056

14. Jiménez B, Volpert OV, Crawford SE, Febbraio M, Silverstein RL, Bouck N. Signals leading to apoptosis-dependent inhibition of neovascularization by thrombospondin-1. *Nat Med.* (2000) 6:41–8. doi: 10.1038/71517
15. Galvao AM, Ramilo DW, Skarzynski DJ, Lukasik K, Tramontano A, Mollo A, et al. Is FAS/Fas ligand system involved in equine corpus luteum functional regression? *Biol Reprod.* (2010) 83:901–8. doi: 10.1095/biolreprod.110.084699
16. Galvão A, Henriques S, Pestka D, Lukasik K, Skarzynski D, Mateus LM, et al. Equine luteal function regulation may depend on the interaction between cytokines and vascular endothelial growth factor: an *in vitro* study. *Biol Reprod.* (2012) 86:187. doi: 10.1095/biolreprod.111.097147
17. Koressaar T, Remm M. Enhancements and modifications of primer design program Primer3. *Bioinformatics.* (2007) 23:1289–91. doi: 10.1093/bioinformatics/btm091
18. Untergasser A, Cutcutache I, Koressaar T, Ye J, Faircloth BC, Remm M, et al. Primer3—new capabilities and interfaces. *Nucleic Acids Res*. (2012) 40:e115. doi: 10.1093/nar/gks596
19. Liebert MA, Reaction RPC. Comprehensive algorithm for quantitative real-time polymerase chain reaction. *J Comput Biol*. (2005) 12:1047–64. doi: 10.1089/cmb.2005.12.1047
20. Pepper MS. Transforming growth factor-beta : vasculogenesis, angiogenesis, and vessel wall integrity. *Cytokine Growth Factor Rev.* (1997) 8:21–43. doi: 10.1016/S1359-6101(96)00048-2
21. Goumans M, Liu Z, Dijke P. TGF-β signaling in vascular biology and dysfunction. *Cell Res.* (2009) 19:116–27. doi: 10.1038/cr.2008.326
22. Geng L, Chaudhuri A, Talmon G, Wisecarver JL, Wang J. TGF-beta suppresses VEGFA-mediated angiogenesis in colon cancer metastasis. *PLoS ONE.* (2013) 8:e59918. doi: 10.1371/journal.pone.0059918
23. Wang Z, Tao J, Wang Z, Gu M. Transforming growth factor- b 1 induces endothelial-to-mesenchymal transition via Akt signaling pathway in renal transplant recipients with chronic allograft dysfunction. *Ann Transplant.* (2016) 21:775–83. doi: 10.12659/AOT.899931
24. Maroni D, Davis JS. TGFB1 disrupts the angiogenic potential of microvascular endothelial cells of the corpus luteum. *J Cell Sci.* (2011) 124(Pt 14):2501–10. doi: 10.1242/jcs.084558
25. Galvão AM, Skarzynski D, Ferreira-Dias G. Luteolysis and the auto-, paracrine role of cytokines from tumor necrosis factor α and transforming growth factor β superfamilies. *Vitam Horm.* (2018) 107:287–315. doi: 10.1016/bs.vh.2018.01.001
26. Mccracken JA, Custer EE, Schreiber DT, Tsang PCW, Keator CS, Arosh JA. Prostaglandins and other lipid mediators a new *in vivo* model for luteolysis using systemic pulsatile infusions of PGF 2α. *Prostaglandins Other Lipid Mediat*. (2012) 97:90–6. doi: 10.1016/j.prostaglandins.2012.01.004
27. Miyamoto A, Shirasuna K, Wijayagunawardane MPB. Blood flow : A key regulatory component of corpus luteum function in the cow. *Domest Anim Endocrinol.* (2005) 29:329–39. doi: 10.1016/j.domaniend.2005.03.011
28. Acosta TJ, Yoshizawa N, Ohtani M, Miyamoto A, De Fisiologia D, Veterinarias FDC, et al. Local changes in blood flow within the early and midcycle corpus luteum after prostaglandin F 2 α injection in the cow. *BMC Vet Res.* (2002) 658:651–8. doi: 10.1095/biolreprod66.3.651
29. Mondal M, Schilling B, Folger J, Steibel JP, Buchnick H, Zalman Y, et al. Deciphering the luteal transcriptome : potential mechanisms mediating stage-specific luteolytic response of the corpus luteum to prostaglandin F 2 alpha. *Physiol Genomics.* (2011) 43:447–56. doi: 10.1152/physiolgenomics.00155.2010
30. Li H, Chen J, Wang X, He MEI, Zhang Z, Cen Y. Nodal induced by hypoxia exposure contributes to dacarbazine resistance and the maintenance of stemness in melanoma cancer stem - like cells. *Oncol Rep.* (2018) 39:2855–64. doi: 10.3892/or.2018.6387
31. Quail DF, Taylor MJ, Walsh LA, Dieters-Castator D, Das P, Jewer M, et al. Low oxygen levels induce the expression of the embryonic morphogen Nodal. *Mol Biol Cell*. (2011) 22:4809–21. doi: 10.1091/mbc.e11-03-0263
32. Lai J, Jan H, Liu L, Lee C, Wang S, Hueng D, et al. Nodal regulates energy metabolism in glioma inducible factor 1 a. *Neuro Oncol.* (2013) 15:1330–41. doi: 10.1093/neuonc/not086
33. Forsythe JOA, Jiang B, Iyer N V, Agani F, Leung SW, Koos RD, et al. Activation of vascular endothelial growth factor gene transcription by hypoxia-inducible factor 1. *Mol Cell Biol*. (1996) 16:4604–13. doi: 10.1128/MCB.16.9.4604
34. Müller K, Ellenberger C, Schoon H. Research in Veterinary Science Histomorphological and immunohistochemical study of angiogenesis and angiogenic factors in the ovary of the mare. *Res Vet Sci*. (2009) 87:421–31. doi: 10.1016/j.rvsc.2009.04.011
35. Labrousse-Arias D, Castillo-Gonzalez R, Rogers NM, Torres-Capelli M, Barreira B, Aragones J, et al. HIF-2alpha-mediated induction of pulmonary thrombospondin-1 contributes to hypoxia-driven vascular remodelling and vasoconstriction. *Cardiovasc Res*. (2016) 109:115–30. doi: 10.1093/cvr/cvv243
36. Greenaway J, Gentry PA, Feige J, Lamarre J, Petrik JJ. Thrombospondin and vascular endothelial growth factor are cyclically expressed in an inverse pattern during bovine ovarian follicle development. *J Cell Physiol.* (2005) 1078:1071–8. doi: 10.1095/biolreprod.104.031120
37. Zalman Y, Klipper E, Farberov S, Mondal M, Wee G, Folger JK, et al. Regulation of angiogenesis-related prostaglandin f2alpha-induced genes in the bovine corpus luteum. *PLoS ONE.* (2012) 86:92. doi: 10.1095/biolreprod.111.095067
38. Alessio M, Monte L De, Scirea A, Gruarin P, Tandon NN, Sitia R. Synthesis, processing, and intracellular transport of CD36 during monocytic differentiation. *PLoS Comput Biol.* (1996) 271:1770–5. doi: 10.1074/jbc.271.3.1770
39. Luiken JJFP, Chanda D, Nabben M, Neumann D, Glatz JFC. Post-translational modifications of CD36 (SR-B2): implications for regulation of myocellular fatty acid uptake. *Mol Basis Dis.* (2016) 1862:2253–8. doi: 10.1016/j.bbadis.2016.09.004

Conflict of Interest: The authors declare that the research was conducted in the absence of any commercial or financial relationships that could be construed as a potential conflict of interest.

frontiers in Endocrinology

ORIGINAL RESEARCH
published: 04 October 2019
doi: 10.3389/fendo.2019.00662

Luteal Lipids Regulate Progesterone Production and May Modulate Immune Cell Function During the Estrous Cycle and Pregnancy

Camilla H. K. Hughes[1], *Remy Bosviel*[2], *John W. Newman*[2,3,4] *and Joy L. Pate*[1]*

[1] *Center for Reproductive Biology and Health, Department of Animal Sciences, Pennsylvania State University, State College, PA, United States,* [2] *West Coast Metabolomics Center, Genome Center, University of California, Davis, Davis, CA, United States,* [3] *Obesity and Metabolism Research Unit, USDA-ARS-Western Human Nutrition Research Center, Davis, CA, United States,* [4] *Department of Nutrition, University of California, Davis, Davis, CA, United States*

Although the corpus luteum (CL) contains high concentrations of lipid in the form of steroid hormone precursors and prostaglandins, little is known about the abundance or function of other luteal lipid mediators. To address this, 79 lipid mediators were measured in bovine CL, using ultra performance liquid chromatography-tandem mass spectrometry. CL from estrous cycle days 4, 11, and 18 were compared and, separately, CL from days 18 of the estrous cycle and pregnancy were compared. Twenty-three lipids increased as the estrous cycle progressed ($P < 0.05$), with nine increasing between days 4 and 11 and fourteen increasing between days 4 and 18. Overall, this indicated a general upregulation of lipid mediator synthesis as the estrous cycle progressed, including increases in oxylipins and endocannabinoids. Only 15-KETE was less abundant in the CL of early pregnancy ($P < 0.05$), with a tendency ($P < 0.10$) for four others to be less abundant. Notably, 15-KETE also increased between estrous cycle days 4 and 18. Ingenuity Pathway Analysis (IPA, Qiagen) indicated that functions associated with differentially abundant lipids during the estrous cycle included leukocyte activation, cell migration, and cell proliferation. To investigate changes in CL during maternal recognition of pregnancy, this lipid dataset was integrated with a published dataset from mRNA profiling during maternal recognition of pregnancy. This analysis indicated that lipids and mRNA that changed during maternal recognition of pregnancy may regulate some of the same functions, including immune cell chemotaxis and cell-cell communication. To assess effects of these lipid mediators, luteal cells were cultured with 5-KETE or 15-KETE. One ng/mL 5-KETE reduced luteal progesterone on day 1 of culture, only in the absence of luteinizing hormone (LH), while 1 ng/mL 15-KETE induced progesterone only in the presence of LH (10 ng/mL). On day 7 of culture, 0.1 ng/mL 15-KETE reduced prostaglandin (PG)F2A-induced inhibition of LH-stimulated progesterone production, while 1 ng/mL 15-KETE did not have this effect. Overall, these data suggest a role for lipid mediators during luteal development and early pregnancy, as regulators of steroidogenesis, immune cell activation and function, intracellular signaling, and cell survival and death.

Keywords: corpus luteum, metabolomics, lipoxygenase, immune cells, progesterone, pregnancy, cell proliferation

OPEN ACCESS

Edited by:
Artur Mayerhofer, Ludwig Maximilian University of Munich, Germany

Reviewed by:
Dariusz Jan Skarzynski, Institute of Animal Reproduction and Food Research (PAN), Poland
Cecily Vauna Bishop, Oregon Health & Science University, United States

***Correspondence:**
Joy L. Pate
jlp36@psu.edu

Specialty section:
This article was submitted to Reproduction, a section of the journal Frontiers in Endocrinology

Received: *26 June 2019*
Accepted: *12 September 2019*
Published: *04 October 2019*

Citation:
Hughes CHK, Bosviel R, Newman JW and Pate JL (2019) Luteal Lipids Regulate Progesterone Production and May Modulate Immune Cell Function During the Estrous Cycle and Pregnancy. Front. Endocrinol. 10:662. doi: 10.3389/fendo.2019.00662

INTRODUCTION

The corpus luteum (CL) originates from the ovulatory follicle and has an incredibly high steroidogenic output. Its primary steroid hormone product is progesterone, which is produced from cholesterol precursor and is the hormone that maintains pregnancy in all mammals, making the CL necessary to normal reproductive function. In the absence of a viable pregnancy, the bovine CL regresses rapidly, in response to prostaglandin (PG) F2A, ceasing progesterone production and allowing another ovulation to occur. Therefore, luteal rescue in the presence of a pregnancy is also imperative for reproduction. Many luteal functions and processes are conserved; therefore, an improved understanding of luteal function in the cow may be applied to our understanding women's health.

The CL is a site of bioactive lipid synthesis. It contains high concentrations of arachidonic acid (1) and luteal tissue uptake of arachidonic acid *in vitro* was greater than the uptake of this prostaglandin precursor in skeletal muscle or ovarian cortex (2). Free arachidonic acid was present in greater concentrations in the CL of the estrous cycle than in the CL of pregnancy on day 18 (1), perhaps providing precursor for the luteal synthesis of PGF2A that is required for luteal regression (3). Intraluteal synthesis of PGEs and prostacyclin and uterine synthesis of PGEs have both been implicated in luteal rescue during early pregnancy (4–7), although this mechanism is not entirely clear.

Although prostaglandin products of arachidonic acid have been studied extensively in the CL, functions of other intraluteal lipids are less well-understood. Arachidonate lipoxygenases may act upon arachidonic acid to form hydroxyeicosatetraenoic acids, lipoxins, and leukotrienes. Uterine infusion of a lipoxygenase inhibitor delayed return to estrous, implicating lipoxins in regulation of estrous cycle length (8) and perhaps in PGF2A synthesis and luteal function. Specific 5-lipoxygenase (ALOX5) products including lipoxins and leukotrienes also altered luteal function in *in vitro* assays. 5-HETE and leukotriene (LT) C4 both reduced progesterone production and 5-HETE also reduced prostacyclin, while LTC4 induced PGF2A. Conversely, LTB4 induced progesterone and PGE2 production in cultured luteal cells (8, 9). These data indicate that leukotrienes and lipoxins may be luteotropic or luteolytic, depending on the molecule, yet little is known about intraluteal concentrations of these lipids.

Fatty acid-derived mediators from other polyunsaturated fatty acids may also have important ovarian functions. Surprisingly, supplementation of fatty acids in the form of flaxseed to transition cows increased the diameter of the corpus luteum (10) and fatty acid supplementation to cows in the form of fish meal resulted in altered omega-3 fatty acid concentrations in plasma and decreased luteal sensitivity to PGF2A, perhaps through a mechanism involving lateral mobility of the prostaglandin F receptor in the cell membrane (11, 12). These data indicate that dietary fatty acid content may alter luteal function.

Despite data indicating an important functional role for bioactive lipids in luteal function, little is known about the patterns of abundance of these lipids in CL during luteal development, maintenance, and rescue, in any species. Therefore, the abundance of lipid mediators, including endocannabinoids and oxylipins from cyclooxygenase (COX), lipoxygenase (LOX), and cytochrome P450 (CYP)-dependent metabolism were profiled in the CL on days 4, 11, and 18 of the estrous cycle and on day 18 of pregnancy. The objectives of this study were to identify lipid mediators that regulate luteal function during these transitions, to integrate the lipid profile with a previously published mRNA profile of CL during maternal recognition of pregnancy, and to determine the effect of a subset of lipids on *in vitro*progesterone production.

METHODS

Animals and Tissue Collection

All procedures were approved by the Penn State University Institutional Animal Care and Use Committee or The Ohio State University Animal Care and Use Committee. Regularly cyclic cows were observed for behavioral signs of estrus and the day of standing estrus was assigned as day 0. For the targeted metabolomics experiment, sixteen dairy cows were used, with four cows/group in four groups. For cows assigned to the day 4 group, upon observation of estrus and a dominant follicle by ultrasound, cows were given an injection of GnRH (Factrel, 100 μg; Zoetis) in order to precisely time ovulation relative to time of collection for these early CL. Cows were slaughtered on day 4 following estrus. For samples collected later than day 4, precise synchrony of ovulation relative to CL collection was not necessary, so no GnRH was given, and CL were collected via colpotomy. For CL of pregnancy, cows were bred by artificial insemination and a uterine flush was performed immediately following CL collection and was examined for embryo fragments to confirm the presence of a viable pregnancy. For all samples, tissue was snap frozen in liquid nitrogen immediately following tissue collection and stored at −80°C thereafter. For *in vitro* experiments, three to five dairy cows were used in each group, CL were collected on day 10–12 of the estrous cycle, and each treatment was applied to cells from each cow. Number of animals per group for these experiments is stated in the figure legend.

Lipid Mediator Extraction and Analysis

Oxylipins and endocannabinoids were isolated using a Waters Ostro™ Sample Preparation Plate. Luteal samples were homogenized and 40 ± 8 mg were added to 2 mL polypropylene tubes spiked with a 5 μL antioxidant solution (0.2 mg/ml solution BHT/EDTA in 1:1 MeOH:water) and 10 μL 1,000 nM analytical deuterated surrogates as previously described (13, 14). Samples were then mixed with 35 μL methanol, 550 μL isopropanol w/10 mM ammonium formate, 1% formic acid and 100 μL water, and the tube was placed in a Geno/Grinder 2010 (SPEX SamplePrep) for 30 s and centrifuged at 10,000 × g for 5 min at room temperature. Supernatants were transferred into the Ostro plate wells and captured in glass inserts containing 10 μL of 20% glycerol in methanol by applying 15 mmHg of vacuum for 10 min. The eluent was dried under vacuum and reconstituted with 100 μL, 1:1 MeOH/ACN (v/v) containing 100 nM of 1-cyclohexyl ureido, 3-dodecanoic acid and 1-phenyl ureido, 3-hexanoic acid urea used as internal standards (gifts from Dr. B. D. Hammock, University of California, Davis).

The samples were then vortexed and filtered at 0.1 μm through PVDF membranes (Millipore) by centrifugation < 4,500 × g (rcf) for 3 min at 6°C. The filtrate was transferred to inserts in amber glass and stored at −20°C for <48 h before analysis by UPLC-MS/MS. Analytes in 5 μL extract aliquot were separated on a 2.1 × 150 mm, 1.7 μm Acquity BEH column (Waters) using published protocols for oxylipins and endocannabinoids (13, 15). All chromatographic and mass spectral acquisition parameters are provided in **Supplemental Tables 1–4**. Samples were held at 10°C. Separated residues were detected by negative mode electrospray ionization for oxylipins and positive mode electrospray ionization for endocannabinoids using multiple reaction monitoring on an API 6500 QTRAP (AB Sciex). Analytes were quantified using internal standard methods and 5- to 7-point calibration curves ($r^2 \geq 0.997$). Calibrants and internal standards were either synthesized [10,11-DHN, 10,11-DHHep, 10(11)-EpHep] or purchased from Cayman Chemical, Avanti Polar Lipids Inc., or Larodan Fine Lipids. Data was processed with AB Sciex MultiQuant version 3.0.2. The internal standards were used to quantify recovery of surrogate standards.

Cell Culture and Progesterone Enzyme-Linked Immunosorbent Assays

For all cell culture experiments, CL from days 10–12 were used. CL were dissociated as previously described (16) and cells were put into culture in serum-free Hams F12 medium supplemented as described previously (16). For progesterone production experiments, all treatments were initiated on day 0. For assessment of progesterone on day 1, medium was collected 18–22 h after cells were initially put into culture. For assessment of progesterone on day 7, medium was changed and fresh treatments were added on days 1, 3, and 5, and medium was collected and assayed for progesterone on day 7. 5-KETE and 15-KETE (Cayman Chemical) were dissolved in EtOH, which was added to medium at a final concentration of 0.0001 and 0.001% v/v, respectively, for 0.1 and 1 ng/mL treatments. Concentrations of lipids were based on tissue concentration of 5-KETE and 15-KETE and calculated using the equation used in Pate (17), with the lower concentration, 0.1 ng/mL, being approximately physiological. Additional treatments were luteinizing hormone (LH; NHPP; 10 ng/mL), PGF2A (Sigma; 10 ng/mL) and LH + PGF2A. Progesterone enzyme-linked immunosorbent assays (ELISA) were performed as previously described for culture medium samples (18), with the following modifications: samples and antibodies were diluted in a buffer of 0.04 M 3-(N-morpholino)propanesulfonic acid, 0.12 M NaCl, 0.01 M EDTA, 0.05% Tween 20, 0.005% chlorhexidine digluconate, and 0.1% gelatin. Antibodies were Goat Antimouse IgG Antibody (2 ug/mL; EMD Millipore) and Monoclonal Progesterone Antibody (57.8 ng/mL; East Coast Bio). Progesterone conjugate (East Coast Bio) was diluted 1:750. Functional range of the progesterone standard curve (Cayman Chemical) was 0.16–10 ng/mL and all samples were diluted so that they fit within the functional range of the assay.

Quantitative PCR

Luteal cells were allowed to adhere overnight, and on day 1, were treated with 0.1, 1, or 100 ng/mL of 5-KETE. 5-KETE was dissolved in ethanol, making final concentrations of ethanol 0.0001, 0.001, and 0.1% v/v, respectively. Cells were collected after 24 h of treatment. In another experiment, luteal cells were treated with 100 ng/mL of 5-KETE for 7 days prior to collection. Quantitative PCR (qPCR) was performed as described previously for cultured luteal cells (19), with the exception that RNA was isolated using the Qiagen RNeasy Plus Mini kit following instructions from the manufacturer.

Statistical and Pathway Analysis

All statistical analysis of targeted metabolomics data was performed using JMP Pro v 13.0 (SAS Institute). Although each experiment was analyzed separately, the same method of analysis was used for each. For each metabolite, normality was assessed using the Shapiro-Wilk test and a Box Cox transformation to obtain normal distributions when distributions that were not normal were encountered. Normal data were then assessed for outliers per treatment group ($N = 4$) using a 95% Dixon test. If detected, outliers were removed from the raw data, missing data was imputed per treatment group using the multivariate singular value decomposition method (20), and the Box Cox transformation was repeated. Students *t*-test or ANOVA with a Tukey *post-hoc* test were used to assess the effect of stage of cycle or pregnancy on lipid abundance for each lipid measured. In all cases, statistical significance was considered when $P < 0.05$. For the experiment comparing early pregnancy to the late estrous cycle, statistical tendencies ($P < 0.10$) were few and significant differences were even fewer. Because the small number of observations per group ($N = 4$/group) resulted in low power, values approaching significance were considered in pathway analyses, though this cutoff was only used for the latter experiment. False discovery rate-adjusted *P*-values (Padj) were also calculated (21) with a false discovery rate of 20%, and are available in **Tables 1**, **2**. However, these adjusted *P*-values were not used to select lipids used in pathway analysis, both because of the low power in this study and because this was a targeted metabolomics study, with relatively few molecules measured, as compared to an untargeted transcriptomics or proteomics study. Principal component analysis was used to determine whether differences among groups within an experiment allowed groups to be distinguished individually. Finally, to identify groups of lipids with similar patterns of expression, hierarchical cluster analysis was performed on lipids from the estrous cycle experiment only. Pathway analysis was conducted in Ingenuity Pathway Analysis (IPA; Qiagen). General lipid pathway information, including precursor, metabolism, and nomenclature information, was obtained from www.hmdb.ca and pubchem.ncbi.nlm.nih.gov. These data are available online as Study ST001245 at the Metabolomics Workbench (https://www.metabolomicsworkbench.org/).

The dataset of lipids that changed during maternal recognition of pregnancy was integrated with a transcriptomics dataset in which CL of the cycle and pregnancy were compared on day 17. In this study, $N = 4$/group and 140 differentially abundant

TABLE 1 | Differentially abundant lipids from CL of days 4, 11, and 18 of the estrous cycle.

Differ between	Cluster	Common name	Chemical Class	General pathway classification	Log2 fold change day 11 vs. 4	Log2 fold change, day 18 vs. 4	*P*-value	*P*-adj[a]
Days 4 and 11	5	5-KETE[b]	Ketone	Lipoxygenase/alcohol dehydrogenase	1.43	1.31	<0.001	0.001
		2-Arachidonylglycerol	Acylglycerol	Endocannabinoid	1.49	1.19	0.011	0.085
	6	19,20-DiHDPA	Vicinal diol	Cytochrome P450/epoxide hydrolase	2.98	4.14	0.006	0.085
		17,18-DiHETE	Vicinal diol	Cytochrome P450/epoxide hydrolase	2.56	3.39	0.009	0.085
		5,15-DiHETE	Non-vicinal diol	Lipoxygenase	3.42	6.30	0.021	0.105
	7	8(9)-EpETrE	Epoxide	Cytochrome P450	3.61	4.86	0.006	0.085
		Linoleic acid	PUFA	Fatty acid	0.93	1.41	0.007	0.085
		Adrenoylethanolamide	Acylethanolamide	Endocannabinoid	1.76	4.20	0.008	0.085
		9,12,13-TriHOME	Triol	Autooxidation	1.38	2.91	0.009	0.085
Days 4 and 18	7	11(12)-EpETrE	Epoxide	Cytochrome P450	2.94	4.29	0.010	0.085
		12(13)Ep-9-KODE[b]	Epoxy ketone	Lipoxygenase	1.56	3.06	0.010	0.085
		Dihomo-γ-Linolenoyl ethanolamide	Acylethanolamide	Endocannabinoid	1.06	3.97	0.012	0.085
		15,16-DiHODE	Vicinal diol	Cytochrome P450/epoxide hydrolase	2.15	3.86	0.016	0.105
		2-Linoleoylglycerol	Acylethanolamide	Endocannabinoid	1.52	3.35	0.018	0.105
		9(10)EpO (epoxystearate)	Epoxide	Cytochrome P450	1.18	2.53	0.023	0.105
		Stearoylethanolamide	Acylethanolamide	Endocannabinoid	1.72	2.06	0.028	0.105
		14(15)-EpETrE	Epoxide	Cytochrome P450	2.50	3.85	0.030	0.105
		15-KETE[b]	Ketone	Lipoxygenase/alcohol dehydrogenase	1.08	1.30	0.030	0.105
		Arachidonoylethanolamide	Acylethanolamide	Endocannabinoid	0.82	2.76	0.031	0.105
		9(10)-EpOME	Epoxide	Cytochrome P450	1.96	3.72	0.039	0.105
		6-trans-Leukotriene B4	Non-vicinal diol	Lipoxygenase	1.47	3.78	0.044	0.105
		8-HETE	Alcohol	Lipoxygenase	1.25	3.95	0.044	0.105
		Arachidonic acid	PUFA	Fatty acid	0.85	1.37	0.044	0.105

[a] *False Discovery Rate adjusted p-values, for false discovery rate of 20%.*

[b] *Indicates a lipid that was also differentially abundant during maternal recognition of pregnancy.*

mRNA were identified (19). These data are available online the NCBI's Gene Expression Omnibus [(22); https://www.ncbi.nlm.nih.gov/geo/], accession number GSE135342.

All statistical analysis for progesterone production and qPCR experiments were performed in SAS 9.4 (SAS Institute). Animal was included as an effect in the model, significance was considered at $P < 0.05$, and for the qPCR experiment, the reference gene, RPL19, was used as a covariate to account for differences in RNA loading and cDNA synthesis.

RESULTS

Lipid Mediator Profile

Seventy-nine lipids were measured in the CL, at four times, day 4, 11, 18 of the estrous cycle, and day 18 of pregnancy (**Supplemental Table 5**). For lipids measured during the estrous cycle, principle component analysis (PCA) was used to reduce the 79 variables into linearly uncorrelated principle components. Only component 1 meaningfully separated the data, explaining 54.4% of the variation in the dataset. The day 4 samples clustered separately from day 11 and 18 samples along component 1, though 1 day 4 sample was more similar to the day 11 and 18 samples than the other 3 day 4 samples. The day 11 and 18 samples did not cluster separately. Analysis of component 1 scores indicated that the day 4 samples differed from the day 11 and 18 groups, but those groups did not differ from each other (**Figure 1A**).

Samples from day 18 of the estrous cycle and pregnancy did not cluster separately when PCA was performed (data not shown). The majority of lipids were less abundant on day 18 of pregnancy than day 18 of the estrous cycle, although this

TABLE 2 | Differentially abundant lipids, and those that tended to be differentially abundant, in CL of day 18 of the estrous cycle and pregnancy.

Common name	Chemical class	General pathway classification	Log2 fold change (pregnant vs. cyclic)	*P*-value	*P*-adj[a]
15-KETE[b]	Ketone	Lipoxygenase/alcohol dehydrogenase	−1.57	<0.001	0.008
5-KETE[b]	Ketone	Lipoxygenase/alcohol dehydrogenase	−0.69	0.063	0.888
12(13)Ep-9-KODE[b]	Epoxy ketone	Lipoxygenase	−1.99	0.083	0.888
alpha-linolenoyl ethanolamide	Acylethanolamide	Endocannabinoid	−3.64	0.084	0.888
15(16)EpODE	Epoxy ketone	Cytochrome P450	−1.70	0.090	0.888

[a] *False Discovery Rate adjusted p-values, for false discovery rate of 20%.*
[b] *Indicates a lipid that was also differentially abundant during the estrous cycle.*

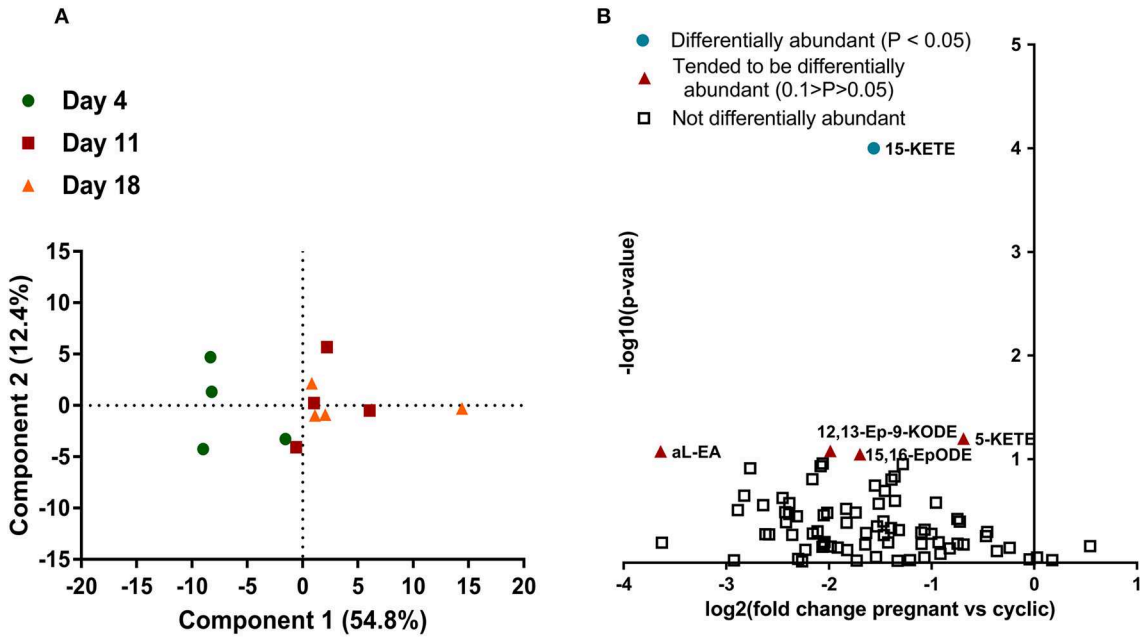

FIGURE 1 | Lipids in the CL during the estrous cycle and early pregnancy ($N = 4$/group). **(A)** Principle component analysis, with each point representing one sample from the lipid profiling experiment. Samples from day 4 are represented with a green circle, samples from day 11 are represented with a red square, and samples from day 18 are represented by an orange triangle. Distance apart on principle components 1 and 2 is a proxy for overall similarity in lipid abundance profile, with closer points being more alike. **(B)** Volcano plot of all lipids measured in the CL on day 18 of the estrous cycle and pregnancy. Each lipid is represented by a point, with the lipids that did not change represented with an open square, the lipids that tended to change represented by an orange triangle, and the lipids that changed ($P < 0.05$) represented by a teal circle. Magnitude of statistical significance is represented in the y-axis, while numerical fold change is represented on the x-axis, with lipids that were greater during the CL of the estrous cycle on the left and lipids that were greater in the CL of pregnancy on the right.

numerical change was small and only resulted in a few lipids that were significantly differentially abundant (**Figure 1B**).

Estrous Cycle-Associated Changes

Cluster analysis was used to determine which lipids had similar patterns of abundance during the estrous cycle, regardless of the detection of a measurable change (**Supplemental Table 5**). Seven clusters were generated, among which three clusters contained 73 of the 79 lipids measured, including all differentially abundant lipids (**Figure 2**). The remaining clusters contained 1 or 2 lipids each, none of which changed (**Supplemental Figure 1**). The cluster with the greatest number of lipids was cluster 7, a cluster in which lipids appeared to increase from day 4 through day 18.

Twenty-three lipids were differentially abundant as the estrous cycle progressed and all increased over time. Among these, fourteen were greater on day 18 than on day 4, with those on day 11 not differing from either of the other two groups. These lipids were all in cluster 7. For nine metabolites, abundances were greater on day 11 than on day 4 and remained greater on day 18. These lipids were in clusters 5, 6, and 7. Among the lipids that were differentially abundant during the estrous cycle, 20 were uniquely differentially abundant only in the estrous cycle, while three were also differentially abundant or tended to be differentially abundant during maternal recognition of pregnancy: 5-KETE, 15-KETE, and 12(13)Ep-9-KODE (**Table 1**). The lipids that changed during luteal development and maintenance may

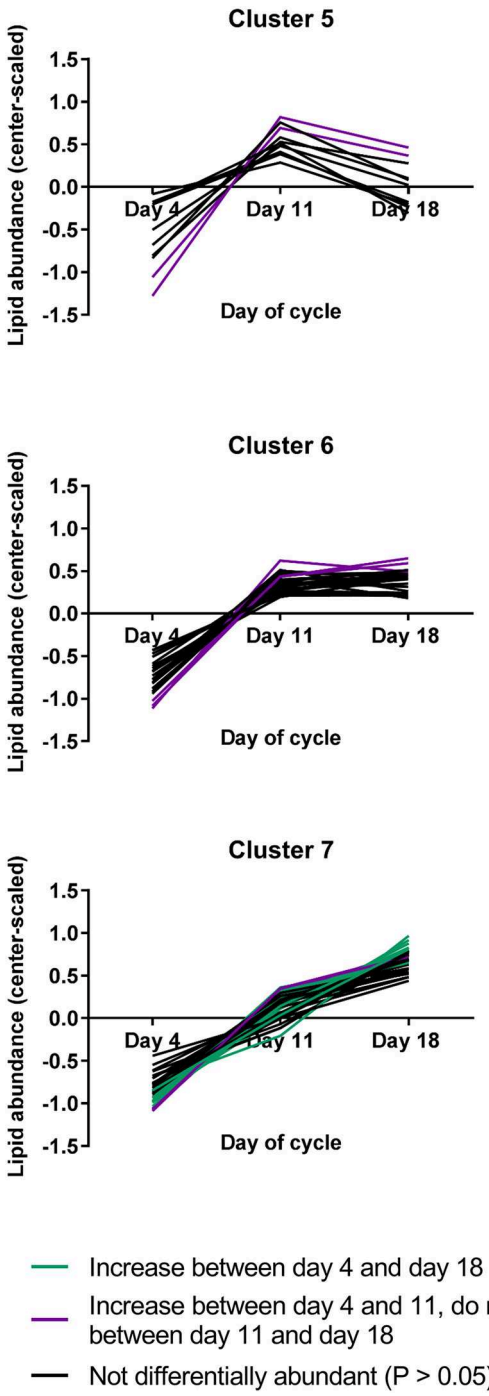

FIGURE 2 | The three lipid abundance clusters that included lipids that changed during the estrous cycle ($N = 4$/group). Lipids that appeared to change but were not statistically differentially abundant are represented by black lines, while lipids that changed between days 4 and 11 are represented by purple lines and lipids that changed between days 4 and 18 are represented by turquoise lines.

be considered in groups of lipids derived from common precursors or in groups synthesized by common enzymes or enzyme groups.

Concentrations of luteal fatty acid epoxides, bioactive products of cytochrome (CYP) P450 metabolism, were altered over the estrous cycle, as were their enzymatic hydrolysis products, the 1,2- or vicinal carbon diols (**Table 1**). Between days 4 and 11 increases were observed in the arachidonate-derived 8(9)-epoxyeicosatrienoic acid (EpETrE), diols from the docosahexenoate-derived diol, 19,20-dihydroxydocosapentenoic acid (DiHDPA), the putative oxidative stress marker 9,12,13-trihydroxyoctadecenoicacid (TriHOME) from linoleate, along with linoleate itself. Between days 4 and 18, 11(12)- and 14(15)-EpETrE concentrations increased, along with the linoleate-derived 9(10)-epoxyoctadecenoic acid (9(10)-EpOME), and the oleate-derived 9(10)-epoxyoctadecanoic acid (EpO). Alpha-linolenate-derived 15,16-dihydroxyoctadecadienoic acid (15,16-DiHODE) also increased at this time.

The two classical endocannabinoids, arachidonoylethanolamide (anandamide) and 2-arachidonylglycerol changed, with anandamide increasing between days 4 and 18, while 2-arachidonylglycerol increased between days 4 and 11. Several related N-acylethanolamides also changed during the luteal phase, including adrenoylethanolamide, dihomo- γ-linolenoyl ethanolamide, and stearoylethanolamide (**Table 1**).

The lipoxygenase pathway results in production of lipoxins and leukotrienes. 8-HETE increased between day 4 and 18, 5-HETE tended to increase between days 4 and 11, 18 ($P = 0.06$), and 15-HETE did not change. On the other hand, the alcohol dehydrogenase dependent ketone metabolites of these alcohols were strongly affected by estrous cycle stage. 5-KETE, derived from 5-HETE, changed between days 4 and 11, while 15-KETE, derived from 15-HETE, changed between days 4 and 18. The linoleate-derived 12(13)-epoxy-9-ketooctadecadienoicacide (12-(13)Ep-9-KODE) changed between days 4 and 18. Concentrations of 6-trans-leuktriene B4 (6-trans-LTB4), a reported decomposition product of the 5-lipoxygenase derived leukotriene C4, also increased between days 4 and 18 (**Table 1**, **Figure 3**).

Ingenuity Pathway Analysis (IPA; Qiagen) was used to determine functions in which differentially abundant lipids from the estrous cycle may be involved. One functional network, including the functions that were associated with the greatest number of lipids, indicated that six differentially abundant lipids may be regulators of immune cell activation, migration, and function (**Figure 4**).

Pregnancy-Associated Changes

During early pregnancy, one lipid mediator, 15-KETE, declined, while four others tended to decline, including 5-KETE, 12(13)Ep-9-KODE, 15(16)EpODE, and alpha-linolenoyl ethanolamide (**Figure 5**). 5-KETE, 15-KETE, 12(13)-Ep-9-KODE are all lipoxygenase-derived metabolites as described above. The alpha-linolenic acid metabolites 15(16)-EpODE from CYP metabolism, and alpha-linolenoyl ethanolamide, an endocannabinoid-like compound were also changed (**Table 2**, **Figure 5**).

In the comparison of CL from day 18 of the cycle and pregnancy, it is difficult to determine whether changes observed

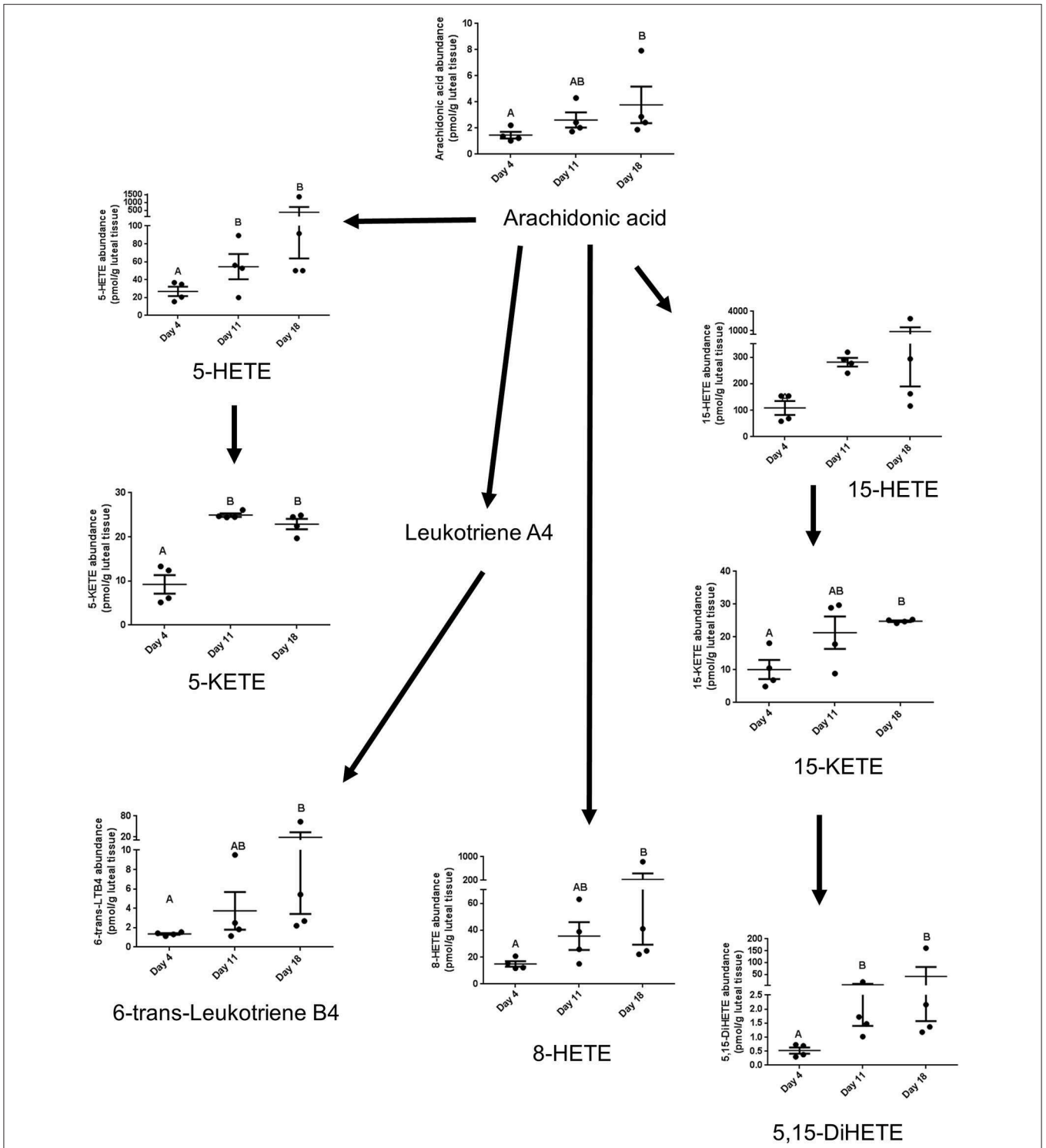

FIGURE 3 | The lipids that are components of the lipoxygenase pathway that were measured in this study, with arrows indicating synthesis relationships between lipids. 6-trans-LTB4 is also a reported decomposition product of the 5-lipoxygenase derived leukotriene C4.

result from exposure of the CL of the cycle to early pulses of PGF2A from the uterus or to conceptus signaling. Therefore, to determine in which group the lipid changed, day 11 CL were compared to CL of pregnancy, only for lipids that changed or tended to change during early pregnancy. Remarkably, 15-KETE and alpha-linolenoyl ethanolamide, which did not

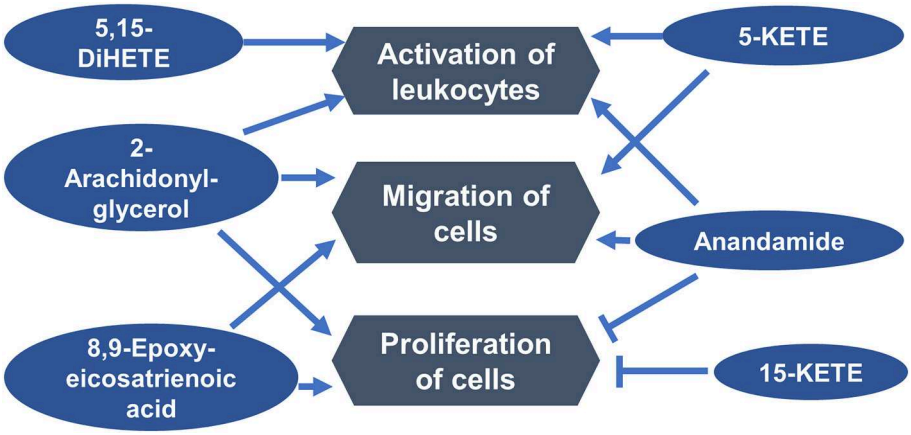

FIGURE 4 | Luteal metabolomics and pathway analysis during the estrous cycle. A functional network showing top functions in which differentially abundant lipids from the estrous cycle may be involved.

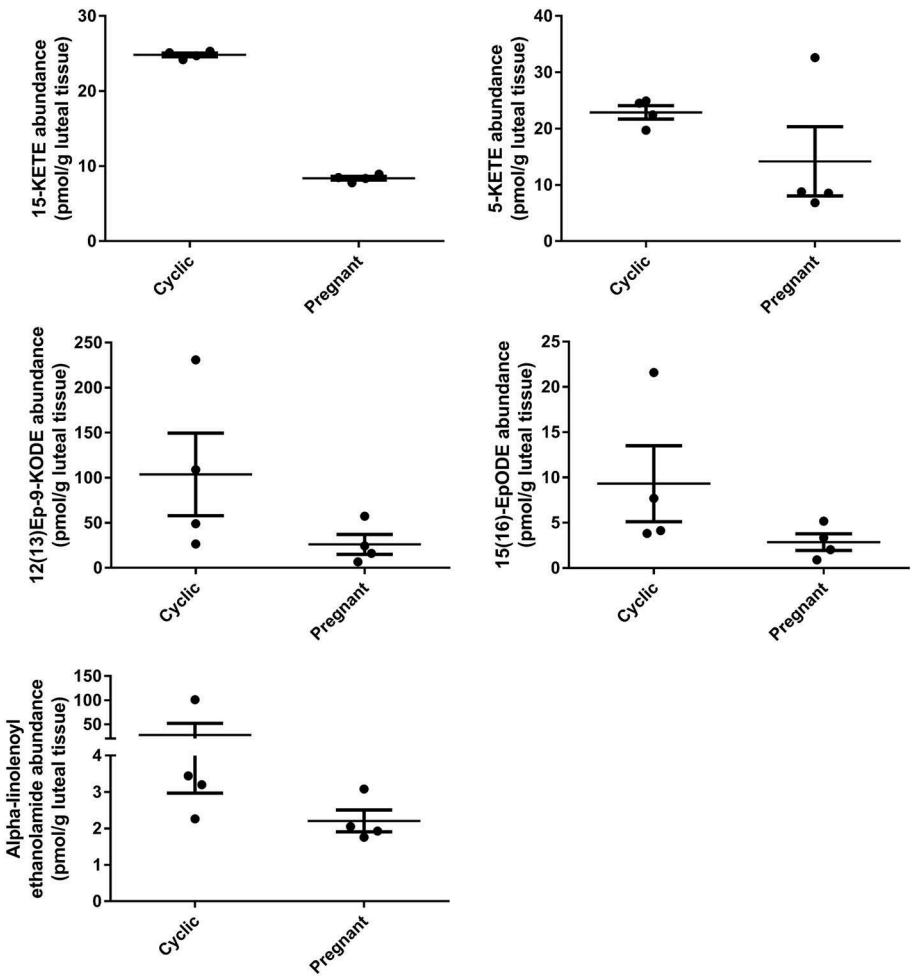

FIGURE 5 | Luteal metabolomics during maternal recognition of pregnancy ($N = 4$/group). Lipids that changed (15-KETE; $P < 0.05$) or tended to change ($P < 0.1$) during maternal recognition of pregnancy.

change between days 11 and 18, were both less in the CL of pregnancy than on day 11 ($P < 0.05$), indicating that they may be downregulated during early pregnancy. A very similar pattern was observed for 5-KETE, though 5-KETE did not differ from day 11 significantly ($P = 0.11$; **Figure 6**). For the other two lipids that tended to change during early pregnancy, no difference between day 11 and pregnancy could be detected.

To generate a more comprehensive profile of luteal changes during maternal recognition of pregnancy, mRNA that were differentially abundant during maternal recognition of pregnancy (19) were integrated with the lipids from this study. Analysis in MetaboAnalyst (23) and in Reactome (24) demonstrated no significantly modulated pathways that included both differentially abundant mRNA and differentially abundant lipids. This indicated no clear enzyme-lipid or lipid-receptor interaction as a result of integration. However, network analysis in IPA (Qiagen) indicated that networks "Lipid metabolism, molecular transport, and small molecule biochemistry" and "DNA replication, recombination and repair, cell death and survival, cellular function and maintenance" involved both differentially abundant lipids and mRNA. Further, these networks indicated that 5-KETE, which tended to be differentially abundant during maternal recognition of pregnancy, may be associated with ERK1/2 and P38 MAPK signaling. One network indicated that 5-KETE may regulate expression of MYC proto-oncogene (*MYC;* **Figure 7A**), which was greater in the CL of the estrous cycle relative to the CL of pregnancy. Therefore, cultured luteal cells were treated with 100 ng/mL 5-KETE for 24 h, to determine if 5-KETE regulates *MYC* in luteal cells (**Figure 7B**). Concentrations of 1 and 0.1 ng/mL for 24 h and 100 ng/mL for 7 days were also tested (data not shown). 5-KETE did not alter *MYC* in cultured luteal cells at any concentration. Functional analysis in IPA indicated that a decrease in 5-KETE, as well as sphingosine kinase 2 and retinoic acid receptor responder 2, may regulate a decrease in chemotaxis of phagocytes during early pregnancy (**Figure 7C**). Additionally, a number of differentially abundant mRNA and alpha-linolenoyl ethanolamide may together be regulators of cellular communication in the CL (**Figure 7D**).

Notably, the precursor of 15-KETE, 15-HETE, was not different during maternal recognition of pregnancy. In the transcriptomics dataset comparing CL of day 17 of the estrous cycle and pregnancy, the mRNA encoding the enzyme responsible for synthesis of 15-KETE, hydroxyprostaglandin dehydrogenase 15-(NAD; *HPGD*), was numerically less ($P = 0.11$) in the CL of pregnancy (**Figure 7E**).

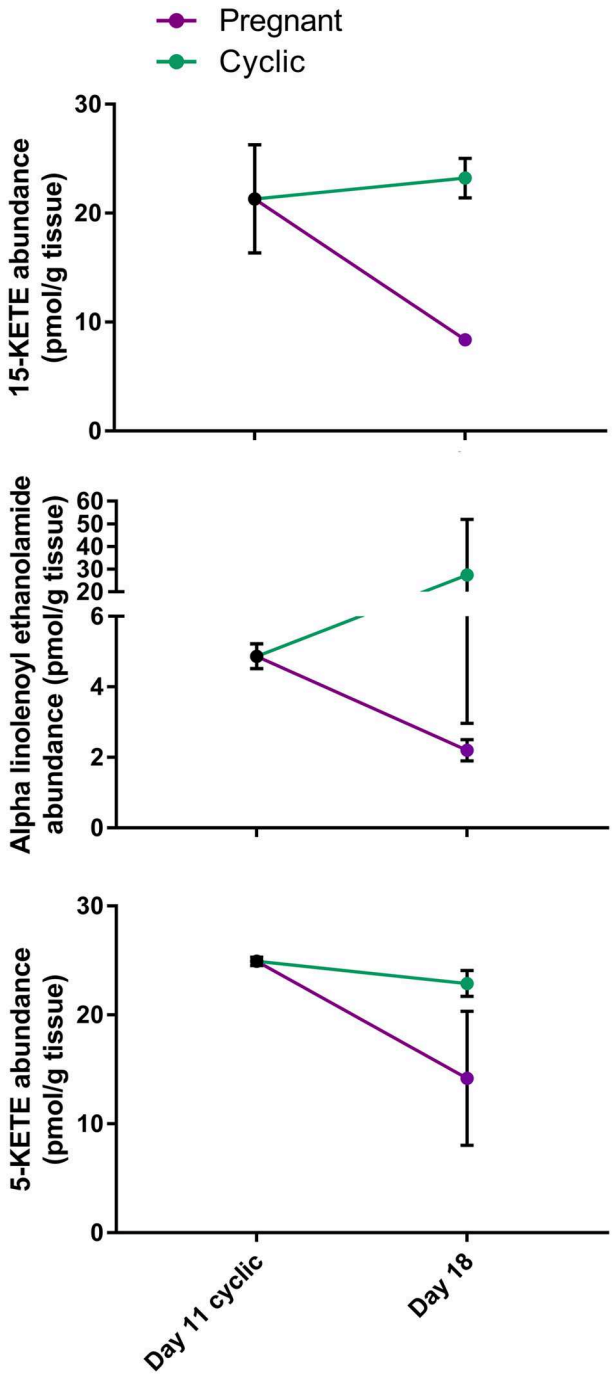

FIGURE 6 | Comparison of lipid abundance on day 11 of the estrous cycle and day 18 of pregnancy. Mean lipid abundance on day 11 is represented by a black circle, with day 18 of the estrous cycle represented in teal and day 18 of pregnancy represented in purple. 15-KETE and alpha-linolenoyl ethanolamide differed ($P < 0.05$) when day 11 of the estrous cycle and day 18 of pregnancy were compared, while 5-KETE demonstrated a similar numerical pattern ($P = 0.11$).

Luteal Progesterone Production in Response to KETEs

5-KETE and 15-KETE changed during the estrous cycle and during maternal recognition of pregnancy and were identified as likely key regulators of physiological functions in luteal cells. To assess effects of these two lipids, luteal cells were cultured with 5-KETE or 15-KETE. On day 1 of culture, 0.1 ng/mL 5-KETE did not alter progesterone in the absence or presence of LH (**Figure 8A**), while 1 ng/mL 5-KETE reduced luteal progesterone, but only in the absence of LH (**Figure 8B**). Conversely, while 0.1 ng/mL 15-KETE had no effect (**Figure 8C**),

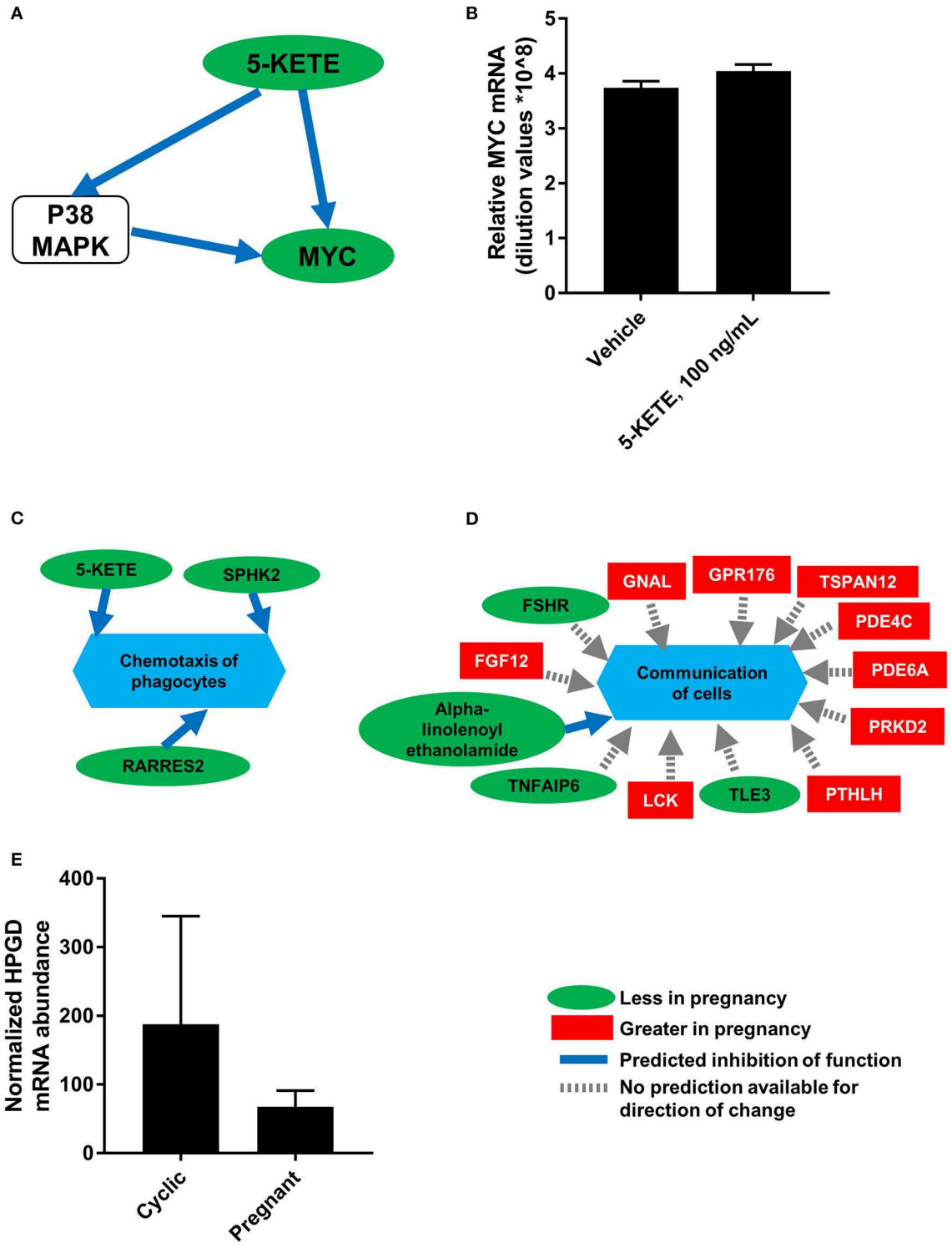

FIGURE 7 | Integration of luteal transcriptomics and metabolomics during maternal recognition of pregnancy [$N = 4$/group for metabolomics and transcriptomics; (19)]. **(A)** The network from IPA indicating a relationship between 5-KETE and MYC, with a green oval indicating less abundance in the CL of pregnancy, a blue arrow indicating predicted inhibition, and a white rounded square indicating a molecule that was not measured. **(B)** Effect of 5-KETE on MYC mRNA abundance in cultured luteal cells ($N = 3$). **(C,D)** Predicted functions of differentially abundant lipids and mRNA from maternal recognition of pregnancy, with a green oval indicating less abundance in the CL of pregnancy, a red square indicating greater abundance in the CL of pregnancy, a blue arrow indicating predicted inhibition, and a gray dashed arrow indicating that no prediction is available for direction of change. **(E)** HPGD abundance on day 17 of the estrous cycle and pregnancy, as measured by transcriptomics; $P = 0.11$.

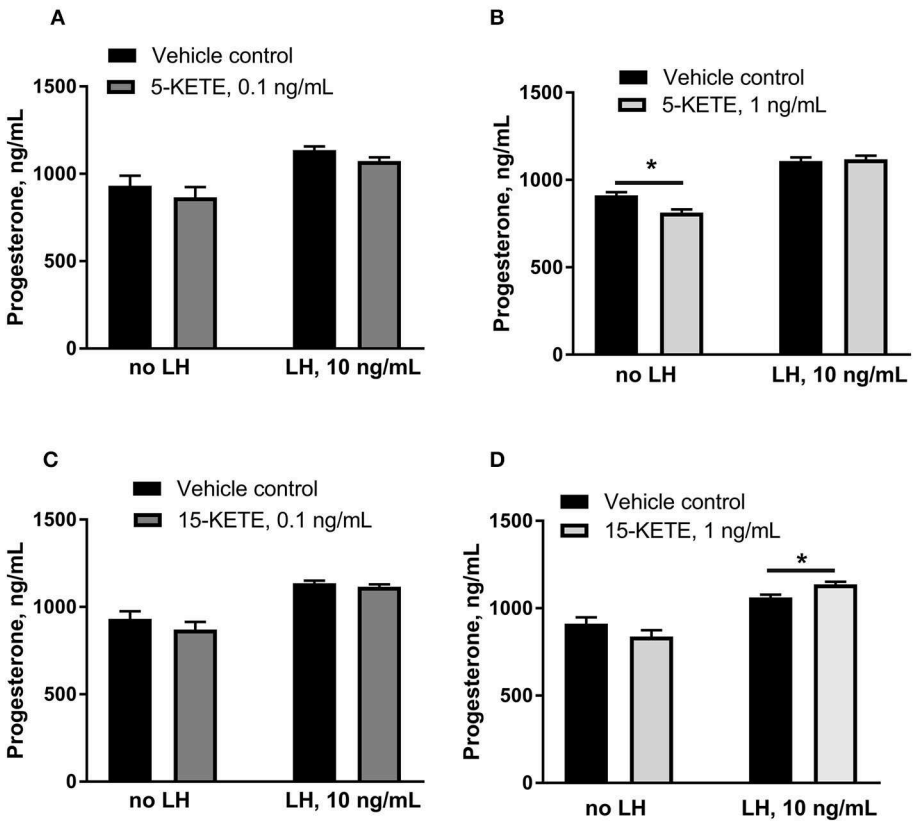

FIGURE 8 | Effect of 5-KETE and 15-KETE on progesterone production in cultured luteal cells on day 1 of culture. Significant differences ($P < 0.05$) between lipid-treated and vehicle control are denoted with a *. The effect of 0.1 ng/mL **(A)** or 1 ng/mL **(B)** 5-KETE and of 0.1 ng/mL **(C)** or 1 ng/mL **(D)** 15-KETE ($N = 5$ and $N = 4$ for without and with LH groups, respectively).

1 ng/mL 15-KETE induced progesterone only in the presence of LH (**Figure 8D**).

Effects of 5-KETE and 15-KETE were also assessed on day 7 of culture, in order to determine whether these lipids altered the PGF2A-induced inhibition of LH-response seen in luteal cells on day 7 of culture (25). 5-KETE did not have any effect on day 7, either alone or in combination with LH or LH + PGF2A (**Figures 9A,B**). However, 0.1 ng/mL 15-KETE reduced the degree to which PGF2A inhibited LH-stimulated progesterone production (**Figure 9C**), whereas 1 ng/mL 15-KETE did not have this effect (**Figure 9D**).

DISCUSSION

The objective of this study was to identify novel lipids that may be either supportive of or deleterious to luteal function and progesterone production. *In silico* pathway analysis indicated that differentially abundant lipids from the metabolic profiling experiment may regulate functions associated with luteal cell-immune cell communication and cell survival and proliferation. Moreover, this profiling allowed identification of lipid regulators of luteal progesterone production and response to PGF2A *in vitro*.

The endocannabinoid family of molecules activate the cannabinoid receptors, CNR1 and CNR2, both G protein-coupled receptors (26). These molecules are derived from membrane phospholipids and include both N-acylethanolamines (including the classical endocannabinoid, anandamide) and 2-acylglycerols (including the classical endocannabinoid, 2-arachidonylglycerol). Members of each of these classes increased over time during the cycle and one more tended to be less in the CL of pregnancy.

CL express the cannabinoid receptors CNR1 and CNR2, as well as fatty acid amide hydrolase (FAAH), which is responsible for the breakdown of endocannabinoids (27). *In vitro* activation of CNR1 or 2, or inhibition of FAAH, reduced progesterone, PGF2A, and PGE1 (28). Importantly, activation of CNR1 and 2 *in vivo* reduced plasma progesterone, luteal weight, and LH receptor abundance (29). Moreover, in CNR1 knockout mice, the luteolytic effect of LPS was lost, with no increase in luteal cyclooxygenase enzymes or PGF2A content, indicating that the mechanism by which LPS induced luteal regression requires endocannabinoid signaling (30). Although only one endocannabinoid, alpha-linolenoyl ethanolamide, tended to be less abundant in the CL of pregnancy, this change may contribute to mechanisms that ensure luteal survival.

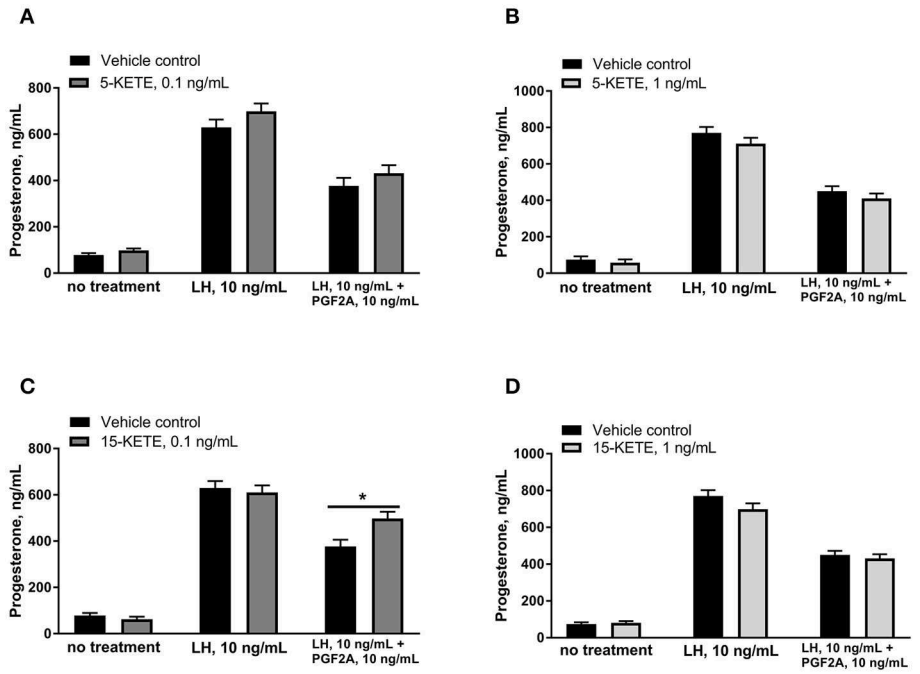

FIGURE 9 | Effect of 0.1 ng/mL **(A)** and 1 ng/mL **(B)** 5-KETE and of 0.1 ng/mL **(C)** and 1 ng/mL **(D)** 15-KETE on progesterone production in cultured luteal cells on day 7 of culture. Significant differences ($P < 0.05$) between lipid-treated and vehicle control are denoted with a * ($N = 4$).

Progesterone increased abundance of FAAH in T lymphocytes (31), indicating that perhaps the high progesterone content of the CL may promote metabolism of endocannabinoids, while the luteolytic cytokine, IFNG (32, 33), decreased abundance of FAAH (31). In addition, stearoylethanolamide has been documented as a proapoptoic factor, particularly in combination with nitric oxide (34). Perhaps the increase in stearoylethanolamide at the end of the estrous cycle makes luteal cells more susceptible to apoptosis during luteal regression. Together, these observations lead to the speculation that increased endocannabinoid abundance could promote luteal regression.

Linoleic acid is an essential fatty acid, meaning that it must be derived from the diet. While little is known about luteal effects of the linoleic acid metabolites measured in this study, linoleic acid itself has been studied extensively and has been demonstrated to decrease PGF2A and PGE2 production by cultured luteal cells, without altering progesterone (35). Feeding a source of omega-6 fatty acids increased linoleic acid content of CL and improved pregnancy rates in beef cattle (36). Given that linoleic acid must be derived from the diet, perhaps luteal tissue uptake and storage of linoleic acid is enhanced between days 4 and 11, to support luteal function or, since free fatty acids were measured, perhaps there is an increase in phospholipase activity and an increase in liberation of linoleic acid from cell membranes.

The three physiologically stable EpETrEs increased in CL as the estrous cycle progressed. These lipids are short-lived vascular inhibitors of functions such as vasoconstriction (37, 38) and blood clotting (39). Their increase over time may enhance blood supply to the CL, thus supporting luteal function. The high rate of progesterone production in the CL requires a large supply of oxygen, and every steroidogenic cell is in contact with a blood vessel.

Surprisingly, no differences were observed in tissue concentrations of PGF2A, PGE2, or 6-keto PGF1A, the stable metabolite of prostacyclin. In a previous report, PGF2A and 6-keto PGF1A content of freshly dispersed luteal cells was measured and reported to be greater on day 5 than on days 10, 15, or 18, with a numerical decline in ratio of 6-keto PGF1A to PGF2A over time (40). A similar decline in ratio was observed here, with ratios of 5.5, 2.3, and 3.2 on days 4, 11, and 18. This supports the results of Milvae and Hansel (40) and indicates that had the number of animals per group in this study been increased and animal-to-animal variation had been reduced, this study would have similar findings. Although Lee et al. (7) reported less intraluteal PGF2A and greater PGE2 on day 16 of ovine pregnancy relative to the same day of the estrous cycle, these CL were likely already regressing on day 16, making comparison with the findings presented here irrelevant. Lukazewska and Hansel (1) reported greater free arachidonic acid concentration in CL of the estrous cycle than CL of pregnancy. In this study, arachidonic acid was slightly greater, although the number of animals per group was more than four times less than in the study of Lukazewska and Hansel (1).

Several lipids of the lipoxygenase pathway changed, both during the estrous cycle and during maternal recognition of pregnancy. LTB4 has previously been reported to increase both PGE2 and progesterone production by luteal cells (9). Lukaszewska and Hansel (1) reported a relatively linear increase in serum progesterone until the time of luteolysis, which may

be supported in part by the luteotrophic effects of LTB4, as it increases during this time.

Members of the lipoxygenase pathway, including 5- and 15-KETE, may regulate infiltration of immune cells. C-C motif chemokine ligand 2 (CCL2), which is an important regulator of immune cell infiltration into the CL (41, 42) and luteal response to PGF2A (43), acted synergistically with 5-KETE to attract monocytes (44). Moreover, the pattern of change in 5-KETE abundance in this experiment is quite similar to the pattern of change in CCL2 in the CL on similar days (45). 15-KETE has been reported to have antiinflammatory properties (46), and indirectly induced immune cell infiltration by increasing abundance of E-selectin on endothelial cells and thus monocyte adhesion (47).

Luteal steroidogenic cells are potent activators of T cells (18), the luteal microenvironment programs resident T cells (48, 49), and alteration in activation state of luteal T cells has been implicated in both luteal regression (50) and luteal rescue (19). Pathway analysis using IPA indicated that four differentially abundant lipids, including 5-KETE and 5,15-DiHETE, and two endocannabinoids, anandamide and 2-arachidonyl-glycerol may regulate activation of leukocytes. Perhaps one mechanism of the ability of luteal steroidogenic cells to alter the function of T cells is through production of paracrine lipid mediators.

It has been reported that 5-KETE elicits its effect on cells by binding to oxoeicosanoid receptor 1 (*OXER1*), a G-protein coupled receptor (51). 5-KETE inhibits cAMP (52), induces calcium influx (53), and induces phosphorylation of p38 MAPK (54), all effects that could lead to the slight but significant 5-KETE-regulated reduction of progesterone observed in the current study. In the presence of LH, however, 5-KETE could not alter progesterone production. Because LH is a potent activator of cAMP, perhaps the moderate effect of 5-KETE was lost in the presence of this potent cAMP activator. 5-HETE, the molecule directly upstream from 5-KETE, inhibited luteal progesterone production in the presence and absence of LH (8, 55). However, in another report, 5-KETE induced StAR and steroid hormone production in adrenal and Leydig cell lines (56), though the mechanism of activation is not clear. The discrepancy between the study of Cooke et al. and this study may be explained by their use of cell lines, rather than the primary cells used here, or by the very high concentration of 5-KETE used in their study.

15-KETE increased progesterone production marginally but significantly, only in the presence of LH. Little is known about the pharmacology of 15-KETE and its receptor has not been identified. However, when cells were treated with a lipoxygenase inhibitor, which inhibited progesterone production, 15-HETE, the direct precursor of 15-KETE, induced progesterone only in the presence of LH, while 5-HETE and 12-HETE had no effect (57). 15-KETE, which increased between day 4 and 18, may also contribute to the change in LH responsiveness observed in luteal cells from older CL relative to younger CL. While LH induced an approximate doubling of progesterone production in dispersed luteal cells from day 5 and 10 of the estrous cycle, it induced a tripling of progesterone over basal in luteal cells from days 15 and 18 of the cycle (40).

During early pregnancy, luteal resistance to PGF2A transiently increases (4, 58, 59). Though this resistance may be due to exposure of CL to IFNT (60, 61), the mechanism of luteal resistance to PGF2A during early pregnancy has eluded researchers. Here, luteal cells treated with the lesser, but not the greater, concentration of 15-KETE, demonstrated reduced ability of PGF2A to inhibit LH response. This indicated a concentration-dependent response of luteal cells to 15-KETE, which was less in the CL of pregnancy. Perhaps the decline in 15-KETE during early pregnancy mediates an increased luteal resistance to PGF2A at that time, consistent with reports of other lipids altering luteal PGF2A response (12).

An *in silico* prediction, based on known regulatory relationships (62) indicated that during early pregnancy, 5-KETE may be a regulator of the transcription factor *MYC* and thus regulate the balance between cell survival and death (63). Despite testing multiple concentrations and times of treatment, no change was detected in *MYC* abundance as a result of 5-KETE treatment. This indicates that the change in luteal concentration of 5-KETE is not driving the change observed in *MYC* during early pregnancy, highlighting the importance of *in vitro* confirmation of *in silico* predictions.

Pathway analysis in IPA predicted that lipids may be regulators of cell proliferation in the CL. Early in the luteal phase, cell proliferation is so rapid that the CL had been compared to the fastest growing tumor. However, proliferation is turned off completely and the size and vascularity of the CL remains constant later in the cycle (64). Notably 15-KETE (65, 66) and anandamide (67) were predicted inhibitors of cell proliferation, including vascular endothelial cell proliferation, in the analysis in IPA. In addition, 5-KETE had a concentration-dependent effect on proliferation in cancer cell lines; high concentrations of 5-KETE inhibited proliferation via the peroxisome proliferator activated receptor gamma pathway (65). Perhaps the lesser concentrations of 5-KETE and 15-KETE in early pregnancy and their increase over time during the estrous cycle mediate the increased bloodflow to the CL during early pregnancy (68) and the decrease in cell proliferation in midcycle CL (64).

In conclusion, targeted metabolomic analysis of luteal tissue lipid mediators was used to identify 5-KETE and 15-KETE as potential key regulators of luteal function during important transitions in the luteal lifespan. Pathway analysis programs predicted lipid involvement in cell migration and chemotaxis, immune cell activation, and regulation of cell proliferation. *In vitro* experiments demonstrated that 5-KETE and 15-KETE were regulators of luteal progesterone and response to PGF2A, but not *MYC* abundance. Lipid regulation of luteal functions is an area that merits further investigation, as these lipids could be key paracrine regulators of luteal steroidogenic, endothelial, and immune cell functions.

DATA AVAILABILITY STATEMENT

All datasets generated for this study are included in the manuscript/**Supplementary Files**.

ETHICS STATEMENT

The animal studies were reviewed and approved by the Pennsylvania State University IACUC or the Ohio State University IACUC.

AUTHOR CONTRIBUTIONS

CH performed integrated omics and pathway and statistical analyses, all *in vitro* experiments, designed the *in vitro* experiments, and wrote the manuscript. JP designed the targeted metabolomics experiments and was involved in experimental design of the *in vitro* experiments, and manuscript preparation. JN and RB performed the LC-MS/MS analyses, performed statistical analyses of targeted metabolomics data, and were involved in manuscript preparation.

FUNDING

Funding provided by the C. Lee Rumberger and Family Endowment to JP and USDA NIFA predoctoral fellowship no. 2017-67011-26062 to CH. Additional support was provided by NIH DK097154 and USDA Project 2032-51530-022-00D and 2032-51530-025-00D. The USDA is an equal opportunity employer and provider.

ACKNOWLEDGMENTS

The authors wish to express gratitude to LM Wetzel for assistance with sample preparation for the targeted metabolomics experiment.

SUPPLEMENTARY MATERIAL

The Supplementary Material for this article can be found online at: https://www.frontiersin.org/articles/10.3389/fendo.2019.00662/full#supplementary-material

REFERENCES

1. Lukaszewska J, Hansel W. Corpus luteum maintenance during early pregnancy in the cow. *J Reprod Fertil.* (1980) 59:485–93. doi: 10.1530/jrf.0.0590485
2. Shemesh M, Hansel W. Stimulation of prostaglandin synthesis in bovine ovarian tissues by arachidonic acid and luteinizing hormone. *Biol Reprod.* (1975) 13:448–52. doi: 10.1095/biolreprod13.4.448
3. Niswender GD, Davis TL, Griffith RJ, Bogan RL, Monser K, Bott RC, et al. Judge, jury and executioner: the auto-regulation of luteal function. *Soc Reprod Fertil Suppl.* (2007) 64:191–206. doi: 10.5661/RDR-VI-191
4. Pratt BR, Butcher RL, Inskeep EK. Antiluteolytic effect of the conceptus and of PGE2 in ewes. *J Anim Sci.* (1977) 45:784–91. doi: 10.2527/jas1977.454784x
5. Silvia WJ, Ottobre JS, Inskeep EK. Concentrations of prostaglandins E2, F2 alpha and 6-keto-prostaglandin F1 alpha in the utero-ovarian venous plasma of nonpregnant and early pregnant ewes. *Biol Reprod.* (1984) 30:936–44. doi: 10.1095/biolreprod30.4.936
6. Milvae RA. Role of luteal prostaglandins in the control of bovine corpus luteum functions. *J Anim Sci.* (1986) 62(Suppl. 2):72–8. doi: 10.1093/ansci/62.2.72
7. Lee J, McCracken JA, Stanley JA, Nithy TK, Banu SK, Arosh JA. Intraluteal prostaglandin biosynthesis and signaling are selectively directed towards PGF2alpha during luteolysis but towards PGE2 during the establishment of pregnancy in sheep. *Biol Reprod.* (2012) 87:97. doi: 10.1095/biolreprod.112.100438
8. Milvae RA, Alila HW, Hansel W. Involvement of lipoxygenase products of arachidonic acid metabolism in bovine luteal function. *Biol Reprod.* (1986) 35:1210–5. doi: 10.1095/biolreprod35.5.1210
9. Korzekwa A, Lukasik K, Skarzynski DJ. Leukotrienes are auto-/paracrine factors in the bovine corpus luteum: an *in vitro* study. *Reprod Domest Anim.* (2010) 45:1089–97. doi: 10.1111/j.1439-0531.2009.01500.x
10. Ulfina GG, Kimothi SP, Oberoi PS, Baithalu RK, Kumaresan A, Mohanty TK, et al. Modulation of post-partum reproductive performance in dairy cows through supplementation of long- or short-chain fatty acids during transition period. *J Anim Physiol Anim Nutr.* (2015) 99:1056–64. doi: 10.1111/jpn.12304
11. Plewes MR, Burns PD, Graham PE, Bruemmer JE, Engle TE, Barisas BG. Effect of fish meal supplementation on spatial distribution of lipid microdomains and on the lateral mobility of membrane-bound prostaglandin F2α receptors in bovine corpora lutea. *Domest Anim Endocrinol.* (2017) 60:9–18. doi: 10.1016/j.domaniend.2017.02.001
12. Plewes MR, Cedillo JC, Burns PD, Graham PE, Bruemmer JE, Engle TE. Effect of fish meal supplementation on luteal sensitivity to intrauterine infusions of prostaglandin F2alpha in the bovine. *Biol Reprod.* (2018) 98:543–57. doi: 10.1093/biolre/ioy003
13. Agrawal K, Hassoun LA, Foolad N, Pedersen TL, Sivamani RK, Newman JW. Sweat lipid mediator profiling: a noninvasive approach for cutaneous research. *J Lipid Res.* (2017) 58:188–95. doi: 10.1194/jlr.M071738
14. La Frano MR, Fahrmann JF, Grapov D, Fiehn O, Pedersen TL, Newman JW, et al. Metabolic perturbations of postnatal growth restriction and hyperoxia-induced pulmonary hypertension in a bronchopulmonary dysplasia model. *Metabolomics.* (2017) 13:32. doi: 10.1007/s11306-017-1170-6
15. Pedersen TL, Newman JW. Establishing and performing targeted multi-residue analysis for lipid mediators and fatty acids in small clinical plasma samples. *Methods Mol Biol.* (2018) 1730:175–212. doi: 10.1007/978-1-4939-7592-1_13
16. Pate JL. Isolation and culture of fully differentiated bovine luteal cells. *Methods Toxicol.* (1993) 3B:360–70.
17. Pate JL. Regulation of prostaglandin synthesis by progesterone in the bovine corpus luteum. *Prostaglandins.* (1988) 36:303–15. doi: 10.1016/0090-6980(88)90072-X
18. Petroff M, Coggeshall KM, Jones LS, Pate JL. Bovine luteal cells elicit major histocompatibility complex class II-dependent T-cell proliferation. *Biol Reprod.* (1997) 57:887–93. doi: 10.1095/biolreprod57.4.887
19. Hughes CK, Maalouf SW, Liu WS, Pate JL. Molecular profiling demonstrates modulation of immune cell function and matrix remodeling during luteal rescue. *Biol Reprod.* (2019) 100:1581–96. doi: 10.1093/biolre/ioz037
20. Baglama J, Reichel L. Augmented implicitly restarted Lanczos bidiagonalization methods. *SIAM J Sci Comput.* (2005) 27:19–42. doi: 10.1137/04060593X
21. Benjamini Y, Hochberg Y. Controlling the false discovery rate: a practical and powerful approach to multiple testing. *J R Stat Soc B.* (1995) 57:289–300. doi: 10.1111/j.2517-6161.1995.tb02031.x
22. Edgar R, Domrachev M, Lash AE. Gene Expression Omnibus: NCBI gene expression and hybridization array data repository. *Nucleic Acids Res.* (2002) 30:207–10 doi: 10.1093/nar/30.1.207
23. Chong J, Soufan O, Li C, Caraus I, Li S, Bourque G, et al. (2018). MetaboAnalyst 4.0: towards more transparent and integrative metabolomics analysis. *Nucleic Acids Res.* (2002) 46:W486–94. doi: 10.1093/nar/gky310
24. Fabregat A, Jupe S, Matthews L, Sidiropoulos K, Gillespie M, Garapati P, et al. The reactome pathway knowledgebase. *Nucleic Acids Res.* (2018) 46:D649–55. doi: 10.1093/nar/gkx1132
25. Pate JL, Condon WA. Effects of prostaglandin F2 alpha on agonist-induced progesterone production in cultured bovine luteal cells. *Biol Reprod.* (1984) 31:427–35. doi: 10.1095/biolreprod31.3.427
26. Fezza F, Bari M, Florio R, Talamonti E, Feole M, Maccarrone M. Endocannabinoids, related compounds and their metabolic routes. *Molecules.* (2014) 19:17078–106. doi: 10.3390/molecules191117078
27. Bagavandoss P, Grimshaw S. Temporal and spatial distribution of the cannabinoid receptors (CB1, CB2) and fatty acid amide hydroxylase in the rat ovary. *Anat Rec.* (2010) 293:1425–32. doi: 10.1002/ar.21181

28. Weems YS, Lewis AW, Neuendorff DA, Randel RD, Weems CW. Endocannabinoid 1 and 2 (CB(1); CB(2)) receptor agonists affect negatively cow luteal function *in vitro*. *Prostaglandins Other Lipid Mediat.* (2009) 90:89–93. doi: 10.1016/j.prostaglandins.2009.09.003
29. Tsutahara NM, Weems YS, Arreguin-Arevalo JA, Nett TM, LaPorte ME, Uchida J, et al. Effects of endocannabinoid 1 and 2 (CB1; CB2) receptor agonists on luteal weight, circulating progesterone, luteal mRNA for luteinizing hormone (LH) receptors, and luteal unoccupied and occupied receptors for LH *in vivo* in ewes. *Prostaglandins Other Lipid Mediat.* (2011) 94:17–24. doi: 10.1016/j.prostaglandins.2010.11.002
30. Schander JA, Correa F, Bariani MV, Blanco J, Cymeryng C, Jensen F, et al. A role for the endocannabinoid system in premature luteal regression and progesterone withdrawal in lipopolysaccharide-induced early pregnancy loss model. *Mol Hum Reprod.* (2016) 22:800–8. doi: 10.1093/molehr/gaw050
31. Maccarrone M, Valensise H, Bari M, Lazzarin N, Romanini C, Finazzi-Agrò A. Progesterone up-regulates anandamide hydrolase in human lymphocytes: role of cytokines and implications for fertility. *J Immunol.* (2001) 166:7183–9. doi: 10.4049/jimmunol.166.12.7183
32. Fairchild DL, Pate JL. Modulation of bovine luteal cell synthetic capacity by interferon-gamma. *Biol Reprod.* (1991) 44:357–63. doi: 10.1095/biolreprod44.2.357
33. Neuvians TP, Schams D, Berisha B, Pfaffl MW. Involvement of pro-inflammatory cytokines, mediators of inflammation, and basic fibroblast growth factor in prostaglandin F 2A-induced luteolysis in bovine corpus luteum. *Biol Reprod.* (2004) 70:473–80. doi: 10.1095/biolreprod.103.016154
34. Maccarrone M, Pauselli R, Di Rienzo M, Finazzi-Agrò A. Binding, degradation and apoptotic activity of stearoylethanolamide in rat C6 glioma cells. *Biochem J.* (2002) 366:137–44. doi: 10.1042/bj20020438
35. May KC, Bobe G, Mueller CJ, Cannon MJ. Conjugated linoleic acid decreases prostaglandin synthesis in bovine luteal cells *in vitro*. *Mol Reprod Dev.* (2011) 78:328–36. doi: 10.1002/mrd.21308
36. Cooke RF. Early career achievement award: supplementing omega-6 fatty acids to enhance early embryonic development and pregnancy establishment in Bos indicus and B. *taurus* beef cows. *J Anim Sci.* (2019) 97:485–95 doi: 10.1093/jas/sky414
37. Metea MR, Newman EA. Signaling within the neurovascular unit in the mammalian retina. *Exp Physiol.* (2007) 92:635–40. doi: 10.1113/expphysiol.2006.036376
38. Hao CM, Breyer MD. Physiologic and pathophysiologic roles of lipid mediators in the kidney. *Kidney Int.* (2007) 71:1105–15. doi: 10.1038/sj.ki.5002192
39. Spiecker M, Liao JK. Vascular protective effects of cytochrome p450 epoxygenase-derived eicosanoids. *Arch Biochem Biophys.* (2005) 433:413–20. doi: 10.1016/j.abb.2004.10.009
40. Milvae RA, Hansel W. Prostacyclin, prostaglandin F2 alpha and progesterone production by bovine luteal cells during the estrous cycle. *Biol Reprod.* (1983) 29:1063–8. doi: 10.1095/biolreprod29.5.1063
41. Townson DH. Immune cell-endothelial cell interactions in the bovine corpus luteum. *Integr Comp Biol.* (2006) 46:1055–9. doi: 10.1093/icb/icl021
42. Nio-Kobayashi J, Kudo M, Sakuragi N, Kimura S, Iwanaga T, Duncan WC. Regulated C-C motif ligand 2 (CCL2) in luteal cells contributes to macrophage infiltration into the human corpus luteum during luteolysis. *Mol Hum Reprod.* (2015) 21:645–54. doi: 10.1093/molehr/gav028
43. Tsai SJ, Juengel JL, Wiltbank MC. Hormonal regulation of monocyte chemoattractant protein-1 messenger ribonucleic acid expression in corpora lutea. *Endocrinology.* (1997) 138:4517–20. doi: 10.1210/endo.138.10.5577
44. Sozzani S, Zhou D, Locati M, Bernasconi S, Luini W, Mantovani A, et al. Stimulating properties of 5-oxo-eicosanoids for human monocytes: synergism with monocyte chemotactic protein-1 and−3. *J Immunol.* (1996) 157:4664–71.
45. Townson DH, O'Connor CL, Pru JK. Expression of monocyte chemoattractant protein-1 and distribution of immune cell populations in the bovine corpus luteum throughout the estrous cycle. *Biol Reprod.* (2002) 66:361–6. doi: 10.1095/biolreprod66.2.361
46. Snyder NW, Golin-Bisello F, Gao Y, Blair IA, Freeman BA, Wendell SG. 15-Oxoeicosatetraenoic acid is a 15-hydroxyprostaglandin dehydrogenase-derived electrophilic mediator of inflammatory signaling pathways. *Chem Biol Interact.* (2015) 234:144–53. doi: 10.1016/j.cbi.2014.10.029
47. Ma G, Pan B, Ren S, Guo C, Guo Y, Wei L, et al. 15-oxoeicosatetraenoic acid mediates monocyte adhesion to endothelial cell. *Lipids Health Dis.* (2017) 16:137. doi: 10.1186/s12944-017-0518-2
48. Poole DH, Pate JL. Luteal microenvironment directs resident T lymphocyte function in cows. *Biol Reprod.* (2012) 86:29. doi: 10.1095/biolreprod.111.092296
49. Walusimbi SS, Pate JL. Luteal cells from functional and regressing bovine corpora lutea differentially alter the function of gamma delta T cells. *Biol Reprod.* (2014) 90:140. doi: 10.1095/biolreprod.114.117564
50. Cannon MJ, Petroff MG, Pate JL. Effects of prostaglandin F 2A and progesterone on the ability of bovine luteal cells to stimulate T lymphocyte proliferation. *Biol Reprod.* (2003) 69:695–700. doi: 10.1095/biolreprod.103.017590
51. Powell WS, Rokach J. Biosynthesis, biological effects, and receptors of hydroxyeicosatetraenoic acids (HETEs) and oxoeicosatetraenoic acids (oxo-ETEs) derived from arachidonic acid. *Biochim Biophys Acta.* (2015) 1851:340–55. doi: 10.1016/j.bbalip.2014.10.008
52. Blättermann S, Peters L, Ottersbach PA, Bock A, Konya V, Weaver CD, et al. A biased ligand for OXE-R uncouples Gα and Gβγ signaling within a heterotrimer. *Nat Chem Biol.* (2012) 8:631–8. doi: 10.1038/nchembio.962
53. Konya V, Blättermann S, Jandl K, Platzer W, Ottersbach PA, Marsche G, et al. A biased non-Gαi OXE-R antagonist demonstrates that Gαi protein subunit is not directly involved in neutrophil, eosinophil, and monocyte activation by 5-oxo-ETE. *J Immunol.* (2014) 192:4774–82. doi: 10.4049/jimmunol.1302013
54. Schratl P, Sturm EM, Royer JF, Sturm GJ, Lippe IT, Peskar BA, et al. Hierarchy of eosinophil chemoattractants: role of p38 mitogen-activated protein kinase. *Eur J Immunol.* (2006) 36:2401–9. doi: 10.1002/eji.200535672
55. Ichikawa F, Yoshimura Y, Oda T, Shiraki M, Maruyama K, Kawakami S, et al. The effects of lipoxygenase products on progesterone and prostaglandin production by human corpora lutea. *J Clin Endocrinol Metab.* (1990) 70:849–55. doi: 10.1210/jcem-70-4-849
56. Cooke M, Di Cónsoli H, Maloberti P, Cornejo Maciel F. Expression and function of OXE receptor, an eicosanoid receptor, in steroidogenic cells. *Mol Cell Endocrinol.* (2013) 371:71–8. doi: 10.1016/j.mce.2012.11.003
57. Taniguchi H, Uenoyama Y, Miyamoto Y, Okuda K. The lipoxygenase pathways are involved in LH-stimulated progesterone production in bovinecorpus luteum. *Prostaglandins Other Lipid Mediat.* (2002) 67:49–60. doi: 10.1016/S0090-6980(01)00174-5
58. Silvia WJ, Niswender GD. Maintenance of the corpus luteum of early pregnancy in the ewe. III. Differences between pregnant and nonpregnant ewes in luteal responsiveness to prostaglandin F2 alpha. *J Anim Sci.* (1984) 59:746–53. doi: 10.2527/jas1984.593746x
59. Silvia WJ, Niswender GD. Maintenance of the corpus luteum of early pregnancy in the ewe. IV. Changes in luteal sensitivity to prostaglandin F2 alpha throughout early pregnancy. *J Anim Sci.* (1986) 63:1201–7. doi: 10.2527/jas1986.6341201x
60. Antoniazzi AQ, Webb BT, Romero JJ, Ashley RL, Smirnova NP, Henkes LE, et al. Endocrine delivery of interferon tau protects the corpus luteum from prostaglandin F2 alpha-induced luteolysis in ewes. *Biol Reprod.* (2013) 88:144. doi: 10.1095/biolreprod.112.105684
61. Bott RC, Ashley RL, Henkes LE, Antoniazzi AQ, Bruemmer JE, Niswender GD, et al. Uterine vein infusion of interferon tau (IFNT) extends luteal life span in ewes. *Biol Reprod.* (2010) 82:725–35. doi: 10.1095/biolreprod.109.079467
62. Sarveswaran S, Chakraborty D, Chitale D, Sears R, Ghosh J. Inhibition of 5-lipoxygenase selectively triggers disruption of c-Myc signaling in prostate cancer cells. *J Biol Chem.* (2015) 290:4994–5006. doi: 10.1074/jbc.M114.599035
63. McMahon SB. MYC and the control of apoptosis. *Cold Spring Harb Perspect Med.* (2014) 4:a014407. doi: 10.1101/cshperspect.a014407
64. Reynolds LP, Grazul-Bilska AT, Killilea SD, Redmer DA. Mitogenic factors of corpora lutea. *Prog Growth Factor Res.* (1994) 5:159–75. doi: 10.1016/0955-2235(94)90003-5
65. O'Flaherty JT, Rogers LC, Chadwell BA, Owen JS, Rao A, Cramer SD, et al. 5(S)-Hydroxy-6,8,11,14-E,Z,Z,Z-eicosatetraenoate stimulates PC3 cell signaling and growth by a receptor-dependent mechanism. *Cancer Res.*

(2002) 62:6817–9. Available online at: https://cancerres.aacrjournals.org/content/62/23/6817.full-text.pdf

66. Wei C, Zhu P, Shah SJ, Blair IA. 15-oxo-Eicosatetraenoic acid, a metabolite of macrophage 15-hydroxyprostaglandin dehydrogenase that inhibits endothelial cell proliferation. *Mol Pharmacol.* (2009) 76:516–25. doi: 10.1124/mol.109.057489
67. DeMorrow S, Glaser S, Francis H, Venter J, Vaculin B, Vaculin S, et al. Opposing actions of endocannabinoids on cholangiocarcinoma growth: recruitment of Fas and Fas ligand to lipid rafts. *J Biol Chem.* (2007) 282:13098–113. doi: 10.1074/jbc.M608238200
68. Pinaffi FLV, Araujo ER, Silva LA, Ginther OJ. Color-Doppler signals of blood flow in the corpus luteum and vascular perfusion index for ovarian and uterine arteries during expansion of the allantochorion in Bos taurus heifers. *Theriogenology*. (2017) 102:35–43. doi: 10.1016/j.theriogenology.2017.07.008

Conflict of Interest: The authors declare that the research was conducted in the absence of any commercial or financial relationships that could be construed as a potential conflict of interest.

frontiers in Endocrinology

ORIGINAL RESEARCH
published: 07 November 2019
doi: 10.3389/fendo.2019.00727

Thrombospondin 1 (THBS1) Promotes Follicular Angiogenesis, Luteinization, and Ovulation in Primates

*Hannah R. Bender†, Genevieve E. Campbell†, Priyanka Aytoda, Allison H. Mathiesen and Diane M. Duffy**

Department of Physiological Sciences, Eastern Virginia Medical School, Norfolk, VA, United States

Angiogenesis is essential to both ovulation and the formation of the corpus luteum. The thrombospondin (THBS) family of glycoproteins plays diverse roles in regulation of angiogenesis, but the role of these vascular regulators in ovulation and luteinization remain to be elucidated. Using the cynomolgus macaque as a model for human ovulation, we demonstrated that levels of THBS1 mRNA and protein in preovulatory follicle granulosa cells increased after the ovulatory gonadotropin surge, with peak levels just before the expected time of ovulation. THBS1 treatment of monkey ovarian microvascular endothelial cells *in vitro* stimulated migration, proliferation, and capillary sprout formation, consistent with a pro-angiogenic action of THBS1. Injection of an anti-THBS1 antibody into monkey preovulatory follicles reduced rates of follicle rupture and oocyte release in response to an ovulatory gonadotropin stimulus when compared with control IgG-injected follicles. Interestingly, two of three oocytes from anti-THBS1 antibody injected follicles were germinal vesicle intact, indicating that meiosis failed to resume as anticipated. Follicles injected with anti-THBS1 antibody also showed reduced granulosa cell layer expansion, endothelial cell invasion, and capillary formation when compared to control IgG-injected follicles. Overall, these findings support a critical role for THBS1 in follicular angiogenesis, with implications for both successful ovulation and corpus luteum formation.

Keywords: luteinizing hormone, neovascularization, ovarian follicle, ovary, oocyte, macaque, granulosa cell, endothelial cell

OPEN ACCESS

Edited by:
Joy L. Pate, Pennsylvania State University, United States

Reviewed by:
Ray Rodgers, University of Adelaide, Australia
Lawrence P. Reynolds, North Dakota State University, United States

***Correspondence:**
Diane M. Duffy
duffydm@evms.edu

†These authors have contributed equally to this work

Specialty section:
This article was submitted to Reproduction, a section of the journal Frontiers in Endocrinology

Received: *26 April 2019*
Accepted: *09 October 2019*
Published: *07 November 2019*

Citation:
Bender HR, Campbell GE, Aytoda P, Mathiesen AH and Duffy DM (2019) Thrombospondin 1 (THBS1) Promotes Follicular Angiogenesis, Luteinization, and Ovulation in Primates. Front. Endocrinol. 10:727. doi: 10.3389/fendo.2019.00727

INTRODUCTION

Angiogenesis is critical for successful ovulation and formation of the corpus luteum (1). New blood vessels form within the dominant follicle in response to the ovulatory gonadotropin surge (2). In primate follicles, capillaries invade the previously-avascular granulosa cell layer before follicle rupture (3). Blockade of key vascular growth factor pathways can prevent both ovulation and luteal formation (1) highlighting the close connection between angiogenesis and ovarian function.

Thrombospondins are a family of vascular regulators, each containing multiple structure/function domains (4). Because of these multiple domains, a molecule of thrombospondin can simultaneously interact with cell surface receptors, extracellular matrix components, matrix remodeling proteases, integrins, and growth factors (4, 5). Thrombospondins have been reported

to be both pro-angiogenic and anti-angiogenic. For example, thrombospondin 1(THBS1) most often acts as an anti-angiogenic factor when THBS1's type 1 repeats interact with CD36 receptors (6). In contrast, pro-angiogenic activity of THBS1 has been reported when the N terminal heparin-binding domain interacts with LRP1 receptors (7, 8).

In the ovary, thrombospondins have been examined in growing follicles, where high THBS1 and THBS2 were associated with decreased vascularity and granulosa cell proliferation but increased granulosa cell apoptosis, perhaps contributing to the processes of follicle development and follicle selection (9–12). Expression of THBS1 and THBS2 decline in both granulosa and theca cells of growing antral follicles as follicle size increases; large preovulatory follicles have low levels of thrombospondins in all follicular cell types (9, 11, 13–15). Very limited information on thrombospondin expression after the LH surge suggests that THBS1 and THBS2 levels may in granulosa and theca cells increase transiently after the LH surge (14). THBS1 and THBS2 expression in the young bovine corpus luteum is highest in vascular endothelial cells and vascular smooth muscle (15), highlighting the role of thrombospondins as vascular regulators.

Ovarian thrombospondin expression and action have been studied in growing follicles up to the antral stage and during the process of luteal regression. However, little is known about thrombospondin expression and action during ovulation and transformation of the follicle into the young corpus luteum. The present studies were conducted to examine the expression of thrombospondin family members in the ovulatory follicle of a primate, the cynomolgus macaque. We demonstrate that THBS1 is an LH-stimulated, pro-angiogenic factor during the transformation of the dominant follicle into the young corpus luteum. *In vivo* and *in vitro* studies confirm that THBS1 is critical to the success of primate ovulation.

MATERIALS AND METHODS

Animals

Whole ovaries and ovarian biopsies were obtained from adult female cynomolgus macaques (Macaca fascicularis) at Eastern Virginia Medical School (Norfolk, VA). All animal protocols were conducted in accordance with the National Institutes of Health's Guide for the Care and Use of Laboratory Animals and were approved by the Eastern Virginia Medical School Animal Care and Use Committee. Animal husbandry was performed as described previously (16). Briefly, adult females (aged 4–8 years) with regular menstrual cycles were routinely observed for menstruation; the first day of menstruation marked day 1 of the cycle. Blood samples were obtained with chemical restraint (ketamine, 5–10 mg/kg body weight) as needed by femoral venipuncture and serum was stored at −20°C. Serum estradiol and progesterone levels were determined using the Immulite 1000 immunoassay system (Siemens Medical Diagnostics Solutions, Rockville, MD). Aseptic surgeries were performed by laparotomy in a dedicated surgical suite under isoflurane anesthesia. Postoperative analgesia was accomplished with buprenorphine and a non-steroidal anti-inflammatory drug (ketoprofen or meloxicam).

Ovarian Stimulation

An ovarian stimulation model was used to obtain ovaries with multiple ovulatory follicles (17). Beginning within 3 days of initiation of menstruation, monkeys received 90 IU of recombinant human follicle stimulating hormone (FSH; Merck and Co., Inc., Kenilworth, NJ) for 6–8 days, followed by 2–3 days of 90 IU of FSH plus 60 IU of recombinant human LH (Serono Reproductive Biology Institute, Rockland, MA) to stimulate the growth of multiple follicles. Animals also received a GnRH antagonist [30 μg/kg Ganirelix (Merck)] daily to prevent an endogenous ovulatory LH surge. Follicular development was monitored by ultrasonography and rising serum estradiol. During aseptic surgery, aspiration of follicles <4 mm was performed before (0), 12, 24, or 36 h after administration of 1000 IU of recombinant human chorionic gonadotropin (hCG; Serono). To inhibit follicular prostaglandin production during the periovulatory interval, some animals were treated as described above; these animals also received the PTGS2 inhibitor celecoxib (32 mg orally every 12 h; Pfizer, New York, NY) beginning with hCG administration and continuing until surgery (16). This treatment has been previously shown to significantly reduce follicular PGE2 levels (16).

Controlled Ovulation With Follicle Injection

A model of controlled ovulation with follicle injection model was used to introduce an antibody into the ovulatory follicle (18). Beginning on day 5–8 of the menstrual cycle, animals were monitored for rising serum estradiol to indicate development of a large pre-ovulatory follicle. Animals then received a GnRH antagonist (Acyline, 60 μg/kg; NICHD, Rockville, MD) to prevent endogenous LH surge concomitant with 80 IU of FSH and 60 IU of LH for 2 days to maintain healthy development of the follicle. On the next day, intrafollicular injection of an antibody against THBS1 (R&D Systems, Minneapolis, MN; AF3074; $n = 4$) or control IgG antibody (Abbiotec, San Diego, CA; $n = 4$) was performed during aseptic surgery; an estimated 10 μg of antibody protein was delivered to each follicle at injection (**Supplemental Table 1**). Immediately post-operatively, 1000 IU hCG (Serono) was administered to initiate ovulatory events. Ovariectomy was performed 48 h after follicle injection and hCG, with ovulation anticipated at about 40 h (19). Ovaries were photographed *in situ* before ovariectomy when possible. In one case (control IgG), the ovulation site was obscured from view *in situ* and was photographed after removal. Data from three of these control IgG ovaries has been previously reported (18); a fourth control IgG-injected ovary was obtained from the same cohort of animals that provided the THBS1 antibody injected ovaries and serves as an additional, contemporary control.

Tissue Preparation

Monkey granulosa cells and oocytes were pelleted from the follicular aspirates by centrifugation at 250 X g. The supernatant (follicular fluid) was removed and stored at −80C. After oocyte removal, a granulosa cell-enriched population of the remaining cells was obtained by Percoll gradient centrifugation (16). Granulosa cells were either used immediately for cell culture or were frozen in liquid nitrogen and stored at −80C. Viability

of granulosa cell-enriched preparations was assessed by trypan blue exclusion and averaged 80%. Whole ovaries were bisected such that at least two ovulatory follicles <4 mm in diameter were present on each piece. Pieces were fixed in 10% formalin and embedded in paraffin.

Quantitative PCR (qPCR)

Levels of mRNA for *THBS1*, *THBS2*, and *THBS4* were assessed by qPCR using a Roche Lightcycler (Roche Diagnostics, Atlanta, GA). Total RNA was obtained from granulosa cells, treated with deoxyribonuclease and reverse transcribed as previously described (20). PCR was performed using the FastStart DNA Master SYBR Green I kit (Roche) following manufacturer's instructions. Primers were designed based on human or monkey sequences and span an intron to prevent undetected amplification of genomic DNA. PCR products were sequenced (Genewiz, South Plainfield, NJ) to confirm amplicon identity (**Supplemental Table 2**). All data are expressed as the ratio of mRNA of interest to *ACTB* mRNA for each sample, where a value of 1.0 indicates the same number of copies of mRNA of interest and copies of *ACTB* in a given mRNA sample.

Histology

Whole ovaries were fixed in 10% formalin for 24 h and embedded in paraffin, oriented such that sections included the follicle apex and follicle wall opposite the apex at the maximal follicle diameter in order to ensure optimal view of the follicle apex (18). Ovaries were serially sectioned at 5 μm with each section retained in order. Every fifth section was deparaffinized in xylene baths, rehydrated through a series of ethanol washes, stained with 30% hematoxylin and 60% eosin (Sigma-Aldrich, St. Louis, MO), and coverslipped with Permount mounting medium (ThermoFisher; Suwanee, GA). Stained sections were imaged using an Olympus microscope with either a DP70 or DP74 digital camera system and associated software (Olympus, Melville, NY). Whole follicle images were assembled from multiple microscopic images of a single tissue section using Image Composite Editor (Microsoft Corp., Redmond, WA).

At least two independent observers performed histologic evaluation of sections from each ovary. Evaluation of sections included identification of the oocyte and (if present) condition of the cumulus (tight/expanded) as well as presence/absence of a rupture site. The size of each rupture site was quantified by measuring the width on the section with the largest rupture site, counting the number of 5 μm sections where the rupture site was present, and using these measurements to calculate the area of an oval.

Western Blot

Granulosa cell lysate preparation and western blot were performed essentially as previously described (3). Briefly, granulosa cell lysates were loaded onto a 3–8% polyacrylamide gradient gel (ThermoFisher). Proteins were transferred to a polyvinylidene fluoride membrane (Immobilon; Millipore, Billerica, MA) and probed using antibodies against THBS1 (0.01 μg/ml; goat; R&D Systems), THBS4 (0.01 μg/ml; goat; R&D Systems), or actin (5 μg/ml; mouse; Millipore) (**Supplemental Table 1**). Membranes were incubated with AP-conjugated secondary antibodies (1:5000; Applied Biosystems; Invitrogen, Carlsbad, CA) and protein bands visualized with Tropix CDP-Star according to the manufacturer's instructions (Applied Biosystems; Invitrogen). Pixel density of each band was quantified by ImageJ (https://imagej.nih.gov/). Each sample is expressed as pixel density of the THBS band divided by the pixel density of the actin band.

Monkey Ovarian Microvascular Endothelial Cells (mOMECs)

Proliferating populations of ovarian microvascular endothelial cells (mOMECs) were obtained from monkey ovulatory follicles, characterized, and maintained as previously described (3).

To assess mOMEC proliferation, cells were grown on glass chamber slides (Nunc, ThermoFisher) until 50% confluent. Cells were incubated overnight in basal media (Lonza, ThermoFisher) with 1% fetal bovine serum (Gibco, Gaithersburg, MD). The next day, cells were treated with recombinant human THBS1 (0.01–1 nM; R&D Systems). After 24 h of treatment *in vitro*, cells were fixed in 10% formalin for Ki67 detection and quantification of proliferating cells by immunocytochemistry as described below.

Migration of mOMECs was assessed as previously described (3) using 6-well plate inserts with 8 μm pores (BD) with cells in basal media inside the insert. Media in the well-consisted of basal media with or without the addition of THBS1 (0.001-1 nM; R&D Systems). For some experiments, THBS1 (1 nM) was preincubated for 24 h at 4C with the THBS1 antibody (R&D Systems), with 4-fold molar excess of antibody. Cells were incubated with treatments for 24 h, then cells on the inside of the insert were removed with a cotton swab. The inserts were fixed in 70% ethanol and stained with hematoxylin and eosin. Five areas of each insert were photographed, and the number of migrated cells was counted for each image.

To assess sprout formation, mOMECs adhered to microcarrier beads were embedded in a fibrin matrix as previously described (3). Basal media plus 0.05 U/mL aprotinin with or without THBS1 (0.01–1 nM; R&D Systems) was added on top of matrixes. Representative beads were photographed before adding treatments (Day 0). For each well, four areas were photographed on Day 1 and Day 2 after initiation of cultures. Beads with sprouts that were entirely within the frame were used to generate sprout counts and measurements. For sprout counts, the number of sprouts per bead was determined, and an average number of sprouts/bead was determined for each treatment group. Sprouts were measured from the edge of the bead to the tip of the longest branch; lengths were averaged for each treatment group.

Human umbilical vein endothelial cells [HUVECs; American Type Culture Collection (ATCC), Manassas, VA] were cultured as described for mOMECs and used as a control primary endothelial cell population.

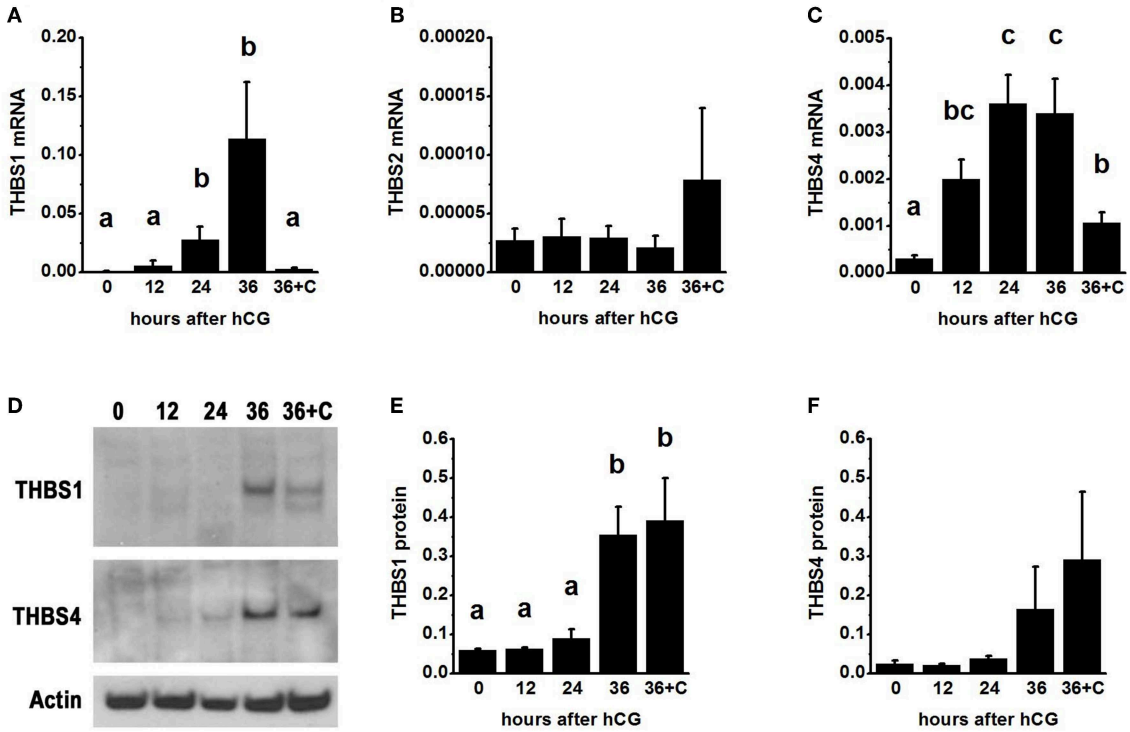

FIGURE 1 | Thrombospondin production by the ovulatory follicle. Granulosa cells were aspirated from monkey ovarian follicles after ovarian stimulation before (0), 12, 24, or 36 h after administration of an ovulatory dose of hCG; additional monkeys received hCG and the PTGS2 inhibitor celecoxib (36+C) 36 h before follicle aspiration. Granulosa cells were assessed by qPCR for mRNA levels of *THBS1* **(A)**, *THBS2* **(B)**, and *THBS4* **(C)**. All *THBS* mRNA levels are expressed relative to *BACT*. Granulosa cell lysates were assessed for THBS1 **(D,E)** and THBS4 **(D,F)** by western blotting and are expressed relative to pan-actin **(D)**. For **(A–C,E,F)**, data are expressed as mean + SEM, $n = 3$–7 samples/treatment. Within each panel, groups with no common letters are different by ANOVA and Duncans *post hoc* test, $p < 0.05$.

Immunohistochemistry

Immunostaining was performed using paraffin-embedded ovaries sectioned at 5 μm essentially as previously described (18). Briefly, tissue sections were heated and deparaffinized. Slides to be used for immunodetection of THBS1 or THBS4 were exposed to antigen retrieval using Tris-ethylenediaminetetraacetic acid (EDTA) as previously described (18). When staining for von Willebrand Factor (VWF) or Ki67, antigen retrieval was not performed. All tissues were blocked with 5% non-immune serum in PBS containing 0.1% Triton X-100. Slides were incubated overnight with primary antibody against THBS1 (2.5 μg/ml; R&D Systems), THBS4 (2.9 μg/ml; R&D Systems), VWF (5 μg/ml; Dako, Carpinteria, CA), or Ki67 (0.35 μg/ml; Dako) (**Supplemental Table 1**) and color-developed using the Vectastain Rabbit ABC kit (Vector Laboratories, Burlingame, CA). Slides were counterstained in hematoxylin, dehydrated, and permanently coverslipped. All images were obtained using an Olympus BX41 microscope fitted with a DP70 digital camera and associated software. Specificity of THBS1 and THBS4 antibody detection were confirmed by preabsorption of the primary antibody with recombinant human peptides (R&D Systems; source) at a molar ratio of 10:1 antigen:antibody at 4C overnight and use of preabsorbed antibody for immunostaining as described above. Omission of the primary antibody served as an additional negative control.

Assessment of Luteinization and Angiogenesis

Granulosa cell layer thickness was assessed as previously described (18). Briefly, an ovarian section stained with hematoxylin and eosin was selected which included the maximal diameter of the follicle and the rupture site (if rupture occurred) or thinnest portion of the remaining follicle wall (if rupture did not occur). The granulosa cell layer immediately opposite the apex or thinnest portion of the remaining follicle wall was assessed. The distance from granulosa cell basement membrane to antral edge of granulosa cells was measured, with a minimum of eight replicate measurements made for each ovarian tissue.

Assessment of endothelial cell invasion into granulosa cell layer (18) was performed using ovarian tissues immunostained for the endothelial cell protein VWF. Endothelial cell invasion into the granulosa cell layer was assessed using a tissue section which included the maximal diameter of the follicle and the rupture site or thinnest portion of the remaining follicle wall. The granulosa cell layer immediately opposite the apex or

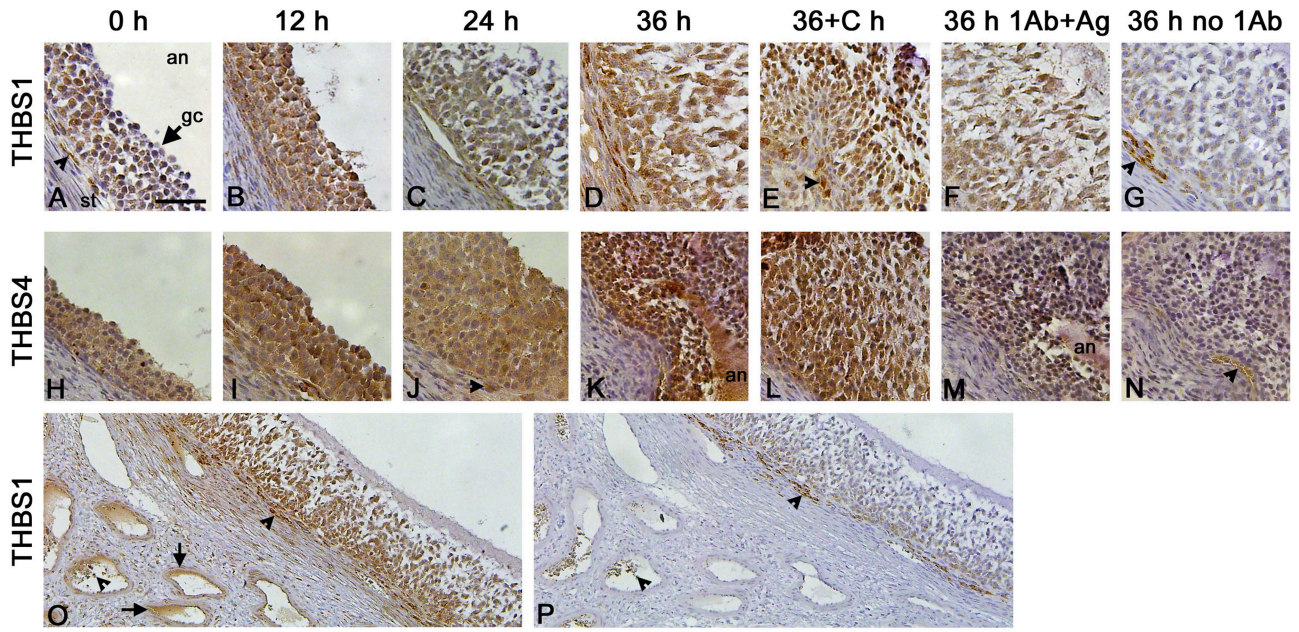

FIGURE 2 | THBS1 and THBS4 immunodetection in monkey ovarian follicles. Immunocytochemical detection (brown) of THBS1 **(A–G)** and THBS4 **(H–N)** was localized to the granulosa cell layer of ovulatory follicles obtained before (0; A,H) and 12 **(B,I)**, 24 **(C,J)**, and 36 **(D,K)** hours (h) after hCG administration as well as 36 h after administration of hCG and celecoxib (36+C h; **E,L**). Images shown are representative of n-3-6 ovaries/treatment. Granulosa cell immunodetection of THBS1 **(F)** and THBS4 **(M)** was reduced after preabsorption of the primary antibody with recombinant human THBS1 or THBS4 and similar to staining observed with no primary antibody **(G,N)**. Nuclei are counterstained blue. All panels are oriented as shown in **(A)**, with stroma (st) in lower left, granulosa cell (gc, arrow) layer central, and follicle antrum (an) in upper right. Arrowheads indicate stromal staining with antibody against THBS1 **(A,E)**, THBS4 **(J)**, and no primary antibody **(G,N)**. Images in **(A–N)** are at the same magnification; bar in **(A)** is 50 μm. Lower magnification images shows immunocytochemical detection of THBS1 **(O)** and no primary antibody **(P)** stained sections of an ovary obtained after ovarian stimulation and 36 h hCG. Staining is apparent in stromal vessels (**O**, arrows). Non-specific staining is indicated near the granulosa cell basement membrane and in vessel lumens in **(O,P)** (arrowheads); bar in **(A)** is 100 μm for images in **(O,P)**.

thinnest portion of the remaining follicle wall was assessed. The distance from the granulosa cell basement membrane to the VWF^+ cell closest to the follicle antrum was determined, with at least five replicate measurements made for each tissue section evaluated.

Three dimensional (3D) modeling of capillary sprouting from stromal vessels was performed as previously described (18). Briefly, four adjacent 5 μm ovarian sections were immunostained for VWF as described above. VWF^+ cells from these adjacent sections were traced into WinSurf software (WinSurf Technology, Hertfordshire, UK) and reconstructed following the manufacturer's instructions.

Data Analysis

Data were assessed for heterogeneity of variance by Bartlett's tests. Data were log transformed when Bartlett's test yielded $p < 0.05$; log-transformed data were subjected to Bartlett's test to confirm that $p > 0.05$. All data sets were assessed by unpaired *t*-test, paired *t*-test, or ANOVA (without or with repeated measures) as indicated in the text and figure legends. ANOVA was followed by Duncan's multiple range test when $p < 0.05$. Statistics were performed using StatPak version 4.12 software; Northwest Analytical, Portland, OR. Significance was assumed at $p < 0.05$. Data are expressed as mean ± SEM.

RESULTS

Ovulatory Follicles Produce Thrombospondins in Response to the Ovulatory Gonadotropin Surge

To examine thrombospondin synthesis and accumulation in the ovulatory follicle, granulosa cells were obtained from monkeys experiencing ovarian stimulation either before (0 h) or 12–36 h after administration of an ovulatory dose of hCG to span the ovulatory interval in primates. Total granulosa cell RNA was assessed for *THBS1*, *THBS2*, and *THBS4*. *THBS1* mRNA was low 0–12 h after hCG and was significantly elevated 24–36 h after hCG (**Figure 1A**). In contrast, *THBS2* mRNA levels were low and unchanging throughout the ovulatory interval (**Figure 1B**). *THBS4* mRNA was low at 0 h and significantly elevated 12–36 h after hCG (**Figure 1C**). Overall, the highest mRNA copy numbers were observed for *THBS1,* with lower copy numbers for *THBS4* and very low copy numbers for *THBS2*.

To determine if changes in *THBS1* and *THBS4* mRNA were accompanied by similar changes in thrombospondin proteins, granulosa cell lysates were subjected to western blotting. THBS1 protein was detected as a single band of 160 MW (**Figure 1D**). Granulosa cell THBS1 was low 0–24 h after hCG, then rose to higher levels at 36 h hCG (**Figure 1E**). THBS4 was detected as a single band of 130 MW (**Figure 1D**). There was no

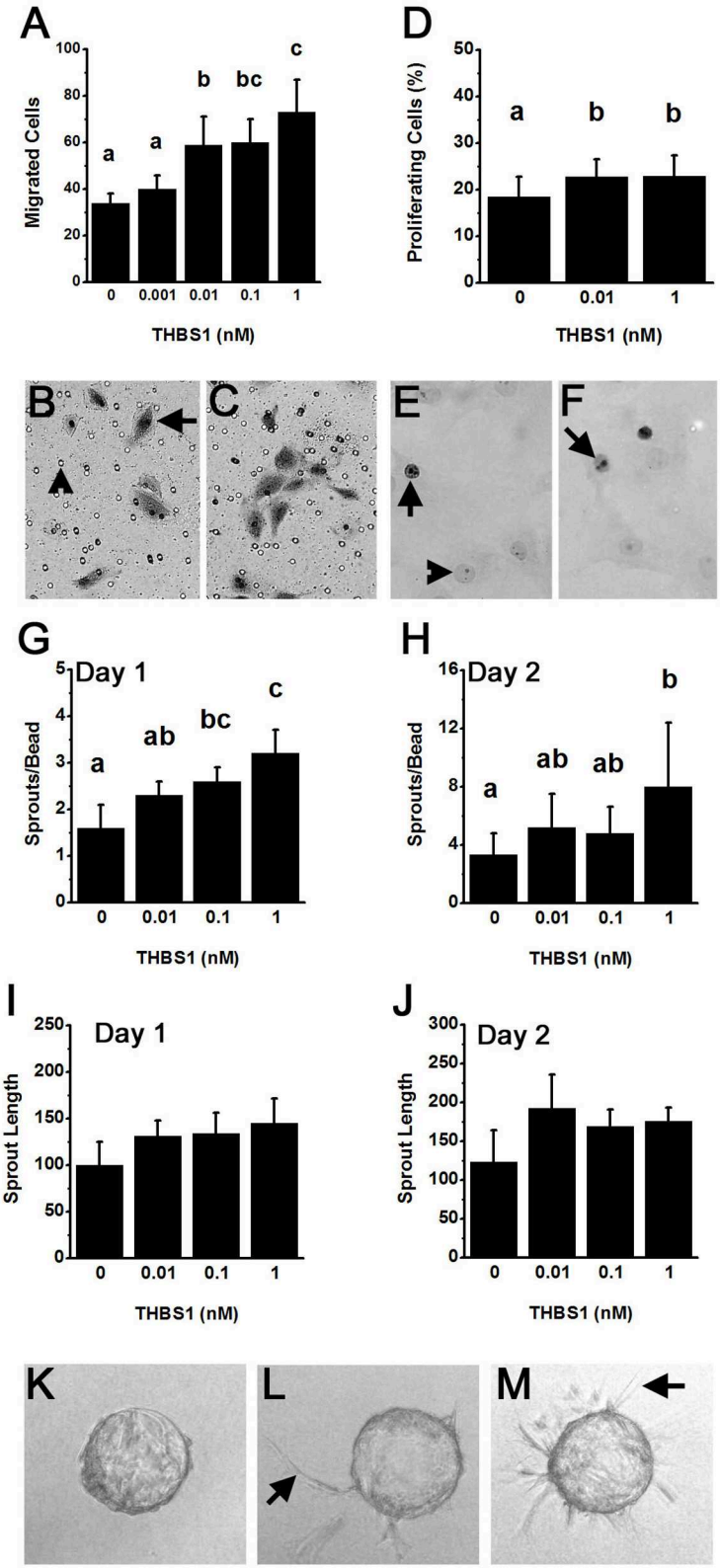

FIGURE 3 | THBS1 is pro-angiogenic *in vitro*. Monkey ovarian microvascular endothelial cells (mOMECs) were treated with human THBS1 protein at concentrations of 0.001–1 nM or no THBS1 (0 nM) as indicated. **(A–C)** Migration was assessed 24 h after plating on a porous membrane and treatment with THBS1. mOMECs (arrow) which migrated through pores (arrowhead) were stained with hematoxylin and eosin, photographed, and counted. Representative membranes from 0 nM

(Continued)

FIGURE 3 | (B) and 1 nM **(C)** treatment groups are shown. **(D–F)** Proliferation was assessed by Ki67 immunodetection in mOMECs cultured for 24 h with THBS1. Ki67 positive (arrows) and negative (arrowhead) cells are indicated in representative images from mOMECs treated with 0 nM **(E)** and 1 nM **(F)** THBS1. Data are expressed as a percentage of Ki67 positive cells among all cells counted. **(G–M)** Sprout formation in response to THBS1 treatment was determined after 1 day **(G,I)** and 2 days **(H,J,L,M)** *in vitro*. mOMECs coating a polymer bead *in vitro* before THBS1 treatment (Day 0; **K**) shows absence of sprouts. Arrows indicate representative sprouts on Day 2 of treatment with no THBS1 **(L)** and 0.1 nM THBS1 **(M)**. Images were quantified for both the number of sprouts (sprouts/bead; **G,H**) and sprout length in μm **(H,J)**. For **(A,D,G–J)**, data are expressed as mean + SEM, $n = 3$–5 samples/treatment. Within each panel, groups with no common letters are different by ANOVA and Duncans *post hoc* test, $p < 0.05$.

significant change in granulosa cell THBS4 protein over the ovulatory interval, though a trend toward increasing THBS4 was noted (**Figure 1F**).

Granulosa cells were the primary ovarian cell type containing immunodetectable thrombospondin proteins. THBS1 was detected in granulosa cells, with little staining present in the ovarian stroma (**Figures 2A–D**). Similarly, THBS4 was detected primarily in granulosa cells (**Figures 2H–K**). Specificity of these primary antibodies was supported by identification of a single band on Western (**Figure 1D**) and confirmed by reduction in immunostaining following preabsorption of the antigen, which appeared similar to the absence of primary antibody, for THBS1 (**Figures 2F,G**) and THBS4 (**Figures 2M,N**). Walls of major stromal vessels also showed evidence of THBS1 immunodetection (**Figure 2O**). Occasional cells in the stroma underlying the granulosa cell basement membrane also showed staining for THBS1 (**Figures 2A,E**) and THBS4 (**Figure 2J**). However, similarly-located cells were stained when the primary antibody was omitted (**Figures 2G,N–P**), so this stromal staining may not represent specific detection of THBS proteins.

Previous studies demonstrated that follicular levels of PGE2, a key ovulatory mediator, increase 24–36 h after hCG in macaque follicles (16). To determine if prostaglandins mediate the hCG-stimulated increase in granulosa cell thrombospondin mRNA or protein levels, additional monkeys experiencing ovarian stimulation also received the PTGS2 inhibitor celecoxib, which blocks follicular prostaglandin synthesis and reduces follicular PGE2 concentrations to very low levels (16). Celecoxib treatment reduced the increase in *THBS1* and *THBS4* mRNAs in granulosa cells collected 36 h after hCG (**Figures 1A,C**). However, celecoxib did not alter granulosa THBS1 and THBS4 protein levels when compared to hCG only after 36 h of treatment (**Figures 1E,F**). Finally, celecoxib treatment did not alter THBS2 mRNA (**Figure 1B**) or result in an apparent change in THBS1 or THBS4 immunodetection in monkey ovarian follicles (**Figures 2E,L**).

THBS1 Regulates Angiogenic Functions *in vitro*

Endothelial cells obtained from monkey ovulatory follicles (mOMECs) were used for *in vitro* studies to explore the role of thrombospondin in angiogenesis of the ovulatory follicle. THBS1 was selected as an agonist for these studies since *THBS1* mRNA was expressed at the high levels in granulosa cells, and THBS1 protein showed significant increase with hCG *in vivo* (**Figure 1**).

Capillary formation involves endothelial cell migration and proliferation to form a new capillary sprout (21). mOMECs showed increased migration in response to THBS1 (**Figures 3A–C**). THBS1 increased mOMEC migration in a dose-dependent manner, with 0.01–1 nM concentrations of THBS1 stimulating an increase in migrated cells (**Figure 3A**). THBS1 also stimulated a small but significant increase in mOMEC proliferation *in vitro* (**Figures 3D–F**).

An *in vitro* model was used to determine if THBS1 stimulated mOMECs to form new capillary-like endothelial cell sprouts (**Figures 3G–M**). THBS1 treatment increased the number of sprouts formed in a dose-dependent manner after 1 day in culture when compared to sprouts formed in media without THBS1 (**Figure 3G**). A similar dose-dependent increases in sprout number was observed after 2 days in culture (**Figure 3H**). THBS1 treatment did not alter sprout length at any dose after 1 day (**Figure 3I**) or 2 days *in vitro* (**Figure 3J**). However, analysis of all sprout length data identified a small but significant increase in sprout length in response to THBS1 treatment when compared with no treatment (ANOVA with two repeated measures, $p < 0.05$).

The ability of THBS1 to stimulate pro-angiogenic actions in mOMECs contrasts with the majority of reports demonstrating a role for THBS1 as an angiogenesis inhibitor (22). For this reason, a common primary endothelial cell population, human umbilical vein endothelial cells (HUVECs), was assessed in our migration assay. There was no difference between the number of migrated HUVECs after 24 h treatment with no THBS1 (14.7 ± 2.7), 0.1 nM THBS1 (10.6 ± 1.1), or 10 nM THBS1 (15.2 ± 2.6) ($p > 0.05$, $n = 3$ independent experiments).

THBS1 Antibody Reduces Ovulation *in vivo*

To examine the role of THBS1 in primate ovulation, luteinization, and follicular angiogenesis, preovulatory monkey follicles were injected with an antibody against THBS1 or control IgG. An ovulatory dose of hCG was administered immediately after follicle injection. The ovary was removed 48 h later, with ovulation is anticipated at about 40 h after the ovulatory gonadotropin stimulus. Serum estradiol and progesterone were not different between treatment groups before or after follicle injection (**Figures 4A,B**). To confirm that the THBS1 antibody neutralizes THBS1 bioactivity, THBS1 was preincubated with the THBS1 antibody before use in the mOMEC migration assay. In these experiments, THBS1 (1 nM) increased migration (**Figure 4C**). Preincubation of THBS1 with the THBS1 antibody reduced migration to levels measured in cells cultured without THBS1. Treatment with the THBS1 antibody alone did not increase or decrease migration compared with untreated cells (**Figure 4C**).

Control IgG-injected ovaries showed evidence of normal ovulation and luteinization. A protruding and bloody ovulatory

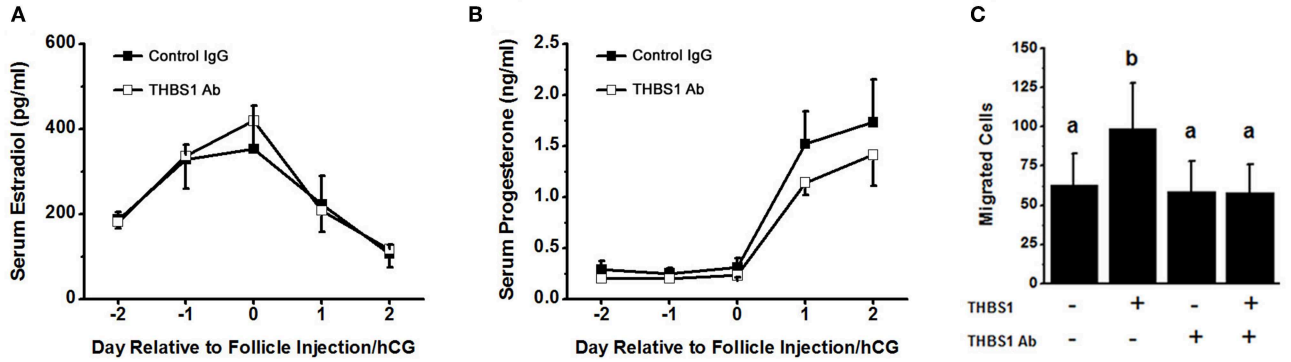

FIGURE 4 | Confirmatory experiments for the intrafollicular antibody injections. Serum levels of estradiol **(A)** and progesterone **(B)** were not different between animals receiving intrafollicular injection of the THBS1 antibody and animals receiving control IgG. For each day, hormone levels were compared by unpaired *t*-test. Data are expressed as mean + SEM, $n = 4$/group. **(C)** THBS1 antibody reduces THBS1 (1 nM)-stimulated mOMEC migration *in vitro*. Within each panel, groups with no common letters are different by ANOVA with 1 repeated measure and Duncans *post hoc* test, $p < 0.05$. Data are expressed as mean + SEM, $n = 3$/group.

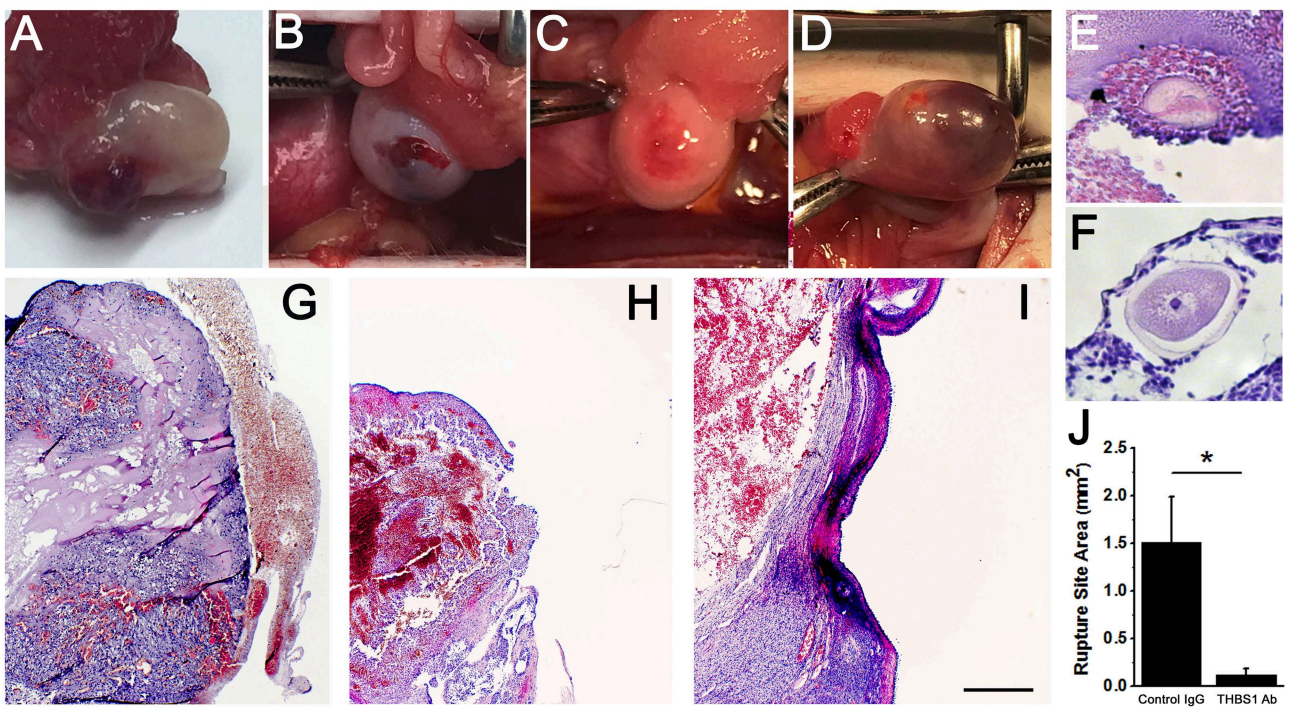

FIGURE 5 | Follicle rupture and oocyte release are compromised after intrafollicular injection with an antibody against THBS1. Ovarian surface at the time of ovary removal after intrafollicular injection of control IgG **(A)** or THBS1 antibody **(B–D)**. Oocytes were located within a THBS1 antibody-injected follicle **(E)** and on the surface of a THBS1 antibody-injected follicle **(F)**. Rupture site after intrafollicular injection of control IgG **(G)**. Rupture sites in follicles injected with the THBS1 antibody were either small **(H)** or absent **(I)**. Tissues shown in **(E–I)** were stained with hematoxylin and eosin. Oocytes **(E,F)** shown at approximately maximal diameter. Images in **(G–I)** are at the same magnification; bar in **(I)** = 0.5 mm. **(J)** Rupture site area after intrafollicular injection with control IgG (IgG) or THBS1 antibody. Groups are different by two-tailed unpaired *t*-test as indicated by $^*p < 0.05$. Data are expressed as mean + SEM, $n = 4$/group.

stigmata was visible on each control IgG-injected ovary at the time of removal at surgery (**Figure 5A**). For each control IgG-injected ovary, the presence of a single rupture site was confirmed upon histological examination (**Table 1**, **Figure 5G**). Oocytes were not identified within any of the control IgG-injected follicles (**Table 1**).

Follicle rupture was reduced in THBS1 antibody-injected ovaries (**Table 1**). Classical ovulatory stigmata were not observed on the surface of any THBS1 antibody-injected ovary (**Figures 5B–D**). Appearances ranged from small disruptions of the ovarian surface (**Figures 5B,C**) to formation of an enlarged hemorrhagic, but unruptured, follicle (**Figure 5D**). Histological

TABLE 1 | Oocyte retention and follicle rupture.

	Control IgG	THBS1 Ab
Oocyte retained in ovary	0/4	2/4
Rupture site present	4/4	2/4

examination showed that two of four THBS1 antibody-injected ovaries possessed very small rupture sites (**Figure 5H**), and two of four showed no breach in the ovarian surface (**Figure 5I**). Overall, THBS1 antibody-injection reduced the area of the ovulation site when compared with control IgG-injected ovaries (**Figure 5J**).

Oocytes were not located in any of the control IgG injected ovaries. However, two oocytes were located within unruptured follicles of THBS1 antibody-injected ovaries (**Table 1**, **Figure 5E**). One additional oocyte in expanded cumulus was located on the exterior surface of a THBS1 antibody-injected ovary, just outside the rupture site (**Figure 5F**). Interestingly, two of the three oocytes identified were germinal vesicle (GV) intact (**Figure 5F**), despite 48 h of exposure to an ovulatory dose of hCG.

THBS1 Antibody Alters Luteinization and Angiogenesis *in vivo*

Control IgG-injected follicles were well-luteinized, with an enlarged granulosa cell layer containing hypertrophied granulosa cells (**Figures 6A,C**). In contrast, the granulosa cell layer of THBS1 antibody-injected follicles was significantly thinner (**Figures 6B,D**). Granulosa cells appeared smaller and more densely packed when compared with control IgG-injected follicles (compare **Figure 6A** with **Figure 6B**; compare **Figure 6G** with **Figure 6I**). Where an expanded granulosa cell layer was noted in THBS1 antibody-injected follicles, the cells had foamy-appearing cytoplasm, which contrasted with the smooth appearance of granulosa cell cytoplasm in control IgG-injected follicles. THBS1 antibody-injected follicles showed more evidence of granulosa cell expansion in the granulosa cells close to the follicle antrum, while granulosa cells along the basement membrane remained more densely packed.

Follicular angiogenesis was evident in both control IgG-injected and THBS1 antibody-injected follicles. Vascular endothelial cells are restricted to the follicle stroma before hCG or the ovulatory LH surge (3). In the present study, staining for VWF identified vascular endothelial cells in the granulosa cell layer of both control IgG-injected and THBS1 antibody-injected follicles obtained 48 h after hCG (**Figures 6A,B**). In control IgG-injected follicles, VWF+ cells extended near to the antral edge of the luteinizing granulosa cells (**Figures 6A,E**), penetrating 89 ± 5% of the granulosa cell layer (**Figure 6F**). 3D modeling shows that VWF+ cells within the granulosa cell layer formed capillary-like networks which initiate at larger stromal vessels and produced a multi-branched network of VWF+ cells within the granulosa cell layer (**Figures 6G,H**). Red blood cells were visible within VWF+ cell-bordered spaces (**Figure 6A**), highlighting the luminal spaces forming within this capillary-like network.

Antibody neutralization of THBS1 reduced angiogenesis in the primate ovulatory follicle. VWF+ cells were located predominantly near the granulosa cell basement membrane of THBS1 antibody-injected follicles (**Figure 6B**). VWF+ cells penetrated less of the granulosa cell layer (**Figure 6E**) when compared to control IgG-injected follicles, reaching only 32 ± 7% of the distance between the granulosa cell basement membrane and the antral edge of the expanding granulosa cell layer (**Figure 6F**). 3D modeling of a THBS1 antibody-injected follicle confirms that VWF+ cells are present among granulosa cells, but groups of VWF+ cells do not connect back to stromal vessels (**Figures 6I,J**). In addition, less branching of capillary-like structures was seen in THBS1 antibody-injected follicles when compared with control IgG-injected follicles (**Figure 6J**). Capillary luminal spaces containing red blood cells were not observed in the THBS1 antibody-injected follicles (**Figure 6B**). However, the antrums of THBS1 antibody-injected follicles contained more numerous red blood cells (**Figures 5D,H,I**) when compared with control IgG-injected follicles (**Figure 5G**).

DISCUSSION

Angiogenesis is an essential component of the ovulatory cascade, since follicular angiogenesis is required for follicle rupture and oocyte release [reviewed in (1)]. Formation of new capillaries within the ovulatory follicle is initiated by the ovulatory LH surge. On a cellular level, angiogenesis is regulated by the coordinated effects of many vascular growth factors. In the primate ovulatory follicle, increased permeability of stromal vessels provides components for follicular fluid and permits immune cell movement from the circulation into the follicle. Vascular remodeling requires both stability and flexibility; stromal vessels must remain intact while new capillaries form and branch into the luteinizing granulosa cell layer. The LH surge has previously been shown to regulate follicular expression of both pro-angiogenic and anti-angiogenic growth factors. In this report, we identify THBS1 as an LH-stimulated vascular growth factor necessary for ovulatory angiogenesis, follicle rupture, and oocyte release in primates.

The LH surge stimulates expression of thrombospondin family members by granulosa cells of monkey ovulatory follicles. *THBS1* and *THBS4* mRNA levels increased by 24 h after administration of the ovulatory gonadotropin stimulus. However, only THBS1 protein levels were increased by 36 h, very near the time of ovulation in this macaque species. Levels of *THBS2* mRNA did not change across the ovulatory interval. Immunostaining showed that granulosa cells are likely the primary source of THBS1 and THBS4 proteins in the ovulatory follicle, with strong staining in the granulosa cell layer. Other cell types of the ovulatory follicle may also express THBS family members. Moderate staining in stromal structures, including walls of established stromal vessels, was also noted. Previous studies in marmosets, cows, and rodent species have identified granulosa cells as the primary source of THBS family members in ovarian follicles (9, 11, 14). Granulosa cell expression of *THBS1* and *THBS2* were reported to be highest in atretic follicles,

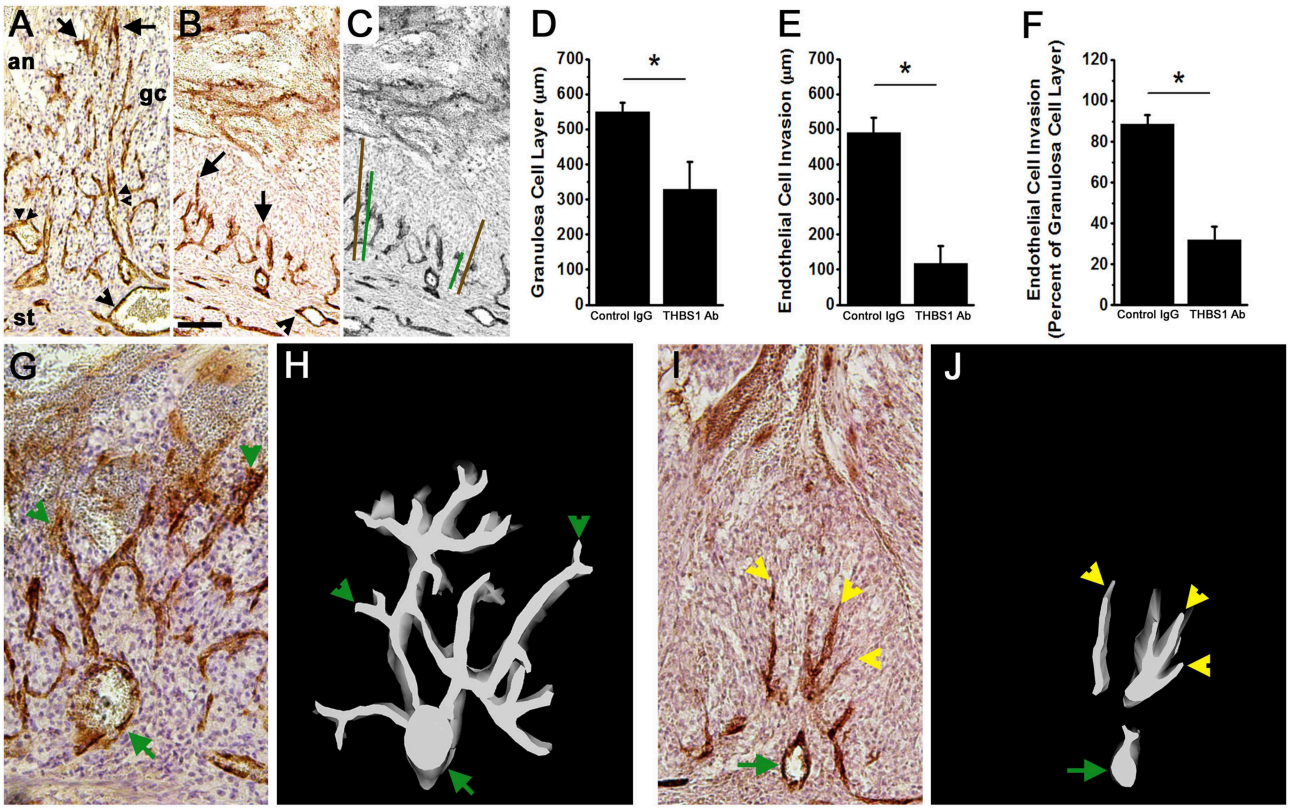

FIGURE 6 | Angiogenesis and luteinization are compromised after intrafollicular injection with an antibody against THBS1. Histological sections of ovaries shown in **Figure 5** were immunostained for VWF (brown) to assess angiogenesis; hematoxylin counterstain. **(A,B)** Endothelial cell invasion into the granulosa cell layer of a control IgG-injected follicle **(A)** and THBS1 antibody-injected follicle **(B)** shows VWF+ cells within the granulosa cell (gc) layer. Arrows indicate VWF+ cells which have invaded furthest from the stroma into the granulosa cell layer. Single arrowheads indicate stromal vessels. Double arrowheads indicate capillary luminal spaces with red blood cells in the control-IgG injected follicle only. **(C)** shows representative measurements of granulosa cell layer thickness (brown lines) and endothelial cell invasion (green lines). **(A–C)** are oriented as shown in **(A)**, with stroma (st) at bottom, granulosa cell (gc) layer central, and follicle antrum (an) at top. Images in **(A–C)** are at the same magnification; bar in **(B)** is 100 µm. Granulosa cell layer thickness **(D)**, endothelial cell invasion **(E)**, and the percent of the granulosa cell layer penetrated by endothelial cells **(F)** after intrafollicular injection with control IgG (IgG) or THBS1 antibody. Groups are different by two-tailed unpaired *t*-test as indicated by $^*p < 0.05$. Data are expressed as mean + SEM, $n = 4$/group. **(H,J)** 3D modeling of endothelial cells (white on black background) is shown alongside **(G,I)** representative VWF immunostained ovarian sections after intrafollicular injection with control IgG **(G,H)** or THBS1 antibody **(I,J)**. Green arrows indicate stromal vessels, green arrowheads indicate capillary-like structures that connect to a stromal vessel, and yellow arrowheads indicate endothelial cells that lack connect to a stromal vessel. **(G–J)** are oriented with antrum at the top, granulosa cells central, and stroma at the bottom of each image/model; **(G,I)** at the same magnification.

ovulatory follicles after the gonadotropin surge, and in the large luteal cells of the developing corpus luteum (9, 11, 14, 15). Both FSH and LH have been shown to stimulate THBS family member expression by granulosa cells *in vitro* (9, 14). This pattern of LH-stimulated THBS family member expression is similar to our previous report of changing VEGF receptor ligands in the monkey ovulatory follicle. In this previous study, follicular VEGFA levels peaked soon after the LH surge while PGF levels peaked at the end of the ovulatory period, just before ovulation (18).

Prostaglandins have been suggested as key regulators of ovarian thrombospondin expression. LH-stimulated elevation of PGE2 and PGF2α levels in primate follicular fluid (17, 23) correlate with peak *THBS1* and *THBS4* mRNAs (**Figure 1**). In the present study, blockade of prostaglandin synthesis with celecoxib prevented the rise in *THBS1* and *THBS4* mRNA observed just before ovulation. However, THBS1 and THBS4 protein levels were not affected. PGE2 is a critical mediator of the ovulatory LH surge (24), and several PGE2 receptors are necessary for ovulation in primates (25). PGF2α increases THBS1 and THBS2 mRNAs in the bovine corpus luteum, where THBS1 plays a role in luteal regression (5). PGF2α receptors present in granulosa cells of the primate ovulatory follicle and young corpus luteum are not capable of signal transduction (26), so the PGF2α pathway is not available to regulate expression of thrombospondins, despite elevated follicular PGF2α levels. PGF2α receptors in primate luteal cells can mediate PGF2α signals later in the luteal phase (26). While prostaglandins are not a key regulators of thrombospondin protein levels in the primate ovulatory follicle, prostaglandins may regulate thrombospondin expression and activity in the primate corpus luteum, especially during luteal regression.

THBS1 is a potent stimulus for follicular angiogenesis *in vitro* and *in vivo*. THBS1 increased monkey ovarian endothelial cell migration and capillary sprout formation *in vitro*. THBS1 only modestly increased endothelial cell proliferation and overall length of capillary sprouts formed *in vitro*. These findings are consistent with a role for THBS1 to promote the differentiation of an endothelial cell into a tip cell, which migrates away from an established vessel and leads the formation of a new capillary sprout (21). THBS1 did not appear to promote the formation of stalk cells, which proliferate and form the tube of the capillary and connects the migrating tip cell to the parent vessel to establish blood flow (21). In the monkey ovulatory follicle *in vivo*, endothelial cells formed branching capillary-like networks that extended from stromal vessels to the antral edge of the luteinizing granulosa cell layer. In contrast, antibody neutralization of THBS1 resulted in limited follicular angiogenesis, even though established stimuli of follicular angiogenesis [such as VEGFA, placental growth factor (PGF), and PGE2 (3, 18, 25, 27, 28)] were likely still present. In THBS1 antibody-injected follicles, endothelial cells showed limited penetration into the granulosa cell layer, with little or no branching of capillary networks. In addition, endothelial cells present in the granulosa cell layer failed to maintain connectivity to nearby stromal vessels. A similar phenotype was seen in a previous study where a follicular administration of a PGF antibody altered follicular angiogenesis and blocked ovulation in primates (18). In branching angiogenesis, the migrating tip cell instructs adjacent endothelial cells to form stalk cells through signaling systems such as the NOTCH pathway (29–31). Failure of stalk cells to form in THBS1 antibody-injected follicles suggests that THBS1 may be involved in communication between tip and stalk cells or for the establishment of the stalk cell phenotype.

THBS1 blockade led to extensive accumulation of red blood cells (RBCs) within the follicle antrum. THBS1 interacts with components of the extracellular matrix (ECM) to support the structural integrity of the ECM and is most often described as an inhibitor of protease activity (32–34). THBS1 neutralization by antibody injection may lead to excessive proteolysis of ECM components, degradation of cell-cell and cell-matrix adhesion proteins, and liberation of matrix-associated growth factors in the stroma surrounding ovulatory follicles. THBS1 neutralization may contribute to the degradation of junctional complexes, creating leaky vessels and thereby increasing vascular permeability (35, 36). For example, THBS1 interacts with integrins and collagen cross-linking sites to mediate cell adhesion and firmly attach endothelial cells to the surrounding matrix; THBS1 also stimulates the phosphorylation of adherens, which form junctions between adjacent endothelial cells (22, 37). Many vascular growth factors, including VEGFA, are associated with ECM; proteolysis liberates these growth factors to establish the gradient that guides tip cells during angiogenesis (38). Without inhibition from THBS1, proteases may excessively liberate growth factors, disrupting gradients that simultaneously promote angiogenesis and create stable vessels (39). Lastly, THBS1 is known to facilitate RBC adhesion to endothelial cells (34, 40). Our 3D model shows that THBS1 is needed for the formation of capillary stalks. In the absence of stalk formation and without THBS1 to promote adhesion of RBCs to endothelial cells, fenestrations in the stromal vessel required for sprouting angiogenesis may provide an opening through which RBCs can flow uncontrolled, contributing to the pooling of RBCs in the follicle antrum (38). The specific mechanism is unknown and will require further investigation. However, through one or perhaps multiple mechanisms, THBS1 may be a key regulator of vascular permeability in the primate ovulatory follicle.

Overall, our studies demonstrate that THBS1 acts as a pro-angiogenic factor as the primate preovulatory follicle transforms into a corpus luteum. Most published reports describe THBS1 as an anti-angiogenic factor [reviewed in (41)]. However, THBS1 can act as a pro-angiogenic factor to promote endothelial cell proliferation, migration, and overall vascular growth (7, 8, 42, 43). Interestingly, pro-angiogenic actions of THBS1 are seen primarily in developing systems, while anti-angiogenic actions of THBS1 are often associated with tumor growth and wound healing (41). Pro-angiogenic actions of THBS1 are typically mediated via the N-terminus region of the molecule, which can interact with cell surface receptors including LRP1 and SDC4 (44). In contrast, anti-angiogenic actions of THBS1 are often mediated via THBS1's type I repeats interacting with CD36 receptors or through sequestration of pro-angiogenic factors such as VEGFA (44). Expression of CD36 in the ovary corresponds with THBS1's established role as an inhibitor of angiogenesis during follicle development, contributing to follicle atresia (14). There is limited information regarding expression of THBS1 receptors in non-human primate or human ovulatory follicles. However, increased CD36 was associated with poor human granulosa cell function (45), while elevated expression of SDC4 in human cumulus cells correlated with improved outcomes for IVF patients (46). The ability of THBS1 to act as a pro-angiogenic or anti-angiogenic factor may also be determined by THBS1 concentration (47), again highlighting the complexity of this system. In the primate ovulatory follicle, pro-angiogenic actions of THBS1 clearly dominate.

THBS1 neutralization *in vivo* significantly compromised ovulation. Injection of the THBS1 antibody resulted in failure of follicle rupture in two of four cases, with two ovaries forming very small rupture sites. Well-controlled proteolysis is essential for rupture (1). Since THBS1 has been reported to inhibit breakdown of many of the connective tissue components present in the follicle wall and surrounding ovarian stroma (32–34), it is somewhat surprising that THBS1 neutralization did not lead to enlarged or multiple ruptures sites. Previous studies support a critical role for ovulatory angiogenesis in ovulatory events including follicle rupture (18, 25, 48, 49), so the positive impact of THBS1 on follicle rupture at ovulation may be secondary to THBS1's pro-angiogenic actions in the follicle. An additional interesting observation is that two of three oocytes identified associated with THBS1-antibody injected follicles did not resume meiosis. Histological observation of the few oocytes available in the present study suggests that at least some degree of cumulus expansion occurred during THBS1 neutralization. Cumulus expansion has been described as a necessary prerequisite

for resumption of oocyte meiosis (50). However, additional pathways promoting oocyte meiotic progression may be independent of cumulus expansion (51, 52). While much remains to be learned, our studies point to a critical role for thrombospondins, and in particular THBS1, as a paracrine regulator of follicular angiogenesis and ovulation in primates. A more complete understanding of THBS1 actions may ultimately enhance treatments for infertility and point to new targets for contraceptive development.

DATA AVAILABILITY STATEMENT

All datasets for this study are included in the manuscript/**Supplementary Files**.

ETHICS STATEMENT

Whole ovaries and ovarian biopsies were obtained from adult female cynomolgus macaques (Macaca fascicularis) at Eastern Virginia Medical School (Norfolk, VA). All animal protocols were conducted in accordance with the National Institutes of Health's Guide for the Care and Use of Laboratory Animals and were approved by the Eastern Virginia Medical School Animal Care and Use Committee.

AUTHOR CONTRIBUTIONS

HB, GC, PA, AM, and DD each contributed data to this manuscript, was involved in preparation of the manuscript, and approved the final version of this manuscript. DD obtained funding and performed statistical analysis.

ACKNOWLEDGMENTS

Recombinant human FSH and Ganirelix were generously provided by Merck & Co. The Eunice Kennedy Shriver National Institute of Child Health and Human Development provided Acyline and funding support (Grant P01 HD071875 to DD).

SUPPLEMENTARY MATERIAL

The Supplementary Material for this article can be found online at: https://www.frontiersin.org/articles/10.3389/fendo.2019.00727/full#supplementary-material

REFERENCES

1. Duffy DM, Ko C, Jo M, Brannstrom M, Curry TE. Ovulation: parallels with inflammatory processes. *Endocr Rev.* (2019) 40:369–416. doi: 10.1210/er.2018-00075
2. Fraser HM, Duncan WC. Vascular morphogenesis in the primate ovary. *Angiogenesis.* (2005) 8:101–16. doi: 10.1007/s10456-005-9004-y
3. Trau HA, Davis JS, Duffy DM. Angiogenesis in the primate ovulatory follicle is stimulated by luteinizing hormone via prostaglandin E2. *Biol Reprod.* (2015) 92:15. doi: 10.1095/biolreprod.114.123711
4. Adams JC, Lawler J. The thrombospondins. *Cold Spring Harb Perspect Biol.* (2011) 3:a009712. doi: 10.1101/cshperspect.a009712
5. Farberov S, Basavaraja R, Meidan R. Thrombospondin-1 at the crossroads of corpus luteum fate decisions. *Reproduction.* (2018) 157:R73–R83. doi: 10.1530/REP-18-0530
6. Dawson DW, Pearce SF, Zhong R, Silverstein RL, Frazier WA, Bouck NP. CD36 mediates the *in vitro* inhibitory effects of thrombospondin-1 on endothelial cells. *J Cell Biol.* (1997) 138:707–17. doi: 10.1083/jcb.138.3.707
7. Orr AW, Elzie CA, Kucik DF, Murphy-Ullrich JE. Thrombospondin signaling through the calreticulin/LDL receptor-related protein co-complex stimulates random and directed cell migration. *J Cell Sci.* (2003) 116:2917–27. doi: 10.1242/jcs.00600
8. Orr AW, Pedraza CE, Pallero MA, Elzie CA, Goicoechea S, Strickland DK, et al. Low density lipoprotein receptor-related protein is a calreticulin coreceptor that signals focal adhesion disassembly. *J Cell Biol.* (2003) 161:1179–89. doi: 10.1083/jcb.200302069
9. Greenaway J, Gentry PA, Feige JJ, Lamarre J, Petrik JJ. Thrombospondin and vascular endothelial growth factor are cyclically expressed in an inverse pattern during bovine ovarian follicle development. *Biol Reprod.* (2005) 72:1071–8. doi: 10.1095/biolreprod.104.031120
10. Greenaway J, Lawler J, Moorehead R, Bornstein P, Lamarre J, Petrik J. Thrombospondin-1 inhibits VEGF levels in the ovary directly by binding and internalization via the low density lipoprotein receptor-related protein-1 (LRP-1). *J Cell Physiol.* (2007) 210:807–18. doi: 10.1002/jcp.20904
11. Thomas FH, Wilson H, Silvestri A, Fraser HM. Thrombospondin-1 expression is increased during follicular atresia in the primate ovary. *Endocrinology.* (2008) 149:185–92. doi: 10.1210/en.2007-0835
12. Osz K, Ross M, Petrik J. The thrombospondin-1 receptor CD36 is an important mediator of ovarian angiogenesis and folliculogenesis. *Reprod Biol Endocrinol.* (2014) 12:21. doi: 10.1186/1477-7827-12-21
13. Higuchi T, Fujiwara H, Yamada S, Tatsumi K, Kataoka N, Itoh K, et al. Co-expression of integrin-associated protein (IAP/CD47) and its ligand thrombospondin-1 on human granulosa and large luteal cells. *Mol Hum Reprod.* (1999) 5:920–6. doi: 10.1093/molehr/5.10.920
14. Petrik JJ, Gentry PA, Feige JJ, Lamarre J. Expression and localization of thrombospondin-1 and−2 and their cell-surface receptor, CD36, during rat follicular development and formation of the corpus luteum. *Biol Reprod.* (2002) 67:1522–31. doi: 10.1095/biolreprod.102.007153
15. Berisha B, Schams D, Rodler D, Sinowatz F, Pfaffl MW. Expression and localization of members of the thrombospondin family during final follicle maturation and corpus luteum formation and function in the bovine ovary. *J Reprod Dev.* (2016) 62:501–10. doi: 10.1262/jrd.2016-056
16. Seachord CL, Vandevoort CA, Duffy DM. Adipose-differentiation related protein: a gonadotropin- and prostaglandin-regulated protein in primate periovulatory follicles. *Biol Reprod.* (2005) 72:1305–14. doi: 10.1095/biolreprod.104.037523
17. Duffy DM, Dozier BL, Seachord CL. Prostaglandin dehydrogenase and prostaglandin levels in periovulatory follicles: implications for control of primate ovulation by PGE2. *J Clin Endocrinol Metab.* (2005) 90:1021–7. doi: 10.1210/jc.2004-1229
18. Bender HR, Trau HA, Duffy DM. Placental growth factor is required for ovulation, luteinization, and angiogenesis in primate ovulatory follicles. *Endocrinology.* (2018) 159:710–22. doi: 10.1210/en.2017-00739
19. Weick RF, Dierschke DJ, Karsch FJ, Butler WR, Hotchkiss J, Knobil E. Periovulatory time course of circulating gonadotropic and ovarian hormones in the rhesus monkey. *Endocrinology.* (1973) 93:1140–7. doi: 10.1210/endo-93-5-1140
20. Duffy DM, Seachord CL, Dozier BL. Microsomal prostaglandin E synthase-1 (mPGES-1) is the primary form of PGES expressed by the primate periovulatory follicle. *Hum Reprod.* (2005) 20:1485–92. doi: 10.1093/humrep/deh784

21. Herbert SP, Stainier DYR. Molecular control of endothelial cell behaviour during blood vessel morphogenesis. *Nat Rev.* (2011) 12:551–64. doi: 10.1038/nrm3176
22. Huang T, Sun L, Yuan X, Qiu H. Thrombospondin-1 is a multifaceted player in tumor progression. *Oncotarget.* (2017) 8:84546–58. doi: 10.18632/oncotarget.19165
23. Dozier BL, Watanabe K, Duffy DM. Two pathways for prostaglandin F2a synthesis by the primate periovulatory follicle. *Reproduction.* (2008) 136:53–63. doi: 10.1530/REP-07-0514
24. Duffy DM, Stouffer RL. Follicular administration of a cyclooxygenase inhibitor can prevent oocyte release without alteration of normal luteal function in rhesus monkeys. *Hum Reprod.* (2002) 17:2825–31. doi: 10.1093/humrep/17.11.2825
25. Kim SO, Harris SM, Duffy DM. Prostaglandin E2 (EP) receptors mediate PGE2-specific events in ovulation and luteinization within primate ovarian follicles. *Endocrinology.* (2014) 155:1466–75. doi: 10.1210/en.2013-2096
26. Kim SO, Markosyan N, Pepe GJ, Duffy DM. Estrogen promotes luteolysis by redistributing prostaglandin F2a receptors within primate luteal cells. *Reproduction.* (2015) 149:453–64. doi: 10.1530/REP-14-0412
27. Coultas L, Chawengsaksophak K, Rossant J. Endothelial cells and VEGF in vascular development. *Nature.* (2005) 438:937–45. doi: 10.1038/nature04479
28. Trau HA, Brannstrom M, Curry TEJ, Duffy DM. Prostaglandin E2 and vascular endothelial growth factor A mediate angiogenesis of human ovarian follicular endothelial cells. *Hum Reprod.* (2016) 31:436–44. doi: 10.1093/humrep/dev320
29. Noguera-Troise I, Daly C, Papadopoulos NJ, Coetzee S, Boland P, Gale NW, et al. Blockade of Dll4 inhibits tumour growth by promoting non-productive angiogenesis. *Nature.* (2006) 444:1032–7. doi: 10.1038/nature05355
30. Leslie JD, Ariza-Mcnaughton L, Bermange AL, Mcadow R, Johnson SL, Lewis J. Endothelial signalling by the notch ligand delta-like 4 restricts angiogenesis. *Development.* (2007) 134:839–44. doi: 10.1242/dev.003244
31. Suchting S, Freitas C, Le Noble F, Benedito R, Breant C, Duarte A, et al. The Notch ligand Delta-like 4 negatively regulates endothelial tip cell formation and vessel branching. *Proc Natl Acad Sci USA.* (2007) 104:3225–30. doi: 10.1073/pnas.0611177104
32. Silverstein RL, Leung LL, Harpel PC, Nachman RL. Complex formation of platelet thrombospondin with plasminogen. Modulation of activation by tissue activator. *J Clin Invest.* (1984) 74:1625–33. doi: 10.1172/JCI111578
33. Bentley AA, Adams JC. The evolution of thrombospondins and their ligand-binding activities. *Mol Biol Evol.* (2010) 27:2187–97. doi: 10.1093/molbev/msq107
34. Chistiakov DA, Melnichenko AA, Myasoedova VA, Grechko AV, Orekhov AN. Thrombospondins: a role in cardiovascular disease. *Int J Mol Sci.* (2017) 18:E1540. doi: 10.3390/ijms18071540
35. Katayama T, Kusanagi Y, Kiyomura M, Ochi H, Ito M. Leukocyte behaviour and permeability in the rat mesenteric microcirculation following induction of ovulation. *Hum Reprod.* (2003) 18:1179–84. doi: 10.1093/humrep/deg248
36. Csanyi G, Yao M, Rodriguez AI, Al Ghouleh I, Sharifi-Sanjani M, Frazziano G, et al. Thrombospondin-1 regulates blood flow via CD47 receptor-mediated activation of NADPH oxidase 1. *Arterioscler Thromb Vasc Biol.* (2012) 32:2966–73. doi: 10.1161/ATVBAHA.112.300031
37. Yan Q, Murphy-Ullrich JE, Song Y. Structural insight into the role of thrombospondin-1 binding to calreticulin in calreticulin-induced focal adhesion disassembly. *Biochemistry.* (2010) 49:3685–94. doi: 10.1021/bi902067f
38. Ribatti D, Crivellato E. "Sprouting angiogenesis", a reappraisal. *Dev Biol.* (2012) 372:157–65. doi: 10.1016/j.ydbio.2012.09.018
39. Hanahan D. Signaling vascular morphogenesis and maintenance. *Science.* (1997) 277:48–50. doi: 10.1126/science.277.5322.48
40. Wautier MP, El Nemer W, Gane P, Rain JD, Cartron JP, Colin Y, et al. Increased adhesion to endothelial cells of erythrocytes from patients with polycythemia vera is mediated by laminin alpha5 chain and Lu/BCAM. *Blood.* (2007) 110:894–901. doi: 10.1182/blood-2006-10-048298
41. Lawler J. Thrombospondin-1 as an endogenous inhibitor of angiogenesis and tumor growth. *J Cell Mol Med.* (2002) 6:1–12. doi: 10.1111/j.1582-4934.2002.tb00307.x
42. Chen J, Somanath PR, Razorenova O, Chen WS, Hay N, Bornstein P, et al. Akt1 regulates pathological angiogenesis, vascular maturation and permeability *in vivo*. *Nat Med.* (2005) 11:1188–96. doi: 10.1038/nm1307
43. Staniszewska I, Zaveri S, Del Valle L, Oliva I, Rothman VL, Croul SE, et al. Interaction of alpha9beta1 integrin with thrombospondin-1 promotes angiogenesis. *Circ Res.* (2007) 100:1308–16. doi: 10.1161/01.RES.0000266662.98355.66
44. Resovi A, Pinessi D, Chiorino G, Taraboletti G. Current understanding of the thrombospondin-1 interactome. *Matrix Biol.* (2014) 37:83–91. doi: 10.1016/j.matbio.2014.01.012
45. Wu RX, Dong YY, Yang PW, Wang L, Deng YH, Zhang HW, et al. CD36-and obesity-associated granulosa cells dysfunction. *Reprod Fertil Dev.* (2019) 31:993–1001. doi: 10.1071/RD18292
46. Wathlet S, Adriaenssens T, Segers I, Verheyen G, Van De Velde H, Coucke W, et al. Cumulus cell gene expression predicts better cleavage-stage embryo or blastocyst development and pregnancy for ICSI patients. *Hum Reprod.* (2011) 26:1035–51. doi: 10.1093/humrep/der036
47. Bornstein P. Thrombospondins function as regulators of angiogenesis. *J Cell Commun Signal.* (2009) 3:189–200. doi: 10.1007/s12079-009-0060-8
48. Hazzard TM, Rohan RM, Molskness TA, Fanton JW, D'amato RJ, Stouffer RL. Injection of anti-angiogenic agents into the macaque preovulatory follicle: disruption of corpus luteum development and function. *Endocrine.* (2002) 17:199–206. doi: 10.1385/ENDO:17:3:199
49. Wulff C, Wilson H, Wiegand SJ, Rudge JS, Fraser HM. Prevention of thecal angiogenesis, antral follicular growth, and ovulation in the primate by treatment with vascular endothelial growth factor trap R1R2. *Endocrinology.* (2002) 143:2797–807. doi: 10.1210/endo.143.7.8886
50. Robker RL, Hennebold JD, Russell DL. Coordination of ovulation and oocyte maturation: a good egg at the right time. *Endocrinology.* (2018) 159:3209–18. doi: 10.1210/en.2018-00485
51. Richard S, Baltz JM. Preovulatory suppression of mouse oocyte cell volume-regulatory mechanisms is via signalling that is distinct from meiotic arrest. *Sci Rep.* (2017) 7:702. doi: 10.1038/s41598-017-00771-y
52. Vigone G, Shuhaibar LC, Egbert JR, Uliasz TF, Movsesian MA, Jaffe LA. Multiple cAMP phosphodiesterases act together to prevent premature oocyte meiosis and ovulation. *Endocrinology.* (2018) 159:2142–52. doi: 10.1210/en.2018-00017

Conflict of Interest: The authors declare that the research was conducted in the absence of any commercial or financial relationships that could be construed as a potential conflict of interest.

frontiers in Endocrinology

ORIGINAL RESEARCH
published: 13 November 2019
doi: 10.3389/fendo.2019.00715

Global Transcriptomic Analysis of the Canine *corpus luteum* (CL) During the First Half of Diestrus and Changes Induced by *in vivo* Inhibition of Prostaglandin Synthase 2 (PTGS2/COX2)

Miguel Tavares Pereira[1], *Felix R. Graubner*[1], *Hubert Rehrauer*[2], *Tomasz Janowski*[3], *Bernd Hoffmann*[4], *Alois Boos*[1] *and Mariusz P. Kowalewski*[1]*

[1] Vetsuisse Faculty, Institute of Veterinary Anatomy, University of Zurich, Zurich, Switzerland, [2] Functional Genomics Center Zurich (FGCZ) ETH/UZH, Zurich, Switzerland, [3] Department of Animal Reproduction, University of Warmia and Mazury, Olsztyn, Poland, [4] Clinic for Obstetrics, Gynaecology and Andrology, Faculty of Veterinary Medicine, Justus Liebig University, Giessen, Germany

The canine luteal phase exhibits several peculiarities compared with other species. In early diestrus, the *corpus luteum* (CL) is, at least in part, independent of gonadotropins, and prostaglandins (PGs) appear to be among its main regulators. This was also observed with the inhibition *in vivo* of COX2, when also transcriptional capacity, vascularization and immune-related factors were affected. Here, we aimed to further investigate the potential effects of PGs withdrawal on the CL transcriptome by performing deep RNA sequencing (RNA-Seq). Samples from a previous *in vivo* study were used; bitches were treated for 5, 10, 20, or 30 days after ovulation with firocoxib (Previcox®), a PTGS2/COX2 inhibitor, or a placebo. Analysis of results was performed with SUSHI (framework from FGCZ) and with pathways and functional networks analyzers. Time-dependent effects were also investigated and used for quality control. More highly represented differentially expressed genes (DEGs, $P < 0.01$, FDR < 0.1) in the early CL (days 5 and 10) referred to proliferation and immune system, while in the mature CL (days 20 and 30) they were related with steroidogenesis. The absence of genes concomitantly affected by the treatment at all time-points suggested stage-dependency in the observed effects. Little effect was observed on days 5 and 10. Day 20 had the highest number of DEGs ($n = 1{,}741$), related with increased immune response. On day 30, DEGs found ($n = 552$) referred to decreased steroidogenesis and vascularization. Our results suggest the presence of strong compensatory effects in the early CL and multidirectional effects toward gonadotropin-dependency of the CL after COX2 inhibition.

Keywords: canine (dog), *corpus luteum*, prostaglandins, transcriptome (RNA-seq), diestrus

OPEN ACCESS

Edited by:
Marc Yeste,
University of Girona, Spain

Reviewed by:
Antonio Galvao,
Babraham Institute (BBSRC), United Kingdom
Jens Vanselow,
Leibniz Institute for Farm Animal Biology, Germany

***Correspondence:**
Mariusz P. Kowalewski
kowalewskipl@yahoo.de;
kowalewski@vetanat.uzh.ch

Specialty section:
This article was submitted to Reproduction, a section of the journal Frontiers in Endocrinology

Received: *05 May 2019*
Accepted: *03 October 2019*
Published: *13 November 2019*

Citation:
Tavares Pereira M, Graubner FR, Rehrauer H, Janowski T, Hoffmann B, Boos A and Kowalewski MP (2019) Global Transcriptomic Analysis of the Canine corpus luteum (CL) During the First Half of Diestrus and Changes Induced by in vivo Inhibition of Prostaglandin Synthase 2 (PTGS2/COX2). Front. Endocrinol. 10:715. doi: 10.3389/fendo.2019.00715

INTRODUCTION

The *corpus luteum* (CL) has a central role in pregnancy through its production of progesterone (P4). In dogs, it plays an even more prominent role because it regulates the entire diestric phase. Indeed, the absence of placental steroidogenic activity in this species makes the CL the sole source of pregnancy-supporting P4 (1, 2). Following exceptionally strong preovulatory luteinization (3), the CL continues to develop following ovulation. As in other species, this is supported by the formation of a dense vascular network (4, 5). Serum P4 levels vary greatly among animals and peak between days 15 and 30 after ovulation. Shortly thereafter, luteal function starts to diminish, accompanied by decreasing levels of P4 and signs of cellular degeneration (6–8). The function of the CL is actively terminated in pregnant bitches shortly before parturition (around day 60 after ovulation) during prepartum luteolysis. This is associated with increased circulating prostaglandin (PG)F2α, apparently produced by the fetal placenta (1, 9–12). Interestingly, no such active mechanism is observed in the absence of pregnancy (12, 13). There is no uterine luteolysin in non-pregnant dogs and hysterectomy does not affect CL function (12, 13). Consequently, non-pregnant bitches present a physiological pseudopregnancy, with circulating P4 levels similar to those in pregnant animals (14, 15). It appears thus, that in lacking an active luteolytic principle, the CL life span of non-pregnant dogs is regulated by some intrinsic regulatory mechanisms. At the regulatory level, the canine CL also presents some species-specific peculiarities compared with other domestic animals. Both LH and prolactin (PRL) have luteotropic roles in the canine CL (16–18). However, PRL appears to be the predominant factor and appears to be required for CL maintenance starting around day 25 after ovulation (19, 20). It is noteworthy that ablation of the hypophysis had less effect on CL function in the first 2–4 weeks after ovulation (17). Consequently, the canine CL presents a transitory independence on gonadotropins in its earlier stages, progressing to a gonadotropin-dependent stage at mid-diestrus, with PRL then acting as the predominant luteotropic factor (17, 18, 20).

The initial observation of increased expression of COX2/PTGS2 and PGE2 synthase (PTGES) in early CL stages suggested PGs as possible important regulators of this organ in the dog (21, 22). Further investigations showed direct effects of PGE2 in early canine luteal cells, in which it could increase steroidogenic acute regulatory (STAR) protein expression and P4 production (23). Following these clues, the effects of PGs on CL function were explored *in vivo* (3, 24). For this, firocoxib (Previcox, Merial Ltd.), a specific inhibitor of COX2, was used to treat bitches from the day of ovulation up to 30 days later, with the aim of causing functional withdrawal of PGs (3, 24). In fact, the expression of PTGES and intra-CL levels of PGE2 and PGF2α were significantly decreased by this treatment (3). It also affected the steroidogenic capacity of the CL (decreased expression of 3βHSD and STAR), and suppressed the levels of circulating P4 (3, 24). Furthermore, the decreased nuclear size of luteal cells induced by this treatment was related to their decreased transcriptional capacity (24). These observations showed a causality between COX2 and the PTGES-dependent synthesis of PGE2 in the CL and established PGs as important modulators of CL function (3, 24).

It appears, however, that PGs might have broader effects on the regulation of CL function in addition to steroidogenesis. COX2 inhibition decreased the expression of the PRL receptor (PRLR) while, in parallel, PGE2 could increase the expression of PRLR in isolated canine luteal cells (3). This suggested an indirect role of PGE2, through the enhancement of PRLR expression, to support the luteotropic function of PRL. Based on this, and on the fact that PGE2 could also increase the expression of endothelin receptor B (ETB; important vasodilator) (25), the effects of PGs withdrawal on luteal vascular and immune factors were further investigated (26). The stabilization of blood vessels was negatively affected by the treatment, while the expression of different pro-inflammatory factors was increased (26). Concomitantly, the presence of strong compensatory effects was implied.

Considering the peculiarities of the canine luteal phase, the present study aimed to investigate additional potential effects of withdrawal of PGs on CL physiology. For this, we used samples from a previously reported *in vivo* study (3, 24, 26), and performed a deep RNA sequencing (RNA-Seq) by applying Next Generation Sequencing (NGS) technology. With this approach, we expected to provide deeper understanding of the importance of PGs at different stages of CL development: its early gonadotropin-independence, then its transition to dependence on hypophyseal hormones, and finally the dependence of the mature CL mainly on PRL. Time-dependent changes in the CL transcriptome associated with its development were also investigated in control samples.

MATERIALS AND METHODS

Tissue Samples

This is a follow-up study utilizing tissue material collected in preceding *in vivo* studies (3, 24, 26). Animal experiments were approved by the responsible ethics committee (permit 54/2008) of the University of Warmia and Mazury in Olsztyn, Poland. Briefly, mixed-breed bitches of different ages (2–7 years old) were monitored by vaginal cytology and P4 measurements for the onset of spontaneous estrus. The day when circulating P4 levels exceeded 5 ng/ml was considered the day of ovulation (day 0). Animals were then randomly assigned to four control and four treated groups, receiving orally and daily either a placebo or 10 mg/kg of firocoxib (Previcox, Merial Ltd), respectively. Treatment was maintained for 5, 10, 20 or 30 days after ovulation. Ovaries were collected by ovariohysterectomy on the last day of treatment. *Corpora lutea* were dissected from surrounding ovarian tissue and preserved in RNAlater at −80°C until further use, as described before (23).

RNA Isolation and Purification

TRIzol reagent (Invitrogen, Carlsbad, CA, USA) was used to isolate total RNA, following the manufacturer's instructions. A primary evaluation of RNA purity and concentration was performed with a NanoDrop 2000C spectrophotometer (ThermoFisher Scientific AG, Reinach, Switzerland). Further purification of RNA was performed with the RNeasy Mini Kit

(Qiagen GmbH, Hilden, Germany), using the RNA Cleanup protocol provided. RNA integrity was assessed with the Agilent 2200 TapeStation System. RNA integrity numbers (RIN) ranged from 8.0 to 9.8.

RNA-Sequencing and Data Evaluation

Next Generation Sequencing (NGS, RNA-Seq)

Sequencing of RNA with NGS was performed to obtain a quantitative evaluation of gene expression. A total of 32 samples available for this follow-up study were allotted to the following groups: $n = 5$ for day 5 control, $n = 4$ for day 5 treated, $n = 4$ for either day 10 control and day 10 treated, $n = 3$ for either day 20 control and day 20 treated, $n = 4$ for day 30 control and $n = 5$ for day 30 treated. RNA-Seq was performed on $n = 4$ animals/group (control and treated) from days 5, 10, and 30, and $n = 3$ animals/group from day 20 after ovulation. Library preparation, cluster generation and sequencing were performed as previously described (27). All samples were processed at the same time to avoid possible batch effects. In brief, the Qubit (1.0) Fluorometer (Life Technologies, Carlsbad, CA, USA) and Bioanalyzer 2100 (Agilent, Waldbronn, Germany) were used to evaluate the quantity and quality of isolated RNA. To be processed further, samples needed to have a 260/280 nm ratio between 1.8 and 2.1 and a 28S/18S ratio within 1.5–2.0. In the succeeding steps, the TruSeq RNA Sample Prep Kit v2 (Illumina, Inc., San Diego, CA, USA) was used. Total RNA samples (100–1,000 ng) were enriched by poly-A selection and reverse-transcribed to obtain double-stranded cDNA. Additionally, fragmentation, end-repair and polyadenylation steps were performed on cDNA samples before ligation of TruSeq adapters containing the index for multiplexing. PCR was used for selective enrichment of fragments containing TruSeq adapters on both ends, and the quality and quantity of the enriched libraries obtained were assessed with the Qubit (1.0) fluorometer and Caliper GX LabChip GX (Caliper Life Sciences Inc., Hopkinton, MA, USA). Finally, libraries were normalized to 10 nM in Tris-Cl 10 mM with Tween 20.

Cluster generation was performed with 2 nM of pooled normalized libraries on the cBOT System with the TruSeq PE Cluster Kit v4-cBot-HS or TruSeq SR Cluster Kit v4-cBot-HS (Illumina, Inc). Sequencing was performed with the Illumina HiSeq4000 with single end 125 bp using the TruSeq SBS Kit v4-HS (Illumina, Inc.). The raw data (.fastq files) obtained were used for downstream analysis. Additionally, they were also deposited in NCBI's Gene Expression Omnibus and are accessible through GEO Series accession number GSE130369.

Data Analysis

The initial analysis of data was performed with the framework SUSHI (28, 29), developed by the Functional Genomics Center of Zurich (FGCZ ETH/UZH, Zurich, Switzerland). Spliced Transcripts Alignment to a Reference (STAR) software was used to align the RNA-Seq dataset (30) to a reference canine genome, the Ensembl genome build CanFam3.1 (http://www.ensembl.org/Canis_familiaris/Info/Index). Gene expression values were obtained with the function *featureCounts* from the R package Rsubread (31). A minimum average of 10 reads in at least one group of replicates was required to consider a gene as detected. After reads counting, initial quality control and explorative analysis were performed with the SUSHI framework.

For differential expression analysis different contrasts (pairwise comparisons) were defined and gene differential expression for each contrast was assessed with the generalized linear model approach from the Bioconductor package DESeq2 (32). This was performed as previously described (27), using the Wald test to assess the significance of differential expression. Next, correction of multiple testing was obtained with the Benjamini-Hochberg algorithm that computes False Discovery Rate (FDR, adjusted *P*-value). Finally, thresholds of *P*-value $<$ 0.01 and adjusted *P*-value $<$ 0.1 (i.e., FDR $<$ 10%) were applied. The complete differentially expressed genes (DEGs) lists obtained for each contrast were used for downstream analyses and are provided in **Supplemental Table 1** (for time-dependent effects) and **Supplemental Table 2** (for treatment-induced effects).

Functional characterization of DEGs for each contrast was performed by identifying different functional terms, resorting to available bioinformatics resources. The identification of over-represented functional categories (i.e., gene ontologies) and their enrichment scores were calculated using the web-based Panther software [http://pantherdb.org, (33)]. This analysis was further supported and complemented with the web-based software Enrichr [http://amp.pharm.mssm.edu/Enrichr/, (34)]. The identification and visualization of enriched functional biological networks was obtained with the application ClueGO v2.5.1 (35) for the software platform Cytoscape v3.6 (36). The software Ingenuity Pathway Analysis (IPA, Qiagen, Redwood City, CA, USA) was used to predict the most significantly affected canonical pathways and identify possibly involved upstream regulators. Lists of up to 10 representative genes involved with particular functional terms (gene ontologies, functional networks, canonical pathways and upstream regulators) from each contrast are presented in **Supplemental Table 3**. In addition, Venn diagram was generated to identify DEGs concomitantly affected by treatment in different contrasts. For this analysis, the thresholds were defined for *P*-value $<$ 0.01 and fold-change for up- (log2Ratio $\geq$ 1) and down-regulation (log2Ratio $<$ -1). Full lists of DEGs used as input for Venn diagram and genes present on each intersection are provided in **Supplemental Table 4**.

Expression of Selected Target Genes by Semi-quantitative Real-Time TaqMan qPCR

Further validation of the RNA-Seq data obtained and analysis of specific functional pathways suggested by our analysis were performed through evaluation of the mRNA expression of 20 selected candidate target genes, by semi-quantitative real-time (TaqMan) qPCR. All available samples were used for qPCR experiments ($n = 32$). A complete list of primers used, TaqMan probes and pre-designed (i.e., commercially-available) TaqMan systems is presented in **Table 1**. Self-designed primers and 6-carboxyfluorescein (6-FAM) and 6-carboxytetramethylrhodamine (TAMRA) labeled probes were designed and ordered from Microsynth AG (Balgach,

TABLE 1 | List of gene symbols, corresponding gene names and TaqMan systems used for real time qPCR.

Gene	Name	Accession number	Primer sequence		Product length (bp)
IDO1	Idoleamine 2,3-dioxygenase 1	XM_532793.5	Forward	5′-TGA TGG CCT TAG TGG ACA CAA G-3′	116
			Reverse	5′-TCT GTG GCA AGA CCT TTC GA-3′	
			TaqMan probe	5′-CAG CGC CTT GCA CGT CTG GC-3′	
SULT1E1	Sulfotransferase family 1E member 1	MK728829	Forward	5′-AAC AGA TGG CAT CTC CTA GAG TAG TG-3′	100
			Reverse	5′-CGG CAA AGA TAG ATC ACC TTA CAG T-3′	
			TaqMan probe	5′-CCA TCT GCC AGT TGA ACT TCT TCC AGC C-3′	
TBXAS1	Thromboxane A synthase 1	XM_005629559.1	Applied Biosystems, prod. no. Cf01022701_m1		105
PTGDS	Prostaglandin D synthase	NM_001003131.1	Applied Biosystems, prod. no. Cf02622002_m1		85
TGFβ1	Transforming growth factor beta 1	NM_001003309.1	Applied Biosystems, prod. no. Cf02623324_m1		83
TGFβR1	Transforming growth factor beta receptor 1	XM_014117881.1	Applied Biosystems, prod. no. Cf02687913_m1		110
ICAM1	Intercellular adhesion molecule 1	NM_001003291.1	Applied Biosystems, prod. no. Cf02690470_u1		124
NODAL	Nodal growth differentiation factor	XM_546146.3	Applied Biosystems, prod. no. Cf02711306_u1		149
FAS	Fas cell surface death receptor	XM_005636650.1	Applied Biosystems, prod. no. Cf02651136_m1		118
FASLG	Fas ligand	NM_001287153.1	Applied Biosystems, prod. no. Cf02625215_s1		89
NFκB1	Nuclear factor kappa B subunit 1	NM_001003344.1	Applied Biosystems, prod. no. Cf02689968_m1		119
NFκBIa	NFKB inhibitor alpha	XM_537413.5	Applied Biosystems, prod. no. Cf02741714_m1		129
PDGF B	Platelet derived growth factor subunit B	NM_001003383.1	Applied Biosystems, prod. no. Cf02626637_m1		109
FGF1	Fibroblast growth factor 1	XM_014108102.1	Applied Biosystems, prod. no. Cf02716346_g1		77
FGF2	Fibroblast growth factor 2	XM_003432481.3	Applied Biosystems, prod. no. Cf03460065_g1		147
THBS1	Thrombospondin 1	XM_544610.5	Applied Biosystems, prod. no. Cf02701399_m1		88
PPARγ	Peroxisome proliferator activated receptor gamma	NM_001024632.2	Applied Biosystems, prod. no. Cf02625640_m1		92
EGLN1	PHD2/egl-9 family hypoxia inducible factor 1	XM_546089.4	Applied Biosystems, prod. no. Cf02713521_m1		115
NR4A1	Nuclear receptor subfamily 4 group A member 1	NM_001003227.1	Applied Biosystems, prod. no. Cf02719047_s1		113
HSD17B7	Hydroxysteroid 17β dehydrogenase 7	XM_014111264.1	Applied Biosystems, prod. no. Cf02657821_m1		82
PTK2	Protein tirosine kinase 2	XM_005627993.2	Applied Biosystems, prod. no. Cf02684608_m1		104
EIF4H	Eukaryotic translation initiation factor 4H	XM_014114129.1	Applied Biosystems, prod. no. Cf02713640_m1		136
KDM4	Lysine (K)-specific demethylase 4A	XM_005629106.2	Applied Biosystems, prod. no. Cf02708629_m1		96

Switzerland). The design of *IDO1* primers and probes was based on published canine CDS sequences while for *SULT1E1* molecular cloning of the canine sequence was required and this was performed by a subcloning approach using the pGEM-T vector, as described previously (22, 37, 38) (sequence submitted to GenBank under accession number MK728829). Commercially-available systems were obtained from Applied Biosystems. The efficiency of PCR reactions was evaluated to ensure approximately 100% (39).

Elimination of genomic DNA contamination, reverse transcription (RT) and semi-quantitative real-time TaqMan qPCR (RT-qPCR) were performed following the manufacturers' and our previously published protocols (22, 39). Briefly, total RNA samples were treated with the RQ1 RNase-free DNase kit (Promega, Dübendorf, Switzerland) to eliminate possible genomic DNA contamination. Random hexamers were used as primers in the subsequent RT reactions, employing reagents obtained from Applied Biosystems. For RT-qPCR, all samples were run in duplicates in 96-well optical plates, using autoclaved water and RNA not subjected to RT (minus-RT control) instead of cDNA as negative controls. Reactions were run in an automated fluorometer ABI PRISM 7500 Sequence Detection System (Applied Biosystems) and were set as follows: initial denaturation for 10 min at 95°C followed by 40 cycles of 15 s at 95°C and 1 min at 60°C each. Relative quantification was done by applying the comparative Ct method (ΔΔCt). RT-qPCR data were normalized with three reference genes: PTK2, EIF4H, and KDM4. Based on the RNA-Seq data collected herein, these genes were found to be stably expressed in all samples examined using the online tool RefFinder and NormFinder software (40, 41). Since RT-qPCR data were unevenly distributed, logarithmic transformation was performed and results are presented as geometric means (Xg) ± geometric standard deviation (SD). The evaluation of treatment-induced effects was performed with

a two-tailed Student's *t*-test, comparing the treatment group with the control group at each time point (day). Additionally, time-related changes in the expression of target genes were evaluated in control animals using the Kruskal-Wallis test (non-parametric ANOVA) followed by Dunn's test. All statistical tests were performed with GraphPad 3 (GraphPad Software Inc., San Diego, CA, USA) and values of $P < 0.05$ were considered statistically significant.

RESULTS

Initial Evaluation of Sequencing Results

Initial exploratory analysis of the sequencing data obtained was performed with the CountQC app provided in the SUSHI framework. This function allowed assessment of homogeneity and correlations between samples, as well as clustering of high variance features among all samples submitted for RNA-Seq. The analysis of samples correlation matrix (**Supplemental Image 1A**) indicated the presence of some variation among all sequenced samples. Based on the analysis of this matrix and gene expression scatter plots (not shown), samples 10/1 and 30/1 controls, and 10/2 and 30/1 treated with Previcox, were considered outliers and removed from the dataset for further analysis. This allowed a more homogeneous correlation between samples within each group (**Supplemental Image 1B**). Further observation of the correlation matrix indicated a higher homogeneity among samples of each control group compared with the respective treated groups (**Supplemental Image 1B**). This was also suggested by the more homogeneous clustering of samples and genes visible on the heatmap, with 2,000 genes exhibiting higher variance among control samples (**Supplemental Image 1C**) compared with the one that contained all analyzed samples (**Supplemental Image 1D**). Clustering observed on the heatmap with the 2,000 genes showing higher variance among all analyzed samples (**Supplemental Image 1D**) also suggested that, apart from effects on the immune system and negative regulation of cellular processes on day 20, passage of time appeared to have a higher global impact on CL expression of these genes than COX2 inhibition. This was further visualized using a principal component analysis (PCA) plot of the same 2,000 genes with higher variance among all samples (**Figure 1**). Thus, samples appeared to be segregated based on time-point of analysis, with those samples from days 5 and 10 being proximally distributed on a cluster and samples from days 20 and 30 on the other side of the plot. The scattered distribution of samples treated up to day 20 after ovulation indicates stronger effects of treatment in this group (**Figure 1**).

Time-Dependent Effects

Samples available for the present study were representative of different regulatory stages of early CL development, i.e., the early developing, gonadotropin-independent CL (days 5 and 10), and the mature CL in transition and during its dependence on gonadotropins (days 20 and 30, respectively). Close similarity between samples from days 5 and 10 on the one end, and days 20 and 30 on the other end, was also suggested from the PCA plot (**Figure 1**). Therefore, when evaluating the effects of time on the CL transcriptome, samples were grouped accordingly with differential expression analysis (pairwise comparison) being performed for the contrast "Days 20+30 control over days 5+10 control." This analysis was performed using the DESeq2 package for Bioconductor and genes were assumed to be differentially expressed if $P < 0.01$ and FDR < 0.1. Of the total set of 19,856 genes, 13,332 genes were considered expressed (above the threshold of 10 reads per gene). DEGs accounted for 3,484 features with 1,681 being up- and 1,803 down-regulated at days 20+30 compared with the early developing CL (days 5+10; **Table 2**, **Figure 2A**). A detailed list of all DEGs affected by time is provided in **Supplemental Table 1**. Additional representation of DEGs in Volcano plots, filtered by FDR < 0.1 and log2Ratio > 0.5, is provided in **Supplemental Image 2A**. Following this, functional characterization of DEGs was performed. First, the pairwise comparison was classified according to Gene Ontology (GO) terms related to the domain biological process (BP). Panther software was used to calculate enrichment scores for each term, and results were further corroborated with Enrichr. Lists of up to ten (n = 10) representative genes for different functional terms, as well as upstream regulators and networks identified in the following steps, are presented in **Supplemental Table 3**.

Genes more highly represented at early CL stages (days 5+10) compared to days 20+30 were strongly associated with (**Figure 2A**, **Supplemental Table 3**): cell-cell adhesion ($P =$ 2.40E-3), locomotion ($P =$ 1.28E-3), immune system process ($P =$ 1.27E-3), metabolic process ($P =$ 9.67E-4) and cellular process ($P =$ 2.73E-4). On the other hand, functional terms over-represented in the mature CL (days 20+30) included (**Figure 2A**, **Supplemental Table 3**): fatty acid biosynthetic process ($P =$ 1.26E-3), fatty acid metabolic process ($P =$ 2.96E-4), lipid metabolic process ($P =$ 1.12E-6), phospholipid metabolic process ($P =$ 2.35E-3), protein localization ($P =$ 1.64E-3), intracellular protein transport ($P =$ 1.04E-3), transport ($P =$ 3.12E-5) and localization ($P =$ 1.22E-4).

Using as input the lists of upregulated and downregulated DEGs for this contrast (**Supplemental Table 1**), enriched functional networks were grouped and visualized with the ClueGO plug-in for the platform Cytoscape (**Figure 2B**, **Supplemental Table 3**, **Supplemental Image 3A**). Among the more highly represented functional networks observed on days 5 and 10 were those referring to cell signaling and metabolism, extracellular matrix, apoptosis and, in greater numbers, networks related to immune function (**Figure 2B**, **Supplemental Table 3**). On the other hand, networks mainly observed on days 20 and 30 were associated with intracellular transport and (lipids) metabolism (**Supplemental Table 3**, **Supplemental Image 3A**).

The prediction of the most significantly affected signaling pathways was obtained from IPA software by using the list of DEGs as input ($P < 0.01$, FDR < 0.1). Among the most enriched canonical pathways predicted to be activated by the passage of time were those related to (**Supplemental Table 3**): cholesterol synthesis/steroidogenesis (superpathway of cholesterol biosynthesis, $P =$ 4.90E-5; cholesterol biosynthesis I, $P =$ 1.20E-4; cholesterol biosynthesis II, $P =$ 1.20E-4; and cholesterol biosynthesis III, $P =$ 1.20E-4). On the other hand, among

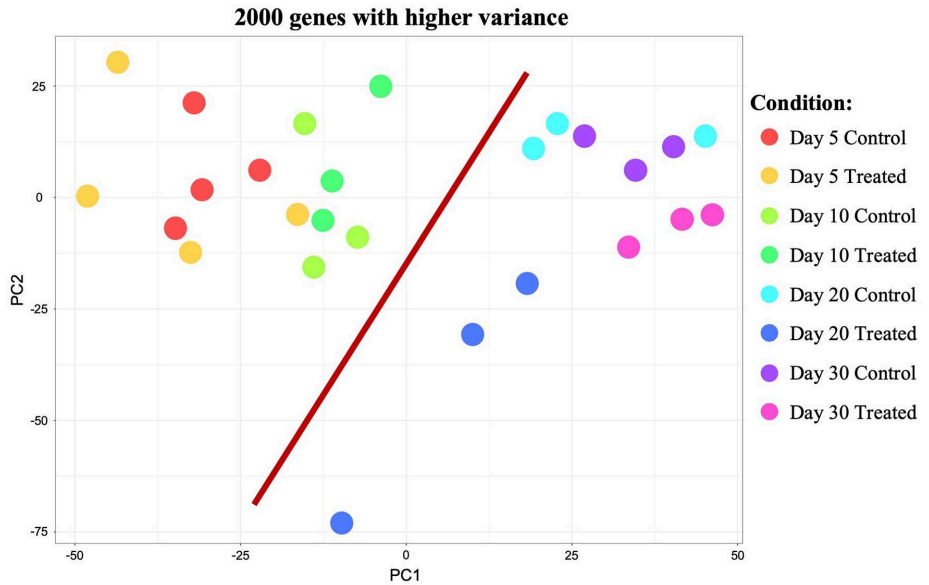

FIGURE 1 | Principal component analysis (PCA) plot of all samples showing the 2,000 genes that presented higher variance. Distribution of samples appears to be mainly based on the effect of time (highlighted by red bar separating samples from days 5 and 10 from samples from days 20 and 30). Samples distribution and scattering also suggest stronger effects of treatment on day 20 than on the other time points studied.

TABLE 2 | Summary of differential expression analysis (pairwise comparison) for all selected contrasts investigated in the present study.

Contrasts	Days 20+30 C over days 5+10 C	Day 5 T over day 5 C	Day 10 T over day 10 C	Day 20 T over day 20 C	Day 30 T over day 30 C
Total DEGs ($P < 0.01$, FDR < 0.1)	3,484	74	2	1,741	552
Number of genes with counts above threshold (10 reads per gene)	13,332	13,428	13,280	13,477	13,187
Upregulated genes	1,681	47	1	1,146	306
Downregulated genes	1,803	27	1	595	246

significant pathways that were predicted to be inhibited by time were those related to (**Supplemental Table 3**): cellular proliferation (EIF2 signaling, $P = 7.94E-16$; mTOR signaling, $P = 3.98E-12$), cell cycle (cyclins and cell cycle regulation, $P = 3.63E-7$), ECM production (inhibition of matrix metalloproteases, $P = 1.86E-4$) and immune function (leukocyte extravasation signaling, $P = 3.55E-8$; acute phase response signaling, $P = 5.89E-6$; IL8 signaling, $P = 3.63E-5$; chemokine signaling, 4.68E-5; dendritic cell maturation, $P = 1.8E-4$).

The analysis of DEGs with IPA allowed additional identification of upstream regulators possibly affecting expression of the DEGs obtained. Among the predicted upstream regulators, the following factors were identified: transforming growth factor β 1 (TGFβ1, $P = 7.27E-33$), tumor necrosis factor (TNF, $P = 5.88E-26$), beta-estradiol ($P = 3.08E-22$), platelet-derived growth factor BB (PDGF BB, $P = 1.08E-18$), interferon gamma (INFγ, $P = 3.47E-15$), progesterone (P4, $P = 3.86E-15$), insulin growth factor 1 (IGF1, $P = 3.85E-13$), nuclear factor kappa B inhibitor alpha (NFκBIα, $P = 5.86E-13$) and prostaglandin (PG) E2 receptor 2 (PTGER2/EP2, $P = 9.5E-12$) (**Supplemental Table 3**).

Treatment-Induced Effects

Differential Expression Analysis (Pairwise Comparison) and Venn Diagram

The effects of treatment with Previcox on the transcriptome of CL tissue were assessed by differential expression analysis, in which treated samples were compared with control samples at the respective time-points (days 5, 10, 20 and 30). Thus, the following contrasts were defined: "day 5 treated over day 5 control," "day 10 treated over day 10 control," "day 20 treated over day 20 control," and "day 30 treated over day 30 control." As described for time-dependent effects, the DESeq2 package for Bioconductor was used to obtain lists of DEGs. The thresholds of $P < 0.01$ and FDR < 0.1 were applied to consider a gene as being differently expressed. For all contrasts, a total of 19,856 genes were identified; only genes with at least 10 reads were considered as expressed and included in further analyses. A summary of

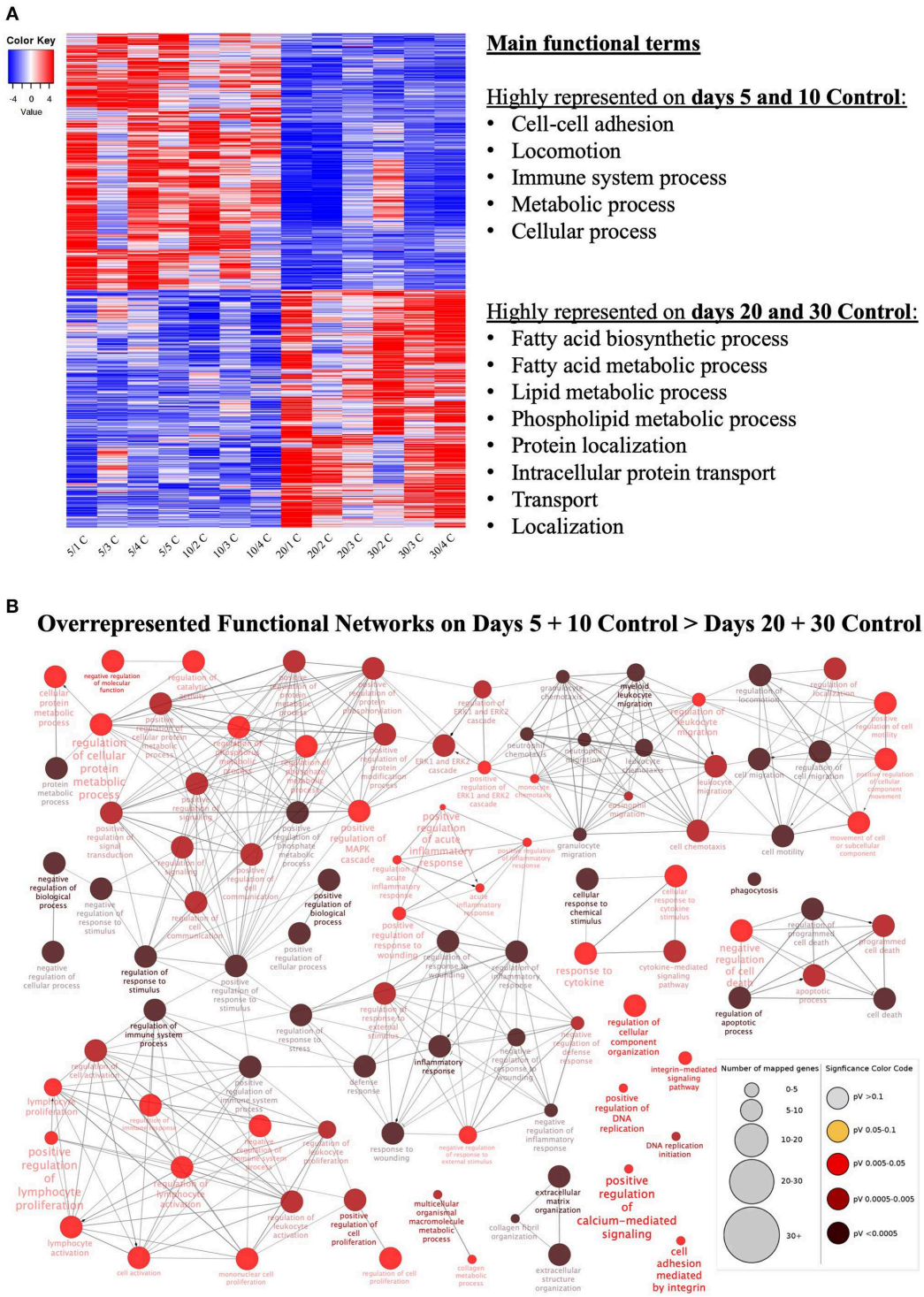

FIGURE 2 | Functional categorization of differentially expressed genes (DEGs) affected at selected time points (contrast "days 20+30 control over days 5+10 control"). **(A)** Heatmap of 3,484 DEGs in the contrast "days 20+30 over days 5+10 control." Gradient of high to low expression of each gene relative to average expression is indicated by red to blue colors. 1,803 genes were more highly expressed in early (days 5 and 10) CL stages whereas 1,681 genes were more highly expressed in mid-diestrus (days 20 and 30) stages ($P \leq 0.01$, FDR ≤ 0.1). Representative overrepresented functional terms in each group of upregulated genes are listed (statistical details are provided in the text and **Supplemental Table 3**). Entire list of DEGs is provided as **Supplemental Table 1**. **(B)** Functional networks found for downregulated DEGs from the contrast "days 20+30 control over days 5+10 control." Overrepresented functional terms of days "5+10 control" are shown. Redundant or non-informative terms were removed and the networks obtained were manually rearranged. Number of mapped genes is indicated by the node size, while significance of functional terms is denoted by node color (represented in legend at the right bottom corner). Networks more highly represented on days 5 and 10 control (developing gonadotropin-independent CL) were related to immune function, extra-cellular matrix (ECM), intracellular signaling and apoptosis.

DEGs analysis is presented in **Table 2**, while full lists of DEGs in response to all treatments at every time-point are presented in **Supplemental Table 2**.

For the contrast at day 5, after being filtered ($P < 0.01$, FDR < 0.1), 74 genes were considered to be DEGs, of which 47 were upregulated and 27 downregulated after treatment. As for the contrast "day 10 treated over day 10 control," the expression of genes varied greatly individually, and resulted in only 2 DEGs filtered by the applied *P*-value/FDR thresholds. Following this low number of DEGs found at day 10, no functional characterization could be performed for this contrast. In the contrast for day 20, 1,741 genes met the criteria of $P < 0.01$ and FDR < 0.1, making this the treatment-related contrast with the highest number of DEGs. Of these DEGs, 1,146 were more highly expressed in the day 20 treated group, while 595 were more highly expressed in the day 20 control group. Finally, for the contrast "day 30 treated over day 30 control" 552 genes were differently expressed ($P < 0.01$, FDR < 0.1), comprising 306 up- and 246 down-regulated features in response to prostaglandin withdrawal. Further representation of DEGs (FDR < 0.1; log2ratio > 0.5) for the contrasts "day 5 treated over day 5 control," "day 20 treated over day 20 control," and "day 30 treated over day 30 control" in form of Volcano Plots are shown in **Supplemental Image 2B–D**.

In an attempt to identify genes that would be simultaneously affected by COX2-inhibition at different time-points of the CL life span, the intersections of DEGs from the contrasts at days 5, 20, and 30 were visualized with a Venn diagram (**Figure 3A**). The input DEGs were filtered for $P < 0.01$ and log2Ratio < -1 (downregulated) and log2Ratio > 1 (upregulated), and a complete list of genes from each intersection is provided in **Supplemental Table 4**. Thirty-two genes were simultaneously affected by treatment on days 5 and 20, while 78 were shared among days 20 and 30. Despite the time difference, 4 genes were still found to be simultaneously affected on days 5 and 30. However, no gene was concomitantly affected by prostaglandin withdrawal at the different time-points.

Functional Annotations, Networks, and Pathways

Further characterization of DEGs for each contrast was performed by identifying different enriched functional terms. The analysis flow was similar to the one applied in differential expression analysis of time-related effects: functional terms (GOs) were identified with Panther and Enrichr, functional networks were visualized with Cytoscape, and prediction of affected canonical pathways and upstream regulators involved was done by IPA. For input, DEGs were filtered by $P < 0.01$ and FDR < 0.1; lists of representative genes are provided in **Supplemental Table 3**.

Contrast "day 5 treated over day 5 control"

The main functional terms related to genes more highly expressed in treated samples from day 5 were (**Figure 3B**, **Supplemental Table 3**): positive regulation of intracellular transport ($P = 3.48E-8$), regulation of cell motility ($P = 1.31E-6$), regulation of cell migration ($P = 7.40E-6$), regulation of cellular component movement ($P = 2.59E-6$) and regulation of locomotion ($P = 2.84E-6$). Due to low numbers of input DEGs, no significant gene ontologies could be identified among the DEGs downregulated by treatment at this early gonadotropin-independent luteal phase. This also accounts for the Cytoscape analysis of functional networks from up- and down-regulated genes.

Enriched pathways predicted to be activated by IPA were mostly related to (**Supplemental Table 3**): cytoskeleton/cell movement/cell division (RhoA signaling, $P = 1.10E-6$; actin cytoskeleton signaling, $P = 4.07E-5$; signaling by Rho family GTPases, $P = 6.31E-5$; regulation of actin-based motility by Rho, $P = 1.07E-4$). Additionally, the pathways death receptor signaling ($P = 5.50E-6$) and leukocyte extravasation signaling ($P = 2.75E-4$) were also predicted to be activated by treatment, while the RhoGDI signaling ($P = 5.13E-7$) pathway was predicted to be deactivated. Among the predicted upstream regulators, actin alpha cardiac muscle 1 (ACTC1, $P = 7.59E-6$), PDGF BB ($P = 3.13E-5$), actin alpha 2 (ACTA2, $P = 2.1E-4$), TNF ($P = 2.78E-4$), and TGFβ1 ($P = 9.94E-E4$) were found (**Supplemental Table 3**).

Contrast "day 20 treated over day 20 control"

For this contrast, the following main terms more highly represented in the treated mature CL during its transition to gonadotropin dependence on day 20 were found (**Figure 3C**, **Supplemental Table 3**): cell proliferation ($P = 4.78E-4$), regulation of cell cycle ($P = 7.06E-5$), cell-cell adhesion ($P = 9.85E-4$), locomotion ($P = 5.58E-5$), response to external stimulus ($P = 1.20E-3$), cell differentiation ($P = 1.84E-4$), regulation of phosphate metabolic process ($P = 2.03E-4$), developmental process ($P = 1.93E-5$), cellular component organization or biogenesis ($P = 6.12E-4$) and metabolic process ($P = 1.46E-3$). High functional variation was found for DEGs in control samples on day 20, yielding only low enrichment scores without strongly enriched functional terms, and without any strongly enriched functional networks. This differed from the CL samples derived from dogs treated for 20 days with Previcox, in which strongly over-represented networks were found, referring to cell differentiation, cell death, gene expression, translation and signaling, hormone regulation and immune function (**Figure 4**, **Supplemental Table 3**).

In response to Previcox treatment, the significant canonical pathways that were predicted to be activated (**Supplemental Table 3**) were related by IPA analysis to cellular proliferation/growth (EIF2 signaling, $P = 5.01E-21$; mTOR signaling, $P = 1.86E-9$) and immune function (toll-like receptor signaling, $P = 1.66E-4$; adrenomedulin signaling pathway, $P = 1.20E-3$; and acute phase response signaling, $P = 4.37E-3$; NFκB signaling, $P = 4.47E-3$; IL6 signaling, $P = 4.47E-3$). Additionally, the relaxin signaling ($P = 4.68E-4$) pathway was also predicted to be activated while the angiopoietin signaling ($P = 4.47E-3$) pathway was predicted to be deactivated. The list of top upstream regulators for the observed effects included (**Supplemental Table 3**): β-estradiol ($P = 6.66E-23$), PDGF BB ($P = 9.63E-20$), TGFβ1 ($P = 2.26E-15$), IL1β ($P = 1.1E-14$), TNF ($P = 4.27E-14$), PGE2 ($P = 3.68E-11$), NFκBIA ($P = 1.45E-10$),

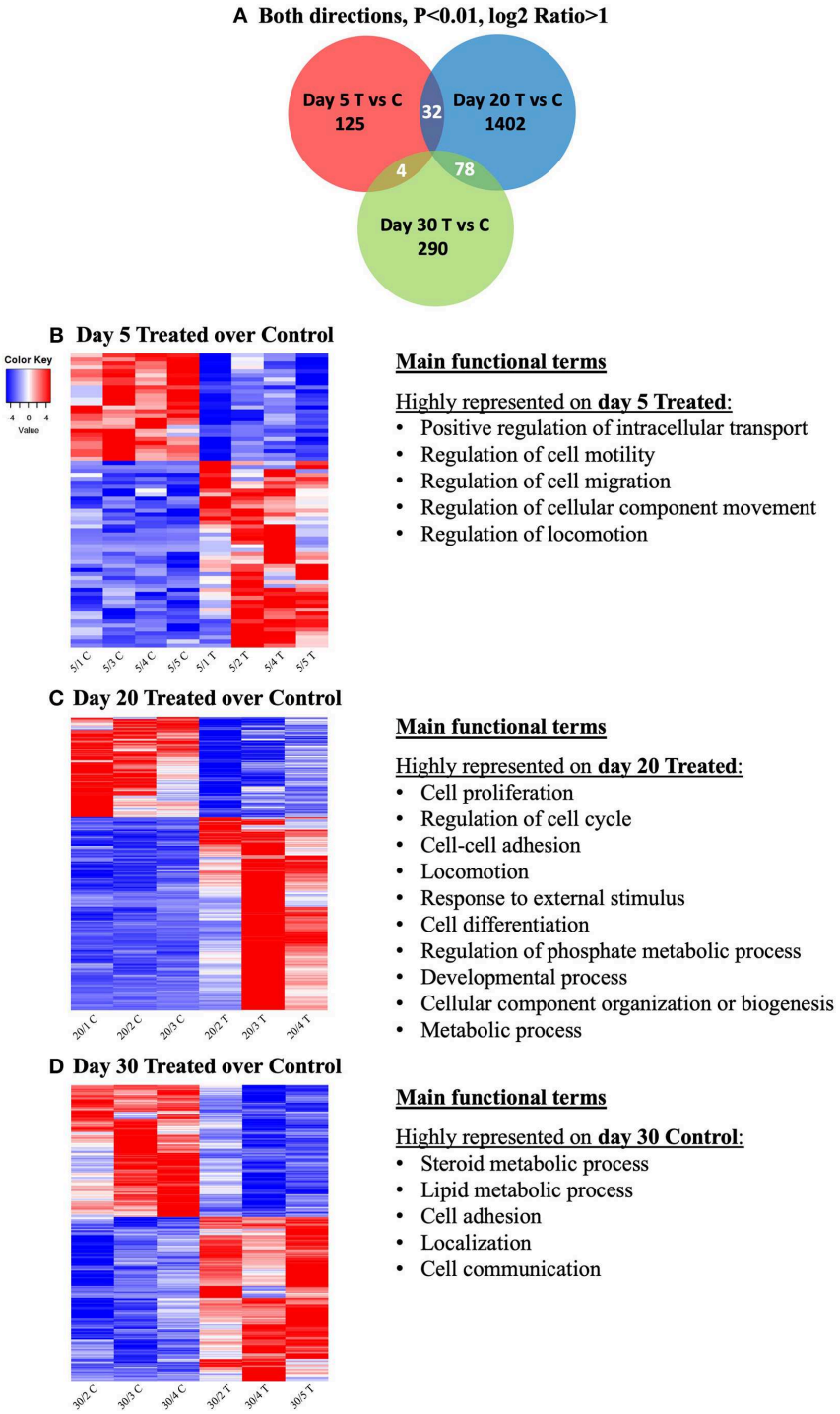

FIGURE 3 | Venn diagram showing the distribution and overlap of differentially expressed genes (DEGs) induced by treatment at different time-points **(A)**. Lists of DEGs from the contrasts "day 5 treated over day 5 control," "day 20 treated over day 20 control," and "day 30 treated over day 30 control" were used as input data. Thresholds were defined for *P*-value < 0.01 and fold-change for up (log2Ratio ≥ 1) and downregulated (log2Ratio ≤ -1) genes. No gene was found to be concomitantly affected by treatment in all groups. Complete list of genes from each contrast and intersection are present in **Supplemental Table 4**. Heatmap and overrepresented functional terms present in differentially expressed genes (DEGs) induced by treatment at different studied time-points **(B–D)**. Gradient of high to low expression of each gene relative to average expression is indicated by red to blue colors. Main significant overrepresented functional terms (gene ontologies) in each group of upregulated genes are listed (statistical details are provided in the text and **Supplemental Table 3**). Entire list of DEGs is provided as **Supplemental Table 2**. **(B)** Heatmap of 74 DEGs of the contrast "day 5 treated over day 5 control" and representative significant overrepresented functional terms in "day 5 treated" are shown. **(C)** Heatmap of 1,741 DEGs of the contrast "day 20 treated over day 20 control" and representative significant overrepresented functional terms at "day 20 treated". **(D)** Heatmap of 552 DEGs of the contrast "day 30 treated over day 30 control" and representative overrepresented functional terms in "day 30 control".

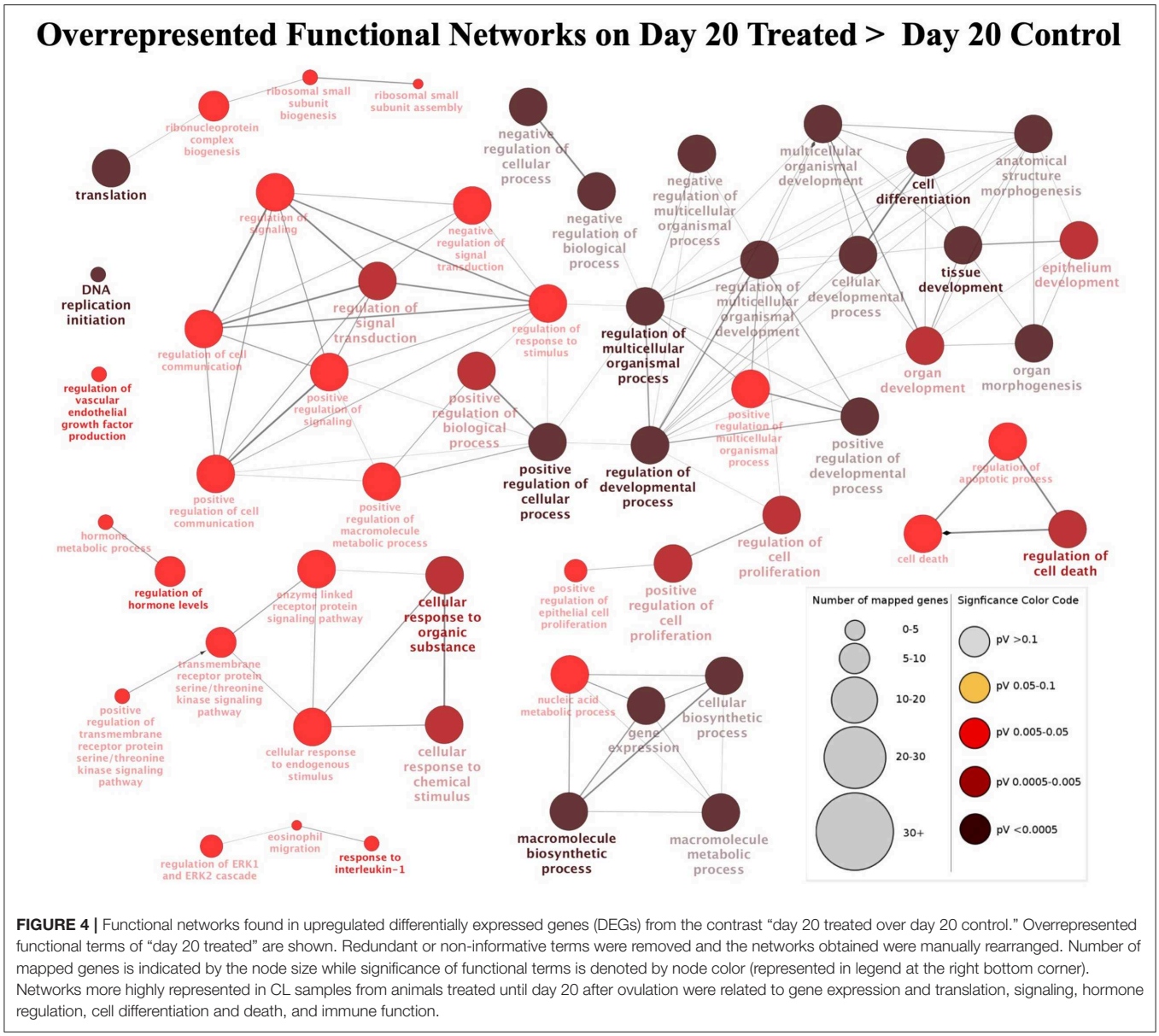

FIGURE 4 | Functional networks found in upregulated differentially expressed genes (DEGs) from the contrast "day 20 treated over day 20 control." Overrepresented functional terms of "day 20 treated" are shown. Redundant or non-informative terms were removed and the networks obtained were manually rearranged. Number of mapped genes is indicated by the node size while significance of functional terms is denoted by node color (represented in legend at the right bottom corner). Networks more highly represented in CL samples from animals treated until day 20 after ovulation were related to gene expression and translation, signaling, hormone regulation, cell differentiation and death, and immune function.

Fas cell surface death receptor (FAS, $P = 1.89E\text{-}9$) and P4 ($P = 2.14E\text{-}9$).

Contrast "day 30 treated over day 30 control"

Genes higher expressed in day 30 control samples were related with the following functional terms (**Figure 3D**, **Supplemental Table 3**): steroid metabolic process ($P = 2.32E\text{-}4$), lipid metabolic process ($P = 1.07E\text{-}4$), cell adhesion ($P = 1.33E\text{-}3$), localization ($P = 1.82E\text{-}3$) and cell communication ($P = 8.96E\text{-}4$). No significantly enriched GO and networks could be found for genes upregulated in response to treatment on day 30, which was restricted by higher functional variation of identified DEGs. However, in control samples functional networks related to nitric oxide synthesis and angiogenesis were found to be highly enriched (**Supplemental Table 3**, **Supplemental Image 3B**).

Interestingly, canonical pathways predicted to be deactivated by treatment in mature CL at day 30 were related with (**Supplemental Table 3**): cholesterol synthesis/steroidogenesis (superpathway of cholesterol biosynthesis, $P = 1.35E\text{-}7$; cholesterol biosynthesis I, $P = 6.31E\text{-}6$; cholesterol biosynthesis II, $P = 6.31E\text{-}6$; cholesterol biosynthesis III, $P = 6.31E\text{-}6$), immune signaling (acute phase response signaling, $P = 1.91E\text{-}4$; NFκB signaling, $P = 3.47E\text{-}4$; TGFβ signaling, $P = 5.13E\text{-}3$; IL8 signaling, $P = 6.61E\text{-}3$; leukocyte extravasation signaling, $P = 8.71E\text{-}3$) and vascularization (VEGF signaling, $P = 3.31E\text{-}3$; PDGF signaling, $P = 1.48E\text{-}3$). With regard to cellular proliferation, the EIF2 signaling ($P = 3.16E\text{-}13$) pathway was predicted to be activated, while the mTOR signaling ($P = 2.63E\text{-}7$) pathway was predicted to be deactivated. Among the top upstream regulators predicted with IPA software were

(**Supplemental Table 3**): TNF (P = 1.89E-10), peroxisome proliferator-activated receptor gamma (PPARγ, P = 9.22E-5), TGFβ1 (P = 9.58E-5), fibroblast growth factor 2 (FGF2, P = 1.44E-4) and NFκBIA (P = 2.25E-4).

Expression of Candidate Target Genes

The expression of candidate genes was investigated by semi-quantitative (TaqMan) qPCR in 32 samples from the different available groups. All results for time-dependent and treatment effects are cumulatively presented in **Supplemental Table 5**. Extracted, significant results were prepared for the main document and are shown in **Tables 3**, **4**. The functional groups chosen for validation of transcriptional analysis included: eicosanoid synthases (*TBXAS1*, *PTGDS*), immune factors (*TGFβ1*, *TGFβR1*, *ICAM1*, *IDO1*, *NODAL*, *FAS*, *FASLG*, *NFκB1*, *NFκBIA*), growth factors (*PDGF B*, *FGF1*, *FGF2*), vascular regulators (*THBS1*), hypoxia-related factors (*EGLN1*/PHD2), nuclear receptors (*PPARG*, *NR4A1*) and steroid-related factors (*HSD17B7*, *SULT1E1*). Expression of all candidate genes was detected in all tissues and, generally, a good correlation was found between RNA-Seq and RT-qPCR results. Additionally, no significant changes in the expression of *EGLN1* and *PDGF B* could be found in response to treatment or passage of time.

Time-Dependent Effects

Changes in candidate gene expression associated with time were assessed in control samples. All significant effects observed with the passage of time (including statistical analysis) are presented in **Table 3**. Time-related effects were observed for: *TBXAS1*(P = 0.0006), *PTGDS* (P = 0.0153), *TGFβR1* (0.0017), *ICAM1* (P = 0.0003), *FAS* (P = 0.0015), *FASLG* ($P < 0.0001$), *NFκBIA* (P = 0.0006), *FGF1* (0.0031), *FGF2* (P = 0.0032), *THBS1* ($P < 0.0001$), *PPARγ* (P = 0.0183) and *HSD17B7* ($P < 0.0001$) (**Table 3**, **Supplemental Table 5**). Despite that $P < 0.05$ was obtained for *NFκB* (P = 0.0408) with the ANOVA test, no significant effect was obtained in the multiple comparisons test ($P > 0.05$, **Table 3**, **Supplemental Table 5**).

The expression of most target genes was downregulated with the passage of time. Expression of *TBXAS1*, *ICAM1*, *FAS*, *FASLG,* and *THBS1* was significantly higher in early developing CL stages (days 5 and/or 10) and decreased toward CL maturation (days 20 and/or 30). The expression of *PTGDS*, *NFκBIA*, and *PPARγ* was significantly higher on day 10 than on day 20. *TGFβR1* and *FGF2* expression was the lowest on day 30 compared with days 5 and 20 or only with day 20, respectively. In a different direction, the expression of *FGF1* significantly increased from day 5 to day 30. Finally, *HSD17B7* had the lowest expression at day 5, increasing during later stages of CL development.

Treatment-Induced Effects

Effects of Previcox treatment were assessed in all available samples by comparing expression of candidate genes in treated and control groups at each time-point (days 5, 10, 20, and 30). No significant changes ($P > 0.05$) in the expression of *FGF1* and *HSD17B7* were obtained in response to treatment in any of the comparisons studied (**Supplemental Table 5**), even if their expression was predicted to be modulated by NGS on days 30 and 20. Additionally, no significant changes in the expression of any of the candidate genes could be observed on day 10 (**Supplemental Table 5**). In the pairwise comparison on day 5, *TGFβ1* and *THBS1* exhibited increased expression in response to treatment, while *FASLG*, *FGF2* and *SULT1E1* were downregulated (for details, including statistical analysis, see **Table 4A**). At day 20, higher expression of *TGFβR1* and *FGF2* was observed in control samples (**Table 4B**). In a different direction, several factors were upregulated by treatment on day 20: *TBXAS1*, *PTGDS*, *ICAM1*, *NODAL*, *FAS*, *FASLG*, *NFκB1*, *NFκBIA*, *THBS1*, *PPARG*, *NR4A1*, and *SULT1E1* (**Table 4B**). Finally, on day 30, treatment decreased the expression of *IDO1* and increased the expression of *FGF2* (**Table 4C**).

DISCUSSION

General Considerations

Among many species-specific regulatory features, the presence of a transitional gonadotropin independence in the developing canine CL is certainly one of the most intriguing (17, 20). It positions the dog as a valuable model for investigating CL development without the dominant effects of hypophyseal hormones that are observed, e.g., in livestock (42, 43). As described previously, PGs, mainly PGE2, are considered to be among the most important regulators of CL function during its independence from gonadotropins (3, 23, 24). It also became apparent that PGE2 might have a broader role in the canine CL, regulating luteal sensitivity to other hormones (e.g., PRL) and exerting vasoactive and immunomodulatory actions (3, 25, 26). Consequently, the wide spectrum of direct and indirect effects of PGs in the canine CL encouraged us to perform the present NGS-based study. The ultimate goal was to better understand the different roles that PGs might play in the CL transcriptome and, thereby, to elucidate other possible regulatory mechanisms induced by PGs in the CL. Taking advantage of access to control samples covering the time span between days 5 and 30 after ovulation, i.e., during the development and maturation of the CL, transcriptional changes were also assessed in these samples with regard to the effects of time. In agreement with our previous reports (3, 24, 26), large variations in gene expression were observed in the CL of Previcox-treated dogs. This may be at least partially explained by the small number of animals per group and individual variations in gene expression. However, as can be seen from the analysis of the sequencing data presented herein, treatment with Previcox itself seemed to be an additional cause for these fluctuations. In fact, samples from control groups showed a higher correlation with each other than samples from treated groups. This could also be observed on the heatmap analysis of the 2,000 genes with higher variance, showing more homogeneous clustering when only control samples were used. As discussed elsewhere, individual variations and pharmacokinetics may have played an important role in the lower homogeneity observed in treated groups (26). The evaluation of both PCA and heatmap plots also suggested a more homogeneous clustering of samples divided between early and mature CL than by application of treatment. It seemed,

TABLE 3 | Relative gene expression of target candidate genes affected by time in control animals.

Target	Group	RGE	SD+/SD–	ANOVA *P*-value	Dunn's test
TBXAS1	Day 5 control	3.95	1.57/1.12	0.0006	5C vs. 20C – $P < 0.05$ 10C vs. 20C – $P < 0.01$ 10C vs. 30C – $P < 0.05$
	Day 10 control	6.02	8.98/3.6		
	Day 20 control	1.75	0.86/0.58		
	Day 30 control	2.25	2.66/1.22		
PTGDS	Day 5 control	6.17	6.69/3.21	0.0153	10C vs. 20C – $P < 0.05$
	Day 10 control	15.02	18.43/8.28		
	Day 20 control	4.39	3.95/2.08		
	Day 30 control	6.74	14.58/4.61		
TGFβR1	Day 5 control	6.28	3.51/2.25	0.0017	5C vs. 30C – $P < 0.001$ 20C vs. 30C – $P < 0.05$
	Day 10 control	5.15	6.45/2.86		
	Day 20 control	6.49	4.86/2.78		
	Day 30 control	2.85	1.98/1.17		
ICAM1	Day 5 control	5.35	10.74/3.57	0.0003	5C vs. 20C – $P < 0.01$ 5C vs. 30C – $P < 0.01$ 10C vs. 20C – $P < 0.05$
	Day 10 control	3.23	1.76/1.14		
	Day 20 control	1.69	0.9/0.59		
	Day 30 control	1.83	0.77/0.54		
FAS	Day 5 control	2.61	1.01/0.73	0.0015	5C vs. 20C – $P < 0.01$ 5C vs. 30C – $P < 0.01$
	Day 10 control	2.33	2.43/1.19		
	Day 20 control	1.4	0.38/0.3		
	Day 30 control	1.45	0.77/0.5		
FASLG	Day 5 control	4.59	2.66/1.68	<0.0001	5C vs. 20C – $P < 0.01$ 5C vs. 30C – $P < 0.001$ 10C vs. 20C – $P < 0.05$ 10C vs. 30C – $P < 0.01$
	Day 10 control	4.2	2.05/1.38		
	Day 20 control	2.3	0.51/0.41		
	Day 30 control	1.85	1.13/0.7		
NFκB1	Day 5 control	1.63	0.63/0.46	0.0408	No significant effects in group comparisons
	Day 10 control	2.13	1.0/0.68		
	Day 20 control	1.35	0.72/0.47		
	Day 30 control	1.41	0.68/0.46		
NFκBIa	Day 5 control	2.4	3.85/1.48	0.0006	10C vs. 20C – $P < 0.001$
	Day 10 control	4.11	6.81/2.56		
	Day 20 control	1.2	0.33/0.26		
	Day 30 control	1.75	0.88/0.58		
FGF1	Day 5 control	3.2	1.57/1.05	0.0031	5C vs. 30C – $P < 0.01$
	Day 10 control	5.47	8.77/3.37		
	Day 20 control	4.98	2.05/1.45		
	Day 30 control	6.45	3.23/2.15		
FGF2	Day 5 control	3.63	2.04/1.31	0.0032	20C vs. 30C – $P < 0.01$
	Day 10 control	3.45	2.18/1.34		
	Day 20 control	4.65	1.46/1.11		
	Day 30 control	2.22	0.82/0.6		
THBS1	Day 5 control	8.91	5.75/3.5	<0.0001	5C vs. 20C – $P < 0.001$ 5C vs. 30C – $P < 0.001$
	Day 10 control	4.85	3.59/2.06		
	Day 20 control	1.97	1.4/0.82		
	Day 30 control	2.91	2.45/1.33		
PPARγ	Day 5 control	2.2	1.28/0.81	0.0183	10C vs. 20C – $P < 0.05$
	Day 10 control	4.08	6.75/2.54		
	Day 20 control	1.66	0.41/0.33		
	Day 30 control	1.89	0.9/0.61		
HSD17B7	Day 5 control	1.9	1.04/0.67	<0.0001	5C vs. 10C – $P < 0.05$ 5C vs. 20C – $P < 0.001$ 5C vs. 30C – $P < 0.001$
	Day 10 control	4.58	3.53/1.99		
	Day 20 control	7.7	1.74/1.42		
	Day 30 control	6.16	8.03/3.48		

Relative gene expression (RGE) is presented for each group as the geometric mean and geometric standard deviation (SD). Non-parametric ANOVA (Kruskal-Wallis) analysis was followed by Dunn's test. Only results considered statistically significant ($P < 0.05$) are presented. Blue ANOVA indicates higher gene expression in early control groups (days 5 and/or 10); red ANOVA indicates higher gene expression in mid-diestrus control groups (days 20 and/or 30); black ANOVA indicates no specific changing pattern between early and mid-diestrus control groups (i.e., between days 5 and/or 10 and days 20 and/or 30).

TABLE 4 | Relative gene expression of target candidate genes affected by treatment at each analyzed time-point.

Target gene	TaqMan real time PCR					NGS results	
	RGE/contr.	SD+/SD–	RGE/treat.	SD+/SD–	*P*-value	*P*-value	Log2 ratio
A. Day 5 treated over control							
TGFβ1	1.58	0.4/0.32	2.67	1.84/1.09	0.0017	0.02148	0.4632
FASLG	4.59	2.66/1.68	2.44	1.35/0.87	0.0013	0.03313	−1.4
FGF2	3.63	2.04/1.31	2.14	1.46/0.87	0.009	0.163	−1.136
THBS1	8.91	5.75/3.5	14.07	5.98/4.2	0.0129	0.2279	0.6146
SULT1E1	7.97	7.27/3.8	4.18	4.33/2.13	0.0023	0.003543	3.094
B. Day 20 treated over control							
TBXAS1	1.75	0.86/0.58	4.25	4.41/2.17	0.005	0.003262	2.014
PTGDS	4.39	3.95/2.08	28.31	28.06/14.09	<0.0001	7.43E-05	2.637
TGFβR1	6.49	4.86/2.78	2.18	1.91/1.02	0.0013	0.04251	−0.8656
ICAM1	1.69	0.9/0.59	16.76	23.31/9.75	<0.0001	4.21E-07	3.765
NODAL	4.5	11.64/3.24	262.07	227.7/121.8	<0.0001	2.98E-09	5.04
FAS	1.4	0.38/0.3	2.6	1.01/0.73	0.0003	0.006776	0.8808
FASLG	2.3	0.51/0.41	5.73	3.05/1.99	<0.0001	0.008149	2.836
NFκB1	1.35	0.72/0.47	2.42	1.04/0.73	0.0064	0.005073	0.932
NFκBIa	1.2	0.33/0.26	5.69	2.62/1.8	<0.0001	7.41E-10	2.01
FGF2	4.65	1.46/1.11	2.37	2.41/1.19	0.0162	0.4982	−0.6664
THBS1	1.97	1.4/0.82	12.77	10.58/5.79	<0.0001	0.0007533	2.55
PPARγ	1.66	0.41/0.33	5.56	7.24/3.14	0.0006	7.94E-08	2.283
NR4A1	4.96	3.03/1.88	43.73	44.88/22.15	<0.0001	2.11E-07	3.616
SULT1E1	6.62	6.63/3.31	17.15	32.76/11.25	0.0396	0.001586	2.63
C. Day 30 treated over control							
IDO1	4.75	6.1/2.67	1.63	0.97/0.61	0.0003	0.0002207	−3.172
FGF2	2.22	0.82/0.6	3.57	2.36/1.42	0.0088	0.765	−0.2163

Relative gene expression (RGE) is presented for each group (contr., control group; treat., treated group) as the geometric mean and geometric standard deviation (SD+/SD–). Student's t-test was applied to test the effect of treatment at each analyzed time-point. Only results considered statistically significant (P < 0.05) are presented. Blue t-test indicates higher gene expression in the control group, while red indicates higher gene expression in treated groups.

thus, that time had a great impact on the transcriptional changes observed among the samples studied.

Time-Dependent Effects

Showing homogenous distribution of gene expression, with a clear distinction between the early and mature CL, time-dependent effects were examined in control samples and additionally served for quality control. When compared with developing CL (days 5 and 10), more highly represented genes in the mature CL (days 20 and 30) related to lipid biosynthesis/metabolism. The canonical pathways predicted to be upregulated at this stage were related to cholesterol biosynthesis. Cholesterol is a substrate required for steroid hormone synthesis. An increase of its production is probably required for the observed increased steroidogenic output from the CL at this time. As also confirmed by the qPCR analysis, the expression of *HSD17B7* (known as PRLR-associated protein) was found to increase with maturation of the CL. Together with other isoforms of 17βHSD, this enzyme is responsible for the conversion of estrone into estradiol, a more potent estrogen (44, 45). Considering the high variation in circulating 17β-estradiol (E2) during the canine diestrus (1), together with the concomitantly increased expression of aromatase (CYP19) (46), it is plausible that the observed increase in *HSD17B7* expression could be involved in the local provision of estrogens in the canine CL. Reflecting the increasing steroidogenic capacity of the CL, following their initial post-ovulatory decrease, E2 levels increase during the course of diestrus in the dog, roughly following the P4 secretion profiles (13, 47). The expression of the estrogen receptors, ESR1/ERα and ESR2/ERβ, has been confirmed in the canine CL (46). Nevertheless, the involvement of estrogens in regulating canine CL function remains underexplored, even though some attempts were made to shed light on the underlying mechanisms (6, 46). Functional terms more highly represented on days 5 and 10 after ovulation were mainly related to immune function and proliferative mechanisms, such as locomotion, cell-cell adhesion, extracellular matrix organization, and regulation of the ERK1/2 cascade. Accordingly, pathways related to cell cycle, proliferation and immune function, were predicted to be inactivated following CL maturation, i.e., at days 20/30 of

the CL lifespan. The apparently increased immune activity in the developing canine CL is in accordance with its previously reported increased infiltration by macrophages, monocytes and lymphocytes at this stage (48, 49). Furthermore, regarding immune regulation, TNF was among the top predicted upstream regulators involved in the CL transcriptomic changes observed in response to time. Similarly, an increased expression of *TNFα* and its receptor *TNFR2* on day 5 compared with mature CL stages was reported previously (26). Here, the expression of *FAS* and *FASLG*, factors belonging to the TNF superfamily, was also found to be more highly expressed in early than in mature CL at mid-diestrus (days 5/10 over 20/30). Their increased expression at that time was corroborated by the qPCR results. The role of the FAS/FASLG system in luteolysis, as extrinsic inducers of apoptosis, has been widely described in different species (50–54). With regard to the early CL, FAS was also observed to be increased in bovine CL as early as at day 5 after ovulation, provoking the question of possible non-apoptotic FAS signaling in regulating CL function (55). Indeed, FAS has been shown to affect some downstream non-apoptotic signaling pathways, such as NFκB (56). Thus, although the role of FAS/FASLG in the developing CL is still unknown, it could be also related with immune-mediated tissue reorganization and proliferation. Similar to FAS/FASLG, thrombospondins (THBS) have been associated with luteolytic events, responding to PGF2α and acting as anti-angiogenic factors by inhibiting the pro-angiogenic FGF2 (57, 58). Similar to the rat (59), and as also found by our qPCR analysis, increased expression of *THBS1* was detected in early CL stages and decreased toward mid-diestrus in mature CL (days 20 and 30). Within the early CL stage, an intense angiogenic activity is observed. Thus, the increased expression of *THBS1* appears paradoxical and is not fully understood. It appears plausible that *THBS1* could act as a limiter of vascular overgrowth, as suggested by others (59). However, it should be mentioned that the protein availability of this factor, as well as the availability of its receptors, were not investigated in the present study, but certainly merit further attention.

Regarding eicosanoids, modulation of CL function is classically seen as a balance between the luteotropic function of PGE2 and the luteolytic activity of PGF2α. In the canine CL, the expression of PGE2 synthase (PTGES) and PGE2 receptor 2 (PTGER2/EP2) decreases with the passage of time (21). This expression pattern could explain inhibition of the eicosanoid signaling pathway predicted by IPA software. Accordingly, similar time-dependent effects were observed herein in the expression of *TBXAS1* and PGD2-synthase (*PTGDS)*, which decreased from the early to the mid-luteal phase in the transcriptional analysis (further confirmed by qPCR). Both eicosanoids have been predominanty characterized in other systems. Thus, whereas thromboxane 2 (TBXA2) has been related to platelet aggregation, myocardial ischemia and bronchoconstriction, PGD2 has been extensively described as a regulator of body temperature and sleep cycle, vasodilation, smooth muscles relaxation and bronchoconstriction (60–62). With regard to the reproductive systems, the inhibition of TBXAS leads to increased cAMP-dependent steroidogenesis in Leydig cells (63). As for PGD2, in males it acts as an activator of the Sox9 gene and is, therefore, pivotal in testicular organogenesis (64, 65). However, to the best of our knowledge, nothing is known about the modulatory effects these two eicosanoids might have on CL function. Strikingly, PGD2 can undergo spontaneous dehydration into different J prostanoids, such as 15d-PGJ2 (66, 67). This prostaglandin can mediate pro-inflammatory mechanisms through different pathways, but also affects anti-inflammatory responses, mainly through the nuclear receptor PPARγ (68). Expression of PPARγ decreased between days 10 and 20 in qPCR analysis, and is an alternative receptor for several different factors, including eicosanoids and fatty acids, with regulatory roles in fatty acid metabolism, cell differentiation and inflammation (69). Among other regulatory effects, PPARγ has an indirect role in potentiating the expression of STAR by upregulating cJUN (70). In the CL of pregnant dogs, it was stably expressed during the whole diestrus (39). However, here we observed increased expression of this receptor in early CL stages, similar to the two eicosanoid-synthases studied. Thus, it seems plausible that also in the dog PPARγ provides an alternative pathway for possible modulatory effects of PGD2-derived prostanoids in the CL.

Collectively, our analysis indicates that during the transition from the early developing to the mature CL a decrease in immune activity and tissue proliferation occurs, expectedly accompanied by its increased steroidogenic capacity. Additionally, among the predicted top upstream regulators, different hormones and PGE2 receptor 2 (PTGER2/EP2) were present, which are known to exhibit time-dependent changes in their expression in the CL during canine diestrus (14, 21). Taking into consideration that these functional changes and the expression of different genes were previously investigated and/or were expected, as mentioned elsewhere, the analysis of time-dependent effects served also as a primary validation of the Next Generation Sequencing methodology. Besides this, the expression patterns of *TBXAS*, *PTGDS*, *FAS/FASLG*, *NFκB/NFκBIA*, *THBS1*, *PPARγ*, and *HSD17B7* in the canine CL were described and discussed for the first time herein. All of these factors may serve functional roles in the development of CL in the canine species and thus constitute topics worthy of more attention in the future.

Treatment-Induced Effects

The functional suppression of COX2, and the consequent withdrawal of PGs, had variable effects on the different groups studied. The numbers of DEGs found for each studied time-point were also variable, being lower in gonadotropin-independent CL stages (days 5 and 10) than during the transition period and at gonadotropin dependency (days 20 and 30, respectively). Interestingly, the highest number of DEGs (1,741) was found in CL from dogs treated with Previcox for 20 days. This, together with the absence of genes commonly affected by treatment in all groups, reinforces the time and developmental stage-dependent effects of COX2 suppression on CL transcriptional activity. Furthermore, the presence of possible compensatory mechanisms for the withdrawal of PGs was suggested previously (3, 26) and appears to be a part of the inherent regulation of CL function in the dog. At the same time, the possible presence of such mechanisms advocates caution in the evaluation and

interpretation of the results obtained because they might be induced by these mechanisms, rather than being directly linked to the function of PGs.

Gonadotropin-Independent Stage of CL

This stage relates to the early, developing CL treated with Previcox over 5 and 10 days. Large individual and functional variations in the response to treatment were observed at this time at the transcriptome level, with fewer genes passing the applied stringent *P*-value and FDR criteria. Nevertheless, functional terms related to cellular movement and division dominated at day 5 after ovulation in response to Previcox. Additionally, the predicted activation of cell movement and cytoskeleton-related pathways was mainly due to the increased expression of factors like actins, laminin and myosin observed in the transcriptome analysis. In preceding studies, significant effects of treatment at this time-point showed decreased expression of STAR, PRLR and PTGES, the latter one being associated with lower levels of intra-CL PGE2 (3). However, no significant effects were observed regarding transcriptional capacity, vascularization or immune function (24, 26). Here, as detected by qPCR, expression of the growth factor *FGF2* was decreased by Previcox treatment, while *THBS1* was upregulated. Considering the aforementioned interaction between these factors, the expression pattern of *FGF2* and *THBS1* suggests a disruptive effect of this treatment on angiogenic mechanisms. The inhibitory effects on vascularization appear even more plausible when the increased expression of *TGFβ1* after treatment is considered. In fact, growth and capillary morphogenesis of endothelial cells isolated from bovine CL were diminished by this cytokine (71). Additionally, in the present study qPCR also detected decreased expression of *FASLG* in Previcox-treated CL. If, as described above, this factor is usually associated with anti-angiogenic activity, its increased expression in early CL stages could imply a positive role of *FASLG* in CL angiogenesis, which appears to be affected after treatment. Although hypothetical, this idea deserves further attention in the future.

Regarding other functional mechanisms, as indicated by qPCR, the gene expression of *SULT1E1* decreased after Previcox treatment. As indicated elsewhere, the auto/paracrine effects of estrogens in the canine CL have been proposed before (6, 46). SULT1E1 sulfoconjugates estrogens, disrupting their capacity to bind to their receptors and, in this way, preventing their actions on target tissues (72). Thus, the observed decrease of *SULT1E1* expression in response to treatment might disturb the balance of locally active estrogens in the CL, presumably as a part of the compensatory mechanisms following the withdrawal of PGs.

The effects of Previcox treatment on day 10 appeared less pronounced at the transcriptome level. In previous studies, however, we observed that inhibition of COX2 at day 10 decreased the expression of PTGES, consequently significantly decreasing the intra-CL levels of PGE2, and this was associated with a significant decrease in circulating P4 levels (3, 24). These previous findings apparently contrast with the low number of DEGs observed in the present analysis. It appears, however, plausible that the variation among the treated samples could be the culprit for the negative output from this analysis, in particular with regard to the applied adjusted *P*-value (FDR), accounting for multiple testing but not for the biological diversity in the response to the applied anti-COX2 insult.

Transition Toward Gonadotropin Dependence

This stage of the CL relates to the transitional period of development toward its gonadotropin dependence, represented in our study by day 20 after ovulation (17, 18). In fact, day 20 was the time-point most affected by treatment. At this time, the CL appears to be more susceptible to insults targeting its functionality. The main functional terms overrepresented in Previcox-treated samples at this day were related to cellular proliferation and immune response. This fits well with the previously reported reduced size of the nuclei of steroidogenic cells and increased expression of some pro-inflammatory interleukins (e.g., IL1β or IL6) in response to Previcox at this day (24, 26). In the present NGS analysis, IL1β and IL6 were also found to be differentially expressed after treatment. The activation of several immune system-related canonical pathways was predicted by IPA software, and increased expression of other pro-inflammatory factors, e.g., *ICAM1*, *NODAL*, *FAS*, *FASLG*, and *NFκB1,* was further confirmed by qPCR. This apparently increased reactivity of the immune system was accompanied by negative effects induced by the treatment at this time-point on the steroidogenic machinery, mirrored in the decreased expression of 3βHSD and STAR (3, 24). These findings suggest predominantly negative effects of treatment on CL function at this stage.

With regard to vascular function, in addition to the previously found increased expression of endothelin-1 (END1) and downregulation of angiopoietin 1 (ANGPT1) at day 20 of treatment (26), here, increased expression of the anti-angiogenic *THBS1* and decreased levels of *FGF2* were identified. With this, the postulated negative impact of PGs withdrawal on CL vascular activity was further substantiated.

Contrasting with the decreased expression of *SULT1E1* at day 5 of treatment, its expression was elevated during the transitional phase at day 20 in the CL of Previcox-treated dogs. SULT1E1 was also elevated in the CL in mid-pregnant dogs undergoing luteolysis after treatment with an antigestagen (27), suggesting that the local withdrawal of estrogens could be related with decreased CL activity. The apparently suppressed expression of *HSD17B7* ($P = 0.0608$) at day 20 of treatment further strengthens the idea of possible involvement of estrogens in CL function. On the other hand, we also observed strongly increased expression of the nuclear factor *NR4A1* (also referred to as Nur77) in response to Previcox. This expression pattern was further confirmed by qPCR. Several functions were previously described for this receptor. The expression of NR4A1 was increased in the CL of bitches, cows and rats in response to treatment with the luteolysin PGF2α (73–75). This receptor is also known to be an important regulator of inflammation [reviewed in (76)]. Thus, it is plausible that the increased expression of this nuclear receptor might be related to the increased inflammatory response observed at this CL stage to the Previcox insult. Nevertheless, its exact functions in the canine CL remain to be determined. Due to the versatile effects of NR4A1 in different organs and systems, its possible actions on the CL appear worthy of more attention in the future.

The increased expression of *TBXAS*, *PTGDS,* and *PPARγ* observed in transcriptomic and qPCR analyses at day 20 after Previcox treatment could represent possible compensatory mechanisms, as suggested in previous reports (3, 26). As mentioned elsewhere, PPARγ acts as an alternative receptor for prostaglandins (68, 69). Besides its potential to upregulate the pro-steroidogenic cJUN (70), it was shown to repress the activity of NFκB (77, 78). Indeed, increased expression of cJUN was proposed previously to counteract the negative effects of Previcox (26).

Cumulatively, in accordance with our previous findings (26), the functional inhibition of COX2, besides suppressing intra-CL PGE2 content (3), led to activation of CL immune system-related factors and pathways. It also negatively affected vascularization of the CL during its functional transition to the gonadotropin-dependent stage. The regulatory effects upon PPARγ and NFκB, the reciprocal interactions between FGF and THBS or even possible modulatory effects on locally produced estrogens, could possibly be involved in the maintenance of CL tissue homeostasis at this time in a PG-dependent manner.

Gonadotropin-Dependent CL Stage

In this comparison, the stage of CL development refers to mid-diestrus, represented by day 30. During this time, the maintenance of CL function is primarily dependent on PRL (19, 20). Day 30 showed the second highest number of DEGs in response to Previcox treatment. Also, in the Venn diagram analysis, days 20 and 30 shared the highest number of simultaneously affected genes, even if signaling pathways represented by these genes indicated their different functional status.

At day 30, the fully mature CL exhibits high steroidogenic capacity. This was reflected in the functional terms overrepresented at day 30 in control samples compared with their Previcox-treated counterparts. These included, e.g., steroidogenic and lipid metabolic processes, which were less represented in the CL of treated dogs. The analysis of functional pathways corroborated these observations, revealing cholesterol synthesis and steroidogenesis among the prevalent pathways affected by the treatment. Interestingly, in this contrast, the effects of the treatment appeared diverse and affected genes with higher functional variations. On the other hand, as indicated above, contrasting with day 20 of treatment, the immune system-related functional pathways (e.g., NFκB- and TGFβ-signaling) appeared less represented at day 30 in the treated CL. Their importance was, however, underlined by placing their respective associated factors among the top upstream regulators. Thus, besides TNF and PPARγ, TGFβ1 and NFκBIA (NFκB-associated factor) were also identified by IPA software. By adding new information, these results also fit well with the previously reported increased presence of CD4-expressing macrophages infiltrating the CL in response to treatment with Previcox at day 30 of treatment (26). Activation of the immune system was further indicated in the data set presented here by the strong suppression of IDO1 expression at day 30 of treatment. Being a rate-limiting enzyme in tryptophan catabolism, IDO1 function is considered to be a checkpoint in the activation of leukocytes by exerting immunosuppressive actions (79). Interestingly, and as indicated above, despite the proximities in the development time, maturation stage and steroidogenic capacity of the CL between days 20 and 30 after ovulation, the effects evoked upon the immune system at these two time-points by Previcox appeared to diverge, further highlighting the time-dependent effects of PGs withdrawal in the canine CL.

Final Remarks

As shown in this and previous studies, treatment of dogs with Previcox affects multiple CL components and functions (3, 24, 26). In accordance with these observations, broad effects of COX2 inhibition were observed in the deep RNA-Seq analysis performed herein. These effects were clearly stage-dependent. Day 20, marking the transitional period toward gonadotropin-dependence, was the most affected by COX2-inhibition, identifying this period as the most sensitive stage of CL development to functional PGs withdrawal. It appears that at this stage the intrinsic regulatory mechanisms become unstable, while the luteotropic effects of PRL may be affected by treatment (3). This could also affect the strong compensatory mechanisms present in earlier stages, rendering the mature CL less capable of stabilizing its transcriptome in response to the insult caused by Previcox treatment. Indeed, it appears that the early CL is more resistant to PGs withdrawal, suggesting that this organ is intrinsically regulated and bears strong compensatory mechanisms. With maturation of the CL, its transcriptome becomes more sensitive to COX2 inhibition.

Mechanisms related to cellular proliferation, immune system and vascularization are undoubtedly involved in the proper development of the CL. Accordingly, here, deeper insights have been provided into the regulatory mechanisms underlying CL development, identifying several factors and pathways that could play roles in this process. Some of these, such as THBS1 and FAS/FASLG, are known for their involvement in the termination of CL function, but their role in CL formation is still not well-understood. Additionally, the modulatory effects of estrogens and PPARγ in the canine CL are still obscure and may play important luteotropic roles. Finally, the increased expression of *TBXAS* and *PTGDS* in early CL stages supports the idea that other PGs, besides PGE2, may play an important role in regulating and supporting the canine CL.

Apparently, by investigating transcriptomic effects, and being based on gene expression patterns, the information presented herein is not definitive and further functional and protein expression-related studies are needed to support these findings and hypotheses. Nevertheless, our analyses with Previcox-treated dogs clearly reveal broader regulatory roles linked to PGs in CL function, besides the luteotropic support of steroidogenesis by PGE2 or the luteolytic signaling of PGF2α. With this, the translational aspect of the present study in relation to other domestic animal species is obvious.

Our study falls into the clinical trials category and Previcox was used orally, as recommended by the manufacturer. This might have weakened effects on the target tissue due to its metabolism, even though 10 mg/kg of firocoxib, double the clinically recommended dosage, was used (in consultation with the manufacturer regarding safety). Despite causing disturbances in CL function, in none of the dogs was the luteal phase terminated. From the clinical point of view, this is important information because administration of Previcox appears to be safe for CL function and maintenance in non-pregnant, and presumably, also in pregnant dogs.

DATA AVAILABILITY STATEMENT

The datasets generated for this study can be found in NCBI's Gene Expression Omnibus, Series accession number GSE130369.

ETHICS STATEMENT

Animal experiments were approved by the responsible ethics committee (permit 54/2008) of the University of Warmia and Mazury in Olsztyn, Poland.

AUTHOR CONTRIBUTIONS

MTP was involved in developing the concept of the present study, experimental design, generating data, analysis and interpretation of data, and drafting of the manuscript. FG was involved in knowledge transfer, and in the laboratory part of the project, as well as in critical discussion of data. HR contributed knowledge transfer, critical discussion and interpretation of data, and editing the manuscript. TJ was involved in design of the *in vivo* study and tissue collection, knowledge transfer, critical discussion of data, and revision of the manuscript. BH was involved in design of the *in vivo* study. BH and AB were involved in knowledge transfer, critical discussion of data, and revision of the manuscript. MPK designed and supervised the project, and was involved in interpretation of the data, and drafting and revision of the manuscript. All authors read and approved the final manuscript.

FUNDING

This work was in part supported by The Swiss National Science Foundation (SNSF) research grant numbers 31003A_160251 and 31003A_182481 to MPK.

ACKNOWLEDGMENTS

Authors are thankful to Dr. Barry Bavister for careful editing of the manuscript. The technical expertise and contribution of Ricardo Fernandez Rubia is greatly appreciated. Part of the laboratory work was performed using the logistics at the Center for Clinical Studies, Vetsuisse Faculty, University of Zurich.

SUPPLEMENTARY MATERIAL

The Supplementary Material for this article can be found online at: https://www.frontiersin.org/articles/10.3389/fendo.2019.00715/full#supplementary-material

Supplemental Table 1 | List of differentially expressed genes (DEGs) found in the contrast "days 20+30 control over days 5+10 control." All genes listed passed the criteria of $P < 0.01$ and FDR < 0.1 (False Discovery Rate, adjusted *P*-value).

Supplemental Table 2 | List of differentially expressed genes (DEGs) found in the contrasts "day 5 treated over day 5 control," "day 10 treated over day 10 control," "day 20 treated over day 20 control," and "day 30 treated over day 30 control." All genes listed passed the criteria of $P < 0.01$ and FDR < 0.1 (False Discovery Rate, adjusted *P*-value).

Supplemental Table 3 | Lists of representative genes (up to 10) and statistical analysis details of particular GO terms, particular functional networks, representative canonical pathways and top upstream regulators.

Supplemental Table 4 | Complete list of genes presented in Venn diagram from the contrasts "day 5 treated over day 5 control," "day 20 treated over day 20 control," and "day 30 treated over day 30 control" and each intersection.

Supplemental Table 5 | Relative gene expression and statistical analysis of all target candidate genes investigated with regard to time-dependent and treatment-induced effects. Relative gene expression (RGE) is presented for each group as the geometric mean and geometric standard deviation. For time-dependent effects, non-parametric ANOVA (Kruskal-Wallis) analysis was used, followed by Dunn's test. For the assessment of effects of treatment, Student's *t*-test was applied at each time-point analyzed. $P < 0.05$ was considered significant.

Supplemental Image 1 | Initial explorative analysis of the sequencing dataset. Samples correlation matrix and heatmaps were obtained by using CountQC app provided in the SUSHI framework. In **(A,B)**, "K" and "Ctrl" relate to control samples while "P" and "Treat" relate to Previcox-treated samples. **(A)** Sample correlation matrix containing all samples submitted for RNA-Seq and considering all genes present. Samples 10/1 (10_K_1) and 30/1 (30_K_1) controls, and 10/2 (10_P_2) and 30/1 (30_P_1) treated, exhibited low correlation coefficients compared with other samples from the same group and were removed from further analysis. **(B)** Sample correlation matrix containing final list of samples used in the present analysis and considering all genes present. Control groups appear to have higher homogeneity than respective treated groups. **(C)** Heatmap of 2,000 genes with higher variance among all control samples. Gene ontologies (GOs) shown were obtained with Enrichr. Samples show apparent better clustering than in **(D)**, the heatmap of 2,000 genes with higher variance among all samples analyzed (control and treated).

Supplemental Image 2 | Volcano plots of differentially expressed genes (DEGs; FDR < 0.1, Log2Ratio > 0.5) affected by the passage of time (**A**: contrast "days 20+30 control over days 5+10 control") or induced by treatment (**B**: contrast "day 5 treated over day 5 control;" **C**: contrast "day 5 treated over day 5 control;" **D**: contrast "day 5 treated over day 5 control").

Supplemental Image 3 | Functional networks found in the upregulated differentially expressed genes (DEGs) from the contrast "days 20+30 control over days 5+10 control" and in the downregulated DEGs from the contrast "day 30 treated over day 30 control." Functional networks were obtained with the ClueGO application for Cytoscape. The functional terms overrepresented in each group are shown. Redundant or non-informative terms were removed and the networks obtained were manually rearranged. Number of mapped genes is indicated by the node size while significance of functional terms is denoted by node color (represented in legend at the right bottom corner). **(A)** Networks more highly represented on days 20 and 30 control (mature CL) were related to intracellular transport and lipid metabolism. **(B)** Networks more highly represented in CL samples from control animals on day 30 after ovulation were related to nitric oxide synthesis and angiogenesis.

REFERENCES

1. Hoffmann B, Höveler R, Nohr B, Hasan SH. Investigations on hormonal changes around parturition in the dog and the occurrence of pregnancy-specific non conjugated oestrogens. *Exp Clin Endocrinol.* (1994) 102:185–9. doi: 10.1055/s-0029-1211280
2. Nishiyama TTS, Ito M, Kimura J, Watanabe G, Taya K, Takeishi M. Immunohistochemical study of steroidogenic enzymes in the ovary and placenta during pregnancy in the dog. *Anat Hist Embryol.* (1999) 28:125–9. doi: 10.1046/j.1439-0264.1999.00170.x
3. Kowalewski MP, Ihle S, Siemieniuch MJ, Gram A, Boos A, Zdunczyk S, et al. Formation of the early canine CL and the role of prostaglandin E2 (PGE2) in regulation of its function: an *in vivo* approach. *Theriogenology.* (2015) 83:1038–47. doi: 10.1016/j.theriogenology.2014.12.006
4. Fraser HM, Wulff C. Angiogenesis in the corpus luteum. *Reprod Biol Endocrinol.* (2003) 1:88. doi: 10.1186/1477-7827-1-88
5. Kamat BR, Brown LF, Manseau EJ, Senger DR, Dvorak HF. Expression of vascular permeability factor/vascular endothelial growth factor by human granulosa and theca lutein cells. Role in corpus luteum development. *Am J Pathol.* (1995) 146:157–65.
6. Hoffmann B, Büsges F, Engel E, Kowalewski MP, Papa PC. Regulation of corpus luteum-function in the bitch. *Reprod Domest Anim.* (2004) 39:232–40. doi: 10.1111/j.1439-0531.2004.00508.x
7. Kowalewski MP. Luteal regression vs. prepartum luteolysis: regulatory mechanisms governing canine corpus luteum function. *Reprod Biol.* (2014) 14:89–102. doi: 10.1016/j.repbio.2013.11.004
8. Kowalewski MP, Gram A, Kautz E, Graubner FR. The dog: nonconformist, not only in maternal recognition signaling. *Adv Anat Embryol Cell Biol.* (2015) 216:215–37. doi: 10.1007/978-3-319-15856-3_11
9. Gram A, Buchler U, Boos A, Hoffmann B, Kowalewski MP. Biosynthesis and degradation of canine placental prostaglandins: prepartum changes in expression and function of prostaglandin F2alpha-synthase (PGFS, AKR1C3) and 15-hydroxyprostaglandin dehydrogenase (HPGD). *Biol Reprod.* (2013) 89:2. doi: 10.1095/biolreprod.113.109918
10. Gram A, Fox B, Buchler U, Boos A, Hoffmann B, Kowalewski MP. Canine placental prostaglandin E2 synthase: expression, localization, and biological functions in providing substrates for prepartum PGF2alpha synthesis. *Biol Reprod.* (2014) 91:154. doi: 10.1095/biolreprod.114.122929
11. Kowalewski MP, Beceriklisoy HB, Pfarrer C, Aslan S, Kindahl H, Kucukaslan I, et al. Canine placenta: a source of prepartal prostaglandins during normal and antiprogestin-induced parturition. *Reproduction.* (2010) 139:655–64. doi: 10.1530/REP-09-0140
12. Luz MR, Bertan CM, Binelli M, Lopes MD. Plasma concentrations of 13,14-dihydro-15-keto prostaglandin F2-alpha (PGFM), progesterone and estradiol in pregnant and nonpregnant diestrus cross-bred bitches. *Theriogenology.* (2006) 66:1436–41. doi: 10.1016/j.theriogenology.2006.01.036
13. Hoffmann B, Höveler R, Hasan SH, Failing K. Ovarian and pituitary function in dogs after hysterectomy. *J Reprod Fertil.* (1992) 96:837–45. doi: 10.1530/jrf.0.0960837
14. Concannon PW. Reproductive cycles of the domestic bitch. *Anim Reprod Sci.* (2011) 124:200–10. doi: 10.1016/j.anireprosci.2010.08.028
15. Steinetz BG, Goldsmith LT, Harvey HJ, Lust G. Serum relaxin and progesterone concentrations in pregnant, pseudopregnant, and ovariectomized, progestin-treated pregnant bitches: detection of relaxin as a marker of pregnancy. *Am J Ver Res.* (1989) 50:68–71.
16. Concannon PW. Effects of hypophysectomy and of LH administration on luteal phase plasma progesterone levels in the beagle bitch. *J Reprod Fert.* (1980) 58:407–10. doi: 10.1530/jrf.0.0580407
17. Okkens AC, Dieleman SJ, Bevers MM, Lubberink AAME, Willemse AH. Influence of hypophysectomy on the lifespan of the corpus luteum in the cyclic dog. *J Reprod Fertil.* (1986) 77:187–92. doi: 10.1530/jrf.0.0770187
18. Onclin K, Verstegen J, Concannon PW. Time-related changes in canine luteal regulation: *in vivo* effects of LH on progesterone and prolactin during pregnancy. *J Reprod Fertil.* (2000) 118:417–24. doi: 10.1530/jrf.0.1180417
19. Concannon PW, Weinstein S, Whaley S, Frank D. Suppression of luteal function in dogs by luteinizing hormone antiserum and by bromocriptine. *J Reprod Ferti.* (1987) 81:175–80. doi: 10.1530/jrf.0.0810175
20. Okkens AC, Bevers MM, Dieleman SJ, Willemse AH. Evidence for prolactin as the main luteotrophic factor in the cyclic dog. *Vet Q.* (1990) 12:193–201. doi: 10.1080/01652176.1990.9694266
21. Kowalewski MP, Mutembei HM, Hoffmann B. Canine prostaglandin E2 synthase (PGES) and its receptors (EP2 and EP4): expression in the corpus luteum during dioestrus. *Anim Reprod Sci.* (2008) 109:319–29. doi: 10.1016/j.anireprosci.2007.11.023
22. Kowalewski MP, Schuler G, Taubert A, Engel E, Hoffmann B. Expression of cyclooxygenase 1 and 2 in the canine corpus luteum during diestrus. *Theriogenology.* (2006) 66:1423–30. doi: 10.1016/j.theriogenology.2006.01.039
23. Kowalewski MP, Fox B, Gram A, Boos A, Reichler I. Prostaglandin E2 functions as a luteotrophic factor in the dog. *Reproduction.* (2013) 145:213–26. doi: 10.1530/REP-12-0419
24. Janowski T, Fingerhut J, Kowalewski MP, Zdunczyk S, Domoslawska A, Jurczak A, et al. *In vivo* investigations on luteotropic activity of prostaglandins during early diestrus in nonpregnant bitches. *Theriogenology.* (2014) 82:915–20. doi: 10.1016/j.theriogenology.2014.07.005
25. Gram A, Latter S, Boos A, Hoffmann B, Kowalewski MP. Expression and functional implications of luteal endothelins in pregnant and non-pregnant dogs. *Reproduction.* (2015) 150:405–15. doi: 10.1530/REP-15-0256
26. Tavares Pereira M, Gram A, Nowaczyk RM, Boos A, Hoffmann B, Janowski T, et al. Prostaglandin-mediated effects in early canine corpus luteum: *in vivo* effects on vascular and immune factors. *Reprod Biol.* (2019) 10:100–11. doi: 10.1016/j.repbio.2019.02.001
27. Zatta S, Rehrauer H, Gram A, Boos A, Kowalewski MP. Transcriptome analysis reveals differences in mechanisms regulating cessation of luteal function in pregnant and non-pregnant dogs. *BMC Genomics.* (2017) 18:757. doi: 10.1186/s12864-017-4084-9
28. Hatakeyama M, Opitz L, Russo G, Qi W, Schlapbach R, Rehrauer H. SUSHI: an exquisite recipe for fully documented, reproducible and reusable NGS data analysis. *BMC Bioinformatics.* (2016) 17:228. doi: 10.1186/s12859-016-1104-8
29. Qi W, Schlapbach R, Rehrauer H. RNA-seq data analysis: from raw data quality control to differential expression analysis. *Methods Mol Biol.* (2017) 1669:295–307. doi: 10.1007/978-1-4939-7286-9_23
30. Dobin A, Davis CA, Schlesinger F, Drenkow J, Zaleski C, Jha S, et al. STAR: ultrafast universal RNA-seq aligner. *Bioinformatics.* (2013) 29:15–21. doi: 10.1093/bioinformatics/bts635
31. Liao Y, Smyth GK, Shi W. The Subread aligner: fast, accurate and scalable read mapping by seed-and-vote. *Nucleic Acids Res.* (2013) 41:e108. doi: 10.1093/nar/gkt214
32. Love MI, Huber W, Anders S. Moderated estimation of fold change and dispersion for RNA-seq data with DESeq2. *Genome Biol.* (2014) 15:550. doi: 10.1186/s13059-014-0550-8
33. Mi H, Huang X, Muruganujan A, Tang H, Mills C, Kang D, et al. PANTHER version 11: expanded annotation data from Gene Ontology and Reactome pathways, and data analysis tool enhancements. *Nucleic Acids Res.* (2017) 45:D183–9. doi: 10.1093/nar/gkw1138
34. Chen EY, Tan CM, Kou Y, Duan Q, Wang Z, Meirelles GV, et al. Enrichr: interactive and collaborative HTML5 gene list enrichment analysis tool. *BMC Bioinformatics.* (2013) 14:128. doi: 10.1186/1471-2105-14-128
35. Bindea G, Mlecnik B, Hackl H, Charoentong P, Tosolini M, Kirilovsky A, et al. ClueGO: a Cytoscape plug-in to decipher functionally grouped gene ontology and pathway annotation networks. *Bioinformatics.* (2009) 25:1091–3. doi: 10.1093/bioinformatics/btp101
36. Shannon P, Markiel A, Ozier O, Baliga NS, Wang JT, Ramage D, et al. Cytoscape: a software environment for integrated models of biomolecular interaction networks. *Genome Res.* (2003) 13:2498–504. doi: 10.1101/gr.1239303
37. Kautz E, Gram A, Aslan S, Ay SS, Selcuk M, Kanca H, et al. Expression of genes involved in the embryo-maternal interaction in the early-pregnant canine uterus. *Reproduction.* (2014) 147:703–17. doi: 10.1530/REP-13-0648
38. Kowalewski MP, Michel E, Gram A, Boos A, Guscetti F, Hoffmann B, et al. Luteal and placental function in the bitch: spatio-temporal changes in prolactin receptor (PRLr) expression at dioestrus, pregnancy and normal and induced parturition. *Reprod Biol Endocrinol.* (2011) 9:109. doi: 10.1186/1477-7827-9-109

39. Kowalewski MP, Meyer A, Hoffmann B, Aslan S, Boos A. Expression and functional implications of peroxisome proliferator-activated receptor gamma (PPARgamma) in canine reproductive tissues during normal pregnancy and parturition and at antiprogestin induced abortion. *Theriogenology.* (2011) 75:877–86. doi: 10.1016/j.theriogenology.2010.10.030
40. Andersen CL, Ledet-Jensen J, Ørntoft T. Normalization of real-time quantitative reverse transcription-pcr data: a model-based variance estimation approach to identify genes suited for normalization, applied to bladder and colon cancer data sets. *Cancer Res.* (2004) 64:5245–50. doi: 10.1158/0008-5472.CAN-04-0496
41. Vandesompele J, De Preter K, Pattyn F, Poppe B, Van Roy N, De Paepe A, et al. Accurate normalization of real-time quantitative RT-PCR data by geometric averaging of multiple internal control genes. *Genome Biol.* (2002) 3:RESEARCH0034. doi: 10.1186/gb-2002-3-7-research0034
42. Hoffmann B, Schams D, Bopp R, Ender ML, Gimenez T, Karg H. Luteotrophic factors in the cow: evidence for lh rather than prolactin. *Reproduction.* (1974) 40:77–85. doi: 10.1530/jrf.0.0400077
43. Szafranska B, Ziecik AJ. Active and passive immunization against luteinizing hormone in pigs. *Acta Physiol Hung.* (1989) 74:253–8.
44. Nokelainen P, Peltoketo H, Vihko R, Vihko P. Expression cloning of a novel estrogenic mouse 17 beta-hydroxysteroid dehydrogenase/17-ketosteroid reductase (m17HSD7), previously described as a prolactin receptor-associated protein (PRAP) in rat. *Mol Endocrinol.* (1998) 12:1048–59. doi: 10.1210/me.12.7.1048
45. Stocco C, Telleria C, Gibori G. The molecular control of corpus luteum formation, function, and regression. *Endocr Rev.* (2007) 28:117–49. doi: 10.1210/er.2006-0022
46. Papa PC, Hoffmann B. The corpus luteum of the dog: source and target of steroid hormones? *Reprod Domest Anim.* (2011) 46:750–6. doi: 10.1111/j.1439-0531.2010.01749.x
47. Onclin K, Verstegen J. Secretion patterns of plasma prolactin and progesterone in pregnant compared with nonpregnant dioestrous beagle bitches. *J Reprod Fertil Suppl.* (1997) 51:203–8.
48. Hoffmann B, Büsges F, Baumgärtne W. Immunohistochemical detection of CD4-, CD8- and MHC II-expressing immune cells and endoglin in the canine corpus luteum at different stages of dioestrus. *Reprod Domestic Anim.* (2004) 39:391–5. doi: 10.1111/j.1439-0531.2004.00520.x
49. Nowaczyk RM, Jursza-Piotrowska E, Gram A, Siemieniuch MJ, Boos A, Kowalewski MP. Cells expressing CD4, CD8, MHCII and endoglin in the canine corpus luteum of pregnancy, and prepartum activation of the luteal TNFalpha system. *Theriogenology.* (2017) 98:123–32. doi: 10.1016/j.theriogenology.2017.05.003
50. Pru JK, Hendry IR, Davis JS, Rueda BR. Soluble Fas ligand activates the sphingomyelin pathway and induces apoptosis in luteal steroidogenic cells independently of stress-activated p38(MAPK). *Endocrinology.* (2002) 143:4350–7. doi: 10.1210/en.2002-220229
51. Quirk SM, Cowan RG, Joshi SG, Henrikson KP. Fas antigen-mediated apoptosis in human granulosa/luteal cells. *Biol Reprod.* (1995) 52:279–87. doi: 10.1095/biolreprod52.2.279
52. Quirk SM, Harman RM, Huber SC, Cowan RG. Responsiveness of mouse corpora luteal cells to fas antigen (CD95)-mediated apoptosis. *Biol Reprod.* (2000) 63:49–56. doi: 10.1095/biolreprod63.1.49
53. Roughton SA, Lareu RR, Bittles AH, Dharmarajan AM. Fas and fas ligand messenger ribonucleic acid and protein expression in the rat corpus luteum during apoptosis-mediated luteolysis. *Biol Reprod*. (1999) 60:797–804. doi: 10.1095/biolreprod60.4.797
54. Taniguchi H, Yokomizo Y, Okuda K. Fas-Fas ligand system mediates luteal cell death in bovine corpus luteum. *Biol Reprod.* (2002) 66:754–9. doi: 10.1095/biolreprod66.3.754
55. Duncan A, Forcina J, Blirt A, Townson D. Estrous cycle-dependent changes of Fas expression in the bovine corpus luteum: influence of keratin 8/18 intermediate filaments and cytokines. *Reprod Biol Endocrinol.* (2012) 10:90. doi: 10.1186/1477-7827-10-90
56. Barnhart BC, Legembre P, Pietras E, Bubici C, Franzoso G, Perer ME. CD95 ligand induces motility and invasiveness of apoptosis-resistant tumor cells. *EMBO J.* (2004) 23:3175–85. doi: 10.1038/sj.emboj.7600325
57. Farberov S, Meidan R. Functions and transcriptional regulation of thrombospondins and their interrelationship with fibroblast growth factor-2 in bovine luteal cells. *Biol Reprod.* (2014) 91:58. doi: 10.1095/biolreprod.114.121020
58. Gospodarowicz D, Neufeld G, Schweigerer L. Molecular and biological characterization of fibroblast growth factor, an angiogenic factor which also controls the proliferation and differentiation of mesoderm and neuroectoderm derived cells. *Cell Differ.* (1986) 19:1–17. doi: 10.1016/0045-6039(86)90021-7
59. Petrik JJ, Gentry PA, Feige J-J, LaMarre J. Expression and localization of thrombospondin-1 and−2 and their cell-surface receptor, CD36, during rat follicular development and formation of the corpus luteum1. *Biol Reprod.* (2002) 67:1522–31. doi: 10.1095/biolreprod.102.007153
60. Breyer RM, Bagdassarian CK, Myers SA, Breyer MD. Prostanoid receptors: subtypes and signaling. *Annu Rev Pharmacol Toxicol.* (2001) 41:661–90. doi: 10.1146/annurev.pharmtox.41.1.661
61. Hata AN, Breyer RM. Pharmacology and signaling of prostaglandin receptors: multiple roles in inflammation and immune modulation. *Pharmacol Ther.* (2004) 103:147–66. doi: 10.1016/j.pharmthera.2004.06.003
62. Urade Y, Hayaishi O. Prostaglandin D2 and sleep/wake regulation. *Sleep Med Rev.* (2011) 15:411–8. doi: 10.1016/j.smrv.2011.08.003
63. Wang X, Yin X, Schiffer RB, King SR, Stocco DM, Grammas P. Inhibition of thromboxane a synthase activity enhances steroidogenesis and steroidogenic acute regulatory gene expression in MA-10 mouse Leydig cells. *Endocrinology.* (2008) 149:851–7. doi: 10.1210/en.2007-0470
64. Malki S, Nef S, Notarnicola C, Thevenet L, Gasca S, Méjean C, et al. Prostaglandin D2 induces nuclear import of the sex-determining factor SOX9 via its cAMP-PKA phosphorylation. *EMBO J.* (2005) 24:1798–809. doi: 10.1038/sj.emboj.7600660
65. Moniot B, Declosmenil F, Barrionuevo F, Scherer G, Aritake K, Malki S, et al. The PGD2 pathway, independently of FGF9, amplifies SOX9 activity in Sertoli cells during male sexual differentiation. *Development.* (2009) 136:1813–21. doi: 10.1242/dev.032631
66. Fitzpatrick FA, Wynalda MA. Albumin-catalyzed metabolismof prostaglandin D2. *J Biol Chem.* (1983) 258:11713–8.
67. Kikawa Y, Narumiya S, Fukushima M, Wakatsuka H, Hayaishi O. 9-Deoxy-delta 9, delta 12-13,14-dihydroprostaglandin D2, a metabolite of prostaglandin D2 formed in human plasma. *Proc Natl Acad Sci USA.* (1984) 81:1317–21. doi: 10.1073/pnas.81.5.1317
68. Herlong JL, Scott TR. Positioning prostanoids of the D and J series in the immunopathogenic scheme. *Immunol Lett.* (2006) 102:121–31. doi: 10.1016/j.imlet.2005.10.004
69. Komar CM. Peroxisome proliferator-activated receptors (PPARs) and ovarian function–implications for regulating steroidogenesis, differentiation, and tissue remodeling. *Reprod Biol Endocrinol.* (2005) 3:41. doi: 10.1186/1477-7827-3-41
70. Kowalewski MP, Dyson MT, Manna PR, Stocco DM. Involvement of peroxisome proliferator-activated receptor γ in gonadal steroidogenesis and steroidogenic acute regulatory protein expression. *Reprod Fertil Dev.* (2009) 21:909–22. doi: 10.1071/RD09027
71. Maroni D, Davis JS. TGFB1 disrupts the angiogenic potential of microvascular endothelial cells of the corpus luteum. *J Cell Sci.* (2011) 124:2501–10. doi: 10.1242/jcs.084558
72. Song WC. Biochemistry and reproductive endocrinology of estrogen sulfotransferase. *Ann N Y Acad Sci.* (2001) 948:43–50. doi: 10.1111/j.1749-6632.2001.tb03985.x
73. Atli MO, Bender RW, Mehta V, Bastos MR, Luo W, Vezina CM, et al. Patterns of gene expression in the bovine corpus luteum following repeated intrauterine infusions of low doses of prostaglandin F2alpha. *Biol Reprod.* (2012) 86:130. doi: 10.1095/biolreprod.111.094870
74. Qi L, Guo N, Wei Q, Jin P, Wang W, Mao D. The involvement of NR4A1 and NR4A2 in the regulation of the luteal function in rats. *Acta Histochem.* (2018) 120:713–9. doi: 10.1016/j.acthis.2018.07.007
75. Ucar EH, Cetin H, Atli MO. Effect of multiple low-dose PGF2alpha injections on the mature corpus luteum in non-pregnant bitches. *Theriogenology.* (2018) 113:34–43. doi: 10.1016/j.theriogenology.2018.01.018

76. Murphy EP, Crean D. Molecular interactions between NR4A orphan nuclear receptors and NF-kappaB are required for appropriate inflammatory responses and immune cell homeostasis. *Biomolecules.* (2015) 5:1302–18. doi: 10.3390/biom5031302
77. Delerive P, de Bosscher K, Besnard S, Berghe WV, Peters JM, Gonzalez FJ, et al. Peroxisome proliferator-activated receptor a negatively regulates the vascular inflammatory gene response by negative cross-talk with transcription factors NF-kB and AP-1. *J Biol Chem.* (1999) 45:32048–54. doi: 10.1074/jbc.274.45.32048
78. Kim EK, Kwon KB, Koo BS, Han MJ, Song MY, Song EK, et al. Activation of peroxisome proliferator-activated receptor-gamma protects pancreatic beta-cells from cytokine-induced cytotoxicity via NF kappaB pathway. *Int J Biochem Cell Biol.* (2007) 39:1260–75. doi: 10.1016/j.biocel.2007.04.005
79. Moon YW, Hajjar J, Hwu P, Naing A. Targeting the indoleamine 2,3-dioxygenase pathway in cancer. *J Immunother Cancer.* (2015) 3:51. doi: 10.1186/s40425-015-0094-9

Conflict of Interest: The authors declare that the research was conducted in the absence of any commercial or financial relationships that could be construed as a potential conflict of interest.

frontiers in Endocrinology

ORIGINAL RESEARCH
published: 14 November 2019
doi: 10.3389/fendo.2019.00724

Functional and Morphological Characterization of Small and Large Steroidogenic Luteal Cells From Domestic Cats Before and During Culture

Michał M. Hryciuk[1]*, *Beate C. Braun*[1], *Liam D. Bailey*[2] and *Katarina Jewgenow*[1]

[1] Department of Reproduction Biology, Leibniz Institute for Zoo and Wildlife Research, Berlin, Germany, [2] Department of Evolutionary Genetics, Leibniz Institute for Zoo and Wildlife Research, Berlin, Germany

The current study aimed to isolate, culture and characterize small (SLC) and large (LLC) steroidogenic cells from the *corpora lutea* (CL) of non-pregnant domestic cats. Isolation of feline SLC was based on an enzymatic digestion of luteal tissue, whereas LLC were obtained by mechanical disruption of CL. To assess function of both cell types, progesterone secretion and mRNA expression of selected genes involved in steroid and prostaglandin synthesis were measured, as well as relative transcript abundance of hormone receptors and anti-oxidative enzymes, before and during culture. The cells were cultured for 3 or 5 days without gonadotropins. Isolated feline SLC and LLC had different sizes (12 ± 3 μm vs. 34 ± 5 μm, respectively), morphologies (amount of lipid droplets) and behaved differently in culture. SLC attached and proliferated or spread quickly, but lost their steroidogenic function during culture (significant decrease in progesterone secretion and expression of steroidogenic genes). The expression of receptors for gonadotropins and prolactin also decreased. Prostaglandin synthase (*PTGS2*) decreased steadily over time, whereas mRNA expression of *PGE2* synthase (*PGES*) increased. The gene expression of anti-oxidative enzyme glutathione peroxidase 4 (*GPX4*), also increased during culture, but not of superoxide dismutase 1 (*SOD1*). In comparison to SLC, LLC did not attach to culture plates, secreted more progesterone per inoculated cells and maintained steroidogenic function during culture. Expression of prostaglandin synthases (*PTGS2* and *PGES*) was almost non-detectable. The gene expression of hormone receptors for prostaglandin F2 alpha (*PTGFR*), gonadotropins (*LHCHR* and *FSHR*), and prolactin (*PRLR*), as well as of anti-oxidative enzymes (*GPX4*, *SOD1*), increased over time. To conclude, we successfully isolated and cultured different types of feline steroidogenic luteal cells and comprehensively characterized both isolated cell types. This knowledge can be used to better understand the CL lifecycle in felines more broadly, and the established cell cultures will provide a foundation for future studies on luteolytic and luteotrophic factors in the domestic cat, and for comparison with other feline species, particularly lynx.

Keywords: cat, luteal cells, steroid production, prostaglandins, gonadotropin reception

OPEN ACCESS

Edited by:
Joy L. Pate,
Pennsylvania State University,
United States

Reviewed by:
John S. Davis,
University of Nebraska Medical Center, United States
Paul Tsang,
University of New Hampshire,
United States

***Correspondence:**
Michał M. Hryciuk
hryciuk@izw-berlin.de

Specialty section:
This article was submitted to Reproduction, a section of the journal Frontiers in Endocrinology

Received: *13 May 2019*
Accepted: *08 October 2019*
Published: *14 November 2019*

Citation:
Hryciuk MM, Braun BC, Bailey LD and Jewgenow K (2019) Functional and Morphological Characterization of Small and Large Steroidogenic Luteal Cells From Domestic Cats Before and During Culture. Front. Endocrinol. 10:724. doi: 10.3389/fendo.2019.00724

INTRODUCTION

The *corpus luteum* is a transient endocrine gland which forms on the mammalian ovary at the place of ovulation. The main function of *corpora lutea* (hereafter CL) is the production of progesterone, which is essential for the establishment and maintenance of pregnancy. CL are also known to synthesize and express receptors for hormones, e.g., sex steroids (1), prostaglandins (2), and gonadotropins (3).

Luteal cell cultures provide a valuable tool to study the functionality of CL, as previously described in many mammalian species like humans (4), rhesus monkeys (5), cows (6), pigs (7), sheep (8, 9), goats (10), rats (11), mice (12), dogs (13), and domestic cats (14). CL are composed of both small and large steroidogenic luteal cells, as well as non-steroidegenic cells such as fibroblasts, endothelial cells, pericytes, and immune cells (15). Small luteal cells (SLC) originate from *theca interna*, whereas large luteal cells (LLC) mainly originate from granulosa cells although they can also arise from SLC (16). Others have reported that theca and granulosa cell, *in vitro*, are able to transform into luteal cells (17, 18). The most prominent difference between SLC and LLC is their size, but the two types of luteal cells differ also in their steroidogenic capacity (4, 8, 11, 19–21), morphology (22), function (4), behavior in culture (11), and responsiveness to hormones (11, 20).

The domestic cat is a seasonal polyestrous species with ovulation induced by mating or by other intensive stimuli. Spontaneous ovulation, however, might also occur when there are no mating partners (23). Thus, CL that form following ovulation are present in either pregnant or non-pregnant luteal phases. The life cycle of pregnancy and the cycle CL was previously described by Dawson (24) and Amelkina et al. (25), and was divided into formation, development/maintenance and regression stages. At the formation stage, growth of the gland is caused by division of steroidogenic and non-steroidegenic cells, vascularization and hypertrophy of steroidogenic cells (24). As CL age, feline steroidogenic cells change their size, shape and degree of vacuolisation. Based on morphology and hormonal activity, there are no differences between similar stages of CL in pregnant and non-pregnant cycles (25). However, based on serum progesterone, the duration of pregnancy is 66 days (26), in contrast to 40 days for a non-pregnant cycle (27). The CL of pregnancy achieve their maximal size 10–16 days after coitus (24). The highest hormonal activity has been determined at around 21 days following ovulation and then decreases until parturition (28). In the case of a non-pregnant cycle, P4 serum concentrations also peak around 21 days post ovulation and drop to baseline at around day 40 (28).

In most mammalian species, CL usually regress to *corpora albicantia* after pregnancy or at the end of the luteal phase of the ovarian cycle. An exception is the so called "persistent CL" which can be found on the ovary outside of these periods. Persistent CL are considered a pathological disorder and are connected to hormonal disruption and infertility, e.g., in cows (29, 30). In contrast, physiologically persistent and hormonally active CL have been described in lynx (31, 32). The lynx CL persist on the ovary for at least 2 years (33) and continuously produce progesterone (P4) (31, 34) at a level comparable to the serum levels of domestic cats during early pregnancy (5–10 ng/mL) (28). It has been suggested that the permanent progesterone levels in lynxes prevent further ovulations and in doing so, turn a polyestrous cycle into a monoestrous pattern (33). This feature is unique within the feline family and demands comparative investigation of luteal function between lynxes and cats.

The aim of the current study was to establish a cell culture system for steroidogenic luteal cells from the domestic cat. We separated small (SLC) and large (LLC) luteal cells from domestic cat CL of development/maintenance stages and cultured them for up to 3 or 5 days. Both cell types were analyzed for basal progesterone secretion (without gonadotropin stimulation) *in vitro* and RNA expression of selected genes involved in steroidogenesis and prostaglandin synthesis as well as hormone receptors and anti-oxidative enzymes before and during culture. The characterized cell culture system will provide a foundation for future studies on potential luteolytic and luteotrophic factors in the domestic cat, and for comparison to lynx species, especially with regards to the function of persistent CL.

MATERIALS AND METHODS

This study was approved by the Internal Committee for Ethics and Animal Welfare of the IZW (2017-02-02). All chemicals used in these experiments were purchased from Merck KGaA, Darmstadt, Germany unless otherwise stated.

Ovaries and *Corpora lutea*

Ovaries were obtained from non-pregnant domestic cats after routine ovariectomy at animal shelter of Berlin. The ovariectomia were not related to the purpose of the experiment. Ovaries were transported to the laboratory in HEPES-MEM medium, supplemented with 3 g/L BSA and 1x Antibiotic Antimycotic Solution in 50 mL tubes (Sarstedt AG & Co. KG, Nümbrecht Germany). Upon arrival, ovaries were isolated from surrounding tissues and washed twice in Dulbecco PBS (DPBS), and checked for the presence of CL indicating a non-pregnant luteal cycle. CL were isolated and washed in fresh DPBS. Half of one CL per animal was fixed in Bouin solution and used for identifying the stage of the luteal life cycle as described by Amelkina (25). For the purpose of the experiments, luteal cell cultures from 17 queens were made, of which 9 were defined as development/maintenance stage. Due to the small size of cat CL, 0.3×10^6 SLC and 0.1×10^6 on average LLC were able to be isolated from one CL. Thus, a full experimental trial including gene expression analysis on both cell types obtained from the same domestic cat was only possible in six cases. The data from these selected experiments ($n = 3$ for experiment A; $n = 3$ for experiment B) were compiled for statistical analysis. All other experiments contributed to the microscopic and steroidogenic characterization (see below) of SCL and LLC.

Experimental Design

For each experiment (A and B), three independent cell culture trials (each trial from one cat) were performed. From a pair of ovaries, CL were equally pooled into two groups to isolate small

and large luteal cells resulting in two independent cell suspension of SLC and LLC.

Initially, each cell suspension was set on a certain cell concentration (see below) and divided into 12 technical replicates of 150 μL (**Figure 1**); three of them were immediately used as a control. The control samples were subjected to gene expression analysis (see below). In the Experiment A, the remaining nine replicates were aliquoted into 96-well plate and were cultured for 1, 2, or 3 days, respectively. On each day of culture, conditioned medium from all replicates was collected for progesterone analysis (see below), and cells were harvested from three replicates for gene expression analysis (see below). Fresh medium was added to the remaining wells of the 96-well plate. In Experiment B, the cell culture was performed for 3, 4, and 5 days. Accordingly, medium changes for progesterone analysis and cell harvest was performed on day 3, 4, and 5, respectively.

Because of this setup, progesterone secretion was measured in 9, 6, and 3 wells on the first, second and third time point, respectively. For relative transcript abundance analysis, three measurements were taken from freshly isolated cells and at each of the three time points of the culture period.

Isolation of Small Luteal Cells (SLC)

Small luteal cells were isolated by a modified enzymatic method (14). CL were placed into a Petri Dish (60 × 10 mm, Thermo Fisher Scientific, Dreieich, Germany) containing medium I (HAM's F12 and MEM Eagle Medium 1:1 supplemented with 0.055 mg/mL gentamicin and 5% FBS), chopped into small pieces and transferred on a 40 μm cell strainer (VWR International, Dresden, Germany), which was placed into another Petri dish. Pieces were covered with medium I supplemented with 0.1% collagenase (types I and II; SERVA Electrophoresis GmbH, Heidelberg, Germany) and 0.005% DNAse I and digested on the strainer for 55 min at 39°C. Thereafter, pieces were gently smashed through the strainer and the obtained suspension was agitated by pipetting and transferred to a glass tube for centrifugation (7 min at 1,000 × g). The cell pellet was resuspended in 2 mL fresh medium I and placed on 40% percoll solution (with DPBS) in a glass tube. After centrifugation for 7 min at 1,000 × g, cells were collected from the interphase between medium I and percoll solution, transferred to 1.5 mL reaction tubes and centrifuged at 500 × g for 4 min. The obtained cell pellet was resuspended in fresh medium I, the cell concentration was determined and set to 200,000 cells per mL (30,000 per 150 μL).

Isolation of Large Luteal Cells (LLC)

Large luteal cells were isolated by a mechanical method. CL were chopped and smashed through a cell dissociation sieve (380 μm) placed into a Petri Dish (60 × 15 mm, Thermo Fisher Scientific) with medium II (HAM's F12 and MEM Eagle Medium, 1:1 (v:v) supplemented with 0.055 mg/mL gentamicin and 1% FBS). To remove pieces of tissue, cell suspension was filtered through cell strainer (35 μm) connected to a 5 mL polystyrene round bottom tube (BD Biosciences Discovery Labware, Canaan, USA) and centrifuged for 7 min at 1,000 × g. The cell pellet was resuspended with medium II and placed on 20% percoll solution (with DPBS) in a glass tube and centrifuged for 7 min at 1,000 × g. Large luteal cells were collected from the interphase between medium II and percoll solution, transferred to 1.5 mL reaction tubes and washed by centrifugation for 4 min at 500 × g. After re-suspension in fresh medium II, the cell concentration was determined and set to 67,000 cells per mL (10,000 per 150 μL).

Cell Culture

Tissue Culture Plates (96-well, Sarstedt) were coated with 15 μl of 0.2% Collagen R (SERVA) diluted 1:10 with DPBS. The collagen solution was evenly distributed on the bottom of wells and left to dry under the hood for 7 h. Coated plates were stored at 6°C until use.

Small and large luteal cells were cultured separately in 150 μL medium I and II, respectively, (see cell concentration above) at 39°C, 5% CO_2. Concentration of FBS in medium for SLC and LLC was different because this ingredient may inhibit responsiveness of the steroidogenic cells toward LH (35). Our aim was to establish conditions for future functional studies; therefore, we have tested medium with 1 and 5% of FBS on SLC and LLC during culture period. In the preliminary experiments, SLC required minimum 5% of FBS in medium. Lower concentration of FBS caused that SLC did not proliferate or spread as fast as in wells with 5% of FBS. There was also much more cell debris, which may indicate on cells death caused by unsuitable medium. For LLC, no difference was observed between the cells in a medium supplemented with 1 and 5% of FBS.

Medium change was performed by replacing 130 μL conditioned medium by freshly prepared medium. For SLC, collected medium was centrifuged for 4 min at 500 × g and then transferred to a new reaction tubes. LLC are not adherent cells, therefore collected medium was centrifuged, then supernatant was transferred to a new reaction tube and a potential pellet with LLC was resuspended with fresh medium and returned to corresponding well. On the day of medium change, the conditioned medium was frozen for hormone analysis at −20°C. In addition, cells from three culture wells were harvested for mRNA analysis. To collect cells from the dish, they were overlayed with Trypsin-EDTA solution (100 μL, 15 min at 39°), and transferred to 1.5 mL reaction tubes contained 100 μL medium. Then, wells were washed twice with medium 500 × g for 4 min. Harvested cells were stored in RNAlater at −20°C, until RNA isolation.

Microscopic Analysis and Cell Measurement

Luteal cell cultures were analyzed under an Axiovert 200M microscope (Carl Zeiss, Oberkochen, Germany) equipped with a ProgRes® camera using the CapturePro 2.10.01 program (JENOPTIK Optical systems GmbH, Berlin, Germany). Digital photos were obtained from freshly isolated SLC and LLC, and were used to determine mean cell diameter with the help of imaging software (cell∧D, Olympus Soft Imaging Solutions GmbH, Münster, Germany). For each cell suspension ($n = 7$) a minimum of 10 cells were measured to characterize size of isolated cells.

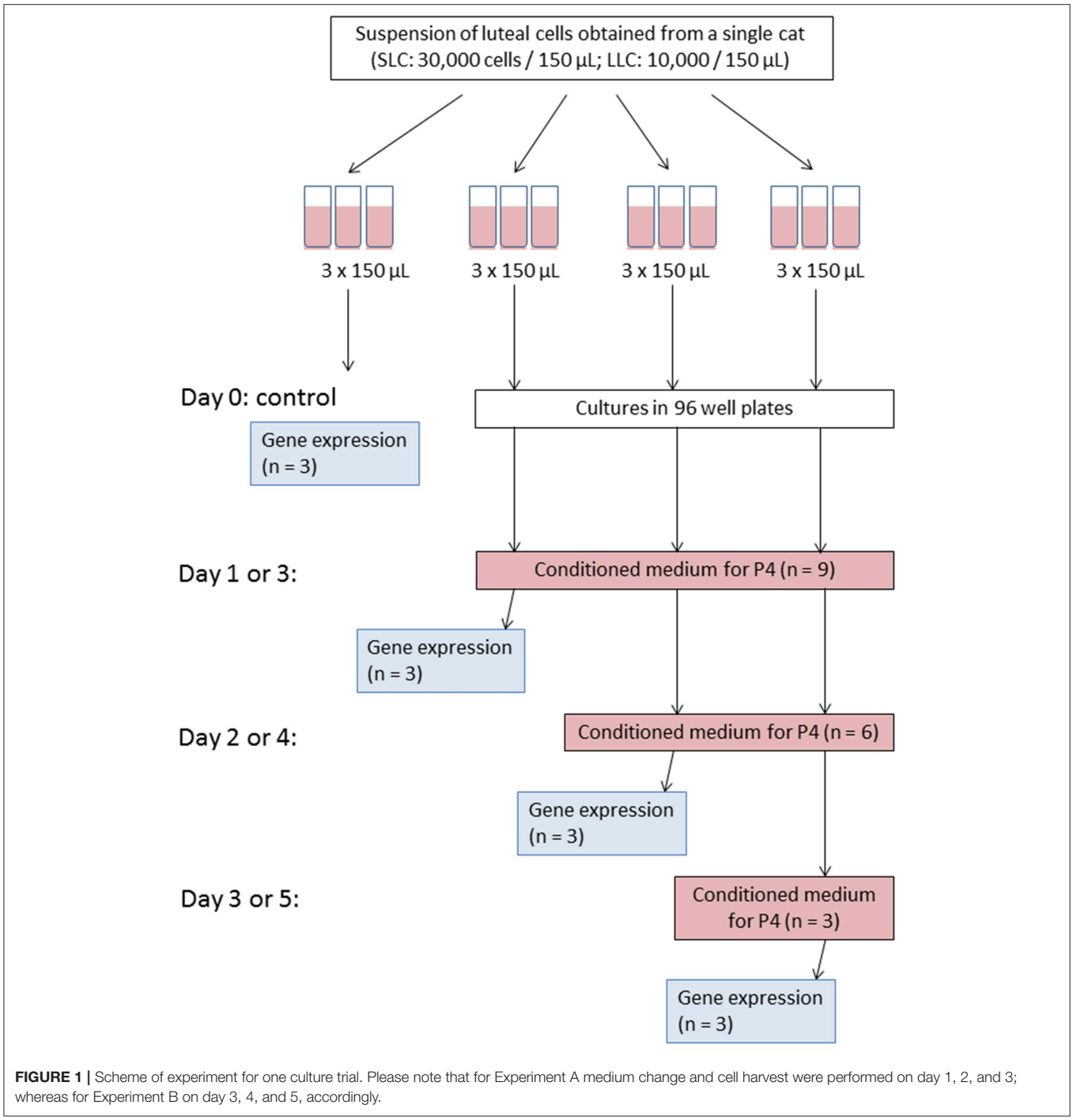

FIGURE 1 | Scheme of experiment for one culture trial. Please note that for Experiment A medium change and cell harvest were performed on day 1, 2, and 3; whereas for Experiment B on day 3, 4, and 5, accordingly.

HSD3B Assay for Identification of Steroidogenic Luteal Cells

For identification of steroidogenic luteal cells, a modified 3β-hydroxysteroid dehydrogenase (HSD3B) activity assay was performed (36) on cell cultures where there were not enough isolated cells for a complete experimental trial. In brief, luteal cells were fixed with 1% formaldehyde in DPBS (15 min, 39°C). Thereafter, they were washed twice in DPBS and incubated for 24 h in staining solution (PBS containing 0.25 mM nitrotetrazolium blue chloride (NBT), 0.1% BSA, 1.5 mM β-nicotinamide adenine dinucleotide hydrate (NAD+), 0.2 mM pregnenolone and 2 mM EDTA). After incubation, cells were washed in DPBS and analyzed under the microscope (Carl Zeiss). Staining control was performed by adding trilostane (2 mM) to the staining solution. Trilostane inhibits specifically the activity of 3β-hydroxysteroid dehydrogenase (37).

Progesterone Determination by Enzyme-Linked Immunosorbent Assay (ELISA)

Progesterone extraction was performed with modifications as described before (38). In detail, medium samples (100 μL) obtained after each medium change were transferred to test tubes (16 × 130 mm, Carl Roth GmbH + Co. KG, Karlsruhe, Germany) followed by addition of 900 μL of PBS and 2.5 mL of methyl-tert-butyl ether/petroleum ether (v:v; 3:7). After shaking for 30 min, the tubes were placed into a freezer (−80°C) for 15 min. Subsequently, the organic phase was decanted into a new tube (16 × 100 mm, Corning Incorporated, New York, USA) and evaporated under a stream of N_2 for 10 min at 50°C. Thereafter, samples were quickly dissolved in 80 μl of 100% methanol, and diluted with 120 μl of distilled water. Recovery values for extraction control samples were in a range 92.3–111.8% for medium I and 90.3–107.9% for medium II. The samples were stored at −20°C until determination of progesterone by ELISA.

Progesterone (P4) analyses were carried out with an in-house microtiter plate enzyme immunoassay as described earlier (39) using a commercial P4 antibody (Sigma P1922, raised in rats to progesterone) and 4-pregnen-3,20-dione-3-CMO-peroxidase label. The cross-reactivities to other steroids were as follows: 4-pregnen-3,20-dione (progesterone), 100%; 5a-pregnan-3,20-dione, 31%; 5a-pregnan-3b-ol-20-one, 18%; 5-pregnen-3b-ol-20-one, 12%; 4-pregnen-3aol-20-one, 4.2%; <0.1% for 5b-pregnan-3a,20adiol, 4-pregnen-20a-ol-3-one, 5b-pregnan-3a-ol-20-one, 5a-pregnan-20a-ol-3-one, 5a-pregnan-3a,20 a-diol, 5a-pregnan-3b,20a-diol, testosterone, estradiol, and cortisol. For ELISA measurements, we used 20 μL of sample extract, which was dispensed on a plate with 100 μL of an enzyme dilution and then 100 μL of antibody solution was added. Intra assay coefficients for two biological samples with low and high concentration were 12.0 and 4.5%, respectively. The respective inter assays were 13.8 and 10.0%. We confirm linearity of extraction method and parallelism of diluted samples.

Sequence Analysis of Genes of Interest

At the beginning of the present study, sequence information was confirmed for some genes of interest, while only predicted sequences were known for others. Thus, in order to design primers suitable for real-time PCR, the predicted sequences must be confirmed. Feline gene sequences were previously confirmed for prostaglandin endoperoxide synthase 2 (*PTGS2*) (40), prostaglandin E2 synthase (*PTGES*) (41), cytochrome P450 family 11 subfamily A polypeptide 1 (*CYP11A1*) (38), 3β-hydroxysteroid dehydrogenase type 1 (*HSD3B1*) (38), prostaglandin E receptor 2 (*PTGER2*) (2), and prostaglandin F receptor (PTGFR) (2). However, gene sequences need to be confirmed for luteinizing hormone receptor (*LHCGR*), prolactin receptor (*PRLR*), follicle stimulating hormone receptor (*FSHR*), glutathione peroxidase 4 (*GPX4*), and superoxide dismutase 1 (SOD1) (see GenBank accession numbers for all genes in **Table 1**). To accomplish this, total RNA was isolated from feline *corpora lutea* tissues according to the innuSPEED Tissue RNA/innuPREP DNase I Digest Kit (*PRLR, FSHR, GPX4, SOD1*; Analytik Jena AG, Jena, Germany) or the Precellys Tissue RNA/peqGOLD DNase I Digest Kit (*LHCGR*; Peqlab, part of VWR International GmbH) as described in Amelkina et al. (43). Reverse transcription of total RNA into single-stranded cDNA (ss cDNA) was performed with the RevertAid First Strand cDNASynthesis Kit (Thermo Scientific, Schwerte, Germany). For the polymerase chain reaction (PCR) primers were purchased from BioTeZ Berlin Buch GmbH (Berlin, Germany) or Merck KGaA. Primer information is listed in **Table 1**. Based on feline ss cDNA templates partial cDNA sequences were amplified using the Expand High FidelityPLUS PCR system (Roche Diagnostics Deutschland GmbH, Mannheim, Germany), as described before (44). The PCR conditions were: 94°C for 2 min; followed by 35 cycles of denaturation (94°C) for 30 s (*LHCGR*, *PRLR*–sequence part 1) or 60 s (*PRLR*–sequence part 2, *FSHR*, *GPX4*, *SOD1*), annealing (see temperatures in **Table 1**) for 30 s (*LHCGR, PRLR-1*) or 60 s (*PRLR-2, FSHR, GPX4, SOD1*), elongation (72°C) for 30 s (*LHCGR*), 60 s (*PRLR*–sequence part 1), 120 s (*PRLR*–sequence part 2, *GPX4, SOD1*), or 150 s (*FSHR*); and a final elongation at 72°C for 7 min. For *PRLR-1* and *FSHR* the purified PCR products were ligated to the pJET 1.2 vector (Thermo Scientific) and transformed in DH5alpha cells (Life Technologies GmbH, Darmstadt, Germany). The *LHCGR* product was ligated into the pCR4-TOPO TA vector and transformed in TOP10 cells (both Life Technologies GmbH). The PCR-products of *PRLR*–sequence part 2, *GPX4* and *SOD1* and positive clones of *FSHR*, *LHCGR* and *PRLR*–sequence part 1 were sequenced by the Services in Molecular Biology GmbH (Dr. M. Meixner, Brandenburg, Germany).

mRNA Expression Analysis by Real-Time PCR

Isolation of total RNA was performed by NucleoSpin® RNA Plus XS (Macherey-Nagel GmbH & Co. KG, Berlin, Germany) according to manufacturer's manual. Concentration and purity of isolated RNA was measured on NanoDrop™ 2000c (Thermo Fisher Scientific). 13 μl of isolated RNA solution was reverse transcribed into cDNA with PrimeScript RT Reagent Kit (TAKARA BIO INC., Kusatsu, Japan) according to the manufacturer's manual, with the exception that Oligo dT primers (25 pmol) and random hexamers (50 pmol) were both used per reaction.

Real-time PCR was performed in CFX96 Real-Time PCR Detection System (Bio-Rad Laboratories GmbH, Munich, Germany) on 96-Well PCR Plates (Bio-Rad) as described before (38). Diluted cDNA was analyzed in a 10 μl reaction volume containing SsoFast EvaGreen Supermix (Bio-Rad) and primers (f.c. 500 nM each). Reactions conditions were: 98°C for 2 min and 40 cycles at 98°C for 8 s and 8 s for primers annealing at different temperatures. Detailed information about primers and annealing temperatures is presented in a **Table 1**. Bio-Rad CFX Manager 3.1 Software was used for quantification data. Serial dilutions of PCR products (*LHCGR, FSHR, GPX4*) or recombinant plasmid carrying desired genes (all other genes) were used for calibration. A normalization factor for qPCR analysis of SLC samples was calculated based on mean values of

TABLE 1 | Sequence of primers used in real-time PCR and for sequence analysis.

Gene	GenBank accession	Species	Primer sequence 5′–3′	TA [°C]	Product size [bp]	Use	References
betaActin	AB051104	*Felis catus*	qfw: GAG CAG GAG ATG GCC ACG qrv: CTC GTG GAT GCC ACA GGA	62	159	a	(42)
GLS	JQ424891	*Felis catus*	qfw: TCC AGC TAT GCT CCA TTG AAG T qrv: TGC AGG AAG ACC AAC ATG G	61	196	a	(38)
TBP	JQ424890	*Felis catus*	qfw: AGA GAG CCC CGA ACC ACT G qrv: TTC ACA TCA CAG CTC CCC AC	62.5	182	a	(38)
CYP11A1	JN165033	*Felis catus*	qfw: CTT CCG GAA CCT GGG CTT qrv: GCA GCG TCC ACC CTC TCT A	61.5	240	a	(38)
HSD3B1	JN127378	*Felis catus*	qfw: GCC CTA CAG GAC CCC AAG A qrv: TTC CAG CAG GAA GGC AAG C	62.5	182	a	(38)
PTGS2/ COX2	EF036473	*Felis catus*	qfw: CAG GAG GTC TTT GGT CTG G qrv: CCT GCT CGT CTG GAA CAA	58	135	a	(2)
PGES/ PTGES	GU059259	*Felis catus*	qfw: TCG CTG CCT CAG AGC CCA qrv: TAG GCC ACG GTG TGC ACC	66	153	a	(2)
PTGER2	EF177829	*Felis catus*	qfw: GAG GGG AAA GGC TGT CCA qrv: GCA AAA ATT GTG AAA GGC AAG	56.5	103	a	(2)
PTGFR	AF272340	*Felis catus*	qfw: GCT GGA GTC CAT TTC TGG TG qrv: CCA CGT TGC CAT TCG AAG	61	104	a	(2)
LHCGR	KP826762*	*Felis catus*	qfw: CCT GGT GTA CAT CGA GCC T qrv: GGA TTC GTT ATT CAT CCC TTG	57.5	199	a	This study
			fw: CAC TCA CCT ATC TCC CTA TC rv: GGA GTG TCT TGG GTG AGC	53	861	b	
PRLR	MH882487*/ MH882488*	*Felis catus*	qfw: GCT CAC ACT CCA GTA CGA AA qrv: TCT GTC CTG GAT ATA AGC TGA	60.5	112	a	This study
			fw1: CTG ATA CAT TTC CTG TAG AAA GAG rv1: TCT GTC CTG GAT ATA AGC TGA	51	635	b	
			fw2: GCT CAC ACT CCA GTA CGA Aa rv2: CCA ATC GTT CCA TTA ATC AAG C	55	1414	b	
FSHR	MH882490*	*Felis catus*	qfw: GCA AAT GTG TTC TTC AAC CTG T qrv: GGA GGT TGG GAA GGT TCT G	59.5	106	a	This study
			fw: CTC AGG ATG TCA TCA TCG G rv: GTG AGA CTT CAG TTA TCC TTT G	53	2045	b	
GPX4	MH882486*	*Felis catus*	qfw: CTT GCA ACC AGT TCG GGA G qrv: CTT GGG CTG GAC TTT CAT CC	58.5	154	a	This study
			fw: CTG TGC TCA GTC CAT GCA C rv: CTT GTG GAG CTA GAG GTA G	53	497	b	
SOD1	MH882489*	*Felis catus*	qfw: GAG AGG CAT GTT GGA GAC CT qrv: GTC ATC TCG TTT CTC GTG GAC	59.5	144	a	This study
			fw: GAG CAT GGA TTC CAC GTC C rv: CTC AGA TCG CAT CCT AGG G	53	364	b	

**Analyzed in this study.*

a, expression study; b, sequence analysis.

relative transcript abundance for beta Actin (*BACT*), glutaminase (*GLS*), and TATA-Box Binding Protein (*TBP)* using qbasePLUS software (Biogazelle, Zwijnaarde, Belgium) (45). For LLC only *BACT* values were used for normalization as GLS and TBP were not detectable in most samples. Mentioned reference genes were previously described by Zschockelt et al. (46) as suitable reference genes for luteal tissue. No template control (NTC) and no reverse transcriptase control (NRT) samples were included in analysis.

Statistical Analysis

All data presented for P4 analysis and gene expression analysis were depicted as mean ± standard deviation for all replicates within same day of experiment A and B and for SLC and LLC.

Each cell culture was isolated from an individual cat and may therefore have differed in their baseline P4 concentration and transcript abundance, meaning that different measurements taken from the same cell culture could not be fully independent. To account for the lack of independence between technical replicates, P4 concentration and transcript abundance were mean centered within each cell culture. The mean value of P4 concentration and transcript abundance was subtracted from each individual measurement, so that all measurements were adjusted to be relative to the mean value of that particular cell culture. With this approach, all statistical tests considered relative changes within a cell culture between time periods rather than absolute change in P4 concentration and transcript abundance. This approach accounts for any differences in absolute P4

TABLE 2 | Progesterone concentration in cell culture medium determined by EIA.

	Type of cells	Medium obtained from culture period:					
		Day 0–1	Day 1–2	Day 2–3	*P*-value	Chi-squared test statistic	df
Experiment A	SLC	4706 ± 2902^{a} pg P4/mL	122 ± 180^{b} pg P4/mL	345 ± 153^{b} pg P4/mL	<0.0001	40.15	2
		5.7 ± 3.46^{a} pg P4/ng RNA	0.7 ± 0.7^{b} pg P4/ng RNA	0.16 ± 0.09^{b} pg P4/ng RNA	<0.001	17.85	2
	LLC	5247 ± 2470^{a} pg/mL	550 ± 235^{b} pg/mL	206 ± 82^{b} pg/mL	<0.0001	40.29	2
		6.55 ± 3.61^{a} pg P4/ng RNA	0.84 ± 0.36^{b} pg P4/ng RNA	0.28 ± 0.19^{b} pg P4/ng RNA	<0.001	17.91	2
		Day 0–3	Day 3–4	Day 4–5			
Experiment B*	SLC	2608 ± 999 pg/mL	48 ± 58 pg/mL	288 ± 185 pg/mL			
	LLC	14431 ± 9447 pg/mL	1867 ± 1851 pg/mL	509 ± 534 pg/mL			

*SLC, small luteal cells; LLC, large luteal cells. Mean values ± standard deviation correspond to 30,000 SLC and 10,000 LLC seeded into wells at the day of initiating cell culture. For each experiment and each cell type, three cell preparations were used to generate P4 concentrations. Values in a second row, describe amount of progesterone produced in one well-normalized with total RNA value for the corresponding well. Non-parametric Kruskal-Wallis test was used for statistical analysis. Chi squared—refers to test statistics and df indicates degrees of freedom. Different superscripted letters indicate significant differences between groups, based on pairwise comparison Wilcoxon rank sum test. *For Experiment B, statistical analysis and normalization values ware not performed because the first values describe amount of progesterone accumulated over 3 days while other values describe amount of P4 accumulated over 1 day period.*

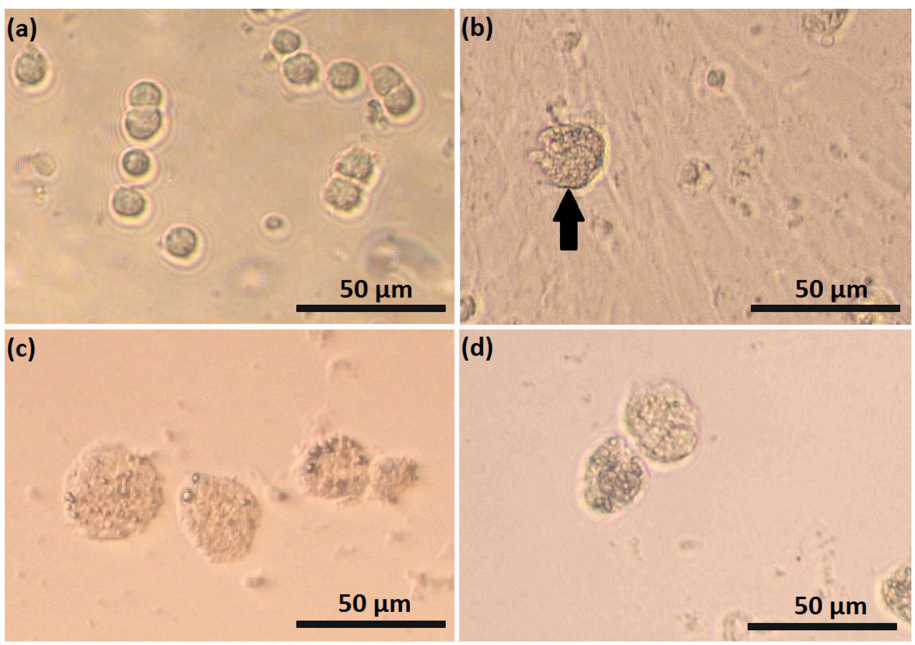

FIGURE 2 | Photomicrographs of small (SLC) and large (LLC)–luteal cell. SLC **(a)** and LLC **(c)** after seeding to culture dish; **(b)** SLC culture at day 5, black arrow indicate on a cell which may have differentiated, **(d)** LLC culture at day 5.

concentration and transcript abundance that may be caused by differences in the individual cat from which cells were isolated.

All analyses were performed in R (R: A language and environment for statistical computing (2018); R Foundation for Statistical Computing, Vienna, Austria; v. 3.5.0). Relative P4 concentration and transcript abundance between time periods was analyzed using a Kruskal-Wallis rank sum test followed by a *post-hoc* pairwise Wilcoxon rank sum test for comparison between group levels using the Benjamini-Hochberg adjustment for multiple testing (47). Analyzing day as a categorical rather than continuous variable gave the possibility to detect non-linear changes in P4 concentration and transcript abundance over time. *P*-values lower than 0.05 were considered statistically significant. Chi-square test statistics and degrees of freedom are provided in result summary tables (**Table 2**, **Tables S1**, **S2**).

The relative transcript abundance for selected genes was depicted as vertical box plot by plotting medians and percentiles (Sigma.Plot 10.0 Systat software GmbH, Erkrath, Germany).

RESULTS

Characterization of Luteal Cells in Culture

Within isolated SLC suspension, 99.3% of cells had diameter smaller or equal to 20 µm, while in isolated LLC, the percentage

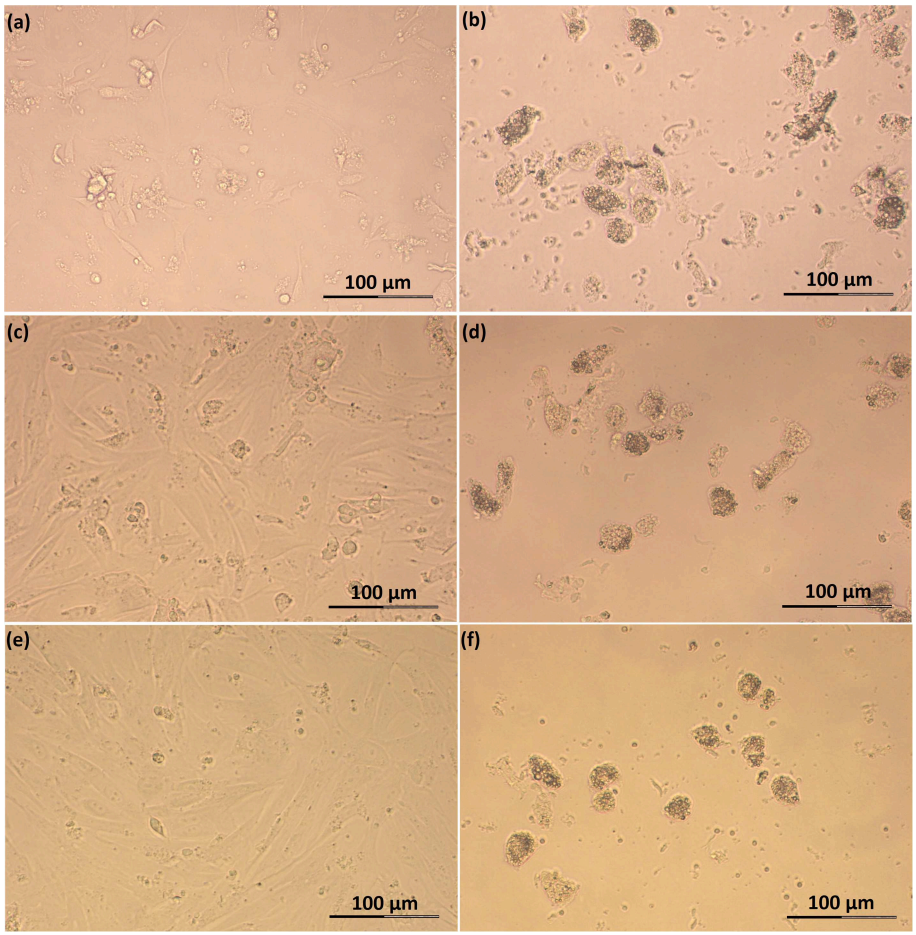

FIGURE 3 | Photomicrographs of SLC and LLC in cell culture during experiment A: **(a)** SLC at day 1, **(b)** LLC at day 1, **(c)** SLC at day 2, **(d)** LLC at day 2, **(e)** SLC at day 3, and **(f)** LLC and day 3. The series of photos are from one individual.

of cells with diameter >20 µm was 99.0%. Sometimes suspension with isolated cells contained cell debris which could not be removed by washing and were not counted.

Feline SLC and LLC varied in morphology and behaved differently in cell culture (**Figure 2**). Isolated SLC had an average diameter of 12 ± 3 µm and were round (**Figure 2a**). After 24 h of culture, the cells attached to the bottom of the culture well and became elongated (**Figures 3a,c,e**, **4a,c,e**). Proliferating or spreading cells covered most of the bottom of a well at around the fourth day of culture. In experiment B, at around the fourth day of culture, visual observations showed that some of the small luteal cells accumulated lipid droplets and detached from the culture plate (**Figures 2b**, **4c,e**). The detached cells looked similar to LLC, as they were large and round. These observations were made only occasionally.

Isolated LLC were almost three times larger than SLC with an average diameter of 34 ± 5 µm (**Figure 2c**). They were round to oval and contained a high amount of lipid droplets. Based on microscopic analysis during the cell culture period, the number and size of lipid droplets in LLC seemed not to change (**Figures 3b,d,f**, **4b,d,f**). LLC did not attach to the cell culture plate, and did not proliferate (**Figure 2d**). According to photographs taken every day, the number of LLC seemed to decrease during the culture period, possibly due to cell death and cell loss by medium change (**Figures 3b,d,f**, **4b,d,f**).

Identification of Steroidogenic Luteal Cells

Suspensions of stained, freshly isolated SLC and LLC clearly indicate their steroidogenic capacity (**Figures 5a,g**, respectively). For SLC around 68% of isolated cells was intensively stained or had partial staining which allowed us to distinguish them from cells without any steroidogenic activity. In contrast to this, all isolated LLC were stained. Among them, around 85% of isolated LLC were characterized by very high steroidogenic activity what was expressed by dark blue color of cells. Another 15% of isolated cells have lower steroidogenic activity, what could be distinguished by lighter blue color. There was still visible difference between LLC with low steroidogenic activity and cells in control staining group.

Small luteal cells were also stained for activity of HSD3B during cell culture. On day 2, most of the attached cells expressed steroidogenic activity (**Figure 5c**, **Figure S1**), while on day 5,

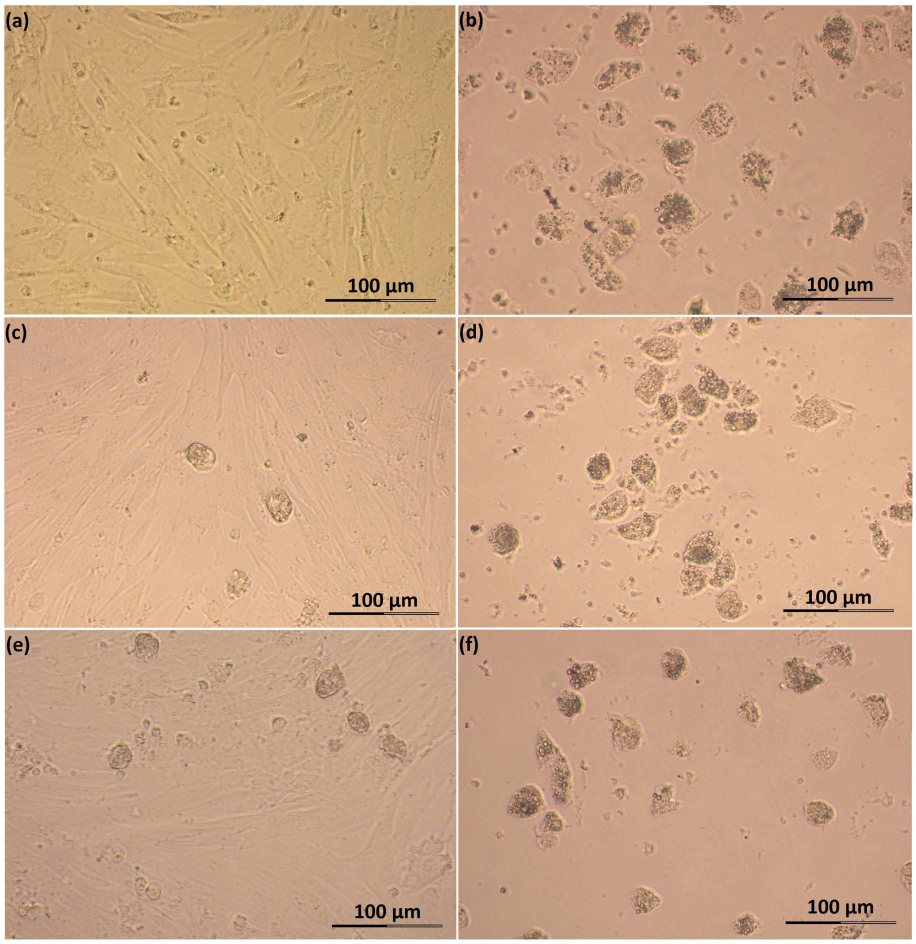

FIGURE 4 | Photomicrographs of SLC and LLC in cell culture during experiment B: **(a)** SLC at day 3, **(b)** LLC at day 3, **(c)** SLC at day 4, **(d)** LLC at day 4, **(e)** SLC at day 5, and **(f)** LLC and day 5. The series of photos are from one individual.

the cells were characterized by partial staining. Remarkably, some cells were intensively colored dark blue and contained round nuclei and numerous large cytoplasmic lipid droplets (**Figure 5e**).

Trilostane was used to specifically block the activity of 3β-hydroxysteroid dehydrogenase, resulting in reduced enzyme activity (**Figures 5b,d,f,h**). The remaining staining after trilostane treatment might indicate other NAD^+-dependent metabolic reactions. In contrast to cell monolayers (SLC on day 5 of culture), crystals of trilostane could not be removed by washing from the cell suspensions.

Progesterone Production

For experiment A, there was a significant difference in P4 concentration between time periods in both SLC and LLC cultures (**Table 2**; $p < 0.001$). In all cases, *post-hoc* pairwise comparison of groups showed that P4 concentration was significantly higher during the first period than either of the later time periods (**Table 2**). Our presented hormone concentrations do not consider changes in cells number during cell culture period. For experiment B, the first measures describe progesterone concentration accumulated over 3 days, while the following measurements describe progesterone accumulated over 1 day period, therefore statistical analysis for this experiment was not performed.

For SLC cultures, P4 concentration in experiment A did not statistically increase between the middle and final time period due to very large variations in cell preparations (**Table 2**). In comparison, P4 concentration in LLC was decreasing progressively between time periods (**Table 2**). However, neither of these differences was significant in *post-hoc* pairwise comparisons.

Concentration of secreted progesterone was higher in the medium obtained from LLC, than from SLC. Thus, LLC produce more progesterone per cell than SLC, because initial number of steroidogenic cells was three times higher for SLC than for LLC.

Expression Analysis by Relative Transcript Abundance

All analyzed genes were detectable (**Figures 6**, **7**, **Tables S1**, **S2**) in luteal cells of domestic cats, but *PTGS2* and *PGES* were present only at very low levels in LLC.

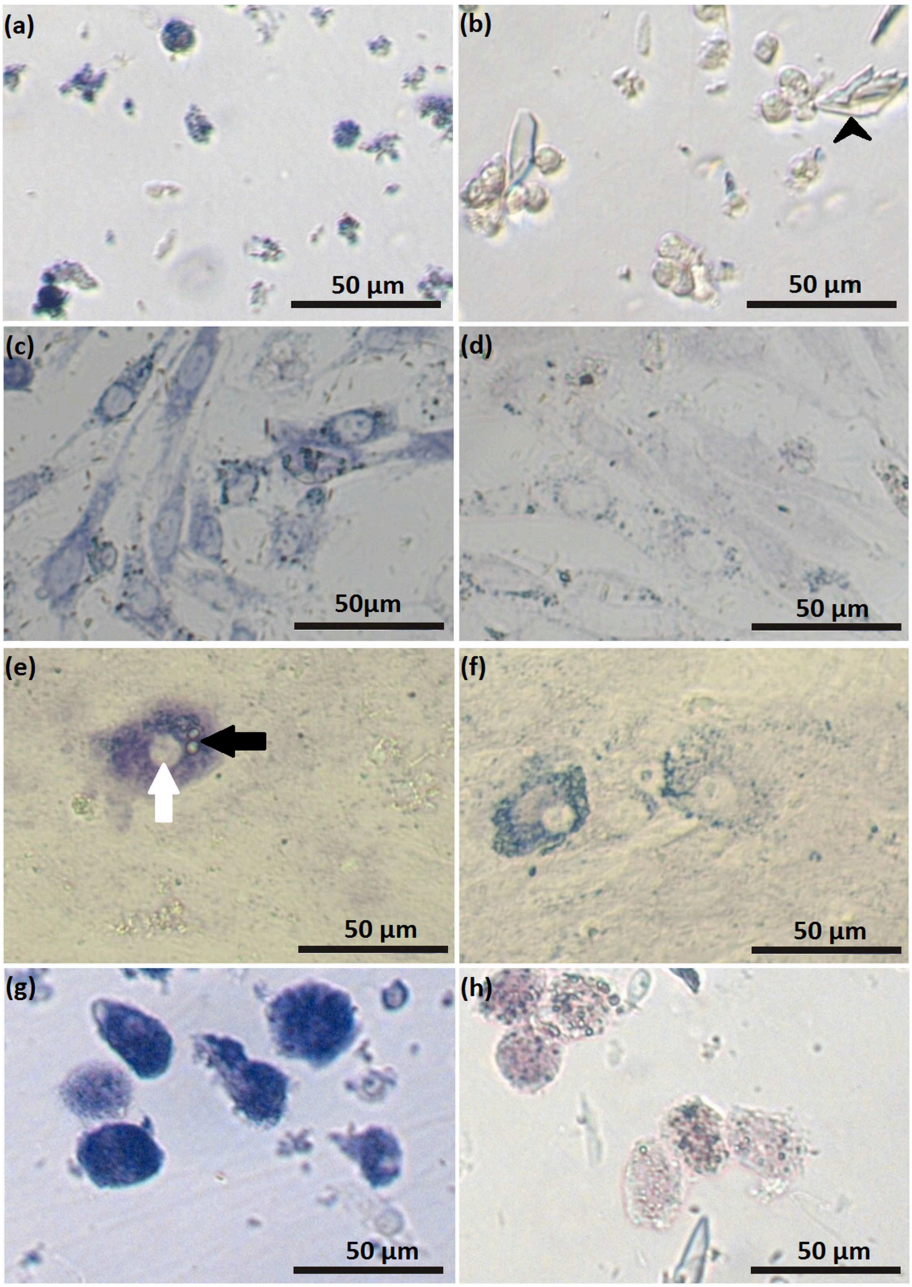

FIGURE 5 | Luteal cells stained for activity of 3β-hydroxysteroid dehydrogenase: freshly isolated small (SLC) luteal cells **(a)**; control staining for freshly isolated SLC **(b)**, black arrowheads indicate crystals of trilostane, which could not be removed from wells with non-adherent cells; SLC at day 2 of cell culture **(c)**; control staining for SLC at day 2 of cell culture **(d)**; SLC at day 5 of cell culture **(e)**, white arrow points to the nucleus, black arrow points to lipid droplets; staining control for SLC at day 5 of cell culture **(f)**; freshly isolated large luteal cells (LLC) **(g)**; control staining freshly isolated LLC **(h)**. In control samples, activity of 3β-hydroxysteroid dehydrogenase was blocked by trilostane.

During SLC culture significant changes were observed for all genes (**Figures 6a,c,e,g,i,k,m,o,q,s,u**, **7a,c,e,g,i,k,m,o,q,s,u**) although the pattern was gene specific. Both steroidogenic enzymes (*CYP11A1* and *HSD3B1*) expressed a similar pattern, with a very strong expression directly after isolation and a significant drop of their RNA abundance after culture (**Figures 6a,c**, **7a,c**). In contrast, enzymes involved in prostaglandin synthesis were characterized by two opposite patterns. Expression of *PTGS2* decreased steadily over the time (**Figure 6e**), whereas PGES expression increased (**Figures 6g**, **7g**). Hormone receptors (**Figures 6i,k,m,o,q**, **7i,k,m,o,q**) showed comparable patterns to the one described for steroidogenic

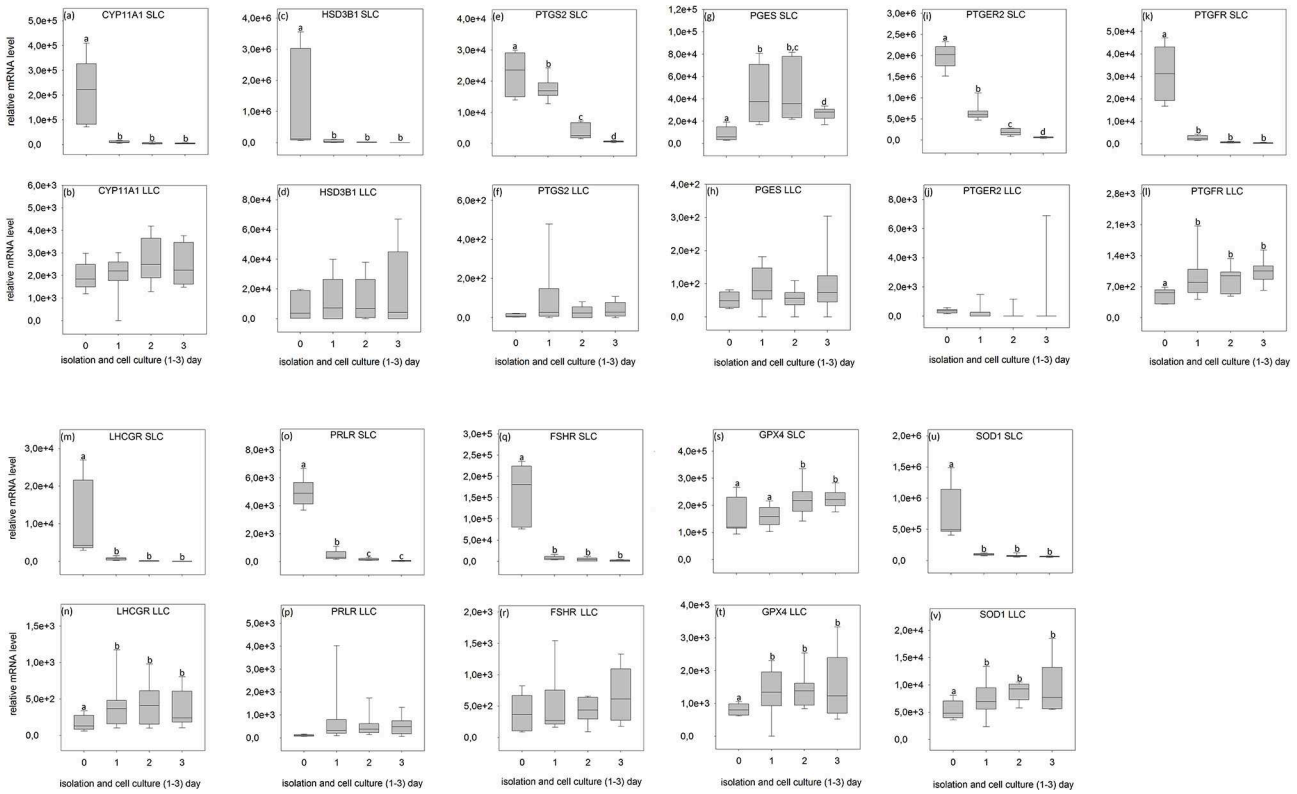

FIGURE 6 | Relative mRNA level of analyzed genes in SLC (small luteal cells) and LLC (large luteal cells) obtained directly after isolation (Day 0) and after 1–3 days of culture (Experiment A). **(a,b)** *CYP11A1*, Cholesterol Side-Chain Cleavage Enzyme, **(c,d)** *HSD3B1*, 3β-hydroxysteroid dehydrogenase type 1, **(e,f)** *PTGS2*, prostaglandin-endoperoxide Synthase 2, **(g,h)** *PGES* - Prostaglandin E synthase, **(i,j)** *PTGER2*, prostaglandin E receptor 2, **(k,l)** *PTGFR*, prostaglandin F receptor, **(m,n)** *LHCGR*, luteinizing hormone/choriogonadotropin receptor, **(o,p)** *PRLR*, prolactin receptor, **(q,r)** *FSHR*, follicle stimulating hormone receptor, **(s,t)** *GPX4*, glutathione peroxidase 4, **(u,v)** *SOD1*, superoxide dismutase 1. Small letters indicate significant differences between groups, based on pairwise comparison Wilcoxon rank sum test.

enzymes. The strongest decrease in expression (274-fold) was observed in *LHCGR* (**Figure 6m**). The anti-oxidative enzyme *GPX4* increased during the time of cell culture (**Figures 6s**, **7s**) whereas *SOD1* expression strongly decreased (**Figures 6u**, **7u**).

For LLC, no significant changes were measured for genes involved in steroid and prostaglandin synthesis (**Figures 6b,d,f,h**, **7b,d,f,h**). However, a significant increase of gene expression during the culture period was measured for hormone receptors (**Figures 6l,n**, **7j,n,p,r**), except *PTGER2, PRLR, FSHR* in experiment A (**Figures 6j,p,r**) and *PTGFR* in experiment B (**Figure 7l**). The two analyzed anti-oxidative enzymes *GPX4* and *SOD1* also increased significantly over time (**Figures 6t,v**, **7t,v**).

DISCUSSION

We describe for the first time separate cultures of small and large luteal cells in domestic cat, accompanied by hormone and gene expression analysis. All culture systems were performed without any stimulation by potential luteotrophic or luteolytic factors, and therefore present the basis for functional studies on cellular activity of SLC and LLC in domestic cats and for comparative studies in other feline species in the future.

We have performed two series of experiments over different time periods, because there is a lack of information about steroidogenic luteal cells from domestic cat at a very first day in cell culture. Available literature for other species characterize cell cultures at different days (7, 9, 10, 14) including directly after isolation (48).

Isolation of Small and Large Feline Luteal Cells and Their Characterization

Isolation of Steroidogenic Cells

Enzymatic digestion of luteal tissue with collagenase and DNase is the common method of luteal cell isolation (4, 49–52). However, this method generally isolates a mixture of small and large luteal cells, which is then purified by centrifugation through a percoll density gradient (4, 51, 52) or by cell sorting (53). In comparison to bovine CL, feline CL are quite small and cell numbers are very low, so the application of flow cytometry is inappropriate. Fortunately, our modified method based on enzymatic digestion allows us to isolate SLC only.

LLC were exclusively obtained through mechanical method. Isolating luteal cells without enzymatic digestion has rarely been used before. Gregoraszczuk (7) reported the use of mechanical

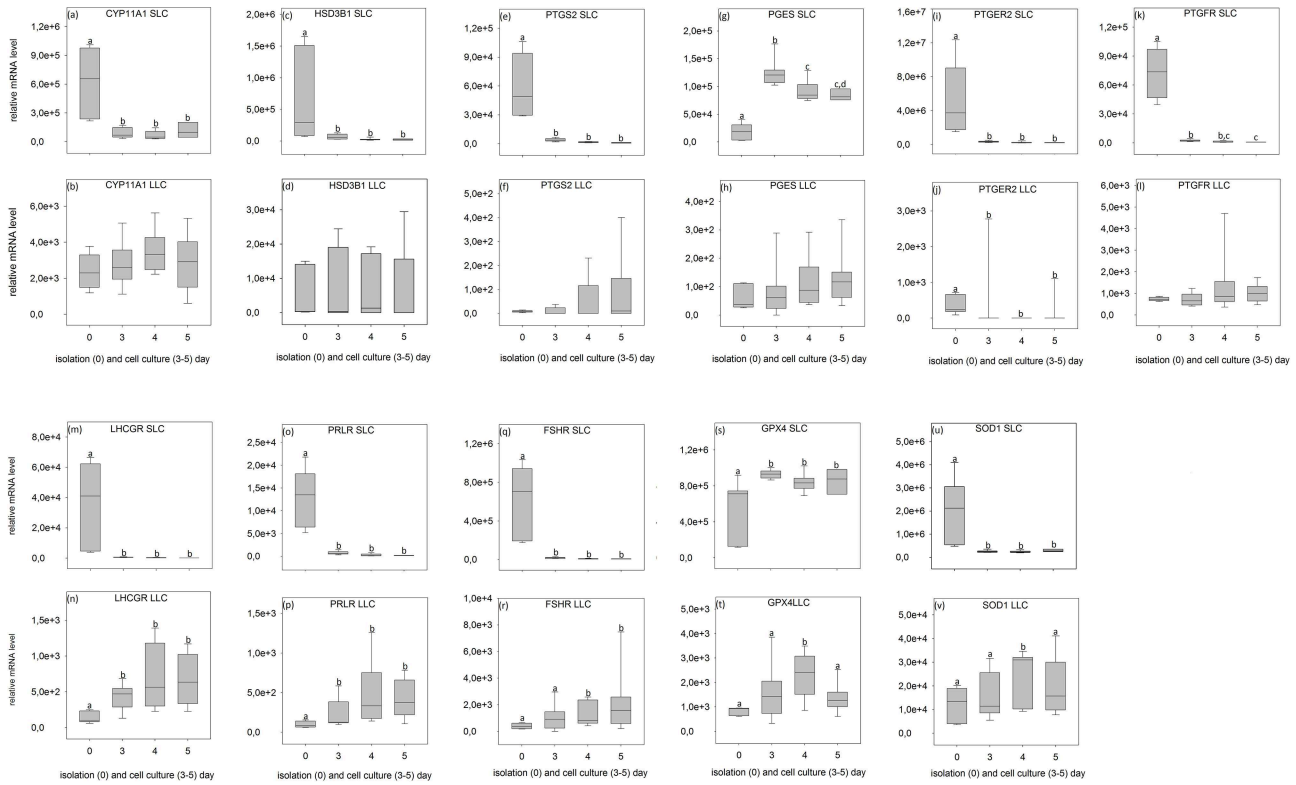

FIGURE 7 | Relative mRNA level of analyzed genes in SLC (small luteal cells) and LLC (large luteal cells) obtained directly after isolation (Day 0) and after 3–5 days of culture (Experiment B). **(a,b)** *CYP11A1*, Cholesterol Side-Chain Cleavage Enzyme, **(c,d)** *HSD3B1*, 3β-hydroxysteroid dehydrogenase type 1, **(e,f)** *PTGS2*, prostaglandin-endoperoxide Synthase 2, **(g,h)** *PGES*, Prostaglandin E synthase, **(i,j)** *PTGER2*, prostaglandin E receptor 2, **(k,l)** *PTGFR*, prostaglandin F receptor, **(m,n)** *LHCGR*, luteinizing hormone/choriogonadotropin receptor, **(o,p)** *PRLR*, prolactin receptor, **(q,r)** *FSHR*, follicle stimulating hormone receptor, **(s,t)** *GPX4*, glutathione peroxidase 4, **(u,v)** *SOD1*, superoxide dismutase 1. Small letters indicate significant differences between groups, based on pairwise comparison Wilcoxon rank sum test.

disruption of porcine luteal through a metal strainer, and Srivastava et al. (54) obtained luteal cells without enzymatic digestion based on migration of cells from tissue pieces (7, 54). Using tissue explants, however, requires time to achieve cell migration, creating colonies and monolayer formation and the composition of cell culture might be uncertain. In comparison, our isolation method allows for the isolation of LLC in a very short time and provides a very good way to distinguish them from SLC. To obtain SLC we have modified the method of Arikan and Yigit (14), who had previously described isolation of feline luteal cells. The selectiveness of the enzymatic method is based on the high sensitivity of feline LLC toward enzymatic digestion in contrast to SLC. The extreme fragility of LLC was discussed earlier for rat (11, 55, 56) and was related to the impact of mechanical forces and enzymes on peculiar morphology of LLC with their extremely high number of intracellular lipid droplets and extensive interdigitation (11, 55).

Characterization of Freshly Isolated SLC and LLC

The two different isolation protocols described here were the basis for our gene expression analysis in both SLC and LLC, although it must be indicated that the data on relative abundance cannot be compared directly between cell types. Due to the comparably low amount of extracted RNA obtained from LLC, only one reference gene could be used for normalization. In addition, the high variation of measurements between the cell isolates did not allow a more detailed statistical analysis.

Nevertheless, some important conclusions can be inferred from the observed gene expression profiles in the two freshly isolated luteal cell populations of domestic cats. Firstly, all tested genes were found to be expressed, but comparison between the different genes revealed some putative quantitative differences. SLC had a very high level of prostaglandin E2 receptor (*PTGER2*) expression (**Figures 6i**, **7i**), followed by genes of steroidogenic enzymes and the antioxidant system (**Figures 6a,c,s,u**, **7a,c,s,u**). Prostaglandins and their receptors were previously reported to play an important role in the maintenance of carnivore CL (2, 13, 57, 58). Interestingly, both prostaglandin synthases (*PTGS2* and *PGES,* **Figures 6e,g**, **7e,g**) and the receptor for PGF2alpha (*PTGFR,* **Figures 6k**, **7k**) were expressed at considerably lower levels compared to *PTGER2* in SLC. This hints to a more pronounced role of PGE reception in SLC. In LLC, both synthases were almost undetectable (*PTGS2* and *PGES;* **Figures 6f,h**, **7f,h**), while *PTGFR* (**Figures 6l**, **7l**) was at the same expression level as the receptor of *PGE2* (**Figures 6j**, **7j**). This may indicate to a comparable sensitivity of LLC toward both prostaglandins. Previous determination of gene expression in luteal tissue of domestic cats, revealed a decreasing

prostaglandin synthesis, once the CL develop from formation toward development/maintenance, accompanied by an increase of prostaglandin receptors, *PTGER4* and *PTGFR* (2).

Also for other analyzed genes, differences in expression patterns between the two steroidogenic luteal cell populations could not previously be identified before using CL tissues. Isolated SLC showed comparatively high expression level for *FSHR* (10–20 times higher, **Figures 6q**, **7q**) in contrast to both, the LH receptor (**Figures 6m**, **7m**) and the prolactin receptor (**Figures 6o**, **7o**). In isolated LLC, the FSH receptor (**Figures 6r**, **7r**) expression level was not different from that of LH (**Figures 6n**, **7n**) and prolactin receptors (**Figures 6p**, **7p**). In our previous studies (unpublished data) on feline luteal tissue, we have determined increasing *FSHR* expression during luteal life span and increasing prolactin receptor expression toward early regression. In contrast, *LHCGR* level decreased toward regression. In other species, luteal LH receptor expression was transiently down regulated in response to the LH-surge, but reactivated in the mid-luteal phase and decreased again with CL regression (59). Domestic cats are induced ovulators and in the case of non-pregnancies a real LH-surge might not occur.

Our two luteal cell populations and their cultures allow for follow-up studies on the response to gonadotrophic stimulation, and provide a better understanding on the role of suggested luteotrophic factors, like LH or prolactin, for the survival of CL; and last but not least, for the physiological persistency of CL described for lynx species (33).

Functional Behavior of Steroidogenic Luteal Cells During Culture

Although being isolated from similar domestic cats, both established luteal cell culture systems were different with regard to medium composition and cell number inoculated into wells. Our aim was to define marginal suitable culture conditions, which would later allow the study of luteotropic factors. Therefore, outcomes of culture cannot be directly compared and will be discussed separately.

Functional Behavior of SLC in Culture

In our cell culture system, SLC morphology was similar to rat luteal cells (11). After seeding, they attached to the cell culture plate within 1 day. Proliferation or cells spreading of feline SLC was ongoing until a confluent monolayer formed at around day 3–4 (**Figures 3a,c,e**, **4a,c,e**). A hint for proliferation is the increasing relative abundance for reference genes per well (data not shown). SLC of domestic cat release less progesterone than LLC (**Table 2**) per inoculated cells. This activity difference was previously described in sheep (21), pigs (19), cows (8, 20), humans (4), and rats (11). In addition, our feline SLC progressively lost their steroidogenic capabilities over the period of cell culture, as shown by decreasing enzyme activity of 3β-hydroxysteroid dehydrogenase (**Figures 5a,c,e**) accompanied by a decrease in mRNA expression of steroidogenic genes during culture (**Figures 6a,c**, **7a,c**). In bovines, SLC divided rapidly in the absence of LH, showed signs of mitosis in culture and lost steroidogenic function (60). Arikan et al. (14) described a steady decline of progesterone production between day 3, 5, and 7 of feline luteal cell in culture (14). In contrast, we did not observe a further decrease of P4 production between day 4 and 5 in SLC (**Table 2**).

Simultaneous determination of steroid production and gene expression as described, might allow us to assess the functionality of the cells in culture. It appears that SLC suffered massively from the isolation procedure and needed at least 1 day to recover within culture. The immediate change in steroid producing activity after inoculation to the culture disk, however, was expected and has been described for rat and bovine luteal cells (11, 61). Unraveling the course of gene activity and hormone production during the first 72 h as described for experiment A, reflected the conversion of SLC *in vivo* (activity at day 0) to probably proliferating (but maybe not non-differentiated) luteal cells between day 1 and 3. Interestingly, we observed a drop in gene expression in some but not all genes. The *PGES* and *GPX4* expression showed a different pattern with a higher expression in cultured cells (**Figures 6g,s**, **7g,s**). In luteal tissue, the *PGES* expression was highest in the formation stage and decreased over luteal life span (2).

Glutathione peroxidase 4, the enzyme which is encoded by the *GPX4* gene, protects cells against membrane lipid peroxidation (62). The expression of this gene did not fall after isolation and in fact increased during the course of culture in SLC. This may have been a reaction to the elevated oxidative stress in the cell culture.

There is evidence that bovine SLC have an ability to differentiate to LLC *in vivo* (16), and this was also described for CL of pseudo-pregnant domestic cats (50). This phenomenon, however, has not previously been described *in vitro*. In the experiments of Hoyer et al. (9), cultured ovine luteal cells significantly increased in size, but this was not described as a cell differentiation. Microscopic analysis of our SLC cultures may indicate that some SLC differentiated into LLC. Around the fourth day of culture, some LLC-like cells were observed occasionally and their number appeared to increase during the culture period (**Figures 4c,e**). At the beginning of differentiation, cells increased in size, acquired more compact and round shape, accumulated lipid droplets within the cytoplasm, and started to detach from the cell culture dish (**Figure 5e**). This culminated in a cell type expressing morphology and size characteristics of LLC (**Figure 2b**). Alternatively those cells can represent cells with diameter $>20\,\mu m$ obtained after isolation, which at the beginning of cell culture flattened on the bottom of a well, but then grew to size typical for LLC and detached from bottom of the well. Another explanation for this may be that cells detached on their way to dying and its bigger size is caused by long time in cell culture, but such a big increase in diameter in dying cells seems unlikely for us.

Enzyme activity for 3ß-hydroxysteroid dehydrogenase of differentiating cells was much more conspicuous (**Figure 5e**) compared to the SLC, but blocking enzyme activity with trilostane was not as pronounced as that of isolated LLC indicating a difference between these two cell types. Trilostane is a synthetic steroid which selectively inhibits 3ß-hydroxysteroid dehydrogenase (37). Thus, the remaining staining indicates a reduction of formazan by other pathways like the activities of lactate dehydrogenase (63) or of alkaline phosphatase (64, 65). Activity for alkaline phosphatase was previously used to discriminate between theca-derived luteal cells and luteal cells

of granulosa cell origin in the pig (66) and the rat (67). In this study we did not specifically select the differentiated luteal cell for expression analysis, but future studies might consider producing and harvesting differentiated SLC to compare their cellular activity with LLC.

Functional Behavior of LLC in Culture

The behavior of feline LLC in culture was different from SLC. LLC did not attach to the culture well and did not proliferate. Similar observations regarding lack of proliferation of LLC were previously made in rats (11). Nelson et al. describes also, that LLC of rat do not flatten out completely in culture. It was explained, most probably as the abundance of lipid droplets in LLC. Based on this information and our observation, we suggest that maybe LLC in domestic cat do not attach to the well surface because of high amount of lipid droplets. LLC numbers declined over the period of study, which was reflected by a massive drop in reference gene expression (data not shown). Although it is not clear whether progesterone is released from cellular depots or produced *de novo* (**Table 2**), intense staining for activity of 3β-hydroxysteroid dehydrogenase after isolation (**Figure 5g**) and stable gene expression of steroidogenic enzymes support luteal cell activity in surviving cells during culture (**Figures 3b,d,f**, **4b,d,f**). We also observed a steady increase in the expression of the receptors for gonadotrophins, prolactin and PGF2alpha (**Figures 6l,n**, **7n,p,r**). Further experiments are needed to test whether and how LLC will react to LH or FSH stimulation or PGF2alpha supplementation. It has been previously suggested that PGF2alpha might change its function from a luteotrophic agent at the start of pregnancy or luteal cycle toward a luteolytic component around parturition. This was supported by the PGFM profile determined throughout pregnancy in domestic cats (68, 69) and the inability to interrupt pregnancies with prostaglandins before day 33 of pregnancy and the need for extremely high doses thereafter (70, 71). Shille and Stabenfeldt (72) showed that high doses and repeated treatments with PGF2alpha in the first trimester had almost negligible effects (72). During the same time period, the highest level of PGF synthase (*PTGF*) was detected in the feline placenta (73). This, together with our observation that LLC isolated from CL in the stage of development/maintenance express PGF2alpha receptor, points to a luteotrophic function of prostaglandin at the beginning of feline luteal cycle.

DATA AVAILABILITY STATEMENT

The datasets generated for this study can be found in the GenBank: MH882487, MH882488, MH882490, MH882486, and MH882489.

ETHICS STATEMENT

Our samples are from routine ovariectomies performed in animal clinics and were not related to the purpose of the experiment.

AUTHOR CONTRIBUTIONS

MH carried out the study, analyzed and interpreted the data, and compiled the manuscript. BB designed the study with respect to gene expression analysis, partly analyzed and interpreted data, discussed the results, critically revised the manuscript, and finally approved the version for submission. LB performed statistics, proofread for English, critically revised the manuscript, and finally approved the version for submission. KJ designed the study with respect to cell culture, discussed the results, critically revised the manuscript, and finally approved the version for submission. All authors approved the final submitted manuscript.

FUNDING

This work was supported by the German Research Foundation (DFG BR 4021/5-1). The publication of this article was funded by the Leibniz Open Access Publishing Fund.

ACKNOWLEDGMENTS

We would like to thank, Katharina Pohling for assistance with maintaining the cell cultures, Sigrid Holz for preparation of histologic slides, and Mareen Albrecht and Katrin Paschmionka for help with hormone analysis. We also would like to thank Shannon Currie for proofreading of the manuscript.

SUPPLEMENTARY MATERIAL

The Supplementary Material for this article can be found online at: https://www.frontiersin.org/articles/10.3389/fendo.2019.00724/full#supplementary-material

Figure S1 | SLC stained for activity of 3β-hydroxysteroid dehydrogenase SLC at day 2 of cell culture **(a)**; control staining for SLC at day 2 of cell culture **(b)**. In control samples, activity of 3β-hydroxysteroid dehydrogenase was blocked by trilostane.

Table S1 | Relative mRNA abundance of genes in small luteal cell cultures (days 1–3 and 3–5) compared to freshly isolated cells (day 0). Results presented as mean values ± standard deviation. *P*-values indicate the result of Kruskal-Wallis test for normalized data, Chi squared—refers to test statistics and df indicates degrees of freedom. Small letters indicate significant differences between groups, based on pairwise comparison Wilcoxon rank sum test. *Indicates that significant differences between groups have the same pattern with expression on day 0 being different from all others days.

Table S2 | Relative mRNA abundance of genes in large luteal cell cultures (days 1–3 and 3–5) compared to freshly isolated cells (day 0). Results presented as mean values ± standard deviation. *P*-values indicate the result of Kruskal-Wallis test for normalized data, Chi squared—refers to test statistics and df indicates degrees of freedom. Small letters indicate significant differences between groups, based on pairwise comparison Wilcoxon rank sum test. *Indicates that significant differences between groups have the same pattern with expression on day 0 being different from all others days.

REFERENCES

1. van den Driesche S, Smith VM, Myers M, Duncan WC. Expression and regulation of oestrogen receptors in the human corpus luteum. *Reproduction*. (2008) 135:509–17. doi: 10.1530/REP-07-0427
2. Zschockelt L, Amelkina O, Siemieniuch MJ, Kowalewski MP, Dehnhard M, Jewgenow K, et al. Synthesis and reception of prostaglandins in *corpora lutea* of domestic cat and lynx. *Reproduction*. (2016) 152:111–26. doi: 10.1530/REP-16-0180
3. Yoshioka S, Abe H, Sakumoto R, Okuda K. Proliferation of luteal steroidogenic cells in cattle. *PLoS ONE*. (2013) 8:e84186. doi: 10.1371/journal.pone.0084186
4. Friden BE, Hagstrom H, Lindblom B, Sjoblom P, Wallin A, Brannstrom M, et al. Cell characteristics and function of two enriched fraction of human luteal cells prolonged culture. *Mol Hum Reprod*. (1999) 5:714–9. doi: 10.1093/molehr/5.8.714
5. Brannian JD, Stouffer RL. Progesterone production by monkey luteal cell subpopulations at different stages of the menstrual cycle: changes in agonist responsiveness. *Biol Reprod*. (1991) 44:141–9. doi: 10.1095/biolreprod44.1.141
6. Gospodarowicz D, Gospodarowicz F. Bovine luteal cells in tissue culture. *Exp Cell Res*. (1972) 75:353–62. doi: 10.1016/0014-4827(72)90440-5
7. Gregoraszczuk E. Steroid hormone release in cultures of pig corpus luteum and granulosa cells: effect of LH, hCG, PRL and estradiol. *Endocrinol Exp*. (1983) 17:59–68.
8. Fitz TA, Mayan MH, Sawyer HR, Niswender GD. Characterization of two steroidogenic cell types in the ovine corpus luteum. *Biol Reprod*. (1982) 27:703–11. doi: 10.1095/biolreprod27.3.703
9. Hoyer PB, Kong W, Crichton EG, Bevan L, Krutzsch PH. Steroidogenic capacity and ultrastructural morphology of cultured ovine luteal cells. *Biol Reprod*. (1988) 38:909–20. doi: 10.1095/biolreprod38.4.909
10. Arikan S, Kalender H, Simsek O. Effects of cholesterol on progesterone production by goat luteal cell subpopulations at two different stages of the luteal phase. *Reprod. Domest Anim*. (2010) 45:e434–9. doi: 10.1111/j.1439-0531.2010.01596.x
11. Nelson SE, McLean MP, Jayatilak PG, Gibori G. Isolation, characterization, and culture of cell subpopulations forming the pregnant rat corpus luteum. *Endocrinology*. (1992) 130:954–66. doi: 10.1210/endo.130.2.1733737
12. Quirk SM, Harman RM, Huber SC, Cowan RG. Responsiveness of mouse *corpora luteal* cells to Fas antigen (CD95)-mediated apoptosis. *Biol Reprod*. (2000) 63:49–56. doi: 10.1095/biolreprod63.1.49
13. Kowalewski MP, Fox B, Gram A, Boos A, Reichler I. Prostaglandin E2 functions as a luteotrophic factor in the dog. *Reproduction*. (2013) 145:213–26. doi: 10.1530/REP-12-0419
14. Arikan S, Yigit AA. Effects of cholesterol and cAMP on progesterone production in cultured luteal cells isolated from pseudopregnant cat ovaries. *Anim Reprod Sci*. (2009) 115:238–46. doi: 10.1016/j.anireprosci.2008.12.003
15. Stocco C, Telleria C, Gibori G. The molecular control of corpus luteum formation, function, and regression. *Endocr Rev*. (2007) 28:117–49. doi: 10.1210/er.2006-0022
16. Alila HW, Hansel W. Origin of different cell types in the bovine corpus luteum as characterized by specific monoclonal antibodies. *Biol Reprod*. (1984) 31:1015–25. doi: 10.1095/biolreprod31.5.1015
17. Meidan R, Girsh E, Blum O, Aberdam E. *In vitro* differentiation of bovine theca and granulosa cells into small and large luteal-like cells: morphological and functional characteristics. *Biol Reprod*. (1990) 43:913–21. doi: 10.1095/biolreprod43.6.913
18. Alexopoulos E, Shahid J, Ongley HZ, Richardson MC. Luteinized human granulosa cells are associated with endogenous basement membrane-like components in culture. *Mol Hum Reprod*. (2000) 6:324–30. doi: 10.1093/molehr/6.4.324
19. Lemon M, Loir M. Steroid release in vitro by two luteal cell types in the corpus luteum of the pregnant sow. *J Endocrinol*. (1977) 72:351–9. doi: 10.1677/joe.0.0720351
20. Ursely J, Leymarie P. Varying response to luteinizing hormone of two luteal cell types isolated from bovine corpus luteum. *J Endocrinol*. (1979) 83:303–10. doi: 10.1677/joe.0.0830303
21. Rodgers RJ, O'Shea JD, Findlay JK. Progesterone production in vitro by small and large ovine luteal cells. *J Reprod Fertil*. (1983) 69:113–24. doi: 10.1530/jrf.0.0690113
22. Fields MJ, Fields PA. Morphological characteristics of the bovine corpus luteum during the estrous cycle and pregnancy. *Theriogenology*. (1996) 45:1295–325. doi: 10.1016/0093-691X(96)00099-4
23. Lawler DF, Johnston SD, Hegstad RL, Keltner DG, Owens SF. Ovulation without cervical stimulation in domestic cats. *J Reprod Fertil Suppl*. (1993) 47:57–61.
24. Dawson AB. The development and morphology of the corpus luteum of the cat. *Anatomical Record*. (1941) 79:155–69. doi: 10.1002/ar.1090790203
25. Amelkina O, Braun BC, Dehnhard M, Jewgenow K. The corpus luteum of the domestic cat: histologic classification and intraluteal hormone profile. *Theriogenology*. (2015) 83:711–20. doi: 10.1016/j.theriogenology.2014.11.008
26. Tsutsui T, Stabenfeldt GH. Biology of ovarian cycles, pregnancy and pseudopregnancy in the domestic cat. *J Reprod Fertil Suppl*. (1993) 47:29–35.
27. Paape SR, Shille VM, Seto H, Stabenfeldt GH. Luteal activity in the pseudopregnant cat. *Biol Reprod*. (1975) 13:470–4. doi: 10.1095/biolreprod13.4.470
28. Verhage HG, Beamer NB, Brenner RM. Plasma-levels of estradiol and progesterone in cat during poly-estrus, pregnancy and pseudopregnancy. *Biol. Reprod*. (1976) 14:579–85. doi: 10.1095/biolreprod14.5.579
29. Lashari MH, Tasawar Z. The effect of PGF2 on persistent corpus luteum in Sahiwal cows. *Int J Livestock Prod*. (2012) 3:1–5. doi: 10.5897/IJLP10.012
30. Magata F, Shirasuna K, Struve K, Herzog K, Shimizu T, Bollwein H, et al. Gene expressions in the persistent corpus luteum of postpartum dairy cows: distinct profiles from the *corpora lutea* of the estrous cycle and pregnancy. *J Reprod Dev*. (2012) 58:445–52. doi: 10.1262/jrd.2011-049
31. Goritz F, Dehnhard M, Hildebrandt TB, Naidenko SV, Vargas A, Martinez F, et al. Non cat-like ovarian cycle in the Eurasian and the Iberian lynx - ultrasonographical and endocrinological analysis. *Reprod Domest Anim*. (2009) 44(Suppl 2):87–91. doi: 10.1111/j.1439-0531.2009.01380.x
32. Painer J, Jewgenow K, Dehnhard M, Arnemo JM, Linnell JD, Odden J, et al. Physiologically persistent *corpora lutea* in Eurasian lynx (*Lynx lynx*) - longitudinal ultrasound and endocrine examinations intra-vitam. *PLoS ONE*. (2014) 9:e90469. doi: 10.1371/journal.pone.0090469
33. Painer J, Goeritz F, Dehnhard M, Hildebrandt TB, Naidenko SV, Sanchez I, et al. Hormone-induced luteolysis on physiologically persisting *corpora lutea* in Eurasian and Iberian lynx (*Lynx lynx* and *Lynx pardinus*). *Theriogenology*. (2014) 82:557–62. doi: 10.1016/j.theriogenology.2014.05.004
34. Jewgenow K, Painer J, Amelkina O, Dehnhard M, Goeritz F. Lynx reproduction–long-lasting life cycle of *corpora lutea* in a feline species. *Reprod Biol*. (2014) 14:83–8. doi: 10.1016/j.repbio.2014.03.002
35. Pate JL, Condon WA. Effects of serum and lipoproteins on steroidogenesis in cultured bovine luteal cells. *Mol Cell Endocrinol*. (1982) 28:551–62. doi: 10.1016/0303-7207(82)90146-0
36. Payne AH, Downing JR, Wong KL. Luteinizing hormone receptors and testosterone synthesis in two distinct populations of Leydig cells. *Endocrinology*. (1980) 106:1424–9. doi: 10.1210/endo-106-5-1424
37. Potts GO, Creange JE, Hardomg HR, Schane HP. Trilostane, an orally active inhibitor of steroid biosynthesis. *Steroids*. (1978) 32:257–67. doi: 10.1016/0039-128X(78)90010-7
38. Braun BC, Zschockelt L, Dehnhard M, Jewgenow K. Progesterone and estradiol in cat placenta–biosynthesis and tissue concentration. *J Steroid Biochem Mol Biol*. (2012) 132:295–302. doi: 10.1016/j.jsbmb.2012.07.005
39. Dehnhard M, Naidenko S, Frank A, Braun B, Goritz F, Jewgenow K. Non-invasive monitoring of hormones: a tool to improve reproduction in captive breeding of the Eurasian lynx. *Reprod Domest Anim*. (2008) 43(Suppl 2):74–82. doi: 10.1111/j.1439-0531.2008.01145.x
40. Siemieniuch MJ, Mlynarczuk JJ, Skarzynski DJ, Okuda K. Possible involvement of oxytocin and its receptor in the local regulation of prostaglandin secretion in the cat endometrium. *Anim Reprod Sci*. (2011) 123:89–97. doi: 10.1016/j.anireprosci.2010.10.015
41. Siemieniuch MJ, Jursza E, Kowalewski MP, Majewska M, Skarzynski DJ. Prostaglandin endoperoxide synthase 2 (PTGS2) and prostaglandins F2alpha and E2 synthases (PGFS and PGES) expression and prostaglandin F2alpha and E2 secretion following oestrogen and/or progesterone stimulation of the feline endometrium. *Reprod Domest Anim*. (2013) 48:72–8. doi: 10.1111/j.1439-0531.2012.02031.x
42. Zschockelt L, Amelkina O, Koster S, Painer J, Okuyama MW, Serra R, et al. Comparative analysis of intraluteal steroidogenic enzymes emphasises the functionality of fresh and persistent *corpora lutea* during pro–and

metoestrus in the lynx. *J Steroid Biochem Mol Biol*. (2015) 154:75–84. doi: 10.1016/j.jsbmb.2015.07.001
43. Amelkina O, Zschockelt L, Painer J, Serra R, Villaespesa F, Braun BC, et al. Apoptosis-related factors in the luteal phase of the domestic cat and their involvement in the persistence of *corpora lutea* in Lynx. *PLoS ONE*. (2015) 10:e0143414. doi: 10.1371/journal.pone.0143414
44. Braun BC, Vargas A, Jewgenow K. The molecular detection of relaxin and its receptor RXFP1 in reproductive tissue of Felis catus and Lynx pardinus during pregnancy. *Reproduction*. (2012) 143:399–410. doi: 10.1530/REP-11-0316
45. Vandesompele J, De Preter K, Pattyn F, Poppe B, Van Roy N, De Paepe A, et al. Accurate normalization of real-time quantitative RT-PCR data by geometric averaging of multiple internal control genes. *Genome Biol*. (2002) 3:research0034. doi: 10.1186/gb-2002-3-7-research0034
46. Zschockelt L, Amelkina O, Siemieniuch MJ, Koster S, Jewgenow K, Braun BC. *corpora lutea* of pregnant and pseudopregnant domestic cats reveal similar steroidogenic capacities during the luteal life span. *J Steroid Biochem Mol Biol*. (2014) 144(Pt B):373–81. doi: 10.1016/j.jsbmb.2014.08.010
47. Yoav B, Hochberg Y. Controlling the False Discovery Rate: A Practical and Powerful Approach to Multiple Testing. *J R Stat Soc Ser B*. (1995) 57:289–300. doi: 10.1111/j.2517-6161.1995.tb02031.x
48. Battista PJ, Condon WA. A role for alternative pathway catecholamines in the regulation of steroidogenesis in cow luteal cells. *J Reprod Fertil*. (1986) 78:275–80. doi: 10.1530/jrf.0.0780275
49. Weber DM, Fields PA, Romrell LJ, Tumwasorn S, Ball BA, Drost M, et al. Functional differences between small and large luteal cells of the late-pregnant vs. nonpregnant cow. *Biol Reprod*. (1987) 37:685–97. doi: 10.1095/biolreprod37.3.685
50. Arikan S, Yigit AA, Kalender H. Size distribution of luteal cells during pseudopregnancy in domestic cats. *Reprod Domest Anim*. (2009) 44:842–5. doi: 10.1111/j.1439-0531.2008.01099.x
51. Batista M, Torres A, Diniz P, Mateus L, Lopes-da-Costa L. Development of a bovine luteal cell in vitro culture system suitable for co-culture with early embryos. *In Vitro Cell Dev Biol Anim*. (2012) 48:583–92. doi: 10.1007/s11626-012-9552-6
52. Wang Z, Chen S, Mo H, Huang Y, Li J, Sun J, et al. A simple and economical method in purifying dairy goat luteal cells. *Tissue Cell*. (2013) 45:269–74. doi: 10.1016/j.tice.2013.03.004
53. Baddela VS, Koczan D, Viergutz T, Vernunft A, Vanselow J. Global gene expression analysis indicates that small luteal cells are involved in extracellular matrix modulation and immune cell recruitment in the bovine corpus luteum. *Mol Cell Endocrinol*. (2018) 474:201–13. doi: 10.1016/j.mce.2018.03.011
54. Srivastava UK, Srivastava SR, Guru PY. Rat luteal cells in tissue culture: a technique for obtaining primary cell culture without enzymatic dissociation. *Indian J Exp Biol*. (1989) 27:602–6.
55. Wilkinson RF, Anderson E, Aalberg J. Cytological observations of dissociated rat corpus luteum. *J Ultrastruct Res*. (1976) 57:168–84. doi: 10.1016/S0022-5320(76)80107-4
56. Luborsky JL, Behrman HR. Isolation and functional aspects of free luteal cells. *Methods Enzymol*. (1985) 109:298–316. doi: 10.1016/0076-6879(85)09095-4
57. Kowalewski MP, Mutembei HM, Hoffmann B. Canine prostaglandin E2 synthase (PGES) and its receptors (EP2 and EP4): expression in the corpus luteum during dioestrus. *Anim Reprod Sci*. (2008) 109:319–29. doi: 10.1016/j.anireprosci.2007.11.023
58. Kowalewski MP, Ihle S, Siemieniuch MJ, Gram A, Boos A, Zdunczyk S, et al. Formation of the early canine CL and the role of prostaglandin E2 (PGE2) in regulation of its function: an *in vivo* approach. *Theriogenology*. (2015) 83:1038–47. doi: 10.1016/j.theriogenology.2014.12.006
59. Choi J, Smitz J. Luteinizing hormone and human chorionic gonadotropin: origins of difference. *Mol Cell Endocrinol*. (2014) 383:203–13. doi: 10.1016/j.mce.2013.12.009
60. Gospodarowicz D, Gospodarowicz F. The morphological transformation and inhibition of growth of bovine luteal cells in tissue culture induced by luteinizing hormone and dibutyryl cyclic AMP. *Endocrinology*. (1975) 96:458–67. doi: 10.1210/endo-96-2-458
61. O'Shaughnessy PJ, Wathes DC. Characteristics of bovine luteal cells in culture: morphology, proliferation and progesterone secretion in different media and effects of LH, dibutyryl cyclic AMP, antioxidants and insulin. *J Endocrinol*. (1985) 104:355–61. doi: 10.1677/joe.0.1040355
62. Imai H, Nakagawa Y. Biological significance of phospholipid hydroperoxide glutathione peroxidase (PHGPx, GPx4) in mammalian cells. *Free Radic Biol Med*. (2003) 34:145–69. doi: 10.1016/S0891-5849(02)01197-8
63. Jelinek D, Flores A, Uebelhoer M, Pasque V, Plath K, Iruela-Arispe ML, et al. Mapping metabolism: monitoring lactate dehydrogenase activity directly in tissue. *J Vis Exp*. (2018) 136:e57760. doi: 10.3791/57760
64. Paavola LG. The corpus luteum of the guinea pig. III Cytochemical studies on the Golgi complex and GERL during normal postpartum regression of luteal cells, emphasizing the origin of lysosomes and autophagic vacuoles. *J Cell Biol*. (1978) 79:59–73. doi: 10.1083/jcb.79.1.59
65. Van Noorden CJ, Jonges GN. Quantification of the histochemical reaction for alkaline phosphatase activity using the indoxyl-tetranitro BT method. *Histochem J*. (1987) 19:94–102. doi: 10.1007/BF01682753
66. Denning-Kendall PA, Guldenaar SE, Wathes DC. Evidence for a switch in the site of relaxin production from small theca-derived cells to large luteal cells during early pregnancy in the pig. *J Reprod Fertil*. (1989) 85:261–71. doi: 10.1530/jrf.0.0850261
67. Sangha GK, Guraya SS. Histochemical changes in acid and alkaline phosphatase activities in the growing follicles and *corpora lutea* of the rat ovary. *Acta Morphol Neerl Scand*. (1988) 26:43–9.
68. Finkenwirth C, Jewgenow K, Meyer HH, Vargas A, Dehnhard M. PGFM (13,14-dihydro-15-keto-PGF(2alpha)) in pregnant and pseudo-pregnant Iberian lynx: a new noninvasive pregnancy marker for felid species. *Theriogenology*. (2010) 73:530–40. doi: 10.1016/j.theriogenology.2009.10.008
69. Dehnhard M, Finkenwirth C, Crosier A, Penfold L, Ringleb J, Jewgenow K. Using PGFM (13,14-dihydro-15-keto-prostaglandin F2alpha) as a non-invasive pregnancy marker for felids. *Theriogenology*. (2012) 77:1088–99. doi: 10.1016/j.theriogenology.2011.10.011
70. Wildt DE, Panko WB, Seager SW. Effect of prostaglandin F2 alpha on endocrine-ovarian function in the domestic cat. *Prostaglandins*. (1979) 18:883–92. doi: 10.1016/0090-6980(79)90125-4
71. Verstegen JP, Onclin K, Silva LD, Donnay I. Abortion induction in the cat using prostaglandin F2 alpha and a new anti-prolactinic agent, cabergoline. *J Reprod Fertil Suppl*. (1993) 47:411–7.
72. Shille VM, Stabenfeldt GH. Luteal function in the domestic cat during pseudopregnancy and after treatment with prostaglandin F2 alpha. *Biol Reprod*. (1979) 21:1217–23. doi: 10.1095/biolreprod21.5.1217
73. Siemieniuch MJ, Jursza E, Szostek AZ, Zschockelt L, Boos A, Kowalewski MP. Placental origin of prostaglandin F2alpha in the domestic cat. *Mediators Inflamm*. (2014) 2014:364787. doi: 10.1155/2014/364787

Conflict of Interest: The authors declare that the research was conducted in the absence of any commercial or financial relationships that could be construed as a potential conflict of interest.

frontiers in Endocrinology

ORIGINAL RESEARCH
published: 15 November 2019
doi: 10.3389/fendo.2019.00774

Proteomic Analysis of Porcine Pre-ovulatory Follicle Differentiation Into Corpus Luteum

*Pawel Likszo, Dariusz J. Skarzynski and Beenu Moza Jalali**

Institute of Animal Reproduction and Food Research, Polish Academy of Sciences, Olsztyn, Poland

The luteinization of the follicular cells, following a LH surge, causes extensive molecular and structural changes in preovulatory follicles (POF) that lead to ovulation and ultimate formation of the corpus luteum (CL). The objective of this study was to identify proteins expressed in porcine POF before the LH surge and a new CL formed, 2–3 days after ovulation, and evaluate proteome changes associated with formation of the CL from a follicle. We used 2D-gel electrophoresis-based proteomics and tandem mass spectrometry followed by a functional analysis using Ingenuity Pathway analysis (IPA) to evaluate functional pathways associated with the luteinization process. Protein lysates were prepared from isolated POFs and from the newly formed CL. A total of 422 protein spots were identified in both structures. A total of 15 and 48 proteins or their proteoforms were detected only in the POFs and CL, respectively. An IPA analysis of a POF proteome showed that most of the follicular proteins were involved in cellular infiltration, endoplasmic stress responses, and the protein ubiquitination pathway. Most of the early luteal proteins were associated with steroid metabolism, cell death and survival, free radical scavenging, and the protein ubiquitination pathway. A comparison of a follicular proteome with that of an early luteal proteome revealed that 167 identified proteins or their proteoforms were differentially regulated between POFs and the newly formed CL ($p < 0.05$ and a fold change of >1.8). Proteins that were significantly more abundant in follicles included cAMP-dependent protein kinase, histone binding protein RBBP4, reticulocalbin, vimentin, and calumenin; more abundant luteal proteins included albumin, farnesyl diphosphate synthase, serine protease inhibitors, elongation factor-1, glutaredoxin, and selenium-binding protein. Proteins that were significantly altered with luteal formation were found to be associated with cholesterol biosynthesis, cell death and survival, and acute phase response. Moreover, upstream regulators of differentially abundant proteins in CL were identified that included insulin growth factor-1, sterol regulatory element-binding transcription factor-1, and nuclear factor erythroid-derived 2. We have identified novel proteins that advance our understanding of (1) processes associated with differentiation of POFs into the CL, (2) possible mechanisms of luteal cell survival, and (3) pathways regulating steroidogenesis in the newly formed CL.

Keywords: preovulatory follicles, luteinization, corpus luteum, porcine, proteomics

OPEN ACCESS

Edited by:
Jens Vanselow, Leibniz Institute for Farm Animal Biology, Germany

Reviewed by:
Monica Beatriz Frungieri, Instituto de Biología y Medicina Experimental (IBYME), Argentina
Aniel Sanchez Puente, Lund University, Sweden

****Correspondence:***
Beenu Moza Jalali
beenu.jalali@pan.olsztyn.pl

Specialty section:
This article was submitted to Reproduction, a section of the journal Frontiers in Endocrinology

Received: *26 April 2019*
Accepted: *23 October 2019*
Published: *15 November 2019*

Citation:
Likszo P, Skarzynski DJ and Moza Jalali B (2019) Proteomic Analysis of Porcine Pre-ovulatory Follicle Differentiation Into Corpus Luteum. Front. Endocrinol. 10:774. doi: 10.3389/fendo.2019.00774

INTRODUCTION

Reproductive efficiency in mammals is dependent on a well-coordinated ovarian cycle that includes follicular development, ovulation, corpus luteum formation, function, and regression in the absence of a pregnancy. The ovulation after the luteinizing hormone (LH) surge leads to the release of the oocyte and differentiation of the ruptured follicle (granulosa and theca cells) into luteal cells of the corpus luteum (CL), a progesterone (P4)-producing transient endocrine gland essential for the establishment and maintenance of early pregnancy. Luteinization primarily involves structural remodeling and changes in the expression of proteins that would initiate differentiation of estrogen-producing granulosa cells to the P4-producing luteal cells. The preovulatory follicles (POF)s under the influence of follicle stimulating hormone (FSH), LH, and growth factors undergo cell proliferation, support oocyte development, and synthesize estrogen (1–6). However, after the LH surge, granulosa cells cease to proliferate and express a different set of genes/proteins to support the luteal phenotype and P4 synthesis (7). The differentiation of the ruptured follicle to the CL is accompanied by changes in the extracellular matrix that allows cell migration. The LH surge induces expression of several MMPs and TIMPs facilitating follicle rupture during ovulation in many species, including pigs (8, 9). The LH also results in the increased expression of growth and angiogenic factors, such as the vascular endothelial growth factor (VEGF), angiopoietin, and their receptor to induce vascularization of the newly formed CL after luteinization (10, 11).

The targeted studies carried out in various species, especially in rodents, using gene knock-out models has elucidated the importance of many genes in the CL formation. Luteinization has been shown to be associated with a change in the expression of genes involved in the cell cycle, such as cyclin-dependent kinases, ovulation, such as cyclooxygenase-2, CATT/enhancer binding protein β (C/EBP), and the P4 receptor, and in cAMP/PKA signaling (12–14). The transcriptomics data related to the luteinization of follicular cells in mouse, rat, bovine, and porcine species has also contributed immensely to our understanding of processes associated with the luteinization of follicular cells (15–19). Despite many similarities between the follicular development, steroidogenesis, and ovulation across the species, there are species specific differences in these processes (20). In pigs, although there have been many reports detailing molecular changes associated with POF development and growth (21–24) and corpus luteum function and regression [reviewed in Ziecik et al. (25)], the studies regarding the luteinization of porcine follicles and CL formation are scarce (26, 27). There is, however, one study detailing the global changes in gene expression of porcine POFs after their luteinization (19); a proteomic analysis of changes associated with formation of the CL from POFs has not been reported yet. The luteinization of granulosa cells is known to start before ovulation (19); however, there are not many reports of regulatory mechanisms associated with ovulation and CL formation. As the formation of CL is essential to the success of pregnancy establishment, a detailed evaluation of molecular changes associated with CL formation was carried out using two-dimensional gel electrophoresis (2D-PAGE) followed by a functional analysis using Ingenuity Pathway analysis to identify processes that differ between these two structures. Owing to the use of porcine models in studies related to ovarian steroidogenesis, biomedical research (28), and a high degree of similarity in protein coding sequences between humans and pig, such a proteomic database might potentially allow for addressing causes of ovulation-related disorders in women. We identified key molecules associated with CL formation, survival, and steroidogenesis, and several novel proteins associated with steroidogenesis were also identified in this study.

MATERIALS AND METHODS

Animals

All procedures involving the use of animals were approved by the Animal Ethics Committee, University of Warmia and Mazury in Olsztyn, Poland, and were conducted in accordance with the national guidelines for agricultural animal care. Porcine ovaries were collected after the animals were slaughtered at a local abattoir and transported to the laboratory in phosphate-buffered saline (PBS) at room temperature. Ovaries were classified using morphological criteria described previously (29). Moreover, the follicular fluid concentrations of hormones estradiol-17 b (E2) and P4 were determined to classify the follicles as POFs before the LH surge. Four to five individual pre-ovulatory follicles more than 6 mm in diameter and that were from one pig were isolated by mechanical dissection. The follicles were punctured and the follicular fluid (FF) was aspirated using an 18-gauge needle fixed to a 5-ml syringe. The oocytes were removed and FF samples were centrifuged at 2,000 g for 15 min at 4°C. Supernatants were analyzed for E2 and P4 concentration using a radioimmunoassay kit (Cisbio International) according to manufacturer's instructions, and the E2:P4 ratios were calculated for each sample. The pre-ovulatory follicular walls from the same animal with E2 to P4 ratio >1.0 were pooled together and snap frozen in liquid nitrogen and stored at −80°C until protein lysate preparation. The CL were collected after 2–3 days of ovulation, characterized morphologically (29), snap frozen and stored at −80°C till further analysis. The POFs and CL used in this study were collected from four individual animals ($n = 4$).

Sample Preparation

Total protein was isolated from 4 to 5 pre-ovulatory follicles collected from same animal and pooled together ($n = 4$), as were the newly formed CL ($n = 4$). The samples were homogenized using a ceramic mortar and pestle and then precooled with liquid nitrogen for at least 1 min. Homogenized frozen tissue was directly transferred into a lysis buffer (30 mM Tris-HCL, 7M urea, 2M thiourea, 4% w/v CHAPS and protease inhibitor). Lysates were sonicated for 4 min in a Sonics Vibra-Cell VCX 120 and centrifuged in a Beckman Ultracentrifuge J2-HS for 30 min at 2,000 g and at 4°C. Protein concentrations were determined using the Bradford method.

Two-Dimensional Gel Electrophoresis (2-DE)

Protein lysates (600 μg) from preovulatory follicles and CL were suspended in rehydration buffer (7M urea, 2M thiourea, 2% w/v CHAPS, 10 mM DTT, 1% v/v IPG buffer pH 4–7 and 0.002% bromophenol blue) in a final volume of 340 μl. The protein samples were loaded on 18 cm Immobiline DryStrips, pH 4–7 (GE Healthcare, Uppsala, Sweden), and rehydrated for 10 h (passive rehydration). The rehydrated strips were focused at 50 μA per strip in an Ettan IPGphor IEF System I (GE Healthcare, Uppsala, Sweden) with the following voltage program: 500 V for 8 h, 1,000 V for 1 h, 8,000 V for 3 h, and 8,000 V for 2.5 h. Prior to gel electrophoresis, focused proteins in the IPG strips were equilibrated in two incubation steps, each lasting 15 min, at room temperature with slow shaking. In the first step, each strip was equilibrated in 10 mL of equilibration buffer (50 mM Tris-HCl pH 6.8, 6M urea, 30% v/v glycerin, 2% w/v SDS and trace of bromophenol blue) supplemented with 1% w/v DTT. The second equilibration step involved alkylation in the same equilibration buffer that contained 2.5% w/v iodoacetamide instead of DTT. For the second dimension analysis, strips were applied onto 12.5% polyacrylamide gels and sealed with 0.5% agarose. The second electrophoresis was run (Bio-Rad) at 40 mA for 30 min, 60 mA for 1.5 h, and 80 mA for 2 h at 4°C. After electrophoresis, gels were fixed in methanol:acetic-acid:water (40:10:50) for 1 h followed by staining using a Coomassive Brilliant Blue G250 (Sigma Aldrich, Saint Louis, USA). The gels were destained and scanned with an ImageScanner II (GE Healthcare).

Image and Data Analysis

The gel images were analyzed using the ImageMaster 2-D Platinum software version 7 from GE Healthcare. For comparison of protein spots between pre-ovulatory follicles and the CL, more than 15 spots in all gels were landmarked and normalized. Only protein spots with reproducible change of a minimum of 1.8-fold increase or decrease in their relative abundance and $p < 0.05$ by one way Anova in four biological replicates were considered significantly altered in the CL as compared to the pre-ovulatory follicle. Each group was performed in triplicate.

Excision of 2D-gel Spots, Tryptic Digestion and MALDI-TOF/TOF Analysis

To define the overall proteome of pre-ovulatory follicles and newly formed CL, clearly visible spots were manually picked from gels and washed for 30 min each in distilled water followed by 50 mM ammonium bicarbonate. Protein spots were digested overnight at 37°C using an in-gel tryptic digestion kit (Thermoscientific, MA) and following manufacturer's instructions. After digestion, the peptides were suspended in 100 μl of 0.1% trifluoroacetic acid (TFA) and desalted using C-18 zip tips (Sigma-Aldrich). The peptides were eluted from the zip tips with 2 μl of 50% acetonitrile in 0.1% TFA and mixed 1: 1 with matrix solution (5 mg/ml solution of α-cyano-4-hydroxycinnamic acid in 50% acetonitrile/0.1% TFA). 1 μl of peptide-matrix mixture was spotted on the MALDI target plate and left to dry at room temperature. The digested peptides were analyzed with a MALDI-MS/MS mass spectrometer, Autoflex-TOF/TOF (Bruker Daltonics, Bremen, Germany) in positive ion reflector mode with an accelerating potential at 20 kV with eight shots per second was also used. The mass spectra were internally calibrated using monoisotpoic [M+H]+ ion peptide calibration standards (Bruker Daltonics) consisting of Angiotensin II (1046.54), Angiotensin I (1296.68), Substance P (1347.73), Bombesin (1619.82), ACTH clip 1 (2093.086), ACTH clip 18 (2465.19), and Somatostatin 28 (3147.471). Mass spectra were processed with the Flex Analysis and Biotool 2.2 software (Bruker Daltonics). Peptide mass finger printing (PMF) and fragment mass spectra (MS/MS) for each individual spot were combined, and an ion search was performed with the MASCOT 2.2 software (Matrix Science) integrated with Biotool 2.2. The Mass Spectrometry Protein Sequence Database (Version 09292005; 2,344,227 sequences) and the National Center for Biotechnology Information non-redundant Sus scrofa protein database were searched with the following MASCOT settings: one incomplete tryptic cleavage allowed; fragment ion mass tolerance of 0.8 Da; parent ion mass tolerance of 0.8 Da; alkylation of cysteine by carbamidomethylation as a fixed odification; oxidation of methionine as a variable modification. For the PMF and MS/MS ion search, statistically significant ($p \leq 0.05$) matches by MASCOT were regarded as correct hits. We identified a total of 451 spots including the proteins that were differentially regulated between pre-ovulatory follicles and the CL. A complete proteomic work flow is depicted in **Supplementary Figure 1**.

Ingenuity Pathway Analysis

IPA (Ingenuity, Mountain View, CA) was used to gain insights into the involvement of all the identified follicular, luteal, and differentially abundant proteins between these two structures in biological pathways and networks. IPA identifies networks of interacting proteins and connects identified proteins in the data set to molecular networks contained within the Ingenuity Knowledge Database. The identified proteins were analyzed using IPA Core analysis to assess functional pathways and upstream regulators that were over represented in the data set. Fisher's exact test was used to calculate a *P*-value for each network and a functional pathway to determine which pathways are significantly linked to input data that is mapped to genes/proteins in the whole Ingenuity Pathways Knowledgebase. We also used IPA Upstream Regulator analysis to identify upstream transcription regulators by Fisher's exact *t*-test. The right-tailed Fisher's exact test, using a threshold of $P < 0.05$ after application of the Benjamini-Hochberg method for multiple testing correction, and z-score (in case of proteins with significantly altered abundances) were used as two statistical measures for identifying significant biofunctions and upstream regulators. The *z*-score value indicated the state of activation (z-score ≥ 2.0) for the analyses. The Upstream Regulator module identified the upstream regulators that might explain the observed changes in protein abundances in our dataset and highlight the biological activities occurring during the luteinization process.

Western Blot

Western-blot analysis was performed to validate the identity of select proteins belonging to categories unfolded protein response, oxidative stress response, cell proliferation and migration, sterol transport, and to quantitatively assess their abundance in select samples. Total protein lysate (25 μg) from a sample of POFs and the CL were resolved by 8% and 10% SDS-PAGE gel electrophoresis. Proteins were transferred onto polyvinylidene difluoride membranes (0.45 μm; Sigma-Aldrich, Saint Louis, USA) at 60 V for 90 min. Membranes were blocked with 5% non-fat milk in TBS-T (Tris buffered saline plus 0.05% Tween 20, pH 7.4) for 1.5 h at room temperature. Subsequently, membranes were washed thrice with TBS-T and incubated with following primary antibodies: rabbit anti-porcine ceruloplasmin, rabbit anti-porcine ERp57 (PDIA3), rabbit anti-porcine vitamin D binding protein (VDBP), mouse anti-porcine selenium binding protein 1 (SELENBP1), rabbit anti-porcine β-actin (Abcam, Cambridge, UK), rabbit anti-porcine aldose reductase (AKR1B1), and mouse anti-porcine heat shock protein (HSP) 60 (Sigma-Aldrich, Saint Louis, USA) diluted in TBS-T at 4°C overnight. The following day, the membranes were washed three times with TBS-T and incubated with anti-rabbit (Sigma-Aldrich, Saint Louis, USA) or anti-mouse (Abcam, Cambridge, UK) polyclonal secondary antibodies conjugated with alkaline phosphatase, diluted in TBS-T for 1.5 h at room temperature. The membranes were washed three times and protein bands were visualized by incubation in a solution of alkaline phosphate buffer (100 mM Tris-HCL, pH 9.5; 100 mM NaCl; 5 mM $MgCl_2$) with an addition of Nitro Blue Tetrazolium (Sigma-Aldrich, Saint Louis, USA) and 5-bromo-4-chloro 3-indolyl phosphate (Sigma-Aldrich, Saint Louis, USA) in the dark. The membranes were washed in deionized water for 1 min to stop the reaction color. The intensity of the protein bands was quantified by measuring optical density using a ChemiDoc^{TM} Touch Imaging System (Bio-Rad, Hercules, CAL, USA). The signal was analyzed using the Image Lab version 5.2 (Bio-Rad, Hercules, CAL, USA) and normalized to β-actin.

Statistical Analysis

The statistical analysis of the Western Blot data was performed by using GraphPad PRISM v.7.0 software (GraphPad Software, Inc., San Diego, CA, USA). To test the changes in the expression of the selected proteins between POFs and the newly formed CL and validate the proteomic results, an unpaired Student's *t*-test followed by a Mann-Whitney post-test were applied with the significance set at $P < 0.05$.

RESULTS

Hormone Assay in Follicular Fluid

The concentration of E2 and P4 in follicular fluid pooled from 5 follicles ranged from 161.41 ± 34.70 ng/mL, 208 ± 36 ng/ml, 251 ± 42 ng/ml, and 229 ± 24 ng/ml for E2 and 109.04 ± 3.28 ng/ml, 168.21 ± 2.9 ng/ml, 176.73 ± 17.23, and 202 ± 2.08 ng/ml for P4, respectively, in four different animals. Follicles were regarded as pre-ovulatory estrogenic when the E2/P4 ratio was more than 1.0 (19).

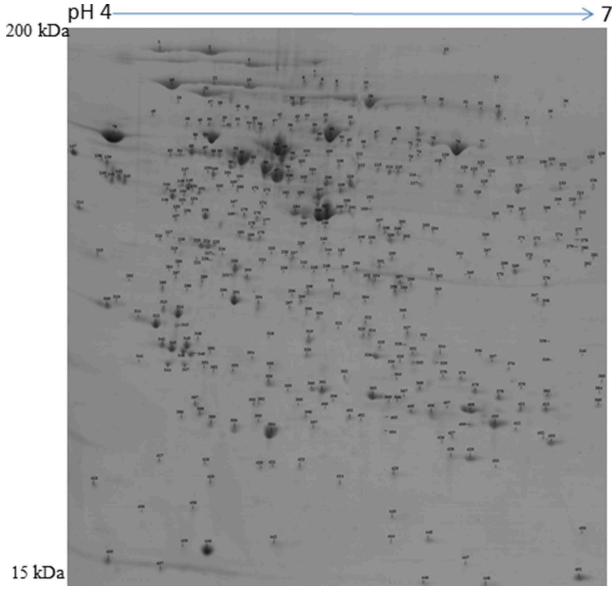

FIGURE 1 | Representative protein map of the porcine preovulatory follicles. Proteins corresponding to spot numbers are listed in **Supplementary Table 1**.

Characterization of Pre-ovulatory Follicular and Newly Formed Corpus Luteum Proteome

A 2D-PAGE of the protein lysates from pooled follicles (>6 mm in size) from the same animal and the CL obtained from porcine ovaries after 2–3 days of ovulation was performed over a pH range of 4–7. Analysis of the 2-DE gels with ImageMasterTM 2D Platinum Software led to visualization of ∼600 spots. The protein spots that were visualized in at least three gels were selected for identification by mass spectrometry. A total of 422 spots corresponding to proteins and their proteforms were identified in the POFs and CL using MALDI-MS/MS analysis (**Figure 1** and **Supplementary Tables 1, 2**). The follicular proteome was predominantly represented by structural proteins: actin, myosin, vimentin, and tubulin; calcium binding proteins: calreticulin, calumenin, and reticulocalbin, and proteins involved in ubiquitin-proteasome system: 26S proteasome non-ATPase regulatory subunit 13 and ubiquitin carboxyl-terminal hydrolase isozyme L1. For functional analysis using Ingenuity Pathway Analysis (IPA), protein IDs were submitted to Biomart and converted to 378 human specific Ensembl gene IDs (http://useast.ensembl.org/biomart). The remaining proteins did not map to human Ensembl gene IDs because they were uncharacterized proteins or unique to *Sus scrofa* (e.g., apolipoprotein R). A functional analysis of all of the POF proteins using IPA revealed that top processes that proteins were associated with included protein ubiquitination (20 proteins), endoplasmic stress response (11 proteins) remodeling of cytoskeleton (7 proteins), and unfolded protein response (7 proteins) (**Table 1**). The luteal proteome was highly represented by protease inhibitors (serpins

TABLE 1 | Functional categories and their associated proteins that are highly represented in POFs and the corpus luteum.

Functional categories	Associated proteins
POFs	
Protein ubiquitination	HSP90AA1, HSP90AB1, GRP78, HSPA8, HSPB1, HSP60, GRP78, PSMA3, PSMA6, PSMB3, PSMD11, SUGT1, TRAP1, UBE2K, PSME2, UCHL1, UCHL3, USP14, PSMD5, PSMD13
Endoplasmic reticulum stress response	HSP90AA1, HSP90AS1, GRP78, GRP94, HSPD1, P4HP, SOD1, UCHL1, ERP44, GORASP2, VCP
Unfolded protein response	CALR, PDIA6, CALU, P4HP, HSPA5, HSPA8, VCP
Remodeling of cytoskeleton	ACTB, ACTG1, ARP5, ACT2, MAPRE1, TUBB, VIM
NEWLY FORMED CORPUS LUTEUM	
Protein ubiquitination	HSP90AA1, HSP90AB1, HSPA9, HSPB1, HSPD1,GRP78, HSPA8, HSPB1, HSP60, GRP78, PSMA3, PSMA6, PSMB3, PSMD11, PSME2, PSMD13, SUGT1, TRAP1, UBE2K, UCHL1, UCHL3, USP14, PSMD5
Steroid synthesis	AKR1C1/C2, AKR1C4, APOA1, APOE, CYB5A, FDPS, IDI1, ODC1, PHB, SET, StAR, G6PD, HMGCS1, HSD17B1, HSD3B1, HSD3B2
NRF2-mediated oxidative stress response	CLPP, FTH, FTL, SOD1, GST, MAPK3, VCP, ACTB, ACG1, USP4, CP, PRDX6, PRDX4, GPX3,
Acute phase response	FGG, FTL, HNRNPK, HP, HPX, RBP4, SERPINA3, AHSG, ALB, CRP, CP, APOA1, C4BPA, MAPK3

and cathepsins) and proteins involved in the transport and synthesis of lipids [steroidogenic acute regulatory protein (STAR), farnesyl diphosphate synthase (FDPS), and aldo-keto reductase family 1 member C4 (AKR1C4)]. The IPA identified proteins that were associated with pathways such as the protein ubiquitination pathway (23 proteins), steroid metabolism (16 proteins), NRF2-mediated oxidative stress response (14 proteins), and acute phase response signaling (14 proteins) (**Table 1**).

Characterization of Proteins Associated With Differentiation of Follicles to CL

To detect changes associated with the transition of POFs to the CL after the LH surge, the protein profiles of POFs and the newly formed CL were compared by 2D-PAGE in the pH range 4–7. From a total of 600 matched spots, 167 significantly altered protein spots in the CL, as compared to the POFs, were identified (average ratio >1.8, $P < 0.05$). Representative 2D gel images depicting significantly altered protein spots in the CL as compared to POF are shown in **Figure 2** and the corresponding identified proteins along with the positive or negative fold change are listed in **Supplementary Tables 3, 4**, respectively. The identified proteins found upregulated in the CL as compared to POF included albumin (ALB), aldose reductase (AKR1B1), aldo-keto reductase family 1 member C4 (AKR1C4), fibrinogen gamma chain (FGG), isopentenyl-diphosphate delta isomerase 1 (IDI1), and fetuin (AHSG). Representative MS/MS spectra of some of the proteins that were differentially regulated between POFs and the CL in this study are shown in **Figure 3** and **Supplementary Figure 2**. Functional annotation of differentially abundant proteins resulted in their association with top molecular and cellular functions including the inhibition of cell death, lipid metabolism, and cell migration (**Figure 4A** and **Table 2**). Furthermore, differentially abundant proteins in the CL were linked to canonical pathways that support the luteinization process and included geranylgeranyl diphosphate biosynthesis I (via Mevalonate), cholesterol biosynthesis, and RhoA signaling (**Supplementary Figure 3** and **Table 2**). The IPA analysis of the significantly altered proteins further identified large number of upstream regulators that could be involved in luteinization-induced altered protein profiles in the CL. Top upstream regulators identified with a positive z-score (z-score > 2.0) included insulin growth factor-1 (IGF-1), nuclear factor erythroid derived (NFE2L2), sterol regulatory element-binding transcription factor 1 (SREBF1), and CCAAT/enhancer binding protein beta (CEBPB) (**Figure 4B** and **Supplementary Table 5**).

Western-Blot Analysis

The 2D-PAGE results were further validated by Western-blot analysis. Six identified proteins that were either upregulated or downregulated in the CL or identified for the first time in the porcine CL (CP and VDBP) were selected for further analysis. Statistical analysis of protein levels relative to beta-actin (ACTB) showed similarities to 2D results. Whereas, an abundance of protein disulfide isomerase 3 and heat shock protein 60 were significantly decreased in CL, AKR1B1 was more abundant in the CL, and proteins CP, SELENBP1, and VDBP were detected only in the CL (**Figure 5**).

DISCUSSION

The aim of the present study was to determine the protein profile of POFs and evaluate the LH surge-induced changes in follicles leading to ovulation and CL formation. This is the first comprehensive proteomic characterization of the porcine POFs to the best of our knowledge that gives an insight into the functional processes associated with follicles. The follicular proteome was highly represented by cytoskeleton-associated proteins, the endoplasmic stress response, and the folding of proteins.

Cytoskeletal Proteins

Cytoskeletal proteins were highly represented in POFs and included actin, tubulin, tropomyosin, and myosin. The genes

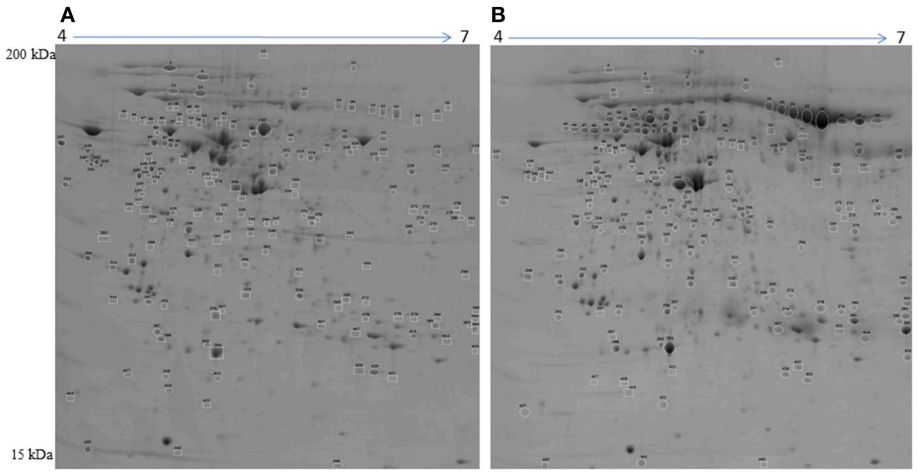

FIGURE 2 | Representative 2D gel image illustrating comparison between **(A)** preovulatory follicles and **(B)** newly formed corpus luteum proteomes. Significantly altered spots ($P < 0.05$) with at least 1.8-fold changes in intensity were identified as upregulated (circles) or downregulated (squares) in POFs or the CL. Spot numbers correspond to the proteins that were identified by mass spectrometry analysis and are presented in **Table 2**. Images are representative of four gel analyses.

corresponding to these proteins were previously described with luteinization of POFs (19). Cytoskeletal proteins play essential roles in changes associated with the differentiation of follicular cells. The expression of cytoskeletal proteins is under the control of FSH in rat granulosa cells, however, there are many reports highlighting the LH-induced morphological changes that involve the remodeling of the actin cytoskeleton, causing granulosa cells to become more rounded during the luteinization process and, more importantly, stimulation of P4 production (30–33). The other POF-associated structural proteins included microtubule-associated protein RP/EB1 (MAPRE1, spot 303 **Supplementary Table 1**) and vimentin. Vimentin existed in many isoforms (49–54 kDa) with a significantly decreased abundance in the CL. The expression of MAPRE1 did not show any significant difference between the POFs and the CL. In rat granulosa cells, an isoform of microtubule-associated proteins, MAP2D is expressed as an FSH responsive, and its expression is known to persist in the luteal cells (34). The MAP2D isoform binds to vimentin during follicular luteal transition. In mice, hCG induces phosphorylation of vimentin and its increased binding to low molecular weight MAP2D leading to vimentin disruption and contraction of granulosa cells which in turn results in an increase in the P4 synthesis (31). We speculate that, in pigs, the follicular expression of vimentin and MAPRE1, which binds to intermediate filaments, might have a similar function due to its reported involvement in follicle development (35).

Endoplasmic Stress Response and Folding of Proteins

The other class of proteins with a high representation in POF was associated with the abrogation of endoplasmic reticulum (ER) stress. The development of a follicle to preovulatory stage is accompanied with an extensive proliferation of the granulosa cell, which leads to hypoxia (36). Such a condition may contribute to ER stress resulting in prosurvival unfolded protein response (UPR) signaling to maintain ER homeostasis (37). In the absence of UPR, ER stress can inhibit cell growth and result in apoptosis as a survival mechanism affecting P4 synthesis (38). The porcine POFs are under ER stress, as we observed POF-specific expression of 78 kDA glucose-regulated protein (GRP78), a central regulator of unfolded protein responses and an important marker of ER stress (39). Calreticulin and calumenin are calcium-binding chaperone proteins and their expression is induced as a result of UPR. Both these proteins were highly abundant in the POFs and are known to alleviate ER stress (40, 41). Additionally, calreticulin knock out female mice were shown to be infertile due to impaired folliculogenesis and decreased ovulatory rates (41), suggesting its importance in female reproduction.

The other class of proteins belonging to UPR that was expressed in POFs was heat shock proteins (HSPs). HSPs belong to the class of multifunctional chaperones that are expressed as a response to stress to protect cells and restore homeostasis (42). HSPs can prevent the incorrect assembly or folding of proteins, reduce apoptosis and increase cell proliferation and survival. We observed that abundances of HSP90, HSP70, and HSP60 were significantly higher in the POFs as compared to the CL, and these proteins existed in many isoforms in POFs. HSPs are known to alleviate the ER stress. In bovine granulosa cells, elevated temperatures induced ER stress, and, as a survival mechanism, an increase in GRP78, HSP70, and HSP90 was observed (43). GRP78 is an important regulator of steroidogenesis; it results in StAR activation at the mitochondria-associated ER membranes (44). The HSP90 also plays a regulatory role in oocyte maturation (45) and reduces stress-induced cell apoptosis by attenuating the caspase pathway (46). Therefore, the higher abundances of HSPs in POFs may be associated with their ability to survive the ER stress and guide the follicle toward ovulation. Interestingly, the expression of HSPs was significantly reduced in the newly formed CL. Heat shock resulting in

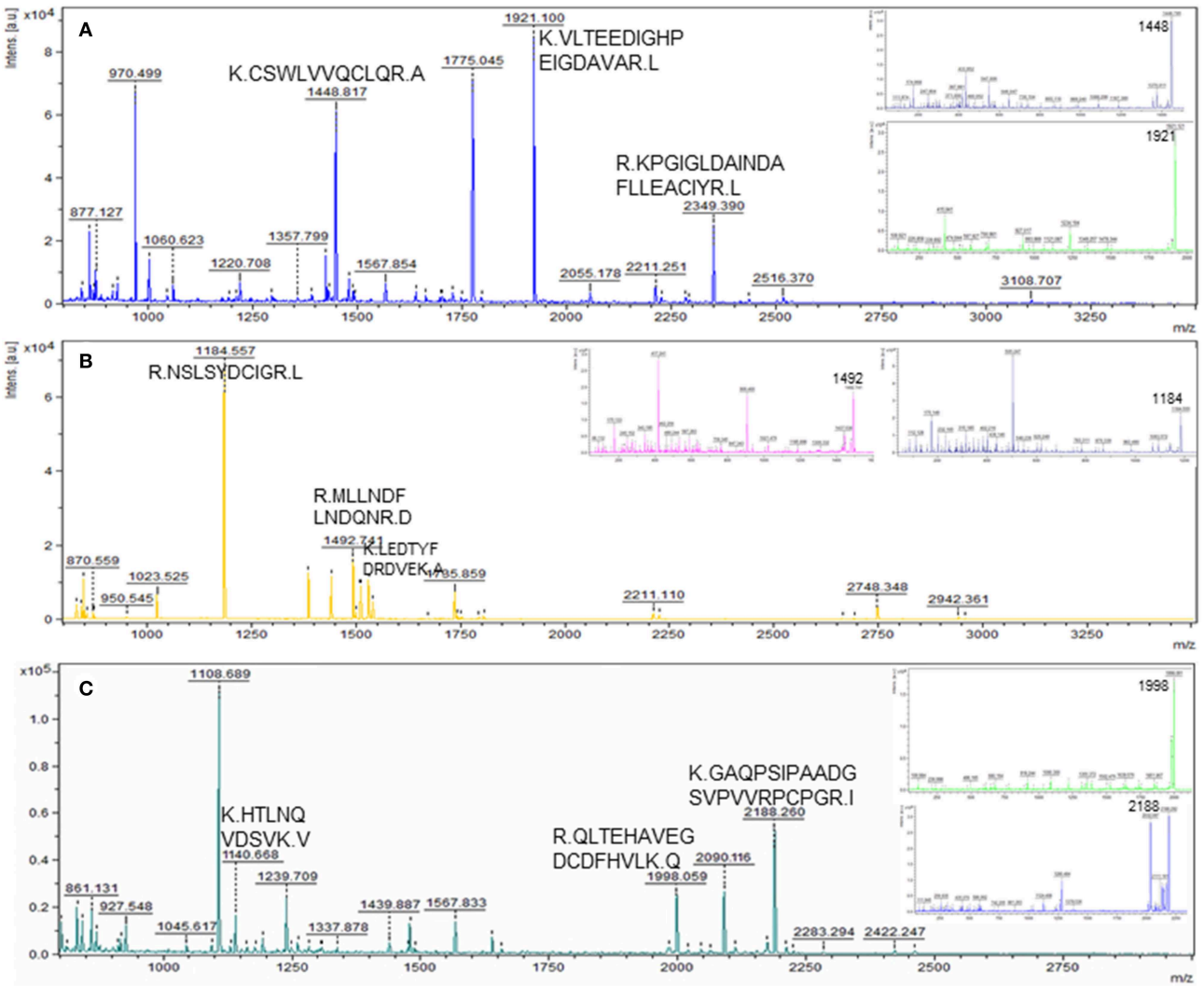

FIGURE 3 | Representative MS and MS/MS (insets) spectra of some of the novel differentially abundant proteins in the CL as compared to POF. Matched peptides with a significant ion score of >30 are shown. **(A)** Peptides KCSWLVVQCLQRA, KVLTEEDIGHPEIGDAVARL, and RKPGIGLDAINDAFLLEACIYRL matched to protein FDPS; **(B)** peptides RNSLSYDCIGRL, RMLLNDFLNDQ NRD, and KLEDTYFDRDVEKA matched to protein HMGCS1; **(C)** peptides KHTLNQVDSV KV, RQLTEHAVEGDCDFHVLKQ, and KGAQPSIPAADGSVPVVRPCPGRI matched to protein AHSG.

elevated expression of HSP70 and HSP90 interferes with the steroid synthesis. It was shown that the expression of HSP70 is related to the downregulation of steroidogenic acute regulatory protein (StAR) and effects steroidogenesis in the rat luteal cells (47). These reports together with the results from present study suggest that whereas, HSPs have a protective role in POFs, there downregulation during luteinization is essential for P4 synthesis.

The LH surge causes differentiation of estrogen-producing follicular cells to the progesterone-producing luteal cells; a change in the abundance of proteins is therefore important for luteal function and survival. The proteins that were highly represented in newly formed CL were associated with biological functions that may be regulated by the LH surge.

Steroid Biosynthesis and Metabolism

In this study, we observed that proteins associated with functional categories such as cholesterol biosynthesis/transport and steroid metabolism were differentially regulated between POFs and the newly formed CL. The cholesterol biosynthesis and metabolism was associated with an increase in the levels of StAR protein, IDI1, AKR1C4, and a decrease in estradiol 17-beta-dehydrogenase 1 (HSD17B1). The other proteins associated with cholesterol biosynthesis in porcine CL were FDPS and GGPS1. The importance of StAR in mediating the steroidogenic response is well documented (7, 48). The new finding of this study related to steroid biosynthesis was the activation of the mevalonate pathway through expression of HMGCS1, FDPS, GGPS1, and IDI1 (**Supplementary Figure 4**). HMGCS1 is a key rate-limiting enzyme in the cholesterol synthesis pathway, and its expression

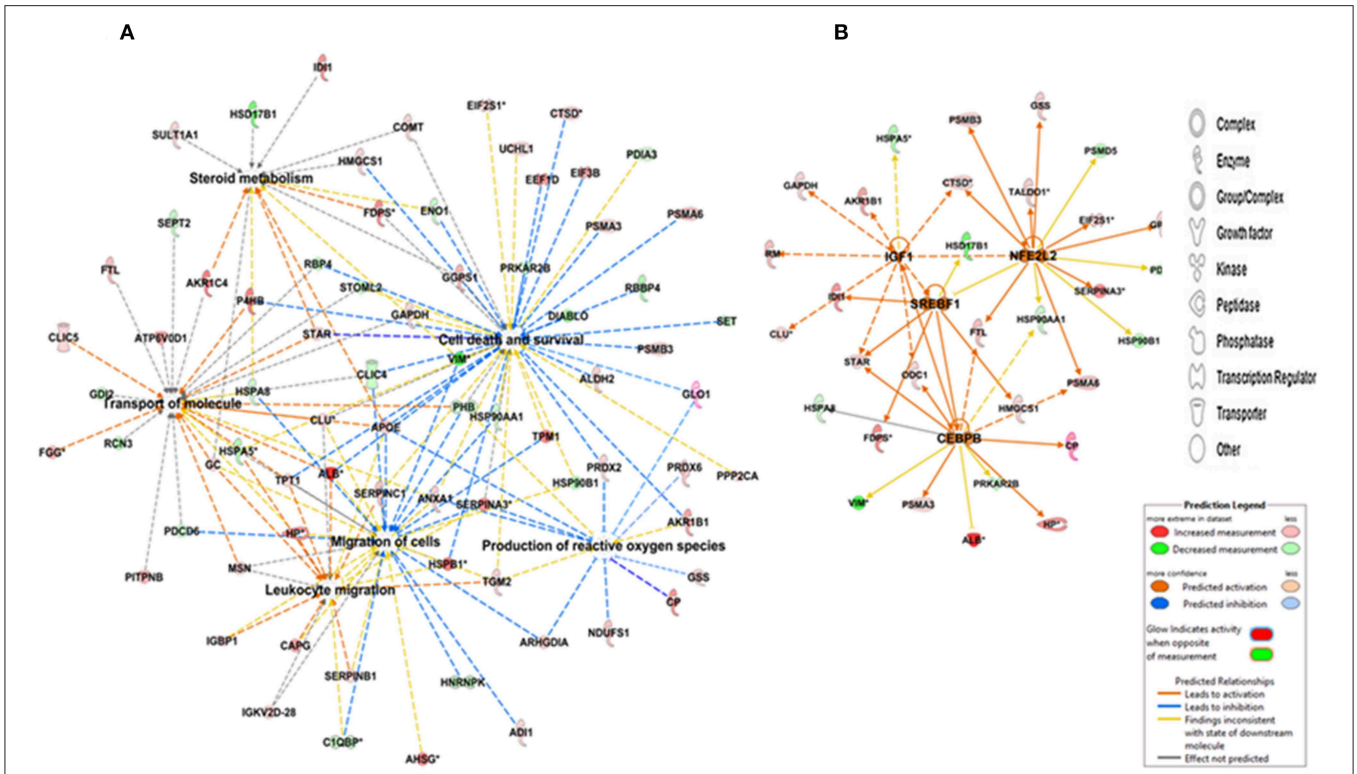

FIGURE 4 | IPA depicting **(A)** networks integrating proteins involved in cell death and survival, cell migration, the scavenging of reactive oxygen species, and lipid metabolism and **(B)** upstream regulators of differentially abundant proteins in the CL. Red and green colors depict an increase or decrease, respectively, in abundance of the proteins in the CL. The color intensity of nodes indicates a fold change increase or decrease associated with a particular protein.

TABLE 2 | IPA analysis overview: canonical pathways and molecular and cellular functions associated with differentially regulated proteins between POFs and the CL.

Top molecular and cellular functions	*P*-value	No. of molecules	Canonical pathways	*P*-value	No. of molecules
Cell death and survival	1.46E-10	45	Acute phase response signaling	8.39E-07	9
Steroid metabolism	6.21E-09	14	Super pathway of geranylgeranyldiphosphate biosynthesis (via mevalonate)	2.19E-06	4
Cellular movement	6.54E-07	39	Superpathway of cholesterol biosynthesis	1.80E-05	4
Molecular transport	7.09E-06	27	RhoA signaling	6.56E-05	6
Free radical scavenging	2.52E-05	13	LXR/RXR signaling	7.19E-05	6

was recently reported in the bovine CL where it was suggested to support the production of high progesterone levels (49). The proteins of this pathway contain sterol response elements and, indeed, transcription factor SREBF1 was identified as an upstream regulator of proteins involved in steroid biosynthesis in our study. In rat ovaries, genes of the mevalonate pathway containing sterol response elements (SRE) were shown to be regulated by LH. It was suggested that LH-induced elevation in steroidogenesis results in decreased levels of cholesterol, which, in turn, activates the transcriptional induction of genes associated with cholesterol biosynthesis (50). IGF-1 regulated many of the proteins associated with steroid biosynthesis. Though the expression and role of IGF-1 has been extensively investigated in follicular growth and development, its role in luteal formation or development has not been investigated at length. However, IGF-I is reported to have steroidogenic actions in early pig corpora lutea (days 4–7 of the estrous cycle), which is lost on later days of the estrous cycle (51). The results of the present study suggest that LH induces cholesterol synthesis through the mevalonate pathway in the porcine CL to support progesterone production by the newly formed CL.

We also observed an increase in proteins involved in the sterol transport that included significantly higher expression of APOE, ALB, PITP, and VDBP (GC) in the CL as compared to POFs. Though the CL can produce cholesterol *de novo* as evidenced by the expression of HMGCS1, other mechanisms

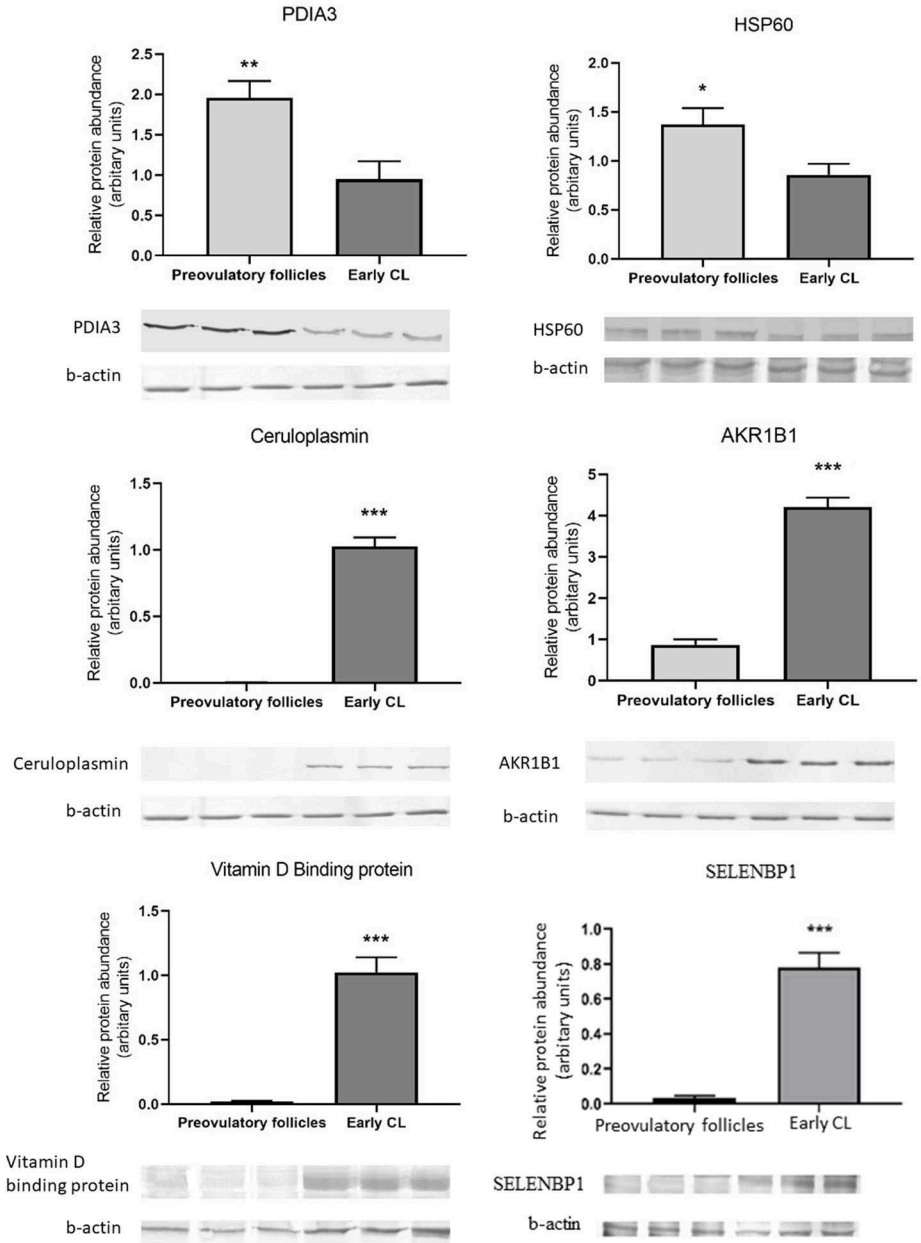

FIGURE 5 | Western blot validation of change in abundances of proteins associated with unfolded protein resonse-PDIA3 and HSP60; oxidative stress response-Ceruloplasmin and AKR1B1; cell proliferation and migration-SELENBP1 and sterol transport-VDBP in newly formed CL as compared to preovulatory follicles. Data are presented as mean ± standard error. $^{*}P \leq 0.05$, $^{**}P \leq 0.01$, $^{***}P \leq 0.001$ by *t*-test.

for obtaining cholesterol are required to meet the need for high progesterone production. This could be achieved by endocytosis of cholesterol-rich low-density lipoproteins (LDL) (52). VDBP belongs to the albumin superfamily, its expression was ∼4.0-fold higher in the CL as compared to POFs, and this study reports its expression for the first time in the CL. IPA analysis grouped it with the proteins associated with cholesterol transport. The known functions of VDBP include its vitamin transport and actin remodeling, however, VDBP has also been shown to bind LDL (53), and we suggest that along with APOE it might transport LDL to the CL for luteal steroidogenesis.

Oxidative Stress Response

The newly formed CL is under oxidative stress due to inflammation-like responses during ovulation after an LH surge and high steroidogenic activity. Inflammation results in the acute phase response (APR), and this was one of the most significant pathways associated with CL formation. We identified APR protein fetuin (AHSG), APR proteins with

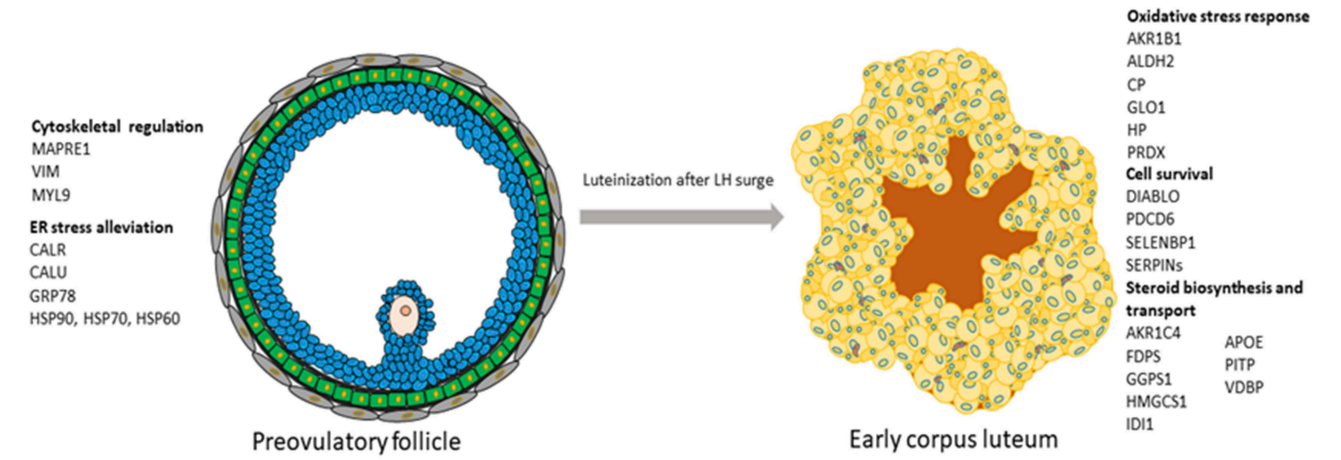

FIGURE 6 | Schematic representation of the processes and their associated proteins that were highly represented either in preovulatory follicles or in early corpus luteum.

antioxidant functions, ceruloplasmin (CP), and haptoglobin (HP) proteoforms in the CL. The role of these proteins in the CL is not known, but AHSG was recently suggested to be a marker of luteinization (54). Oxidative stress is detrimental to the cells; it induces apoptosis, interferes with cholesterol transport, and is associated with luteal regression (55). We observed that proteins involved in the metabolism and scavenging of reactive oxygen species were upregulated in the CL as compared to POFs. The role of antioxidants in the control of CL function has been shown in many studies [reviewed in (55)]. Many of the antioxidant enzymes PRDX6, GSS, GPX3, and GLRX identified here play major roles in removing reactive oxygen species and were identified previously in porcine luteinized follicles (19). The other proteins belonging to anti-oxidative stress response included AKR1B1, ALDH2, CP, and GLO1. Aldo-keto reductases (AKR1B1) and GLO1 are induced in response to oxidative stress and detoxify carbonyl compounds resulting from lipid oxidation (56, 57). The detoxification of carbonyls might result from the binding between glutathione and aldo-keto reductases, resulting in alleviation of oxidative stress in female ovary (56). GLO1 is expressed ubiquitously in cells, and, recently, it has been reported to be expressed in mouse ovary and oocytes where it was shown to abrogate the glycative stress response through components of the SIRT1 functional network (58). Transcription factor NFE2L2 (Nrf2) was detected as the upstream regulator of many of the proteins involved in alleviating oxidative stress response. Nrf2 is an important cytoprotective factor that regulates critical antioxidant and stress-responsive genes. It was shown to be upregulated as a survival mechanism in bovine granulosa cells subjected to oxidative stress (59). Its role in the porcine luteal function is worth further investigation. These findings suggest that in the newly formed CL, besides the expression of well-known components of the antioxidation system, other antioxidants are also expressed to support survival of luteal cells and support P4 production.

Cell Migration and Cell Survival

The other functional categories that were overrepresented in the CL were cell migration and cell survival. The luteinization and ovulation leading to the CL formation is associated with tissue remodeling, differentiation of follicular cells into large and small luteal cells, endothelial cell migration, and an intermixing of these cell types. These processes include modification of the extracellular matrix (ECM) and actin cytoskeleton. ECM remodeling is a interplay between proteinases and protease inhibitors. The expression of serine protease, plasminogen activator (PA), and the protease inhibitor system has been defined in pigs (60). Though uPA and the members of MMP and TIMP family are associated with the remodeling and angiogenesis of the CL in mice, the knock out of uPA did not result in significant changes in ovulation or CL function. It was suggested that other elements might be involved in remodeling during CL formation (7, 61). We observed that functional category cell migration was mainly associated with proteases CTSD and CTSH and protease inhibitors SERPINA3-6 and SERPINA3-8, which were more abundant in the CL. Some of the isoforms of SERPINs were detected only in the CL. Cystein cathepsins and serine proteases are known to degrade extarcellular cellular matrix facilitating ovulation, cell migration, and angiogenesis during CL formation (7, 62). The newly formed CL undergoes extensive tissue growth and vascularization and a balance between proteases and protease inhibitors is important to regulate the proteolysis that could otherwise damage tissue growth and it vascularization. A CL-specific expression of SELENBP1 was observed in this study. The functions of SELENBP1 are largely unknown; however, it is widely investigated in tumor tissues where it is expressed at lower levels, including in ovarian cancer models (63). It is reported to play a role in tumor suppression by controlling cellular proliferation and migration (64). CL formation also involves the fine-tuning of cell proliferation and cell survival after ovulation. It was observed that, whereas proteins promoting cell death, such as PDCD6 and DIABLO, were downregulated,

proteins promoting luteal survival shown to be associated with proteasome subunits were upregulated in the CL. Proteasomes have complex functions, the proteasome-ubiquitin system is also a regulator of proteolytic enzymes, such as MMPs. The inhibitors of proteasomes result in apoptosis in proliferating cells and, on the other hand, in dying cells the same inhibitors can block apoptosis (65). This observation explains their role in both CL development and CL regression.

In conclusion, a number of proteins characterizing POFs were identified. It can be suggested that, in POFs, cytoskeletal proteins, such as vimentin and MAPRE1, are not only associated with changing the shape of follicular cells but also with steroidogenesis. A number of proteins and biological pathways associated with the differentiation of POFs to CL were identified. Some of the proteins that might be regulated by LH and associated with steroidogenesis in the newly formed porcine CL, such as IDI1, FDPS, and HMGCS1, and cell survival, such as the eukaryotic translation factor, PDCD6, DIABLO, and the proteasome ubiquitin system, are reported in this study, thereby providing novel insights into peri-ovulatory regulation of proteins that might play a role in luteinization processes and luteal survival (**Figure 6**). As in bovines (54), the induction of AHSG with the formation of CL observed here can be suggested to be marker of luteinization.

DATA AVAILABILITY STATEMENT

All datasets generated for this study are included in the article/**Supplementary Material**.

ETHICS STATEMENT

All procedures involving the use of animals were approved by the Animal Ethics Committee, University of Warmia and Mazury in Olsztyn, Poland, and were conducted in accordance with the national guidelines for agricultural animal care.

AUTHOR CONTRIBUTIONS

BM designed the experiments. PL and BM performed the experiments. BM, PL, and DS analyzed the results. BM and DS wrote the manuscript. All authors reviewed the manuscript.

FUNDING

This work was supported by a grant from the National Science Center in Poland (DEC- 011/01/B/NZ4/03542) and by statutory funds received by PL from Institute of Animal Reproduction and Food Research, PAS, Olsztyn.

ACKNOWLEDGMENTS

The authors are grateful to Mr. Michal Blitek and W. Krzywiec for sample collection and characterization.

SUPPLEMENTARY MATERIAL

The Supplementary Material for this article can be found online at: https://www.frontiersin.org/articles/10.3389/fendo.2019.00774/full#supplementary-material

REFERENCES

1. Richards JS, Russell DL, Ochsner S, Hsieh M, Doyle KH, Falender AE, et al. Novel signaling pathways that control ovarian follicular development, ovulation, and luteinization. *Recent Prog Horm Res*. (2002) 57:195–220. doi: 10.1210/rp.57.1.195
2. Evans AC. Characteristics of ovarian follicle development in domestic animals. *Reprod Domest Anim*. (2003) 38:240–6. doi: 10.1046/j.1439-0531.2003.00439.x
3. Wu J, Xu B, Wang W. Effects of luteinizing hormone and follicle stimulating hormone on the developmental competence of porcine preantral follicle oocytes grown *in vitro*. *J Assist Reprod Genet*. (2007) 24:419–24. doi: 10.1007/s10815-007-9154-5
4. Lucy MC. Regulation of ovarian follicular growth by somatotropin and insulin-like growth factors in cattle. *J Dairy Sci*. (2000) 83:1635–47. doi: 10.3168/jds.S0022-0302(00)75032-6
5. Hunter MG, Robinson RS, Mann GE, Webb R. Endocrine and paracrine control of follicular development and ovulation rate in farm species. *Anim Reprod Sci*. (2004) 82–3:461–77. doi: 10.1016/j.anireprosci.2004.05.013
6. Palma GA, Argañaraz ME, Barrera AD, Rodler D, Mutto AÁ, Sinowatz F. Biology and biotechnology of follicle development. *Sci World J*. (2012) 2012:938138. doi: 10.1100/2012/938138
7. Stocco C, Telleria C, Gibori G. The molecular control of corpus luteum formation, function, and regression. *Endocr Rev*. (2007) 28:117–49. doi: 10.1210/er.2006-0022
8. Curry TE Jr, Song L, Wheeler SE. Cellular localization of gelatinases and tissue inhibitors of metalloproteinases during follicular growth, ovulation, and early luteal formation in the rat. *Biol Reprod*. (2001) 65:855–65. doi: 10.1095/biolreprod65.3.855
9. Kimura A, Kihara T, Ohkura R, Ogiwara K, Takahashi T. Localization of bradykinin B2 receptor in the follicles of porcine ovary and increased expression of matrix metalloproteinase-3 and−20 in cultured granulosa cells by bradykinin treatment. *Biol Reprod*. (2001) 65:1462–70. doi: 10.1095/biolreprod65.5.1462
10. Fraser HM, Bell J, Wilson H, Taylor PD, Morgan K, Anderson RA, et al. Localization and quantification of cyclic changes in the expression of endocrine gland vascular endothelial growth factor in the human corpus luteum. *J Clin Endocrinol Metab*. (2005) 90:427–34. doi: 10.1210/jc.2004-0843
11. Martelli A, Palmerini MG, Russo V, Rinaldi C, Bernabò N, Di Giacinto O, et al. Blood vessel remodeling in pig ovarian follicles during the periovulatory period: an immunohistochemistry and SEM-corrosion casting study. *Reprod Biol Endocrinol*. (2009) 7:72. doi: 10.1186/1477-7827-7-72
12. Lim H, Paria BC, Das SK, Dinchuk JE, Langenbach R, Trzaskos JM, et al. Multiple female reproductive failures in cyclooxygenase 2-deficient mice. *Cell*. (1997) 91:197–208. doi: 10.1016/S0092-8674(00)80402-X
13. Natraj U, Richards JS. Hormonal regulation, localization, and functional activity of the progesterone receptor in granulosa cells of rat preovulatory follicles. *Endocrinology*. (1993) 133:761–9. doi: 10.1210/endo.133.2.8344215
14. Sterneck E, Tessarollo L, Johnson PF. An essential role for C/EBP in female reproduction. *Genes Dev*. (1997) 11:2153–62. doi: 10.1101/gad.11.17.2153
15. Espey LL, Ujioka T, Russell DL, Skelsey M, Vladu B, Robker RL, et al. Induction of early growth response protein-1 gene expression in the rat ovary in response to an ovulatory dose of human chorionic gonadotropin. *Endocrinology*. (2000) 141:2385–91. doi: 10.1210/endo.141.7.7582

16. Leo CP, Pisarska MD, Hsueh AJ. DNA array analysis of changes in preovulatory gene expression in the rat ovary. *Biol Reprod*. (2001) 65:269–76. doi: 10.1095/biolreprod65.1.269
17. McRae RS, Johnston HM, Mihm M, O'Shaughnessy PJ. Changes in mouse granulosa cell gene expression during early luteinization. *Endocrinology*. (2005) 146:309–17. doi: 10.1210/en.2004-0999
18. Ndiaye K, Fayad T, Silversides DW, Sirois J, Lussier JG. Identification of downregulated messenger RNAs in bovine granulosa cells of dominant follicles following stimulation with human chorionic gonadotropin. *Biol Reprod*. (2005) 73:324–33. doi: 10.1095/biolreprod.104.038026
19. Agca C, Ries JE, Kolath SJ, Kim JH, Forrester LJ, Antoniou E, et al. Luteinization of porcine preovulatory follicles leads to systematic changes in follicular gene expression. *Reproduction*. (2006) 132:133–45. doi: 10.1530/rep.1.01163
20. Foxcroft GR, Hunter MG. Basic physiology of follicular maturation in the pig. *J Reprod Fertil Suppl*. (1985) 33:1–19.
21. Caetano AR, Johnson RK, Ford JJ, Pomp D. Microarray profiling for differential gene expression in ovaries and ovarian follicles of pigs selected for increased ovulation rate. *Genetics*. (2004) 168:1529–37. doi: 10.1534/genetics.104.029595
22. Gladney CD, Bertani GR, Johnson RK, Pomp D. Evaluation of gene expression in pigs selected for enhanced reproduction using differential display PCR and human microarrays: I. Ovarian follicles. *J Anim Sci*. (2004) 82:17–31. doi: 10.2527/2004.82117x
23. Bonnet A, Lê Cao KA, Sancristobal M, Benne F, Robert-Granié C, Law-So G, et al. *In vivo* gene expression in granulosa cells during pig terminal follicular development. *Reproduction*. (2008) 136:211–24. doi: 10.1530/REP-07-0312
24. Sriperumbudur R, Zorrilla L, Gadsby JE. Transforming growth factor-beta (TGFbeta) and its signaling components in peri-ovulatory pig follicles. *Anim Reprod Sci*. (2010) 120:84–94. doi: 10.1016/j.anireprosci.2010.03.003
25. Ziecik AJ, Przygrodzka E, Jalali BM, Kaczmarek MM. Regulation of the porcine corpus luteum during pregnancy. *Reproduction*. (2018) 156:R57–67. doi: 10.1530/REP-17-0662
26. Murphy BD, Gevry N, Ruiz-Cortes T, Cote F, Downey BR, Sirois J. Formation and early development of the corpus luteum in pigs. *Reprod Suppl*. (2001) 58:47–63.
27. Smith MF, McIntush EW, Smith GW. Mechanisms associated with corpus luteum development. *J Anim Sci*. (1994) 72:1857–72. doi: 10.2527/1994.7271857x
28. Hammernik DL. Farm animals are important biomedical models. *Anim Front*. (2019) 9:3–5. doi: 10.1093/af/vfz026
29. Leiser R, Zimmermann W, Sidler X, Christen A. Normal cyclical morphology of the endometrium and ovary of swine. *Tierarztl Prax*. (1988) 16:261–80.
30. Karlsson AB, Maizels ET, Flynn MP, Jones JC, Shelden EA, Bamburg JR. Luteinizing hormone receptor-stimulated progesterone production by preovulatory granulosa cells requires protein kinase A-dependent activation/dephosphorylation of the actin dynamizing protein cofilin. *Mol Endocrinol*. (2010) 24:1765–81. doi: 10.1210/me.2009-0487
31. Flynn MP, Fiedler SE, Karlsson AB, Carr DW, Maizels ET, Hunzicker-Dunnm M. Dephosphorylation of MAP2D enhances its binding to vimentin in preovulatory ovarian granulosa cells. *J Cell Sci*. (2016) 129:2983–96. doi: 10.1242/jcs.190397
32. Aharoni D, Dantes A, Amsterdam A. Cross-talk between adenylate cyclase activation and tyrosine phosphorylation leads to modulation of the actin cytoskeleton and to acute progesterone secretion in ovarian granulosa cells. *Endocrinology*. (1993) 133:1426–36. doi: 10.1210/en.133.3.1426
33. Wu. C., Keivenst VM, O'Toole TE, McDonald JA, Ginsberg MH. Integrin activation and cytoskeletal interaction are essential for the assembly of a fibronectin matrix. *Cell*. (1995) 83:715–24. doi: 10.1016/0092-8674(95)90184-1
34. Salvador LM, Flynn MP, Avila J, Reierstad S, Maizels ET, Alam H, et al. Neuronal microtubule-associated protein 2D is a dual a-kinase anchoring protein expressed in rat ovarian granulosa cells. *J Biol Chem*. (2004) 279:27621–32. doi: 10.1074/jbc.M402980200
35. Day F, Karaderi T, Jones MR, Meun C, He C, Drong A, et al. Large-scale genome-wide meta-analysis of polycystic ovary syndrome suggests shared genetic architecture for different diagnosis criteria. *PLoS Genet*. (2018) 19:e1007813.
36. Monniaux D, Michel P, Postel M, Clement F. Multiscale modeling of ovarian follicular development: From follicular morphogenesis to selection for ovulation. *Biol Cell*. (2016) 108:149. doi: 10.1111/boc.201500087
37. Harada M, Nose E, Takahashi N, Hirota Y, Hirata T, Yoshino O, et al. Evidence of the activation of unfolded protein response in granulosa and cumulus cells during follicular growth and maturation. *Gynecol Endocrinol*. (2015) 31:783–7. doi: 10.3109/09513590.2015.1062862
38. Park HJ, Park SJ, Koo DB, Lee SR, Kong IK, Ryoo JW, et al. Progesterone production is affected by unfolded protein response (UPR) signaling during the luteal phase in mice. *Life Sci*. (2014) 113:60–7. doi: 10.1016/j.lfs.2014.07.033
39. Lee AS. The ER chaperone and signaling regulator GRP78/BiP as a monitor of endoplasmic reticulum stress. *Methods*. (2005) 35:373–81. doi: 10.1016/j.ymeth.2004.10.010
40. Lee JH, Kwon EJ, Kim do H. Calumenin has a role in the alleviation of ER stress in neonatal rat cardiomyocytes. *Biochem Biophys Res Commun*. (2013) 439:327–32. doi: 10.1016/j.bbrc.2013.08.087
41. Tokuhiro K, Satouh Y, Nozawa K, Isotani A, Fujihara Y, Hirashima Y, et al. Calreticulin is required for development of the cumulus oocyte complex and female fertility. *Sci Rep*. (2015) 5:14254. doi: 10.1038/srep14254
42. Vincenz L, Jager R, O'Dwyer M, Samali A. Endoplasmic reticulum stress and the unfolded protein response: targeting the achilles heel of multiple myeloma. *Mol Cancer Ther*. (2013) 12:831–43. doi: 10.1158/1535-7163.MCT-12-0782
43. Alemu TW, Pandey HO, Wondim DS, Gebremedhn S, Neuhof C, Tholen E, et al. Oxidative and endoplasmic reticulum stress defense mechanisms of bovine granulosa cells exposed to heat stress. *Theriogenology*. (2018) 110:130–41. doi: 10.1016/j.theriogenology.2017.12.042
44. Prasad M, Pawlak KJ, Burak WE, Perry EE, Marshall B, Whittal RM, et al. Mitochondrial metabolic regulation by GRP78. *Sci Adv*. (2017) 3:e1602038. doi: 10.1126/sciadv.1602038
45. Metchat A, Akerfelt M, Bierkamp C, Delsinne V, Sistonen L, Alexandre H. Mammalian heat shock factor 1 is essential for oocyte meiosis and directly regulates Hsp90α expression. *J Biol Chem*. (2009) 284:9521–8. doi: 10.1074/jbc.M808819200
46. Lee MW, Park SC, Chae HS, Bach JH, Lee HJ, Lee SH. The protective role of HSP90 against 3-hydroxykynurenine-induced neuronal apoptosis. *Biochem Biophys Res Commun*. (2001) 284:261–7. doi: 10.1006/bbrc.2001.4938
47. Murphy BD, Lalli E, Walsh LP, Liu Z, Soh J, Stocco DM, et al. Heat shock interferes with steroidogenesis by reducing transcription of the steroidogenic acute regulatory protein gene. *Mol Endocrinol*. (2001) 15:1255–63. doi: 10.1210/mend.15.8.0676
48. Niswender GD, Juengel JL, Silva PJ, Rollyson MK, McIntush EW. Mechanisms controlling the function and life span of the corpus luteum. *Physiol Rev*. (2000) 80:1–29. doi: 10.1152/physrev.2000.80.1.1
49. Kfir S, Basavaraja R, Wigoda N, Ben-Dor S, Orr O, Meidan R. Genomic profiling of bovine corpus luteum maturation. *PLoS ONE*. (2018) 13:e0194456. doi: 10.1371/journal.pone.0194456
50. Menon KM, Nair AK, Wang L, Peegel H. Regulation of luteinizing hormone receptor mRNA expression by a specific RNA binding protein in the ovary. *Mol Cell Endocrinol*. (2007) 260–2:109–16. doi: 10.1016/j.mce.2006.03.046
51. Miller EA, Ge Z, Hedgpeth V, Gadsby. JE. Steroidogenic responses of pig corpora lutea to insulin-like growth factor I (IGF-I) throughout the oestrous cycle. *Reproduction*. (2003) 125:241–9. doi: 10.1530/reprod/125.2.241
52. Christenson LK, Devoto L. Cholesterol transport and steroidogenesis by the corpus luteum. *Reprod Biol Endocrinol*. (2003) 1:90. doi: 10.1186/1477-7827-1-90
53. Speeckaert MM, Taes YE, De Buyzere ML, Christophe AB, Kaufman JM, Delanghe JR. Investigation of the potential association of vitamin D binding protein with lipoproteins. *Ann Clin Biochem*. (2010) 47:143–50. doi: 10.1258/acb.2009.009018
54. Baufeld A, Koczan D, Vanselow J. Induction of altered gene expression profiles in cultured bovine granulosa cells at high cell density. *Reprod Biol Endocrinol*. (2017) 15:3–17. doi: 10.1186/s12958-016-0221-6
55. Al-Gubory KH, Garrel C, Faure P., Sugino N. Roles of antioxidant enzymes in corpus luteum rescue from reactive oxygen species-induced oxidative stress. *Reprod BioMed Online*. (2012) 25:551–60. doi: 10.1016/j.rbmo.2012.08.004
56. Fujii J, Iuchi Y, Okada F. Fundamental roles of reactive oxygen species and protective mechanisms in the female reproductive

system. *Reprod Biol Endocrionl*. (2005) 3:43. doi: 10.1186/1477-7827-3-43
57. Brouwers O, Niessen PM, Ferreira I, Miyata T, Scheffer PG, Teerlink T, et al. Overexpression of glyoxalase-I reduces hyperglycemia-induced levels of advanced glycation end products and oxidative stress in diabetic rats. *J Biol Chem*. (2011) 286:1374–80. doi: 10.1074/jbc.M110.144097
58. Emidio GD, Santinia SJ, D'Alessandroa AM, Vetuschic A, Sferra R, Artini PG, Cet al. SIRT1 participates in the response to methylglyoxal-dependent glycative stress in mouse oocytes and ovary. *Biochim Biophys Acta Mol Basis Dis*. (2019) 1865:1389–401. doi: 10.1016/j.bbadis.2019.02.011
59. Khadrawy O, Gebremedhn S, Salilew-Wondim D, Taqi MO, Neuhoff C, Tholen E, et al. Endogenous and exogenous modulation of Nrf2 mediated oxidative stress response in bovine granulosa cells: potential implication for ovarian function. *Int J Mol Sci*. (2019) 20:1635. doi: 10.3390/ijms20071635
60. Politis I, Srikandakumar A, Turner JD, Tsang BK, Ainsworth L, Downey BR. Changes in and partial identification of the plasminogen activator and plasminogen activator inhibitor systems during ovarian follicular maturation in the pig. *Biol Reprod*. (1990) 43:636–42. doi: 10.1095/biolreprod43.4.636
61. Liu K, Wahlberg P, Hagglund AC, Ny T. Expression pattern and functional studies of matrix degrading proteases and their inhibitors in the mouse corpus luteum. *Mol Cell Endocrinol*. (2003) 205:131–40. doi: 10.1016/S0303-7207(03)00147-3
62. Robker RL, Russell DL, Espey LL, Lydon JP, O'Malley BW, Richards JS. Progesterone regulated genes in the ovulation process: ADAMTS-1 and cathepsin L proteases. *Proc Natl Acad Sci USA*. (2000) 97:4689–94. doi: 10.1073/pnas.080073497
63. Huang KC, Park DC, Ng SK, Lee JY, Ni X, Ng WC, et al. Selenium binding protein 1 in ovarian cancer. *Int J Cancer*. (2006) 118:2433–40. doi: 10.1002/ijc.21671
64. Zhang C, Xu W, Pan W, Wang N, Li G, Fan X, et al. Selenium-binding protein 1 may decrease gastric cellular proliferation and migration. *Int J Oncol*. (2013) 42:1620–9. doi: 10.3892/ijo.2013.1850
65. Drexler HC. Programmed cell death and the proteasome. *Apoptosis*. (1998) 3:1–7. doi: 10.1023/A:1009604900979

Conflict of Interest: The authors declare that the research was conducted in the absence of any commercial or financial relationships that could be construed as a potential conflict of interest.

frontiers in Endocrinology

REVIEW
published: 19 November 2019
doi: 10.3389/fendo.2019.00748

Possible Mechanisms for Maintenance and Regression of Corpus Luteum Through the Ubiquitin-Proteasome and Autophagy System Regulated by Transcriptional Factors

*Aamir S. Teeli[1], Paweł Leszczyński[1], Narayanan Krishnaswamy[2], Hidesato Ogawa[3], Megumi Tsuchiya[3], Magdalena Śmiech[1], Dariusz Skarzynski[4] and Hiroaki Taniguchi[1]**

[1] Department of Experimental Embryology, The Institute of Genetics and Animal Breeding, Polish Academy of Sciences, Jastrzebiec, Poland, [2] Indian Veterinary Research Institute, Hebbal Campus, Bengaluru, India, [3] Graduate School of Frontier Biosciences, Osaka University, Suita, Japan, [4] Department of Reproductive Immunology and Pathology, Institute of Animal Reproduction and Food Research, Polish Academy of Sciences, Olsztyn, Poland

OPEN ACCESS

Edited by:
Jens Vanselow,
Leibniz Institute for Farm Animal Biology, Germany

Reviewed by:
Andrea S. Cupp,
University of Nebraska-Lincoln, United States
Katarina Jewgenow,
Leibniz Institute for Zoo and Wildlife Research (LG), Germany

***Correspondence:**
Hiroaki Taniguchi
h.taniguchi@ighz.pl

Specialty section:
This article was submitted to Reproduction, a section of the journal Frontiers in Endocrinology

Received: 29 April 2019
Accepted: 16 October 2019
Published: 19 November 2019

Citation:
Teeli AS, Leszczyński P, Krishnaswamy N, Ogawa H, Tsuchiya M, Śmiech M, Skarzynski D and Taniguchi H (2019) Possible Mechanisms for Maintenance and Regression of Corpus Luteum Through the Ubiquitin-Proteasome and Autophagy System Regulated by Transcriptional Factors. Front. Endocrinol. 10:748. doi: 10.3389/fendo.2019.00748

The corpus luteum (CL) is an important tissue of the female reproductive process which is established through ovulation of the mature follicle. Pulsatile release of prostaglandin $F_{2\alpha}$ from the uterus leads to the regression of luteal cells and restarts the estrous cycle in most non-primate species. The rapid functional regression of the CL, which coincides with decrease of progesterone production, is followed by its structural regression. Although we now have a better understanding of how the CL is triggered to undergo programmed cell death, the precise mechanisms governing CL protein degradation in a very short period of luteolysis remains unknown. In this context, activation of ubiquitin-proteasome pathway (UPP), unfolded protein response (UPR) and autophagy are potential subcellular mechanisms involved. The ubiquitin-proteasome pathway (UPP) maintains tissue homeostasis in the face of both internal and external stressors. The UPP also controls physiological processes in many gonadal cells. Emerging evidence suggests that UPP dysfunction is involved in male and female reproductive tract dysfunction. Autophagy is activated when cells are exposed to different types of stressors such as hypoxia, starvation, and oxidative stress. While emerging evidence points to an important role for the UPP and autophagy in the CL, the key underlying transcriptional mechanisms have not been well-documented. In this review, we propose how CL regression may be governed by the ubiquitin-proteasome and autophagy pathways. We will further consider potential transcription factors which may regulate these events in the CL.

Keywords: ubiquitin-proteasome, autophagy, steroidogenesis, corpus luteum, transcription factors

INTRODUCTION

Corpus luteum (CL) formation, an integral part of the female reproductive process, is accomplished through ovulation of the mature follicle. The CL is a transient organ composed of various cells types. These include endothelial cells, immune cells, and luteal cells, which differentiate from follicular cells (granulosa and thecal cells) following ovulation. The CL development is classified as early, mid, late and regression stages in terms of its growth rate, neovascularisation, and rate of progesterone (P_4) production. In the absence of pregnancy, luteolysis occurs with a decrease in P_4 synthesis and secretion. Conversely, P_4 produced by the CL maintains pregnancy in several species. To produce P_4 in the CL, free cholesterol is transferred to the inner mitochondrial membrane by carrier proteins including steroidogenic acute regulatory protein (STAR). This process involving the P450 cholesterol side-chain cleavage enzyme (p450scc/CYP11A1) converts cholesterol to pregnenolone, the C-21 steroid precursor (1). STAR is a protein that governs the rate-limiting step of gonadal steroidogenesis.

In a non-fertile estrous or menstrual cycle, the CL undergoes luteolysis. In ruminants, pulsatile release of prostaglandin $F_{2\alpha}$ ($PGF_{2\alpha}$) by the uterus leads to regression of luteal cells and renewal of the estrous cycle. The rapid functional regression of the CL, which is characterized by decreased P_4 production, is followed by structural regression. During the structural regression, luteal cells undergo apoptosis (2–5). Failure of this mechanism is associated with dysfunction of the reproductive cycle and infertility. While we understand the process by which the CL undergoes programmed cell death, the mechanisms governing the degradation of a large quantity of CL proteins over a very short period of time is yet to be elucidated.

The ubiquitin-proteasome pathway (UPP) plays an important role in the degradation of unnecessary proteins. During this process, target proteins are first bound to small ubiquitin proteins and degraded. The UPP is a regulatory mechanism that maintains tissue homeostasis in response to various stressors including oxidative stress. This pathway acts through the endoplasmic reticulum (ER) (6). The UPP governs physiological processes in a variety of gonadal cells (7, 8). Emerging evidence suggests that UPP dysfunction leads to pathology within reproductive system (9). Additionally, the unfolded protein response (UPR) signaling pathway, a cellular stress response associated with the ER, is involved in the development, maintenance, and regression of the bovine CL (10). Female mice lacking Beclin1 (*Becn1*), a regulator of autophagy and the UPR system, display a preterm labor phenotype associated with P_4 production dysfunction in ovarian granulosa cells (GCs) (11). Interestingly, GRP78, an ER chaperone protein essential for UPR, plays an integral role in the initiation of steroidogenesis through STAR activation at the mitochondrial membrane (12). Moreover, increased oxidative stress in the ER reduces testosterone production in Leydig cells (13). As such, the UPP and UPR are crucial to degrade unnecessary proteins and maintain cellular homeostasis. Unfortunately, the molecular mechanisms governing UPR function in the CL remain poorly understood.

Similar to the UPP system, autophagy degrades unnecessary proteins through the autophagosome. This process is involved in the metabolism of cellular components associated with the UPP under normal and pathologic conditions. The UPP and autophagy systems are closely related mechanisms that remove unnecessary cellar components. They act cooperatively to maintain cellular homeostasis (14). ER stress is an important trigger of the UPP and autophagy. Recent studies have demonstrated that ER stress and autophagy play important roles in structural regression of CL (15, 16). Together, these results suggest that ER stress-mediated autophagy may play an important role in luteolysis.

In view of these findings, we hypothesize that the UPP and autophagy may play important roles in the functional regulation of the CL and luteolysis. In this review, we will explore the molecular mechanisms governing luteal function and regression as well as its interplay with the proteasome-autophagy system.

FUNCTIONAL LUTEAL REGRESSION AND TRANSCRIPTION FACTORS CONTROLLING CL FUNCTION

Progesterone, the major hormone of CL is elaborated by small and large luteal cells, that are derived from the follicular theca interna and granulosa cells, respectively. The non-steroidogenic component of CL comprises of endothelial cells, pericytes, fibroblasts and immune cells. Small luteal cells are stimulated by luteinizing hormone (LH) which is secreted by the pituitary gland. P_4 secreted by large luteal cells represents the basal P_4 level. The P_4 level derived from small luteal cells is known as LH-induced P_4. The LH receptor is a G protein-coupled receptor with seven membrane spanning domains (17). Once LH binds to its receptor, the second messenger cyclic AMP is released and protein kinase A (PKA) is subsequently activated. PKA phosphorylates various proteins and in turn modulates their function (18). Thereafter, transcription factors induce the expression of steroidogenic enzymes including *STAR*, *Cyp11a*, and 3β-hydroxysteroid dehydrogenase (3β-HSD). STAR plays a role in transporting cholesterol to the mitochondria. P450scc converts cholesterol into pregnenolone in the mitochondria. Pregnenolone is finally converted to P_4 by 3β-HSD in the luteal cells [(19), **Figure 1**].

The regulation of steroidogenesis in the CL involves the temporal expression of genes coding for a variety of steroidogenic enzymes. As the rapid upregulation of steroidogenic enzyme gene expression is required, it is likely that the acute regulation of steroidogenesis in the CL is regulated by transcription factors (**Figure 1**) and change in the expression and activity of these transcription factors trigger functional CL regression. In this regard, NR5A1 (Nuclear Receptor Subfamily 5 Group A Member 1, also known also as adrenal 4 binding protein/steroidogenic factor 1: Ad4BP/SF-1), a regulator of multiple P450 hydroxylases and other components of the steroidogenic program, was first isolated from the adrenal gland (20, 21). Since then, several researchers have identified other transcription factors that regulate the promoter activity of *Star*, *CYP11A1*, *HSD3B2*, and

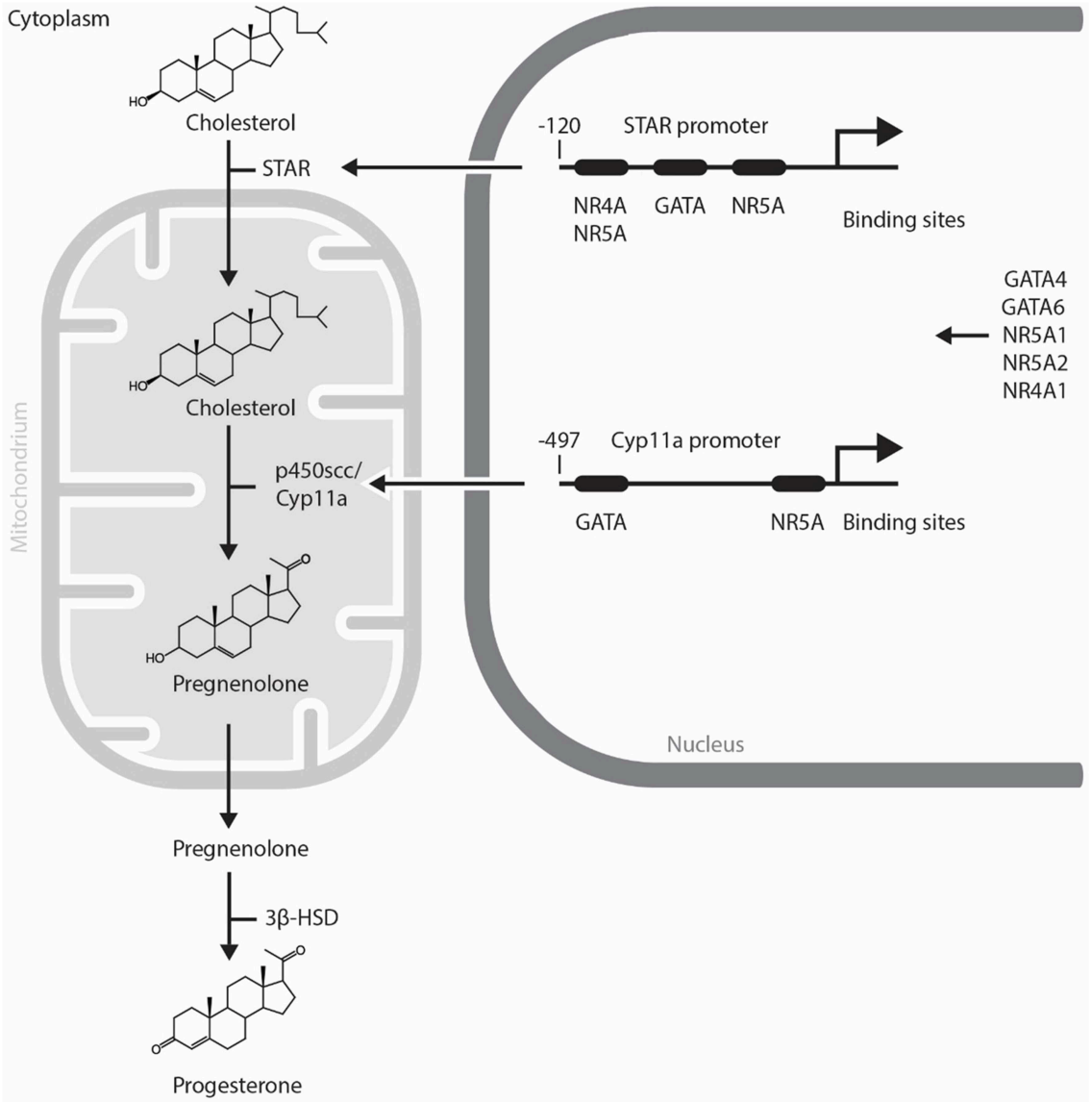

FIGURE 1 | Mechanism of progesterone synthesis and its molecular regulation by GATA and NR5A transcription factors in steroidogenic cells. STAR plays a role in transporting cholesterol to the mitochondria. p450scc converts cholesterol into pregnenolone in the mitochondria. Pregnenolone is finally converted to progesterone by 3β-HSD in steroidogenic cells. STAR and Cyp11a promoters contain evolutionally conserved GATA and NR5A/4A binding sites. GATA, NR4A1, and NR5A transcription factors control the expression of steroidogenic enzymes including STAR, p450scc/Cyp11a. NR5A1, Nuclear Receptor Subfamily 5 Group A Member 1; NR5A2, Nuclear Receptor Subfamily 5 Group A Member 2; NR4A1, Nuclear Receptor Subfamily 4 Group A Member 1; p450scc, cytochrome p450 side-chain cleavage enzyme; STAR, Steroidogenic Acute Regulatory Protein; 3β-HSD, 3β-hydroxysteroid dehydrogenase.

CYP17 [reviewed in (22)]. NR5A1 is abundant in the CL during the midluteal phase and binds to the *Star* promoter *in vivo* (23). Moreover, NR5A1 regulates *Star* and *Cyp11a* gene expressions in luteal cells and the CL of many species (23–26). A luteal cell-specific *Nr5a1* knockout (KO) has not been reported. The ovaries of a newborn mice lacking Nr5a1 in GCs are comparable with wild type; however, Nr5a1-deficient adult females lack CL and suffer from sterility (27).

NR5A2 (also known as Fetoprotein transcription factor: FTF, liver receptor homolog 1: LRH-1), another NR5A family member, is also present in the ovary (28). Interestingly, NR5A2 recognizes the same consensus binding sequence as NR5A1 and may regulate similar steroidogenic enzyme target genes. NR5A2 is the most prominent NR5A factor in the CL (29). Similar to NR5A1, NR5A2 is a potent regulator of steroidogenic gene expression in the CL (23, 29). Luteal specific KO of *Nr5a2* is linked with luteal insufficiency, which suggests that this factor plays a crucial role in luteal formation and function (30). Additionally, *Nr5a1* and *Nr5a2* KO mice individually exhibit luteal disruption with downregulated steroidogenic enzyme gene

expression (functional luteal disruption) and severe structural damage (27, 29, 31). Both these factors, therefore, play prominent roles in luteal function, development, and regression.

While the role of NR4A1 (Nuclear Receptor Subfamily 4 Group A Member 1) in steroidogenesis in the CL is yet to be elucidated, its expression is upregulated by cAMP, a second messenger of several pituitary hormones including LH. NR4A1 is present in the theca cells, GCs, and luteal cells in the human ovary (32, 33). Moreover, NR4A1 is known to regulate *StAR* gene expression activity in mouse Leydig cells (34, 35). On the other hand, NR4A1 levels are upregulated by $PGF_{2\alpha}$ in pseudopregnant rats (36). Further studies are needed to elucidate the control of NR4A1 levels and its role in luteal steroidogenesis.

The gonads also express several GATA factors that are known to regulate steroidogenic gene expression [reviewed in (37)]. In the CL of *Gata4* and *Gata6* conditional double knockdown mice, a reduction in P_4 production is observed along with an acute inhibition of expression of genes in the steroidogenic pathway including *Star*, *Hsd3b1*, and *Cyp11a* [(38), **Figure 2**]. Moreover, *GATA4* and *GATA6* mRNA and protein were identified in bovine CL and it is suggested that GATA6 may be involved in the regulation of *STAR* expression in this species (23). As GATA4 and GATA6 are proposed to physically and functionally interact with NR5A1 and NR5A2 to upregulate steroidogenic enzyme gene transcription via the *HSD3B2* and *Cyp19a* promoter (39), one can expect that they also play important roles in steroidogenesis in the CL. While we have good insights into how steroidogenesis is likely turned on by transcriptional factors in the CL, the mechanism governing its inhibition during functional luteolysis remains obscure. NR0B1 inhibits transcriptional cooperation between GATA4 and NR5A1 in testicular cells, suggesting that it might possibly mediate the inhibitory effect of $PGF_{2\alpha}$ on P_4 in the CL (40, 41).

STRUCTURAL CL REGRESSION AND APOPTOSIS

Reduced P_4 secretion begins during the late luteal phase and leads to CL structural regression. This structural regression occurs through apoptosis which involves nuclear fragmentation (3, 4) as well as caspase 3 and p53 activation (42–44). Detailed information of apoptosis-mediated CL regression is well-reviewed in (45). Our group has identified that apoptosis in bovine CL is induced by the interaction between cytokines and Fas/FasL (46). It is well-established that $PGF_{2\alpha}$ triggers apoptosis during luteolysis. Immune cells and cytokines play important roles in structural luteolysis as evidenced by increased T-lymphocyte and macrophage influx during CL regression (47). In bovine luteal cells, Fas-FasL mediated cell death plays a crucial role in luteal cell apoptosis. This process is induced by interferon gamma (IFNγ) and tumor necrosis factor alpha

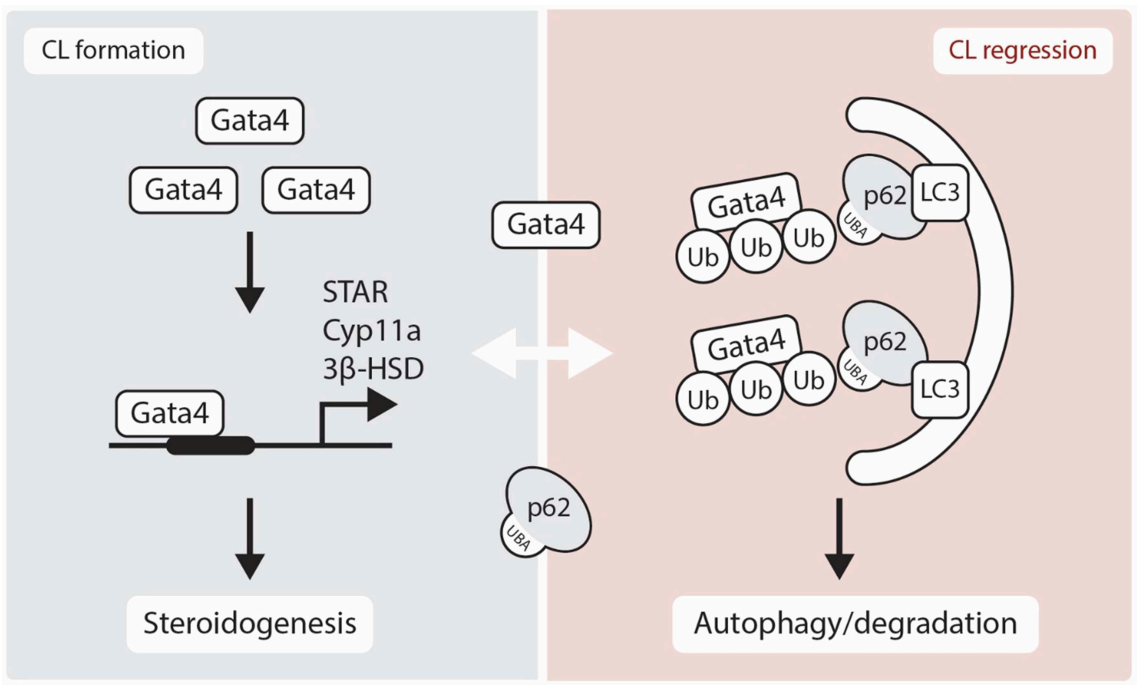

FIGURE 2 | Schematic representation showing the role of GATA4 in luteogenesis and luteolysis. Gata4 is located in the nucleus and regulates several steroidogenic enzymes gene expression. Although p62 is thought to be localized in the cytoplasm, recent studies have suggested that p62 physically interacts with nuclear proteins. Here, we show a hypothetical regulation of GATA4 transcription factor through an interaction with p62 in the luteolytic CL. STAR, Steroidogenic Acute Regulatory Protein; 3β-HSD, 3β-hydroxysteroid dehydrogenase; CYP11A, Cytochrome P450 Family 11 Subfamily A Member; Ub, Ubiquitin; LC3, Microtubule-associated protein 1A/1B-light chain 3; UBA, Ubiquitin-Associated domain.

(TNFα) plays a stimulatory role. Treatment of luteal cells with Fas ligand, in presence of IFNγ and TNFα, leads to the formation of apoptotic bodies, which supports the notion that these cytokines are implicated in luteal regression (46). Moreover, IFNγ and TNFα induce mouse luteal cell apoptosis (48). Macrophages degrade extracellular matrix (ECM) and phagocytize degenerated luteal cells leading to the release of cytokines including TNFα, interleukin-1β (IL-1), and IFNγ (49). The intraluteal TNFα level increases significantly during both spontaneous and induced *in vivo* luteolysis in microdialyzed CL (50). It is, therefore, likely that TNFα stimulates synthesis of luteal $PGF_{2\alpha}$. This modulation of TNFα levels also leads to increased nitrates/nitrites, and stabilization of nitric oxide metabolites (51). TNFα acts in concert with IFNγ to induce luteolysis (46, 52). Hojo et al. (53) have demonstrated that necroptosis is involved in structural regression of CL due to receptor-interacting serine/threonine-protein kinase (RIPK)1 and 3 induction following the treatment of the luteal cells with the inflammatory cytokines IFNγ and TNFα in bovine CL (53). Increased RIPK1 and 3 protein expression is also found in $PGF_{2\alpha}$-induced CL regression, suggesting necroptosis is involved in CL regression. Administration of $PGF_{2\alpha}$ in livestock with functional CL induces luteal regression.

Following functional and structural regression of the CL, proteins in the CL are degraded and removed by regulatory mechanisms. We describe hereafter the proteasome-ubiquitin system and the autophagy mechanisms involved in protein degradation and removal of unnecessary tissue structures.

PROTEASOME AND CL REGULATION

The UPP plays major roles in the degradation of unnecessary proteins. The targeted proteins are bound by small ubiquitin proteins (**Figure 3**). The role of ubiquitin is tightly regulated by several enzymes namely ubiquitin-activating enzyme (E1), ubiquitin-conjugating enzyme (E2), and ubiquitin ligase (E3) (54). On the other hand, the ubiquitinated proteins are degraded by a huge protein complex called the 26S proteasome. The 26S proteasome complex consists of two subclass complexes: the 19S and 20S particles. It is known that the UPP plays important role in the reproductive system (7, 8). Emerging evidence also suggests that dysfunction of the UPS leads to multiple diseases, including the dysfunction of the male and female reproductive tracts (9, 55).

Surprisingly, the UPP system in the CL is not well-characterized and only a very limited number of proteasome genes have been identified in the CL. Nonetheless, the proteasome plays a central role in the degradation of unnecessary proteins, which are labeled with ubiquitin proteins. Since the mammalian CL is renewed after each infertile estrous/menstrual cycle, understanding how its proteins are degraded is an important question that remains unanswered. The proteasome inhibitors MG115 and MG132 reduced both mRNA and protein expression of StAR in the rat adrenal cortex (56). On the other hand, the stability of breast cancer susceptibility gene 1 (*BRCA1*) and its partner BRCA1-associated RING domain protein 1 (BARD1) is regulated by proteasome degradation in human ovarian GCs (57). This regulatory process is also associated with both cAMP-dependent and cAMP-independent steroidogenic

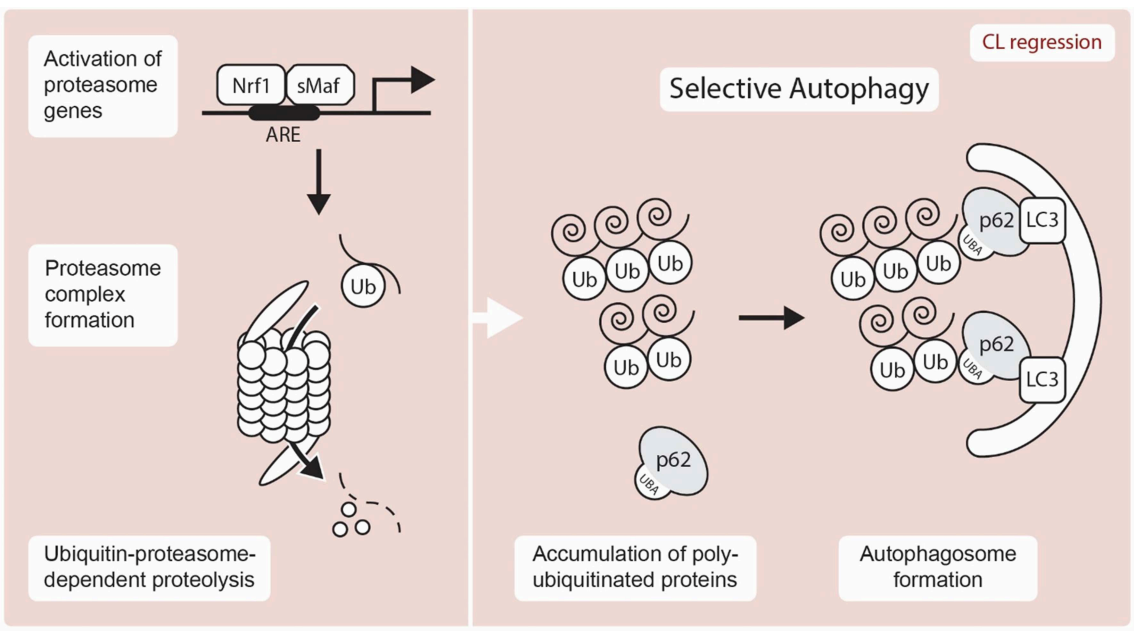

FIGURE 3 | Schematic representation showing UPP and autophagy mediated proteolysis. A transcription factor, Nrf1 is liberated from the ER after stress and translocates to the nucleus, where it induces the expression of proteasome subunit genes through the ARE (antioxidant response element) by hetero-dimerizing with a small Maf (sMaf) protein. Selective autophagy is known to exert proteolysis through the recognition of unnecessary target protein via p62-LC3-autophagosome. Nrf1, NF-E2-related factor 1; sMAF, small musculoaponeurotic fibrosarcoma proteins; ARE, antioxidant response element; Ub, Ubiquitin; LC3, Microtubule-associated protein 1A/1B-light chain 3; UBA, Ubiquitin-Associated domain.

processes. Forskolin-induced *Cyp19a* expression is blocked by MG132 treatment, which suggests that proteasome inhibition downregulates steroidogenesis. It appears that the proteasome-ubiquitin system plays an important role in steroidogenic gene expression and therefore further functional studies about the roles of UPP in luteal steroidogenesis are required. At the molecular level, NF-E2-related factor 1 (NRF1), a transcription factor involved in the stress response, has garnered significant attention due to its implication in protein clearance via the UPP (**Figure 3**). NRF1 is a member of the cap "n" collar (CNC)-bZip transcription factor family and is localized at the ER until an external stressor is present. Upon activation by an external stressor, NRF1 is liberated from the ER and translocates to the nucleus, where it stimulates the expression of proteasome subunit genes via the antioxidant response element (ARE) by hetero-dimerizing with a sMAF (small musculoaponeurotic fibrosarcoma) proteins and to maintain protein homeostasis [(58, 59); **Figure 3**]. Proteasome and deubiquitination enzyme gene expressions are regulated by NRF1 (60, 61). A recent study has demonstrated that deletion of *Nrf1* causes downregulation of several proteasome genes with the accumulation of ubiquitinated proteins and p62/SQSTM1, an autophagy marker (61). Much like ubiquitination, deubiquitination also contributes to proteostasis by regulating cellular levels of free monomeric ubiquitin. However, while Proteasome subunit beta type (*PSMB*) 8 and 9 gene expression, has been identified in the bovine CL (62), the roles of the UPP and its regulation by NRF1 require further study.

UPR AND CL REGRESSION

Another pathway that has been implicated in CL regression is ER stress pathway (10, 15, 63). The ER stress is a cellular phenomenon induced by diverse stimuli disturbing the protein folding in the ER (64, 65). In response to ER stress, UPR pathway is activated to restore the ER homeostasis. The UPR pathway involves the actions of three signaling proteins: protein kinase RNA-like ER kinase (PERK), inositol-requiring enzyme-1/X-box-binding protein (IRE1/XBP-1), and activating transcription factor 6 (ATF6) (66, 67). The PERK and ATF6 are normally in inactive form due to their association with BiP (Binding immunoglobulin Protein; also known as Glucose-regulated protein-Grp78), an ER resident chaperone (**Figure 4**). The main role of the CL is to secrete P_4, which is essential for maintaining pregnancy. While the steroidogenic process diverges into several separate pathways which lead to the synthesis of different steroid products, StAR is significantly involved in this process and regulates the rate-limiting step in P_4 production in the CL. Reduced expression of GRP78, a ER chaperone protein critical for UPR, cause inhibition of StAR protein expression and activity in steroidogenic cells (12). Moreover, female mice lacking Becn1, a regulator of autophagy and the UPR system, have a defect in P_4 production in the ovarian GCs and display a preterm labor phenotype (11). These results suggest that the UPR system may regulate P_4 production through various mechanisms. On the other hand, Skn1, an ortholog of Nrf1-3 in *C. elegans*, regulates UPR signaling and transcription factor genes. SKN-1 contributes to the expression of core UPR factors, *pek-1* and *atf-6* (68). Loss of Skn1 inhibits upregulation of Xbp1 gene expression by ER-stress. Chromatin immunoprecipitation studies indicate that endogenous SKN-1 accumulates at the *xbp-1* site of transcription in the presence of ER stress (**Figure 4**). In the steroidogenic cells, intracellular cholesterol is stored in an esterified form.

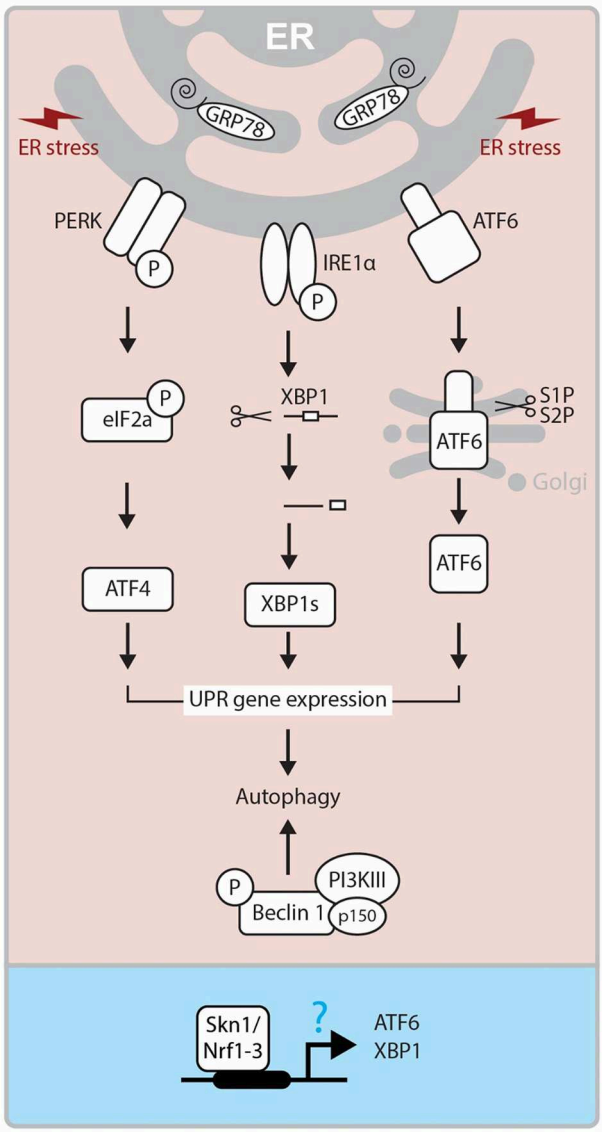

FIGURE 4 | Molecular mechanism of UPR. ER Stress-activated three pathways (IRE, PERK, and ATF6) control the activity of XBP1s, ATF4, ATF6 transcription factors and regulate UPR related gene expressions, which triggers autophagy. On the other hand, Beclin1 forms a complex with PI3KIII and p150, and this also triggers autophagy mechanism. In *Caenorhabditis elegans*, SKN-1, the ortholog of human Nrf1-3, has been reported to regulate ATF6 and XBP1 expressions at the promoter level. ER, endoplasmic reticulum; GRP78, Glucose-regulated protein; PERK, PKR-like eukaryotic initiation factor 2α (eIF2α) kinase; IRE1, inositol-requiring transmembrane kinase/endoribonuclease 1; ATF6, activating transcription factor-6; XBP1, X-box-binding protein 1; XBP1s, spliced XBP1 protein; S1P and S2P, site-1 and site-2 proteases; PI3KIII, Class III PI 3-kinase; Skn1, Protein skinhead-1.

In response to trophic hormone signals coming from the pituitary (e.g., LH, ACTH), cholesterol esterase hydrolyzes cholesterol ester into free cholesterol in target steroidogenic cells. In luteal cells, cholesterol is converted into different types of steroids including P_4 by several steroidogenic enzymes. The gene expression of these enzymes is tightly regulated by several transcription factors. Interestingly, a recent study has revealed that Nrf1 controls cholesterol homeostasis by binding to cholesterol (69). Thus, it is important to determine whether Nrf1 controls steroidogenesis via UPP and UPR modulation in the CL.

As an ER transmembrane protein, IRE1 is essential for UPR and is only activated through binding to unfolded proteins (70). Under the conditions of severe and chronic ER stress, the UPR pathway is not able to cope and cellular dysfunction or death ensues through the activation of both the extrinsic and intrinsic apoptosis pathways (71). Apoptosis is initiated by PERK/eIF2α mediated induction of proapoptotic TF CHOP (Transcriptional factor C/EBP homologous protein), and IRE1 dependent activation of TRAF2 (TNF receptor-associated factor 2). This process stimulates the c-Jun NH2-terminal kinase (JNK) pathway (64, 72). The role of ER stress-mediated apoptosis is well-established in many reproductive events, including follicular atresia (73) and CL regression (10, 15, 63). Yang et al. (15) demonstrated that ER stress markers like Grp78, CHOP, ATF6α and caspase 12 are significantly expressed at the mRNA and protein levels in the late luteal stage during spontaneous and $PGF_{2\alpha}$ induced luteolysis (15). These findings were further supported by decreased expression of ER stress markers and apoptosis in luteal cells treated with tauroursodeoxycholic acid, which functions as a chemical chaperone and reduces ER stress (15, 63). Thus, it is plausible that ER stress-mediated UPR controls both functional and structural luteal regression although further studies are needed to elucidate its molecular mechanism.

AUTOPHAGY AND CL REGRESSION

Redundant cellular components are recognized and transferred to the lysosome by a mechanism known as autophagy. In autophagy, mitophagy selectively degrades mitochondria and pexophagy selectively degrade peroxisomes. Selective autophagy also plays major roles in the degradation of cellular components such as aggregated proteins (74, 75). To recognize target components and properly bring them to the lysosome, an adapter protein involved in autophagy requires at least two domains. One region binds to the target protein and the other domain is necessary for transporting the target to an autophagy mechanism. Autophagy receptor p62 (also known as sequestosome-1) is an adaptor protein which mediates the interaction between selected proteins and autophagosomes. The receptor p62 possesses a LC3-Interacting Region (LIR) motif that interacts with LC3. This interaction allows the receptor p62 to bind to the autophagosomal membrane (**Figure 3**). p62 co-aggregates with the target at the phagophore due to its homopolymerisation property mediated by its PB1(Phox/Bem1p) domain. Interaction of p62 with Atg8/LC3 on the autophagosomal membrane is extremely important for transport. An increase in the expression of LC3-II relative to the expression of LC3-I occurs during autophagy. Although studies on autophagy in the mammalian CL are limited, the link between autophagy and apoptosis is well-established (76, 77). In fact, expression of various autophagy related factors is increased in the late luteal and regression stages of the CL. Increased expression of beclin protein during the late luteal stage in the sow suggests a role in the removal of unwanted proteins during luteolysis (78). LC3-II, an autophagy marker is expressed more in the late than middle stage CL in cattle (42). Similar results were obtained in rat CL as well (16). These findings suggest that autophagy is highly involved in luteal regression in several species. Lipid droplets are unique organelles in the luteal cells enriched with cholesterol esters, that serve as precursor for steroidogenesis. Inhibition of autophagy in luteal cells via deletion of *Becn1* causes failure of lipid droplet formation, and leads to reduced P_4 secretion, demonstrating the critical role of Becn1/ autophagy in luteal steroidogenesis (11). Therefore, the relationship between steroid synthesis and autophagy in the CL should be studied. The p62 receptor exerts its physiological functions including signal transduction regulation, intracellular protein localization (trafficking), and selective autophagy of ubiquitinated proteins through its interaction with various proteins (79). The p62 receptor binds to ubiquitin containing aberrantly aggregated proteins. Since p62 has a ubiquitin associated (UBA) domain and binds to ubiquitinated proteins, p62 plays an important role in selective autophagy. Presently, LC3 and p62 are widely used as autophagy markers. Interestingly, recent studies have revealed that the p62 receptor, a primarily cytoplasmic protein, plays an important role in the nucleus by interacting with several nuclear factors (described below, **Table 1**) that are expressed in the CL (23, 36, 38).

POSSIBLE TRANSCRIPTIONAL REGULATION OF AUTOPHAGY THROUGH THE AUTOPHAGY RECEPTOR P62/SQSTM1 IN THE CL

The nuclear transcription factor GATA4 binds to p62 and is degraded through autophagy [(90), **Figure 2**]. The lysosomal autophagic pathway regulates GATA4 during ionizing radiation-induced and progerin-induced senescence in human mesenchymal stem cells (hMSCs) and fibroblasts, respectively (80, 81). In both fibroblast and hMSCs senescent cells, GATA4 accumulates as a consequence of the loss of physical interaction between p62 and GATA4 (80, 81). While the various functions of GATA factors in luteal P_4 regulation are well-characterized, their role in autophagy is yet to be elucidated (**Figure 2**). Accordingly, SKN-1/Nrf1-3 and ELT-2/GATA transcription factors may regulate the expression of proteasome subunit genes as well as oxidative and heat-stress response genes (91). As NRF family members play prominent roles in the proteasome-autophagy system (61, 92), the relationship between GATA factors and NRF family members in the CL merits further investigation.

TABLE 1 | p62/SQSTM1 interacting nuclear proteins in the regulation of autophagy.

Protein	Biological Process	References
GATA4	GATA family of zinc-finger transcription factors	(80, 81)
ARIP4	AR interacting protein 4-a Rad54 family member and a SNF2 chromatin remodeling factor	(82)
TP53INP1	Tumor Protein P53 Inducible Nuclear Protein-Tumor suppressor/Autophagy	(83)
Rad51	RAD51 Recombinase-DNA damage repair	(84)
PARP-1	Poly (ADP-ribose) polymerase 1-DNA repair	(85)
LC3	Microtubule-associated protein 1A/1B-light chain 3-Autophagy	(86)
AR	Androgen receptor	(87)
PPARα	Peroxisome proliferator-activated receptor alpha	(88)
NR4A1/Nur77	Nerve growth factor IB(NGFIB)/Nur77 /NR4A1-Transcriptional Factor	(89)

Androgen receptor-interacting protein 4 (ARIP4) interacts with sumoylated nuclear receptors such as NR5A1, NR5A2, NR3C1 (GR: glucocorticoid receptor) and NR3C4 (AR: androgen receptor) (93). Multiple studies have shown that steroidogenic genes are regulated by NR5A1. This occurs through direct interaction with transcription factors such as GATA4 (39, 94). The UBA domain of p62 interacts with a novel domain in ARIP4, named SQSTM1/p62 interaction Domain (SID). This domain possesses binding properties similar to ubiquitin. The p62 receptor negatively regulates ARIP4 levels under starvation induced autophagy. This indicates that the interaction between ARIP4 and p62 is involved in the regulation of ARIP4 protein levels during autophagy (82). Considering the dual role of ARIP4 in steroidogenic gene regulation via NR5A1 and autophagy via p62, it will be interesting to further investigate its role during active steroidogenesis and autophagy-mediated CL regression (95, 96).

NR4A, a member of the nuclear receptor superfamily, plays an important role in a variety of cellular processes (97). NR4A1 functions as a nuclear transcriptional factor and activates steroidogenic gene expression in gonadal cells (32, 98). Hu et al. (89) first showed that NR4A1 physically interacts with p62 and accumulates in the mitochondria when mouse embryonic fibroblasts (MEFs) are treated with TNFα and celastrol (89). This suggests that TNFα-mediated apoptosis in the CL may be controlled by NR4A1-dependent regulation of mitochondrial autophagy. Further studies are needed to investigate autophagic regulation of nuclear receptors by p62 in the CL.

TP53 INP1 (tumor protein 53-inducible nuclear protein 1) is a tumor suppressor whose expression is reduced in various cancers. TP53 INP1-LC3 binding occurs via its functional LC3 interaction region (LIR). When TP53 INP1 is highly expressed, TP53 INP1-LC3 interaction is stronger than the p62-LC3 interaction. This inhibits the binding of LC3 to p62 and in turn enhances p62-mediated protein degradation (83). TP53 INP1 also induces autophagy-dependent cell death (83). Since P53 protein is an apoptotic factor in the CL (43), functional analysis of TP53 INP1 in the CL is needed.

PARP-1 [Poly (ADP-ribose) polymerase 1], a key factor in DNA repair, is a partner protein of p62 (85). PARP-1 also binds to LC3 and phosphorylated Unc-51 like autophagy activating kinase 1(ULK1), which are both key factors in autophagy. Rad51 plays a central role in DNA double strand break (DSB) repair through homologous recombination (HR) and also interacts with p62 (84). As autophagy occurs primarily in the cytoplasm, elucidating the role of crosstalk between nuclear localized proteins and autophagy signaling is crucial.

It is worth noting that p62 regulates the binding between Nrf2 and Keap1 (Kelch ECH associating protein 1) although they interact in the nucleus (99). The Nrf2-Keap1 interaction is known to be one of the cellular mechanisms to protect the cells from oxidative stresses. To regulate this mechanism, Nrf2 transcription factor is continuously degraded when its partner protein Keap1 binds. In canonical pathway, the binding of Keap1 controls Nrf2 transcriptional activity (100). However, in non-canonical pathway, p62 binds to Keap1, and this interaction induces a selective autophagy pathway and prevent the interaction between Keap1 and Nrf2 (99). Consequently, Nrf2 transcriptional activity is enhanced and this acts as stress sensor mechanism. To our surprise, many factors identified as nuclear partners of p62 are transcription factors involved in gene regulation of steroidogenic enzymes. Thus, in the near future, the relationship between luteal functional regulation and autophagy-controlled luteal regression will be clarified and we will have better understanding of how luteal function (P_4 production) and regression (apoptosis/autophagy) are orchestrated.

CONCLUSION

Understanding the intracellular homeostatic mechanisms during the maintenance and lysis of CL will pave way for addressing infertility due to luteal dysfunction. Previous research has suggested that dysfunction of the ubiquitin-proteasome and autophagy systems leads to many disorders, including diseases of the male and female reproductive system. However, its molecular basis is not well-studied. We hope that transcriptional regulation of proteasome and autophagy systems during luteolysis will be unraveled in the near future. Elucidation of the transcription factor-proteasome/autophagy axis also could enable efficient recovery from stress situations which will lead to a significant advancement in the field of animal reproduction.

AUTHOR CONTRIBUTIONS

AT and HT conceived, coordinated, wrote and edited the manuscript. AT, NK, HO, and MT wrote, interpreted data, and revised the manuscript. PL, MŚ, and DS edited and revised the manuscript.

FUNDING

This study was supported by a Polish grant from the KNOW (Leading National Research Centre) Scientific Consortium

Healthy Animal - Safe Food, decision of Ministry of Science and Higher Education No. 05-1/KNOW2/2015. This study was also supported by the Polish National Science Center MINIATURA1 (2017/01/X/NZ9/01263) for HT.

ACKNOWLEDGMENTS

The authors thank Dr. Tobias Hohenauer for help with illustrations.

REFERENCES

1. Lavoie HA, King SR. Transcriptional regulation of steroidogenic genes: STARD1, CYP11A1 and HSD3B. *Exp Biol Med*. (2009) 234:880–907. doi: 10.3181/0903-MR-97
2. Bacci ML, Barazzoni AM, Forni M, Costerbosa GL. *In situ* detection of apoptosis in regressing corpus luteum of pregnant sow: evidence of an early presence of DNA fragmentation. *Domest Anim Endocrinol*. (1996) 13:361–72. doi: 10.1016/0739-7240(96)00049-5
3. Juengel JL, Garverick HA, Johnson AL, Youngquist RS, Smith MF. Apoptosis during luteal regression in cattle. *Endocrinology*. (1993) 132:249–54. doi: 10.1210/endo.132.1.8419126
4. Rueda BR, Tilly KI, Botros IW, Jolly PD, Hansen TR, Hoyer PB, et al. Increased bax and interleukin-1beta-converting enzyme messenger ribonucleic acid levels coincide with apoptosis in the bovine corpus luteum during structural regression. *Biol Reprod*. (1997) 56:186–93. doi: 10.1095/biolreprod56.1.186
5. Rueda BR, Wegner JA, Marion SL, Wahlen DD, Hoyer PB. Internucleosomal DNA fragmentation in ovine luteal tissue associated with luteolysis: *in vivo* and *in vitro* analyses. *Biol Reprod*. (1995) 52:305–12. doi: 10.1095/biolreprod52.2.305
6. Reichmann D, Voth W, Jakob U. Maintaining a healthy proteome during oxidative stress. *Mol Cell*. (2018) 69:203–13. doi: 10.1016/j.molcel.2017.12.021
7. Bose R, Manku G, Culty M, Wing SS. Ubiquitin-proteasome system in spermatogenesis. *Adv Exp Med Biol*. (2014) 759:181–213. doi: 10.1007/978-1-4939-0817-2_9
8. Yi YJ, Nagyova E, Manandhar G, Prochazka R, Sutovsky M, Park CS, et al. Proteolytic activity of the 26S proteasome is required for the meiotic resumption, germinal vesicle breakdown, and cumulus expansion of porcine cumulus-oocyte complexes matured *in vitro*. *Biol Reprod*. (2008) 78:115–26. doi: 10.1095/biolreprod.107.061366
9. Hou CC, Yang WX. New insights to the ubiquitin-proteasome pathway (UPP) mechanism during spermatogenesis. *Mol Biol Rep*. (2013) 40:3213–30. doi: 10.1007/s11033-012-2397-y
10. Park HJ, Park SJ, Koo DB, Kong IK, Kim MK, Kim JM, et al. Unfolding protein response signaling is involved in development, maintenance, and regression of the corpus luteum during the bovine estrous cycle. *Biochem Biophys Res Commun*. (2013) 441:344–50. doi: 10.1016/j.bbrc.2013.10.056
11. Gawriluk TR, Ko C, Hong X, Christenson LK, Rucker EB III. Beclin-1 deficiency in the murine ovary results in the reduction of progesterone production to promote preterm labor. *Proc Natl Acad Sci USA*. (2014) 111:E4194–203. doi: 10.1073/pnas.1409323111
12. Prasad M, Pawlak KJ, Burak WE, Perry EE, Marshall B, Whittal RM, et al. Mitochondrial metabolic regulation by GRP78. *Sci Adv*. (2017) 3:e1602038. doi: 10.1126/sciadv.1602038
13. Chen H, Jin S, Guo J, Kombairaju P, Biswal S, Zirkin BR. Knockout of the transcription factor Nrf2: effects on testosterone production by aging mouse Leydig cells. *Mol Cell Endocrinol*. (2015) 409:113–20. doi: 10.1016/j.mce.2015.03.013
14. Lilienbaum A. Relationship between the proteasomal system and autophagy. *Int J Biochem Mol Biol*. (2013) 4:1–26.
15. Yang Y, Sun M, Shan Y, Zheng X, Ma H, Ma W, et al. Endoplasmic reticulum stress-mediated apoptotic pathway is involved in corpus luteum regression in rats. *Reprod Sci*. (2015) 22:572–84. doi: 10.1177/1933719114553445
16. Choi J, Jo M, Lee E, Choi D. The role of autophagy in corpus luteum regression in the rat. *Biol Reprod*. (2011) 85:465–72. doi: 10.1095/biolreprod.111.091314
17. Gilchrist RL, Ryu KS, Ji I, Ji TH. The luteinizing hormone/chorionic gonadotropin receptor has distinct transmembrane conductors for cAMP and inositol phosphate signals. *J Biol Chem*. (1996) 271:19283–7. doi: 10.1074/jbc.271.32.19283
18. Kallen CB, Arakane F, Christenson LK, Watari H, Devoto L, Strauss JF III. Unveiling the mechanism of action and regulation of the steroidogenic acute regulatory protein. *Mol Cell Endocrinol*. (1998) 145:39–45. doi: 10.1016/S0303-7207(98)00167-1
19. Sasano H, Suzuki T. Localization of steroidogenesis and steroid receptors in human corpus luteum. Classification of human corpus luteum (CL) into estrogen-producing degenerating CL, and nonsteroid-producing degenerating CL. *Semin Reprod Endocrinol*. (1997) 15:345–51. doi: 10.1055/s-2008-1068372
20. Morohashi K, Hatano O, Nomura M, Takayama K, Hara M, Yoshii H, et al. Function and distribution of a steroidogenic cell-specific transcription factor, Ad4BP. *J Steroid Biochem Mol Biol*. (1995) 53:81–8. doi: 10.1016/0960-0760(95)00041-W
21. Sadovsky Y, Crawford PA, Woodson KG, Polish JA, Clements MA, Tourtellotte LM, et al. Mice deficient in the orphan receptor steroidogenic factor 1 lack adrenal glands and gonads but express P450 side-chain-cleavage enzyme in the placenta and have normal embryonic serum levels of corticosteroids. *Proc Natl Acad Sci USA*. (1995) 92:10939–43. doi: 10.1073/pnas.92.24.10939
22. King SR, LaVoie HA. Gonadal transactivation of STARD1, CYP11A1 and HSD3B. *Front Biosci*. (2012) 17:824–46. doi: 10.2741/3959
23. Taniguchi H, Komiyama J, Viger RS, Okuda K. The expression of the nuclear receptors NR5A1 and NR5A2 and transcription factor GATA6 correlates with steroidogenic gene expression in the bovine corpus luteum. *Mol Reprod Dev*. (2009) 76:873–80. doi: 10.1002/mrd.21054
24. Liu Z, Simpson ER. Steroidogenic factor 1 (SF-1) and SP1 are required for regulation of bovine CYP11A gene expression in bovine luteal cells and adrenal Y1 cells. *Mol Endocrinol*. (1997) 11:127–37. doi: 10.1210/me.11.2.127
25. Mamluk R, Greber Y, Meidan R. Hormonal regulation of messenger ribonucleic acid expression for steroidogenic factor-1, steroidogenic acute regulatory protein, and cytochrome P450 side-chain cleavage in bovine luteal cells. *Biol Reprod*. (1999) 60:628–34. doi: 10.1095/biolreprod60.3.628
26. Sugawara T, Kiriakidou M, McAllister JM, Kallen CB, Strauss JF III. Multiple steroidogenic factor 1 binding elements in the human steroidogenic acute regulatory protein gene 5'-flanking region are required for maximal promoter activity and cyclic AMP responsiveness. *Biochemistry*. (1997) 36:7249–55. doi: 10.1021/bi9628984
27. Jeyasuria P, Ikeda Y, Jamin SP, Zhao L, De Rooij DG, Themmen AP, et al. Cell-specific knockout of steroidogenic factor 1 reveals its essential roles in gonadal function. *Mol Endocrinol*. (2004) 18:1610–9. doi: 10.1210/me.2003-0404
28. Duggavathi R, Volle DH, Mataki C, Antal MC, Messaddeq N, Auwerx J, et al. Liver receptor homolog 1 is essential for ovulation. *Genes Dev*. (2008) 22:1871–6. doi: 10.1101/gad.472008
29. Zhang C, Large MJ, Duggavathi R, DeMayo FJ, Lydon JP, Schoonjans K, et al. Liver receptor homolog-1 is essential for pregnancy. *Nat Med*. (2013) 19:1061–6. doi: 10.1038/nm.3192
30. Bertolin K, Gossen J, Schoonjans K, Murphy BD. The orphan nuclear receptor Nr5a2 is essential for luteinization in the female mouse ovary. *Endocrinology*. (2014) 155:1931–43. doi: 10.1210/en.2013-1765
31. Meinsohn MC, Morin F, Bertolin K, Duggavathi R, Schoonjans K, Murphy BD. The orphan nuclear receptor liver homolog receptor-1 (Nr5a2) regulates ovarian granulosa cell proliferation. *J Endocr Soc*. (2017) 2:24–41. doi: 10.1210/js.2017-00329
32. Li M, Xue K, Ling J, Diao FY, Cui YG, Liu JY. The orphan nuclear receptor NR4A1 regulates transcription of key steroidogenic enzymes in ovarian theca cells. *Mol Cell Endocrinol*. (2010) 319:39–46. doi: 10.1016/j.mce.2010.01.014

33. Park JI, Park HJ, Choi HS, Lee K, Lee WK, Chun SY. Gonadotropin regulation of NGFI-B messenger ribonucleic acid expression during ovarian follicle development in the rat. *Endocrinology*. (2001) 142:3051–9. doi: 10.1210/en.142.7.3051
34. Martin LJ, Boucher N, Brousseau C, Tremblay JJ. The orphan nuclear receptor NUR77 regulates hormone-induced StAR transcription in Leydig cells through cooperation with Ca2+/calmodulin-dependent protein kinase I. *Mol Endocrinol*. (2008) 22:2021–37. doi: 10.1210/me.2007-0370
35. Martin LJ, Tremblay JJ. The nuclear receptors NUR77 and SF1 play additive roles with c-JUN through distinct elements on the mouse Star promoter. *J Mol Endocrinol*. (2009) 42:119–29. doi: 10.1677/JME-08-0095
36. Qi L, Guo N, Wei Q, Jin P, Wang W, Mao D. The involvement of NR4A1 and NR4A2 in the regulation of the luteal function in rats. *Acta Histochem*. (2018) 120:713–19. doi: 10.1016/j.acthis.2018.07.007
37. Viger RS, Guittot SM, Anttonen M, Wilson DB, Heikinheimo M. Role of the GATA family of transcription factors in endocrine development, function, and disease. *Mol Endocrinol*. (2008) 22:781–98. doi: 10.1210/me.2007-0513
38. Convissar SM, Bennett J, Baumgarten SC, Lydon JP, DeMayo FJ, Stocco C. GATA4 and GATA6 knockdown during luteinization inhibits progesterone production and gonadotropin responsiveness in the corpus luteum of female mice. *Biol Reprod*. (2015) 93:1–10. doi: 10.1095/biolreprod.115.132969
39. Martin LJ, Taniguchi H, Robert NM, Simard J, Tremblay JJ, Viger RS. GATA factors and the nuclear receptors, steroidogenic factor 1/liver receptor homolog 1, are key mutual partners in the regulation of the human 3beta-hydroxysteroid dehydrogenase type 2 promoter. *Mol Endocrinol*. (2005) 19:2358–70. doi: 10.1210/me.2004-0257
40. Sandhoff TW, McLean MP. Repression of the rat steroidogenic acute regulatory (StAR) protein gene by PGF2alpha is modulated by the negative transcription factor DAX-1. *Endocrine*. (1999) 10:83–91. doi: 10.1385/ENDO:10:1:83
41. Tremblay JJ, Viger RS. Nuclear receptor Dax-1 represses the transcriptional cooperation between GATA-4 and SF-1 in Sertoli cells. *Biol Reprod*. (2001) 64:1191–9. doi: 10.1095/biolreprod64.4.1191
42. Aboelenain M, Kawahara M, Balboula AZ, Montasser A, Zaabel SM, Okuda K, et al. Status of autophagy, lysosome activity and apoptosis during corpus luteum regression in cattle. *J Reprod Dev*. (2015) 61:229–36. doi: 10.1262/jrd.2014-135
43. Nakamura T, Sakamoto K. Reactive oxygen species up-regulates cyclooxygenase-2, p53, and Bax mRNA expression in bovine luteal cells. *Biochem Biophys Res Commun*. (2001) 284:203–10. doi: 10.1006/bbrc.2001.4927
44. Trott EA, Plouffe L Jr, Hansen K, McDonough PG, George P, Khan I. The role of p53 tumor suppressor gene and bcl-2 protooncogene in rat corpus luteum death. *Am J Obstet Gynecol*. (1997) 177:327–31. discussion 331–2. doi: 10.1016/S0002-9378(97)70194-7
45. Rolaki A, Drakakis P, Millingos S, Loutradis D, Makrigiannakis A. Novel trends in follicular development, atresia and corpus luteum regression: a role for apoptosis. *Reprod Biomed Online*. (2005) 11:93–103. doi: 10.1016/S1472-6483(10)61304-1
46. Taniguchi H, Yokomizo Y, Okuda K. Fas-Fas ligand system mediates luteal cell death in bovine corpus luteum. *Biol Reprod*. (2002) 66:754–9. doi: 10.1095/biolreprod66.3.754
47. Penny LA, Armstrong D, Bramley TA, Webb R, Collins RA, Watson ED. Immune cells and cytokine production in the bovine corpus luteum throughout the oestrous cycle and after induced luteolysis. *J Reprod Fertil*. (1999) 115:87–96. doi: 10.1530/jrf.0.1150087
48. Jo T, Tomiyama T, Ohashi K, Saji F, Tanizawa O, Ozaki M, et al. Apoptosis of cultured mouse luteal cells induced by tumor necrosis factor-alpha and interferon-gamma. *Anat Rec*. (1995) 241:70–6. doi: 10.1002/ar.1092410110
49. Niswender GD, Juengel JL, Silva PJ, Rollyson MK, McIntush EW. Mechanisms controlling the function and life span of the corpus luteum. *Physiol Rev*. (2000) 80:1–29. doi: 10.1152/physrev.2000.80.1.1
50. Shaw DW, Britt JH. Concentrations of tumor necrosis factor alpha and progesterone within the bovine corpus luteum sampled by continuous-flow microdialysis during luteolysis *in vivo*. *Biol Reprod*. (1995) 53:847–54. doi: 10.1095/biolreprod53.4.847
51. Skarzynski DJ, Bah MM, Deptula KM, Woclawek-Potocka I, Korzekwa A, Shibaya M, et al. Roles of tumor necrosis factor-α of the estrous cycle in cattle: an *in vivo* study. *Biol Reprod*. (2003) 69:1907–13. doi: 10.1095/biolreprod.103.016212
52. Petroff MG, Petroff BK, Pate JL. Mechanisms of cytokine-induced death of cultured bovine luteal cells. *Reproduction*. (2001) 121:753–60. doi: 10.1530/rep.0.1210753
53. Hojo T, Siemieniuch MJ, Lukasik K, Piotrowska-Tomala KK, Jonczyk AW, Okuda K, et al. Programmed necrosis - a new mechanism of steroidogenic luteal cell death and elimination during luteolysis in cows. *Sci Rep*. (2016) 6:38211. doi: 10.1038/srep38211
54. Tanaka K. The proteasome: overview of structure and functions. *Proc Jpn Acad Ser B Phys Biol Sci*. (2009) 85:12–36. doi: 10.2183/pjab.85.12
55. Hu X, Roberts JR, Apopa PL, Kan YW, Ma Q. Accelerated ovarian failure induced by 4-vinyl cyclohexene diepoxide in Nrf2 null mice. *Mol Cell Biol*. (2006) 26:940–54. doi: 10.1128/MCB.26.3.940-954.2006
56. Rucinski M, Tortorella C, Ziolkowska A, Nowak M, Nussdorfer GG, Malendowicz LK. Steroidogenic acute regulatory protein gene expression, steroid-hormone secretion and proliferative activity of adrenocortical cells in the presence of proteasome inhibitors: *in vivo* studies on the regenerating rat adrenal cortex. *Int J Mol Med*. (2008) 21:593–7. doi: 10.3892/ijmm.21.5.593
57. Lu Y, Amleh A, Sun J, Jin X, McCullough SD, Baer R, et al. Ubiquitination and proteasome-mediated degradation of BRCA1 and BARD1 during steroidogenesis in human ovarian granulosa cells. *Mol Endocrinol*. (2007) 21:651–63. doi: 10.1210/me.2006-0188
58. Katsuoka F, Yamamoto M. Small Maf proteins (MafF, MafG, MafK): history, structure and function. *Gene*. (2016) 586:197–205. doi: 10.1016/j.gene.2016.03.058
59. Kim HM, Han JW, Chan JY. Nuclear factor erythroid-2 like 1 (NFE2L1): structure, function and regulation. *Gene*. (2016) 584:17–25. doi: 10.1016/j.gene.2016.03.002
60. Taniguchi H, Okamuro S, Koji M, Waku T, Kubo K, Hatanaka A, et al. Possible roles of the transcription factor Nrf1 (NFE2L1) in neural homeostasis by regulating the gene expression of deubiquitinating enzymes. *Biochem Biophys Res Commun*. (2017) 484:176–83. doi: 10.1016/j.bbrc.2017.01.038
61. Tsuchiya Y, Taniguchi H, Ito Y, Morita T, Karim MR, Ohtake N, et al. The casein kinase 2-nrf1 axis controls the clearance of ubiquitinated proteins by regulating proteasome gene expression. *Mol Cell Biol*. (2013) 33:3461–72. doi: 10.1128/MCB.01271-12
62. Cannon MJ, Pate JL. Expression and regulation of interferon gamma-inducible proteasomal subunits LMP7 and LMP10 in the bovine corpus luteum. *Biol Reprod*. (2003) 68:1447–54. doi: 10.1095/biolreprod.102.010249
63. Park HJ, Park SJ, Koo DB, Lee SR, Kong IK, Ryoo JW, et al. Progesterone production is affected by unfolded protein response (UPR) signaling during the luteal phase in mice. *Life Sci*. (2014) 113:60–7. doi: 10.1016/j.lfs.2014.07.033
64. Sano R, Reed JC. ER stress-induced cell death mechanisms. *Biochim Biophys Acta*. (2013) 1833:3460–70. doi: 10.1016/j.bbamcr.2013.06.028
65. Credle JJ, Finer-Moore JS, Papa FR, Stroud RM, Walter P. On the mechanism of sensing unfolded protein in the endoplasmic reticulum. *Proc Natl Acad Sci USA*. (2005) 102:18773–84. doi: 10.1073/pnas.0509487102
66. Gardner BM, Walter P. Unfolded proteins are Ire1-activating ligands that directly induce the unfolded protein response. *Science*. (2011) 333:1891–4. doi: 10.1126/science.1209126
67. Olzmann JA, Kopito RR, Christianson JC. The mammalian endoplasmic reticulum-associated degradation system. *Cold Spring Harb Perspect Biol*. (2013) 5:10. doi: 10.1101/cshperspect.a013185
68. Glover-Cutter KM, Lin S, Blackwell TK. Integration of the unfolded protein and oxidative stress responses through SKN-1/Nrf. *PLoS Genet*. (2013) 9:e1003701. doi: 10.1371/journal.pgen.1003701
69. Widenmaier SB, Snyder NA, Nguyen TB, Arduini A, Lee GY, Arruda AP, et al. NRF1 is an ER membrane sensor that is central to cholesterol homeostasis. *Cell*. (2017) 171:1094–109.e15. doi: 10.1016/j.cell.2017.10.003
70. Hetz C, Martinon F, Rodriguez D, Glimcher LH. The unfolded protein response: integrating stress signals through the stress sensor IRE1α. *Physiol Rev*. (2011) 91:1219–43. doi: 10.1152/physrev.00001.2011

71. Pincus D, Chevalier MW, Aragon T, van Anken E, Vidal SE, El-Samad H, et al. BiP binding to the ER-stress sensor Ire1 tunes the homeostatic behavior of the unfolded protein response. *PLoS Biol*. (2010) 8:e1000415. doi: 10.1371/journal.pbio.1000415
72. Rasheva VI, Domingos PM. Cellular responses to endoplasmic reticulum stress and apoptosis. *Apoptosis*. (2009) 14:996–1007. doi: 10.1007/s10495-009-0341-y
73. Lin P, Yang Y, Li X, Chen F, Cui C, Hu L, et al. Endoplasmic reticulum stress is involved in granulosa cell apoptosis during follicular atresia in goat ovaries. *Mol Reprod Dev*. (2012) 79:423–32. doi: 10.1002/mrd.22045
74. Svenning S, Johansen T. Selective autophagy. *Essays Biochem*. (2013) 55:79–92. doi: 10.1042/bse0550079
75. Zaffagnini G, Martens S. Mechanisms of selective autophagy. *J Mol Biol*. (2016) 428(9 Pt A):1714–24. doi: 10.1016/j.jmb.2016.02.004
76. Patra S, Panigrahi DP, Praharaj PP, Bhol CS, Mahapatra KK, Mishra SR, et al. Dysregulation of histone deacetylases in carcinogenesis and tumor progression: a possible link to apoptosis and autophagy. *Cell Mol Life Sci*. (2019) 76:3263. doi: 10.1007/s00018-019-03098-1
77. Zhou J, Peng X, Mei S. Autophagy in ovarian follicular development and Atresia. *Int J Biol Sci*. (2019) 15:726–37. doi: 10.7150/ijbs.30369
78. Grzesiak M, Michalik A, Rak A, Knapczyk-Stwora K, Pieczonka A. The expression of autophagy-related proteins within the corpus luteum lifespan in pigs. *Domest Anim Endocrinol*. (2018) 64:9–16. doi: 10.1016/j.domaniend.2018.03.004
79. Mizushima N, Komatsu M. Autophagy: renovation of cells and tissues. *Cell*. (2011) 147:728–41. doi: 10.1016/j.cell.2011.10.026
80. Kang C, Xu Q, Martin TD, Li MZ, Demaria M, Aron L, et al. The DNA damage response induces inflammation and senescence by inhibiting autophagy of GATA4. *Science*. (2015) 349:aaa5612. doi: 10.1126/science.aaa5612
81. Lee JY, Yu KR, Lee BC, Kang I, Kim JJ, Jung EJ, et al. GATA4-dependent regulation of the secretory phenotype via MCP-1 underlies lamin A-mediated human mesenchymal stem cell aging. *Exp Mol Med*. (2018) 50:63. doi: 10.1038/s12276-018-0092-3
82. Tsuchiya M, Isogai S, Taniguchi H, Tochio H, Shirakawa M, Morohashi K, et al. Selective autophagic receptor p62 regulates the abundance of transcriptional coregulator ARIP4 during nutrient starvation. *Sci Rep*. (2015) 5:14498. doi: 10.1038/srep14498
83. Seillier M, Peuget S, Gayet O, Gauthier C, N'Guessan P, Monte M, et al. TP53INP1, a tumor suppressor, interacts with LC3 and ATG8-family proteins through the LC3-interacting region (LIR) and promotes autophagy-dependent cell death. *Cell Death Differ*. (2012) 19:1525–35. doi: 10.1038/cdd.2012.30
84. Hewitt G, Carroll B, Sarallah R, Correia-Melo C, Ogrodnik M, Nelson G, et al. SQSTM1/p62 mediates crosstalk between autophagy and the UPS in DNA repair. *Autophagy*. (2016) 12:1917–30. doi: 10.1080/15548627.2016.1210368
85. Yan S, Liu L, Ren F, Gao Q, Xu S, Hou B, et al. Sunitinib induces genomic instability of renal carcinoma cells through affecting the interaction of LC3-II and PARP-1. *Cell Death Dis*. (2017) 8:e2988. doi: 10.1038/cddis.2017.387
86. Wild P, McEwan DG, Dikic I. The LC3 interactome at a glance. *J Cell Sci*. (2014) 127(Pt 1):3–9. doi: 10.1242/jcs.140426
87. Mitani T, Minami M, Harada N, Ashida H, Yamaji R. Autophagic degradation of the androgen receptor mediated by increased phosphorylation of p62 suppresses apoptosis in hypoxia. *Cell Signal*. (2015) 27:1994–2001. doi: 10.1016/j.cellsig.2015.07.009
88. Diradourian C, Le May C, Cauzac M, Girard J, Burnol AF, Pegorier JP. Involvement of ZIP/p62 in the regulation of PPARalpha transcriptional activity by p38-MAPK. *Biochim Biophys Acta*. (2008) 1781:239–44. doi: 10.1016/j.bbalip.2008.02.002
89. Hu M, Luo Q, Alitongbieke G, Chong S, Xu C, Xie L, et al. Celastrol-induced Nur77 interaction with TRAF2 alleviates inflammation by promoting mitochondrial ubiquitination and autophagy. *Mol Cell*. (2017) 66:141–53.e6. doi: 10.1016/j.molcel.2017.03.008
90. Kobayashi S, Volden P, Timm D, Mao K, Xu X, Liang Q. Transcription factor GATA4 inhibits doxorubicin-induced autophagy and cardiomyocyte death. *J Biol Chem*. (2010) 285:793–804. doi: 10.1074/jbc.M109.070037
91. Keith SA, Maddux SK, Zhong Y, Chinchankar MN, Ferguson AA, Ghazi A, Fisher AL. Graded proteasome dysfunction in caenorhabditis elegans activates an adaptive response involving the conserved SKN-1 and ELT-2 transcription factors and the autophagy-lysosome pathway. *PLoS Genet*. (2016) 12:e1005823. doi: 10.1371/journal.pgen.1005823
92. Kwak MK, Wakabayashi N, Greenlaw JL, Yamamoto M, Kensler TW. Antioxidants enhance mammalian proteasome expression through the Keap1-Nrf2 signaling pathway. *Mol Cell Biol*. (2003) 23:8786–94. doi: 10.1128/MCB.23.23.8786-8794.2003
93. Ogawa H, Komatsu T, Hiraoka Y, Morohashi K. Transcriptional suppression by transient recruitment of ARIP4 to sumoylated nuclear receptor Ad4BP/SF-1. *Mol Biol Cell*. (2009) 20:4235–45. doi: 10.1091/mbc.e08-12-1247
94. Bouchard MF, Taniguchi H, Viger RS. The effect of human GATA4 gene mutations on the activity of target gonadal promoters. *J Mol Endocrinol*. (2009) 42:149–60. doi: 10.1677/JME-08-0089
95. Baba T, Otake H, Inoue M, Sato T, Ishihara Y, Moon JY, et al. Ad4BP/SF-1 regulates cholesterol synthesis to boost the production of steroids. *Commun Biol*. (2018) 1:18. doi: 10.1038/s42003-018-0020-z
96. Syu JS, Baba T, Huang JY, Ogawa H, Hsieh CH, Hu JX, et al. Lysosomal activity maintains glycolysis and cyclin E1 expression by mediating Ad4BP/SF-1 stability for proper steroidogenic cell growth. *Sci Rep*. (2017) 7:240. doi: 10.1038/s41598-017-00393-4
97. Beard JA, Tenga A, Chen T. The interplay of NR4A receptors and the oncogene-tumor suppressor networks in cancer. *Cell Signal*. (2015) 27:257–66. doi: 10.1016/j.cellsig.2014.11.009
98. Martin LJ, Tremblay JJ. The human 3beta-hydroxysteroid dehydrogenase/Delta5-Delta4 isomerase type 2 promoter is a novel target for the immediate early orphan nuclear receptor Nur77 in steroidogenic cells. *Endocrinology*. (2005) 146:861–9. doi: 10.1210/en.2004-0859
99. Komatsu M, Kurokawa H, Waguri S, Taguchi K, Kobayashi A, Ichimura Y, et al. The selective autophagy substrate p62 activates the stress responsive transcription factor Nrf2 through inactivation of Keap1. *Nat Cell Biol*. (2010) 12:213–23. doi: 10.1038/ncb2021
100. Taguchi K, Yamamoto M. The KEAP1-NRF2 system in cancer. *Front Oncol*. (2017) 7:85. doi: 10.3389/fonc.2017.00085

Conflict of Interest: The authors declare that the research was conducted in the absence of any commercial or financial relationships that could be construed as a potential conflict of interest.

frontiers in Endocrinology

REVIEW
published: 29 November 2019
doi: 10.3389/fendo.2019.00832

Perturbations in Lineage Specification of Granulosa and Theca Cells May Alter Corpus Luteum Formation and Function

Mohamed A. Abedel-Majed[1], *Sarah M. Romereim*[2], *John S. Davis*[3,4] *and Andrea S. Cupp*[5]*

[1] *Department of Animal Production, School of Agriculture, University of Jordan, Amman, Jordan,* [2] *Department of Biological Systems Engineering, University of Nebraska-Lincoln, Lincoln, NE, United States,* [3] *Department of Obstetrics and Gynecology, Olson Center for Women's Health, University of Nebraska Medical Center, Omaha, NE, United States,* [4] *VA Nebraska-Western Iowa Health Care System, Omaha, NE, United States,* [5] *Department of Animal Science, University of Nebraska-Lincoln, Lincoln, NE, United States*

Anovulation is a major cause of infertility, and it is the major leading reproductive disorder in mammalian females. Without ovulation, an oocyte is not released from the ovarian follicle to be fertilized and a corpus luteum is not formed. The corpus luteum formed from the luteinized somatic follicular cells following ovulation, vasculature cells, and immune cells is critical for progesterone production and maintenance of pregnancy. Follicular theca cells differentiate into small luteal cells (SLCs) that produce progesterone in response to luteinizing hormone (LH), and granulosa cells luteinize to become large luteal cells (LLCs) that have a high rate of basal production of progesterone. The formation and function of the corpus luteum rely on the appropriate proliferation and differentiation of both granulosa and theca cells. If any aspect of granulosa or theca cell luteinization is perturbed, then the resulting luteal cell populations (SLC, LLC, vascular, and immune cells) may be reduced and compromise progesterone production. Thus, many factors that affect the differentiation/lineage of the somatic cells and their gene expression profiles can alter the ability of a corpus luteum to produce the progesterone critical for pregnancy. Our laboratory has identified genes that are enriched in somatic follicular cells and luteal cells through gene expression microarray. This work was the first to compare the gene expression profiles of the four somatic cell types involved in the follicle-to-luteal transition and to support previous immunofluorescence data indicating theca cells differentiate into SLCs while granulosa cells become LLCs. Using these data and incorporating knowledge about the ways in which luteinization can go awry, we can extrapolate the impact that alterations in the theca and granulosa cell gene expression profiles and lineages could have on the formation and function of the corpus luteum. While interactions with other cell types such as vascular and immune cells are critical for appropriate corpus luteum function, we are restricting this review to focus on granulosa, theca, and luteal cells and how perturbations such as androgen excess and inflammation may affect their function and fertility.

Keywords: follicle, granulosa cell, theca cell, corpus luteum, infertility, differentiation, PCOS, androgen

OPEN ACCESS

Edited by:
Jens Vanselow, Leibniz Institute for Farm Animal Biology, Germany

Reviewed by:
JoAnne Richards, Baylor College of Medicine, United States
Vijay Simha Baddela, Leibniz Institute for Farm Animal Biology, Germany

***Correspondence:**
Andrea S. Cupp
acupp2@unl.edu

Specialty section:
This article was submitted to Reproduction, a section of the journal Frontiers in Endocrinology

Received: *14 June 2019*
Accepted: *14 November 2019*
Published: *29 November 2019*

Citation:
Abedel-Majed MA, Romereim SM, Davis JS and Cupp AS (2019) Perturbations in Lineage Specification of Granulosa and Theca Cells May Alter Corpus Luteum Formation and Function. Front. Endocrinol. 10:832. doi: 10.3389/fendo.2019.00832

INTRODUCTION TO THE DEVELOPMENT AND FUNCTION OF THE OVARY

The ovarian follicle is the structural and functional unit of the mammalian ovary (1–3), which provides the necessary environment for oocyte growth and maturation (1, 3). The corpus luteum, which is derived from the somatic cells of a follicle after the oocyte has been released during ovulation, is a crucial part of pregnancy. Any defects in ovarian function have a negative effect on female reproductive health and fertility (4). In order to fully understand the development of an ovarian follicle and the subsequent formation of the corpus luteum (CL), it is helpful to know the origins of the cells of the ovary. Much of the information provided in this review is based on observations from studies in the bovine with references to human and mouse ovarian development.

Ovarian Development

The assembly of ovarian follicles is the developmental process that mediates the formation of primordial follicles containing an individual oocyte (3, 5–7). Oocytes originate as primordial germ cells (PGC) from the endoderm of the embryonic sac (3, 7). The PGCs migrate by amoeboid movement from the epithelium of the yolk sac into the hindgut and arrive at the gonadal ridges (undifferentiated gonads) (3, 8–10). The PGCs undergo a limited number of mitotic divisions during their passage and upon arrival at the gonadal ridge (10). The gonadal ridges develop as a thickening of the coelomic epithelium on the mesonephros (temporary embryonic kidneys) and make connections with mesonephric tissue by streams of cells called rete-ovarii (3). When PGCs migrate they form oogonial clusters or cysts within the gonadal ridge (6, 11, 12). Mitosis of the oogonia peaks and then ceases during embryonic development, and that early population boom determines the number of germ cells available to all female mammals. Subsequently, the oogonia enter meiosis (8). Following initiation of the meiotic process, the oogonial germ cells enlarge (10) (mice). The meiotic process then leads the oogonial clusters or cysts to break apart to become oocytes surrounded by a single layer of squamous pre-granulosa cells to form primordial follicles (6, 8, 11, 13) (mice and bovine) which establish the ovarian reserve.

Follicle Maturation

The initiation of follicle growth involves the transition of the primordial follicle from the quiescent follicle pool to the growing pool (transitional, primary, secondary, and tertiary) (11, 14, 15) (**Figure 1**). Morphological changes in granulosa from squamous/flattened (less differentiated) to cuboidal epithelial granulosa cells are the histological evidence for the transition from primordial to primary follicles (16, 17) (**Figure 1**). The growth of an oocyte starts immediately after the activation of the primordial follicle. Further, Braw-Tal and Yossefi (16) reported as the number of granulosa cells layers around the oocyte increased there was a corresponding enlargement of the size of oocyte.

The cuboidal granulosa cells in the primary follicle then start to proliferate, transitioning to a secondary follicle which is characterized by multiple layers of granulosa cells surrounding an oocyte (18, 19) (**Figure 1**). When multiple granulosa cell layers have formed in the mammalian ovary, a layer of theca cells differentiate to surround the granulosa cells outside of the basement membrane (14). This layer of theca cells will eventually become two distinct types of theca cells, the inner theca interna and the outer theca externa. The theca interna is a layer of highly vascularized steroidogenic cells, while the theca externa is a loosely organized band of non-steroidogenic cells (20).

Finally, a tertiary (or antral) follicle is formed and is characterized by the presence of a fluid-filled cavity known as an antrum (18, 19) (**Figure 1**). The mural granulosa cells that line the wall of the follicle are critical for steroidogenesis and ovulation; while cumulus granulosa cells surround the oocyte and promote its growth and development (18). Greater numbers of antral follicles present in the ovary are indicative of increased ovarian reserve and are associated with increased fertility in heifers (21).

As an antrum forms, tertiary follicles continue to grow and develop multiple granulosa and theca cell layers (**Figure 1**). The granulosa and theca cells are a site of action for the gonadotropins and a site for production of steroid hormones (22). An increase in gonadotropin releasing hormone from the hypothalamus stimulates gonadotropin release from the pituitary, which promotes follicular growth and estrogen (E2) secretion from the ovaries (23).

Follicle Waves and Ovulation

Receptors for the gonadotropin follicle stimulating hormone (FSH) are localized in the granulosa cells of growing follicles (19, 24). An increase in FSH concentrations during the follicular phase of the reproductive cycle is very important for the development of follicular waves (2–3 waves in cattle and humans), the formation of antral follicles, and the selection of a dominant follicle (the only follicle that keeps growing while other follicles regress and undergo atresia) (25, 26) (**Figure 1**). The dominant follicle grows faster than the rest of the cohort, is more sensitive to FSH, and produces higher levels of estrogen and the regulatory hormone inhibin (2, 19, 27) (**Figure 1**).

Inhibin and estrogen concentrations in the follicular fluid of the dominant follicle have a direct negative feedback effect on FSH release at the anterior pituitary during the mid-follicular phase (2, 19, 28). The granulosa cells of the dominant follicle ultimately acquire LH receptors, a hallmark of a preovulatory follicle (**Figure 1**). Furthermore, increased follicular estradiol production stimulates (**Figure 1**) secretion of the pituitary gonadotropin luteinizing hormone (LH) and eventually induces the LH surge (18, 23). When FSH decreases and LH pulse frequency increases, the dominant follicle becomes more sensitive to LH receptors (LH/CGR) located in both the granulosa and theca cells (19). The LH surge is important in the final maturation and ovulation (follicle rupture) of the dominant follicle (18, 28), as well as in the terminal differentiation of the remaining granulosa and theca cells to form the corpus luteum. The corpus luteum is a transient endocrine structure responsible for secreting progesterone, which is required for preparing the uterus for implantation and maintenance of pregnancy (18).

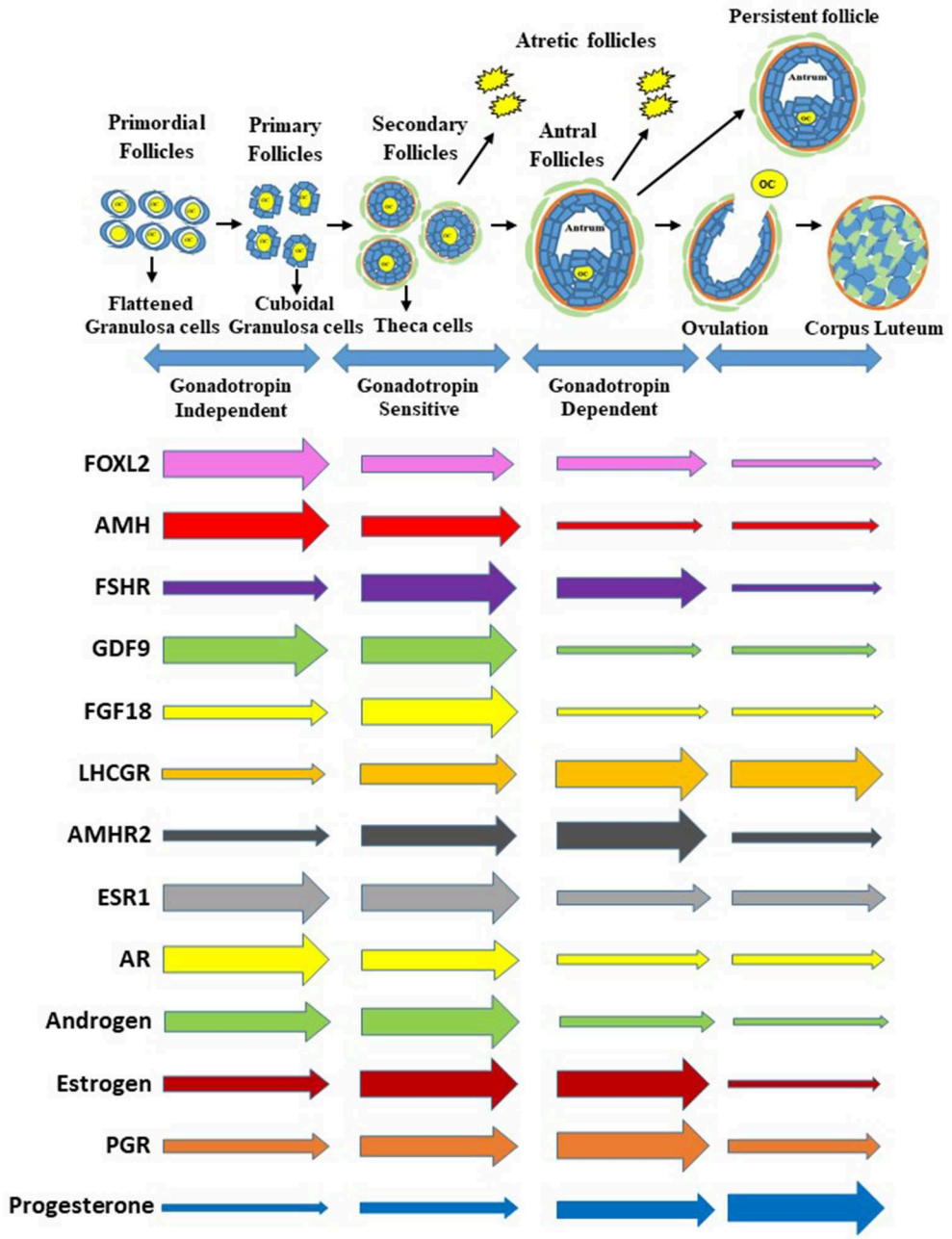

FIGURE 1 | Process of follicle progression from primordial, primary, secondary, and antral follicles through gonadotropin independent, gonadotropin sensitive, and gonadotropin dependent phases to ovulation, development of a persistent follicle, follicular atresia and formation of corpus luteum. Expression of growth factors, hormone receptor genes, and steroids and steroid receptors during each stage of folliculogenesis. The gene expression is representative of the whole follicle or corpus luteum contribution and not individual cells. Furthermore, the size of the arrows at the beginning are not relative to each gene above or below but relative to the horizontal changes through the follicle stages and formation of the corpus luteum.

Corpus Luteum Formation and Function

After ovulation, the somatic cells (theca and granulosa) differentiate into the small luteal cells (SLC) and large luteal cells (LLC), respectively. The development of the corpus luteum into an operational endocrine gland involves growth and development of the steroidogenic cells. Optimal function of the corpus luteum requires the development of an extensive capillary network to deliver nutrients for the production and secretion of the large amounts of progesterone required to preserve pregnancy in most mammalian species. There

are different morphological, physiological, and biochemical characteristics of large and small luteal cells which may reflect different follicular lineages with separate embryological origins (3, 4, 29, 30).

Bovine, ovine and human corpora lutea have two distinct steroidogenic cells with different abilities to produce progesterone (31). During differentiation, both luteal cell types acquire high levels of the key enzymes cholesterol side-chain cleavage P450 (Cytochrome P450 family 11 subfamily A1 or CYP11A1) and 3β-hydroxysteroid-dehydrogenase (3β-HSD or HSD3B) that are required to convert cholesterol into pregnenolone and then progesterone, respectively (32). The activity of these enzymes appears to be present in excess amounts in both small and LLC and does not appear to rate-limiting. The limiting step appears to be the delivery of cholesterol to mitochondria within each cell. The SLC respond to LH with large increases in progesterone secretion, and LLC have an elevated basal rate of progesterone secretion and respond to LH with a modest increase.

The luteal cells of women, monkeys, and rodents have variable responses to LH (30) which may be based on their lipid droplet morphology. Bovine (33) and ovine (34) SLC have larger lipid droplets and the LLC have abundant, dispersed small lipid droplets. The cellular origin of the large luteal cell has generally been ascribed to the granulosa cells in both ruminants and primates. Luteinization of granulosa cells gives rise to cells with cellular features and mRNA expression that are similar to the large luteal cell, whereas luteinization of theca cells gives rise to cells with features like the small luteal cell (35, 36). The origin of the two cell types is observed in the primate based on morphological evidence demonstrating portions of the corpus luteum that are primarily granulosa-lutein cells and other areas that primarily contain smaller theca-lutein cells (37).

LINEAGE SPECIFICATION OF GRANULOSA AND THECA CELLS

Granulosa Cell Lineage

Granulosa cells are interesting in that they are not a uniform population of cells. Some granulosa cells have properties of stem cells including the ability to divide and form colonies (38), divide without contact inhibition (39), and may share properties of endothelial cells (40). All of these may be different depending on the species of reference. During the development of the ovary, granulosa cells may originate from several cell types (**Figure 2**). Early researchers provided evidence that murine granulosa cells developed from both the coelomic epithelium that forms the ovary as well as cells that migrated in from the mesonephros (43, 44). With the advent of conditional knockout mice and fluorescent tags, many of the cell lineages have been refined in the mouse model with further cell lineage differences determined in larger mammals (4, 36). The multiple cellular origins of granulosa cells (where they originate- see **Figures 2**, **3**) may result in altered function and differentiation of these cells later during follicle formation (**Figure 2**) which would affect subsequent corpus luteum development and function upon ovulation. For instance, pregranulosa cells in the bovine (and potentially ovine and human) are derived from gonadal-ridge epithelial-like (GREL) cells. Also stem cells are derived from GREL cells. It is not known if stem cells can also form granulosa cells or different populations of granulosa cells such as mural and cumulus cells. Environmental factors can affect the GREL cells, which may determine if they produce stem cells or pregranulosa cells (3). If the ovarian environment fluctuates based on alterations in cytokines, growth factors, gonadotropins, or steroids it is possible that these granulosa cells might differentiate into populations with different gene expression profiles and function. Thus, further differentiation (luteinization)

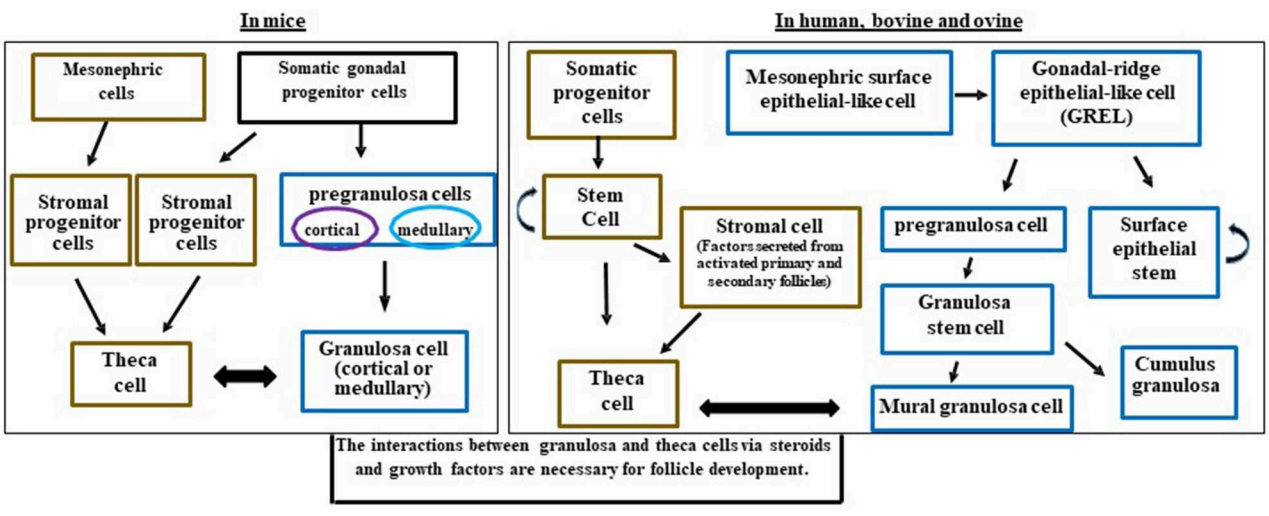

FIGURE 2 | Schematic diagram illustrating the potential and known granulosa and theca cells lineages in the mice, human, bovine, and ovine ovaries and how they interact for follicle development. Somatic progenitor cells have origins from the developing coelomic gonadal epithelium and mesonephric cells. This figure was developed from information in Hummitzsch et al. (3, 41) and Rotgers et al. (42).

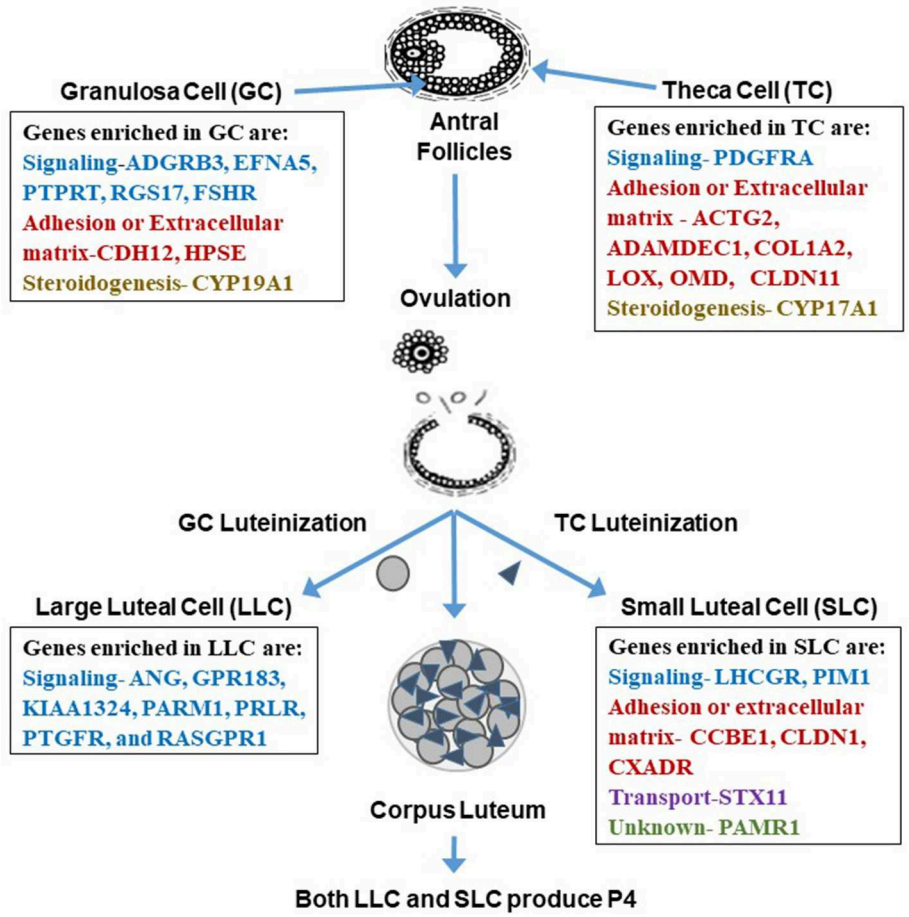

FIGURE 3 | Genes enriched in granulosa cells, theca cells, large luteal cells (LLC), and small luteal cells (SLC). Enriched genes are involved in processes related to signaling, adhesion, extracellular matrix, steroidogenesis, transport, or are unknown. Interestingly, it appears that the categories change from somatic to luteal cells with mainly genes involved in signal transduction enriched in LLC and more adhesion or extracellular matrix genes enriched in SLC. Tables of these enriched genes are in Romereim et al. (36).

of these granulosa cells following ovulation may alter the luteal phenotype and also affect production of progesterone and the ability to maintain pregnancy.

The granulosa cells in mice originate from somatic progenitor cells that come from the coelomic epithelium of the gonad (4, 45, 46). These somatic progenitor cells commit to either pre-granulosa cells or stromal progenitor cells (**Figure 2**) (4, 46). The pregranulosa cells may have different functions and some may not proliferate depending on whether they are medullary or cortical. The medullary cells develop in the initial waves of pregranulosa differentiation and then migrate to and become part of the medullary follicles. In a second wave of pregranulosa cell differentiation, the cortical follicles develop and expand to become the ovarian reserve. A review on these different medullary vs. cortical follicles and the specific markers that differentiate them are presented in detail below (42).

In mice, cortical and medullary granulosa cells (**Figure 2**) commit to different types of pregranulosa cells depending on expression of specific genes. Medullary granulosa cells express the markers *Gata4*$^{+}$/*Cdkn1b*$^{+}$, while cortical pregranulosa cells express *Gata4*$^{+}$/*Lgr5*$^{+}$. The receptor for RESPO1, LGR5, is responsible for continuing development of these granulosa cells. At later stages, the cortical granulosa cells acquire *Cdkn1b*$^{+}$, and as mature cells both cortical and medullary granulosa cells express *FoxL2,* which is critical for maintaining their granulosa-like phenotype. Without *FoxL2* these granulosa cells could revert to a testis (Sertoli-like) or epithelial lineage and express *Sox9*; this also occurs in some granulosa cell tumors (47). Expression of *FoxL2* is dependent on estrogen; thus, steroid environments lacking adequate estrogen may also affect granulosa cell function, proliferation, and development (42).

In larger mammals, the main body of evidence indicates that granulosa cells originate from the mesonephric surface epithelial cells (the temporary embryonic kidney) (**Figure 2**) such as in humans (42) and bovine (3, 41). Mesonephric surface epithelial-like cells break down to form GREL cells that differentiate into pre-granulosa cells and stem cells. The pre-granulosa cells then differentiate into granulosa cells. It is not known if the stem cell

population in addition to self-renewal can also form a population of granulosa cells or other cell types in the ovary (**Figure 2**). GREL cells appear to be located above the mesonephric surface epithelium or to break into this layer and to expand. Thus, the GREL cells may also be contributing to surface epithelial cells, which repair wounds that occur due to ovulation (3, 41, 42, 45, 46). In larger species such as bovine, the pre-granulosa cells also form granulosa "stem" cells which can differentiate into cumulus and mural granulosa cells. The mural granulosa cells are the cell type that later will luteinize into the LLCs because they are the only granulosa cells expressing the LH receptor. Constant communication between granulosa cells and their surrounding environment allows for differentiation, gene expression, growth factor secretion, and cell fate (42).

Theca Cell Lineage

There are many important roles for theca cells in the follicle including crosstalk with granulosa cells for synthesis of androgens and estrogens, as well as providing structural support of the growing follicle as it progresses through the developmental stages to produce a mature and fertilizable oocyte (42, 48). The origins of theca cells have not been definitively identified (4). Some investigators hypothesize that theca cells come from mesonephric cells in mice, humans, and bovine (3, 4, 42, 45, 48, 49) (**Figure 2**).

Other investigators have suggested that theca cells in the mouse originate from the stratified medial aspect of the mesonephric kidney, as they have observed cells with elongated nuclei and an overall appearance of fibroblasts (45, 46). In more recent mouse studies using fluorescent tags to *Wt1* (WT1 transcription factor) and *Gli1* (GLI Family Zinc Finger 1) genes, investigators reported that theca cells come from two sources including ovary-derived *Wt1*+ cells and mesonephros-derived *Gli1*+ cells (4). The expression of Gli1 in theca progenitor cells is induced by the paracrine signals Desert hedgehog (Dhh) and Indian hedgehog (Ihh) from granulosa cells (4). Moreover, Growth differentiation factor 9 (GDF9) from the oocyte induces Dhh/Ihh in granulosa cells (4). In the absence of Dhh and Ihh, ovaries have reduced layers of theca cells around the follicle, decreased steroid production, disrupted folliculogenesis, and fail to form corpora lutea (4). Thus, the recruitment of theca cells from the stroma is regulated by factor(s) produced by granulosa cells at the primary and secondary follicle stages (4, 50).

A previous study in women also demonstrated that theca cells originate from the coelomic epithelium of the gonadal primordium and the neighboring mesonephros under paracrine regulation from granulosa cells (51). Other studies, including those in the bovine, demonstrated that theca cells are recruited from surrounding stromal tissue by factors secreted from an activated primary follicle (3, 41, 49) (**Figure 2**). The actual factors have not been fully identified, but granulosa and oocyte interactions with stroma may cause stroma cells to differentiate into theca cells. It has been proposed that stroma stem cell niches exist in mice, human, and bovine ovaries that allow multiple cell types to be developed depending on the growth factors present (3, 4, 42, 48, 49, 52). Large areas of the ovary including groups of stromal cells surrounding some large blood vessels stain positively for chondroitin/dermatan sulfate epitopes (antibodies 7D4, 3C5, and 4C3) similar to stem cell niches observed in other tissues. These stromal cells may therefore represent a stem cell niche (52). Another study suggested that thecal stem cells are present in mouse ovaries (49). However, these data require further support including determination of whether all the cells or only a proportion of the cells in these stem-cell colonies express genes in the Dhh/Ihh pathway such as *Ptch1* and *2*, *Gli 2* and *3* (49), which would suggest a theca stem cell lineage.

THE STEROIDOGENESIS TIMELINE AND PATHWAYS IN GRANULOSA AND THECA CELLS

The granulosa and theca cells are a site of action for the gonadotropins (hormones secreted by the pituitary gland that act on the gonads) and a site for production of steroid hormones (22, 27, 53). Steroid hormone secretion by ovarian tissues is tightly regulated and crucial to the coordination of reproductive cyclicity (29). Steroidogenesis is the process involving the conversion of cholesterol to androgens, estradiol, and progesterone through a variety of steroid hormone intermediates (54, 55). The enzymes and series of intermediates used in humans and ruminants are collectively called the Δ^5 pathway; whereas steroidogenesis in rodent and pig ovaries can occur through either the Δ^5 or the Δ^4 pathway (24). Granulosa cells and theca cells must act together for ovarian steroidogenesis. The first evidence of both theca and granulosa cells interacting to produce estradiol was reported by Falck (56) indicating estradiol production in rat follicles required both cell types. Ovarian steroid production is critical for normal ovarian processes including follicle growth, differentiation, oocyte maturation, and ovulation (57–59). Ovarian steroids are also required for the normal function and development of several tissues in the female including the uterus, breasts, skeleton, and others (54, 55, 57).

Steroidogenesis in the Developing Ovary

The timing of steroidogenesis in the theca and granulosa cells begins surprisingly early in development. Cells within the mammalian fetal ovary already express steroidogenic enzymes and receptors and have the potential to produce both estrogen and progesterone (60–65). However, because estrogen and progesterone have been demonstrated to inhibit primordial follicle activation (5, 63, 66) and progesterone inhibits follicle assembly *in vitro* (7, 67), ovarian factors must inhibit steroidogenesis to allow these developmental events to occur. Production of estrogen and progesterone by the fetal ovary occurs early in development until the formation of germ cell cords, and then steroidogenesis is inhibited to allow follicle formation/assembly and development of the ovarian reserve (7, 63, 68).

A recent study by da Silva (69) demonstrates that fibroblast growth factor 18 (FGF18) produced by ovigerous cords in the fetal bovine ovary may inhibit production of estrogen during this early development period. FGF18 expression increases at the time when fetal ovarian estrogen and progesterone are declining,

which occurs around the time of follicle assembly. Interestingly, treatment of cultures bovine fetal ovarian explants with FGF18 inhibits production of CYP19A1 and CYP11A1, causing reductions in secretion of both estrogen and progesterone *in vitro* (69). Thus, steroid production occurs early in the ovary from the ovigerous cords, which later become oogonial clusters or cysts; and FGF18 may be a paracrine growth factor that allows for both follicle development and granulosa/theca cell differentiation.

Steroidogenesis During Follicle Maturation and Regulation by Gonadotropins

For estrogen synthesis to occur, cholesterol must first be converted to androgen in theca cells through actions of luteinizing hormone (LH), and androgens are further converted in granulosa cells to estrogens via follicle stimulating hormone (FSH) (27, 57–59) (**Figure 1**). In general, the binding of LH to its receptors on theca cells leads to the conversion of cholesterol into androgens like androstenedione; the androgens then diffuse into the granulosa cells to be converted to estrogens like estradiol by aromatase activity under the regulation of FSH (27, 58) (**Figure 1**). More specific descriptions of each step of the pathway detailing the enzymes and steroid intermediates involved are described below.

Theca cell formation occurs when a maturing follicle contains two or more layers of granulosa cells and coincides with the follicle becoming responsive to LH (48, 70) (**Figure 1**). Binding of LH to its receptor (LHCGR) on theca interna cells leads to signal transduction via G protein-coupled receptors ($G\alpha_s$). Activation of $G\alpha_s$, in turn, stimulates adenylyl cyclase, leading to an elevation in intracellular cAMP levels and subsequent activation of protein kinase A (PKA) (71). This elevation in cAMP and PKA activity promotes steroidogenesis by increasing expression of steroidogenic acute regulatory protein (STAR) as well as by increasing STAR activity via phosphorylation on serine 195 (71). Cholesterol is transported from the cytosol into the inner mitochondrial membrane by STAR in theca cells (57, 72, 73). The movement of cholesterol from the outer to the inner mitochondrial membrane by STAR is believed to be a rate-limiting step in gonadal and adrenal tissues (55, 57, 72).

The granulosa cell expresses receptors for FSH (27, 57). The binding of FSH to its receptor leads to an increase in intracellular cAMP levels and subsequent activation of several pathways including protein mitogen-activated protein kinases (p42/p44 MAPK and p38-MAPK) and phosphatidylinositol 3-kinase (PI3K), which regulate many FSH target genes such as the steroidogenic enzyme *CYP11A1* and *STAR*. In addition, PKA is activated and stimulates the phosphorylation of other regulatory proteins (CREB, β-catenin, AKT, MKP3/DUSP6, p42/44 MAPK, GSK-3ß, FOXO1, and YAP) involved in granulosa cell differentiation and steroidogenesis (27, 74–79).

The timing and magnitude of the expression of genes important to the steroidogenic process is dynamic and controlled by follicle maturation. Expression of *STAR*, *CYP11A1*, *CYP17A1*, and *HSD3B*, and *LHCGR* mRNA is present in preantral follicles (80, 81). Furthermore, expression of these steroidogenic enzymes in theca cells increases as antral follicle growth continues (81). Similar to theca cell steroidogenic mRNA expression, abundance of steroidogenic enzymes in the granulosa cells (P450 aromatase and 17β-HSD) increases as follicles progress from small to large antral stages (80). As follicles mature and near ovulation, large quantities of LH actually decrease the enzymatic activity that promotes estrogen production and instead increase enzymatic activity promoting progesterone production (24) (**Figure 1**).

Thus, conversion of cholesterol to androgens resulting in estrogen requires specific cells types and enzymes within the somatic compartment in the follicle. If these enzymes are over-expressed or not expressed, then this may lead to many different disorders. Excess androgen production is a criterion used to diagnose women with polycystic ovary syndrome (PCOS) (15), a metabolic and reproductive disorder. While the etiology of the PCOS phenotype is not completely known, inappropriate regulation of steroid enzymes or differentiation of somatic cells and inflammation may contribute to this disorder.

GENES EXPRESSED AND ENRICHED IN FOLLICULAR SOMATIC CELLS AND MAY BE MARKERS FOR THECA AND GRANULOSA CELLS

Several genes enriched in the granulosa cell transcriptome were identified as granulosa cell gene markers when compared to theca, LLCs, and SLCs including signaling molecules: Adhesion G Protein Coupled Receptor B3 (*ADGRB3)*, Ephrin-A5 (*EFNA5*), PREDICTED-Protein Tyrosine Phosphatase receptor Type T (*PTPRT*), Regulator of G-Protein signaling 17 (*RGS17*), and Follicle Stimulating hormone receptor (*FSHR)* (**Figure 3**). Additional genes enriched in granulosa cells are involved in cell adhesion and extracellular matrix: Cadherin 12 (*CDH12*), and Heparanase (*HPSE);* and steroidogenesis: Cytochrome P450 family 19 subfamily A polypeptide 1 (*CYP19A1*), the critical enzyme activated by downstream signaling of FSHR to elicit conversion of androgens to estrogen (36, 82). There were also many effector molecules upregulated specifically in granulosa cells related to cell proliferation, survival, DNA replication and repair, and microtubule/chromosome rearrangement including SMADs, PLC, kinases involved in signaling cascades like MAPK3K5, and especially G-protein signaling modulators (36). Moreover, granulosa cells have their own gene expression patterns related to cell functions: cell cycle progression (genes involved in S phase and G2 phase), cellular colony formation (related to proliferation and cellular adhesion), RNA decay, functions associated with G protein and tyrosine kinase receptors, and genes related to FSH signaling protein complex assembly (36).

Genes enriched in theca cells that may be used as markers are genes involved in signaling: Platelet-derived growth factor receptor, alpha polypeptide (*PDGFRA)*; cell adhesion or extracellular matrix development: actin gamma 2 (*ACTG2),* A disintegrin and metalloprotease domain-like decysin 1 (*ADAMDEC1*), Collagen type I alpha 2 chain (*COL1A2)*, Lysyl Oxidase like 1 (*LOXL1),* Osteomodulin *(OMD),* Claudin 11 (*CLDN11),* and steroidogenesis: Cytochrome P450 Family

17 Subfamily A Member 1 *(CYP17A1)* (36, 82) (**Figure 3**). Theca cells have increased gene expression patterns related to metabolism, glycolysis, oxidation of proteins, metabolism of heme, synthesis of carbohydrates, synthesis of sterols, and increased gene expression related to extracellular matrix genes such as decorin, collagens, elastin, and fibrillin (36). Interestingly, in women diagnosed with PCOS, there is a thickening of the cortex of the ovary, which may suggest upregulation of extracellular matrix proteins (83). These ovaries also are more rigid. One of the genes associated with theca cells, fibrillin 3, is a glycoprotein that is associated with the extracellular matrix, and its overexpression may also be linked to the rigid nature of these PCOS ovaries (84).

Genes enriched in granulosa cells vs. theca are mainly those regulating signaling and proliferation of cells in the follicular compartment (36). Furthermore, the expression of *FSHR* is specific to granulosa and not theca whereas *LHGCR* or *LH* is expressed in both theca and granulosa cells (85). Theca cells are enriched in genes that are involved in extracellular matrix and cell adhesion, suggesting theca cells have a more mesenchymal phenotype with more genes regulating stromal composition. Both somatic cells expressed a cell type-specific enzyme that regulates steroidogenesis (CYP19A1 and CYP17A1 in granulosa and theca cells, respectively).

MORPHOLOGICAL CHANGES TO FOLLICULAR SOMATIC CELLS AFTER OVULATION AND LUTEINIZATION

At ovulation, the antral follicle undergoes a remarkable transformation. The somatic follicular cells (theca and granulosa) luteinize into a bloody structure called a corpus hemorrhagicum, which then undergoes maturation to a highly vascularized corpus luteum (86) (**Figures 1**, **3**). In the bovine, the luteinization process starts as granulosa cells and theca interna cells begin to differentiate into large and small luteal cells, respectively (3, 31, 36, 87) (**Figures 1**, **3**). Small and large luteal cells are referred to as parenchymal cells that, together with fibroblasts and endothelial cells, form the basic structure of the corpus luteum (88, 89). Recently, we reported that bovine small and large luteal cell types are highly similar based on overall gene expression profiles, with some notable differences (36). A subsequent report evaluating the differences in gene expression in SLCs and LLCs in bovine corpus luteum confirmed these findings (90).

Both SLCs and LLCs possess LH receptors and synthesize and secrete progesterone (36) (**Figure 1**). Although SLCs are highly responsive to LH, large luteal cells are responsible for 80% of the total progesterone produced by the corpus luteum (91). As the corpus luteum matures, it is proposed that SLCs can increase in number but not in size, whereas large luteal cells can increase in size but not in number during the normal estrous cycle (89). Studies have shown that appropriate numbers of granulosa cells in the developing follicle are critical to provide the minimum population of LLCs needed to maintain progesterone production (92). Environmental factors that affect the proliferation or fate of granulosa cells may reduce luteal cell numbers with adverse effects on progesterone production by the subsequent corpus luteum.

Progesterone targets many tissues, including the hypothalamic-pituitary axis, ovary, oviduct, uterus, cervix, vagina, and mammary gland and embryo (29). Luteal progesterone secretion serves as a local luteal cell survival factor (93), regulates the length of the estrous cycle, and is essential for maintenance of pregnancy (29, 36). Progesterone also regulates the timing of ovulation in livestock species (94). When fertilization of the oocyte and implantation are successful, maternal recognition of pregnancy results in the maintenance of the corpus luteum, which ensures pregnancy maintenance and embryo development (36, 95). Otherwise, the luteolytic cascade would be initiated with the release of prostaglandin F2α in a pulsatile pattern, causing regression of the corpus luteum (36, 95). Anti-luteolytic mechanisms such as secretion of IFNT signaling molecules from the conceptus result in gene expression changes in the LLC and SLC such as increasing expression of ISG15 (interferon-stimulated gene, 15 kDa) (95, 96). Thus, ovarian somatic cells play an essential role in embryonic fate (96).

CHANGES IN GENE EXPRESSION IN THECA AND GRANULOSA CELLS DURING DIFFERENTIATION TO SLCs AND LLCs

The process of luteinization is a dramatic change in the morphology and function of the follicle. This process is initiated by the surge of LH at the time of ovulation. Specific alterations in gene expression occur in theca cells responding to the LH surge that are compatible with a transition to a SLC phenotype including a decrease in expression of *CYP17A1,* Solute carrier family 1 member 3 (*SLC1A3*), TNF receptor-associated factor 5 (*TRAF5),* Tetraspanin 33 (*TSPAN33)*, and Hydroxyprostaglandin dehydrogenase (*HPGD)* concurrent with increased expression of Ras homolog family member B (*RHOB)* (36, 97). There are also alterations in granulosa cell gene expression in response to the LH surge that are compatible with a transition to an LLC phenotype including loss of GC expression of Cytochrome P450 family 19 subfamily A member 1 *(CYP19A1),* Carbohydrate sulfotransferase 8 *(CHST8),* Hydroxysteroid 17B dehydrogenase 1 *(HSD17B1),* Glutamate cysteine ligase catalytic subunit (*GCLC),* Solute carrier family 35 member G1 (*SLC35G1)*, and Alanine amino transferase or Glutamic-pyruvate transaminase) (*GPT*) along with the gain of expression of Pentrax 3 (*PTX3),* Runt-related transcription factor 2 *(RUNX2),* periostin *(POSTN),* Rho-related GTP-binding protein *(RND3),* tissue inhibitor of metalloprotease *1 (TIMP1),* Neurotensin *(NTS),* Fos proto-oncogene *(FOS)*, and regulator of calcineurin 1 (*RCAN1)* (36, 97) (**Figure 3**). These differences in expression of genes also characterize granulosa cells moving from an epithelial cell type to a mesenchymal phenotype as well as a steroidogenesis transition from androgen-centric and estrogen-centric to a progesterone-centric machine, allowing for the production of large quantities of progesterone necessary to support establishment and maintenance of pregnancy.

LUTEAL CELL ENRICHED GENES THAT CAN BE USED AS MARKERS FOR LLCs OR SLCs

In addition to its function as a steroidogenic powerhouse, comparisons of gene expression profiles among granulosa, theca and luteal cells, and bioinformatics analysis predicts that a primary function of the LLC is adhesion (binding of cells, growth of epithelial tissue, and quantity of connective tissue) which is consistent with the changes that occur during luteal formation and LLC differentiation (36). Ultrastructural studies clearly demonstrate that bovine LLCs are closely associated with endothelial cells and have a vast surface area of cellular processes that connect with those cells (98), presumptively providing for adequate nutrition and substrates for progesterone production and easy access for progesterone to enter the blood stream. Genes related to cell signaling were enriched in LLCs including receptors such as Prostaglandin E Receptor 3 (*PTGER3),* Platelet-derived growth factor receptors *(PDGFR),* Prolactin receptor *(PRLR),* Fms related tyrosine kinase 1 (*FLT1),* kinase insert domain receptor *(KDR)*, adrenergic receptor (*ADRA2B*), endothelin receptor (*EDNRB*), Transforming growth factor-beta receptor type 2 (*TGFBR2)*, and TNF receptor superfamily member 21 *(TNFRSF21)* (36) (**Figure 3**). Moreover, the LLC is enriched with genes coding for secreted signaling molecules including Platelet derived growth factor subunit A (*PDGFA),* Parathyroid Hormone Like Hormone *(PTHLH),* Angiogenin (*ANG*)**,** G protein-coupled receptor 183 (*GPR183*), Prostate androgen-regulated mucin-like protein 1 (*PARM1*), Prostaglandin F receptor (*PTGFR*), and RAS guanyl releasing protein 1 **(***RASGPR1***)** (**Figure 3**), genes for angiogenesis including Ephrin-B2 (*EFNB2)*, Platelet-derived growth factor receptor beta *(PDGFRB),* and Vascular *E*ndothelial *G*rowth *F*actor A *(VEGFA*), genes for differentiation of cells including Neurogenic Locus Notch Homolog Protein 3 (*NOTCH3),* Parathyroid Hormone Like Hormone *(PTHLH),* Transforming Growth Factor-beta receptor type 2 (*TGFBR2)*, and *WNT11*, genes for immune and inflammatory responses (chemokines, interleukins, tumor necrosis factor family molecules), genes for synthesis of lipids including Acyl-CoA Oxidase 2 (*ACOX2),* Acyl-CoA Synthetase Long Chain Family Member 4 (*ACSL4),* Cytochrome P450 Family 7 Subfamily B Member 1 (*CYP7B1),* Retinol Dehydrogenase 10 (*RDH10*), and genes related to ion transport including Solute Carrier Family 7 Member 8 (*SLC7A8),* ATPase Na+/K+ transporting subunit beta 2 (*ATP1B2*) (36). Thus, many changes occur in LLC gene expression during differentiation that aid in developing vasculature, regulation of immune cell interactions, and maintenance of progesterone production.

In contrast, as determined by genes specifically enriched in SLCs, bioinformatics revealed their primary function as metabolism, including metabolism of phospholipids, peptides, and sterols as well as regulation of the concentration of ATP (36). Genes enriched in SLCs are signaling molecules including Luteinizing hormone receptor (*LHCGR*), Pim-1 Proto-Oncogene (*PIM1*). SLCs also had three genes enriched involved in adhesion and extracellular matrix including Collagen and Calcium binding EGF (*CCBE1*), Claudin 1 (*CLDN1*), Coxsackie virus and adenovirus receptor (*CXADR*); and Syntaxin 11 (*STX11*) is involved in transport while Peptidase domain containing associated with muscle regeneration 1 (*PAMR1*) gene function is unknown (36) (**Figure 3**). When comparing SLC gene expression to that of LLCs, theca cells, and granulosa cells, SLCs had the greatest number of genes involved in signal transduction including the following: both receptors and ligands related to BMP signaling, complement components involved in immune response, and effector molecules such as kinases and phospholipases (36).

INFLAMMATION CAN AFFECT GRANULOSA AND THECA CELLS WHICH MAY PERTURB CORPUS LUTEUM FORMATION AND FUNCTION

Ovulation is similar to an inflammatory cytokine-mediated response (99, 100) and is associated with an increase in vasodilation, production of prostaglandin, cell proliferation, and secretion of tissue as well as local growth regulatory factors (101, 102). Some studies have suggested that the innate immune system is active in connection with ovulation (101–103). Cytokines are both key modulators of the immune system and contribute to regulation of the ovarian cycle. In fact, the expression and function of innate immune cell-related genes in non-immune cells within the ovary has been reported and provides a novel and important regulatory system during ovulation (104).

Cytokines and chemokines play an important role in ovarian function and follicular development throughout the estrous cycle. One study in early antral follicles (22) found 446 genes in granulosa cells and 248 genes in theca cells, with only 28 regulated genes that were common to granulosa and theca cells. These shared genes were associated with bovine antral follicle development, and they have identified candidate growth factors and cytokines potentially involved in inflammation and cell–cell interactions required for ovarian function such as the following genes: Macrophage inflammatory protein (*MIP1 beta*), Teratocarcinoma-derived growth factor 1 (*TDGF1*), Stromal derived growth factor 1 (*SDF1*; i.e., *CXCL12*), Growth differentiation factor 8 (*GDF8*), Glia maturation factor gamma (*GMFG*), Osteopontin (*SPP1*), Angiopoietin 4 (*ANGPT4*), and Chemokine ligands (*CCL 2, 3, 5*, and *8*) (22).

During the latter stages of follicular development, there is cellular restructuring including follicular wall breakdown, oocyte expulsion and cellular reorganization in preparation for ovulation. These processes are initiated by pro-inflammatory cytokines and chemokines such as interleukin 1α (IL-1α), tumor necrosis factor alpha (TNFα), and chemokine (C-C motif) ligand 4 (CCL4) which stimulate migration of macrophages, monocytes, and leukocytes into the follicle (105). The cytokines indicated above induce an M1 pro-inflammatory phenotype in the infiltrating macrophages that secrete these same pro-inflammatory cytokines, producing a feed-forward mechanism required for ovulation. In some situations such as persistent

follicles (i.e., arrested follicles, such as in PCOS), expression of these pro-inflammatory cytokines is enhanced and may promote increased migration of macrophages, neutrophils, and monocytes into the dominant follicle to potentially reduce granulosa cell proliferation, steroidogenesis and subsequent corpus luteum function (106, 107) (**Figure 4**). Inflammation and cytokines are dramatically higher in follicular fluid from follicles of PCOS patients who are obese (108). In granulosa cells during ovulation, 259 genes were found to be upregulated (2–80-fold) (102). Most of these genes were involved in cytokine signaling to initiate inflammation, innate immunity (102, 109), and cell proliferation factors involved in tissue repair during ovulation (102). The most prominent pathways that represent several modes of cytokine signaling in granulosa cells include MAPK and JAK/STAT signaling (102).

The luteolytic process has also been compared to an acute inflammatory response since it involves infiltration of neutrophils (110–113), macrophages (111, 114–117), and T lymphocytes (111, 115, 116). There is also secretion of cytokines that recruit and potentially trigger leukocytes to become active (118–120). PGF2α rapidly induces many cytokine transcripts in luteal cells (121) such as Tumor necrosis factor alpha (*TNF*) (122, 123), Transforming Growth Factor Beta 1 (*TGFB1*) (123–125), interleukin 1 beta (*IL1B*) (122, 126), and chemokines such as C-C motif chemokine ligand 2 (*CCL2*) (118, 125, 127) and C-X-C motif 8 (*CXCL8*) (112, 113, 123, 125, 126, 128). These cytokines can inhibit progesterone secretion (129–132) and stimulate PGF2α secretion (129, 130, 132). These cytokines can also induce apoptosis in luteal cells (130, 131, 133).

Luteolytic factors secreted by the uterus induce a reduction in blood flow, recruitment and migration of immune cells, reduction in progesterone production, and secretion of pro-inflammatory cytokines within the corpus luteum to induce regression (134, 135). As the intra-luteal concentrations of PGF2α and inflammatory cytokines increase, they may act within an auto-amplification loop until they eventually reach a critical point from which there is no return from the luteolytic cascade (121). Much of the research on immune cells has been conducted in the regressing or late corpus luteum. There is information to suggest that immune cells, mainly macrophages, are present in the corpus luteum (136) and that SLCs produce factors which recruit immune cells (90). Also a recent study demonstrated that depletion of immune cells prior to ovulation blocks ovulation and prevents corpus luteum formation (137).

Several papers have shown that cows with persistent or cystic follicles do have problems ovulating, and women with PCOS also have chronic inflammation. Thus, the types and numbers of immune cells in the follicle may alter ovulation and/or the function and formation of the corpus luteum (**Figure 4**). Lymphocytes do migrate into the corpus luteum and regulate cellular proliferation, steroidogenesis and cell differentiation; however, much needs to be determined about which specific cell types (T, B, Natural Killer; NK) these are and how they might affect any macrophages that are present at the time of ovulation (136). Poole and Pate concluded that, in bovine corpus luteum, the microenvironment regulates the recruitment or differentiation of lymphocyte cells, and these specific lymphocyte cell types (resident T cell lymphocytes) interact

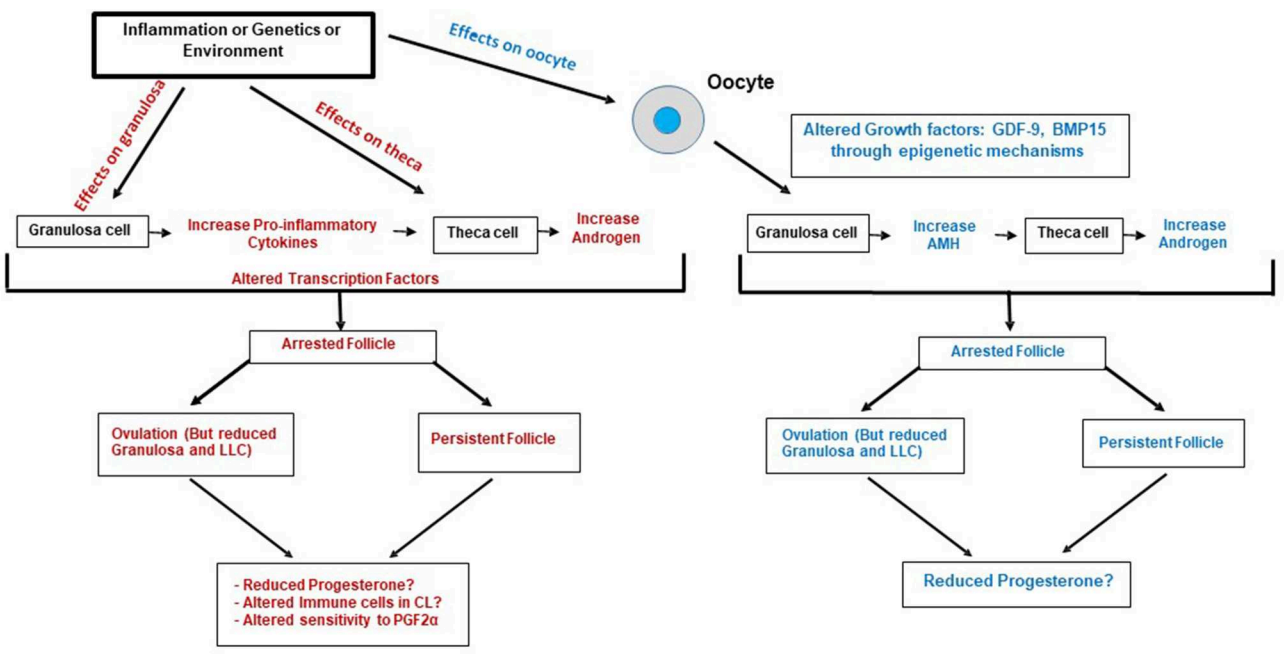

FIGURE 4 | Proposed pathways where Inflammation/Genetics or Environment may cause altered function of individual cells of the follicle (granulosa, oocyte and theca) to alter transcription or expression of genes by epigenetic mechanisms resulting in altered cell to cell communication, arrested follicle development, and anovulation, altered luteal function, and female infertility.

with steroidogenic cells to promote appropriate progesterone production and function of the developing corpus luteum.

A microarray analysis comparing SLC and LLCs determined that gene expression of immune factors were greater in SLCs compared to LLCs in bovine mid-stage corpus luteum, with upregulation of chemokines *CCL2, CCL3, CCL4, CCL5, CCL8,* and *CCL16,* and several CXC chemokines as well as *CX3CL1*. This may suggest that the theca and SLCs have critical functions in directing immune cells to the site of luteal formation to either stabilize its structure, increase progesterone, or enhance vascular development (90).

PERTURBATIONS IN GENE EXPRESSION IN GRANULOSA OR THECA CELLS THROUGH INFLAMMATION AND ALTERED STEROIDOGENESIS MAY ALTER LLCs OR SLCs AND IMPAIR LUTEAL FUNCTION

Stressors During Ovarian Development

Inflammation, environmental stressors, abnormal follicular somatic cell differentiation can result in excess androgens, follicular arrest, anovulation, persistent follicles, and sub-functional corpora lutea, all of which may contribute to female infertility disorders (3, 138) (**Figure 4**). Since steroidogenesis occurs in early fetal life, maternal stressors may perturb cell differentiation of the ovary to alter theca or granulosa cell lineage differentiation and steroid enzyme expression (60–65). Thus, excessive androgen production during the formation of the ovary may affect progenitor cells that give rise to both granulosa cells and theca cells to change their identity. Furthermore, if oocytes or granulosa cells do not express appropriate factors, theca cell differentiation may be altered which may negatively impact formation of the SLCs (and possibly LLCs through cell-cell interaction) and adversely affect the formation and function of the corpus luteum.

Excess Androgens May Affect Follicle Growth and Proliferation of Granulosa Cells

Increased amounts of androgen hormones in the follicular microenvironment are a major factor for follicle arrest (139). Dehydrotestosterone (DHT) treatment reduces granulosa cell cycle progression and FSH-stimulated cell proliferation (140) by decreasing the expression of cell cycle proteins (141). Additionally, DHT stimulates the expression of tumor suppressor gene (*PTEN*) through peroxisome proliferator-activated receptor gamma ($PPAR_{\gamma}$) which in turn suppresses the phosphatidylinositol 3-kinase (PI3K)/AKT signaling pathway, leading to cell cycle arrest and reducing granulosa cell proliferation and viability (142). Several researchers (15, 143) suggest that androgen excess is the most important symptom in PCOS. Women diagnosed with PCOS may have abnormal theca cell function and increased androgens, leading to abnormal ovarian follicular development (15, 144, 145). Excess circulating androgen is associated with ovarian dysfunction and metabolic disorders in women (146). Androgenized rats had fewer estrous cycles and lower numbers of mature and ovulated follicles (142, 145).

TGFβ Family Perturbations Can Alter Granulosa Cell Function

Transforming growth factor beta family growth factors have specific roles in follicle arrest and progression. One TGFβ family member, Anti-Mullerian growth factor (AMH) is produced by large dominant follicles (in humans and bovine) and suppresses other growing follicles until just prior to ovulation (147) (**Figures 1**, **4**), AMH also inhibits FSH-stimulated functions of bovine granulosa cells (147). A majority of women diagnosed with PCOS also have excess granulosa cell production of AMH and another TGFβ family member, follistatin (FST) (148). The excess AMH may be caused by genetic variants in the *AMH* or *AMHR* genes (149) or due to oocyte factors (BMP15 and GDF-9) causing acetylation of histone 3 lysine 27 (H3K27ac) (150) in granulosa cells to enhance *AMH* transcription (**Figure 4**). Furthermore, AMH inhibits aromatase and reduces estrogen production, resulting in excess androgens (151, 152). In human follicles (85) expression of *FST* is positively correlated with *AMH*, *FSHR*, and *AR*. Follistatin and its family member FSTL4 are upregulated in LLCs compared to SLCs (90) in the bovine corpus luteum, suggesting that TGFβ family member secretion (e.g., FST) by LLCs may continue to regulate developing follicles for the subsequent cycle. Thus, alterations in AMH and other TGFβ family members in women diagnosed with PCOS may also indicate changes in their follicles and subsequent corpus luteum function.

Altered Follicular Development and Subsequent Luteal Function

The development and regression of the corpus luteum in ovulatory women with polycystic ovaries have been studied and compared with normally cycling women, and the corpora lutea exhibited no morphological or degenerative differences (153). However, in women with sporadic or chronic anovulation, there is reduced progesterone throughout the menstrual cycle (154) suggesting there is potential for altered luteal function. (155). Additionally, cows with persistent follicles have been demonstrated to develop sub-functional corpus luteum which cannot maintain a pregnancy (156). In androgenized sheep models, the development of PCOS-like phenotypes also results in luteal dysfunction resulting in early pregnancy failure (12). Thus, many facets of luteal function need to be evaluated, including abnormal follicular somatic cell lineage differentiation, to determine how therapies may be employed to maintain progesterone production and promote appropriate luteal formation in mammals.

In summary, anovulation is the leading reproductive disorder in mammalian females. Understanding what affects the ovulation process in order to cause anovulation is essential to improve female fertility. The formation of a functional corpus luteum relies on the appropriate proliferation and differentiation of both granulosa and theca cells. Any disruption in the crosstalk between granulosa and theca cell or differentiation of these cells types alters lineages and gene expression profiles that could negatively impact luteinization and progesterone production.

Moreover, there are a number of autocrine and paracrine factors can affect the formation of the corpus luteum, e.g., growth factors, androgen excess, and inflammatory cytokines as discussed within this review. We hope that this review will spark interest and research to better understand the complex and fascinating processes used during the formation and regression of the corpus luteum.

AUTHOR CONTRIBUTIONS

All authors listed have made a substantial, direct and intellectual contribution to the work, and approved it for publication.

FUNDING

This research was supported by National Institute of Food and Agriculture 2013-67015-20965 and 2017-67015-26450 to AC and JD, NIH HD092263 and HD087402 to AC and JD, University of Nebraska Food for Health Competitive Grants to AC and JD, United States Department of Agriculture Hatch grant NEB26-202/W3112 Accession #1011127 to AC, Hatch–NEB ANHL Accession #1002234 to AC, National Institute of Food and Agriculture postdoctoral fellowship 2016-67012-24697 to SR, and funds from the VA Research and Development Service, and Olson Center for Women's Health to JD.

REFERENCES

1. Bianchi DW, Klinger KW, Vadnais TJ, Demaria MA, Shuber AP, Skoletsky J, et al. Development of a model system to compare cell separation methods for the isolation of fetal cells from maternal blood. *Prenat Diagn*. (1996) 16:289–98. doi: 10.1002/(SICI)1097-0223(199604)16:4<289::AID-PD843>3.0.CO;2-T
2. McGee EA, Hsueh AJ. Initial and cyclic recruitment of ovarian follicles. *Endocr Rev*. (2000) 21:200–14. doi: 10.1210/er.21.2.200
3. Hummitzsch K, Anderson RA, Wilhelm D, Wu J, Telfer EE, Russell DL, et al. Stem cells, progenitor cells, and lineage decisions in the ovary. *Endocr Rev*. (2015) 36:65–91. doi: 10.1210/er.2014-1079
4. Liu C, Peng J, Matzuk MM, Yao HH. Lineage specification of ovarian theca cells requires multicellular interactions via oocyte and granulosa cells. *Nat Commun*. (2015) 6:6934. doi: 10.1038/ncomms7934
5. Kezele P, Skinner MK. Regulation of ovarian primordial follicle assembly and development by estrogen and progesterone: endocrine model of follicle assembly. *Endocrinology*. (2003) 144:3329–37. doi: 10.1210/en.2002-0131
6. Pepling ME. From primordial germ cell to primordial follicle: mammalian female germ cell development. *Genesis*. (2006) 44:622–32. doi: 10.1002/dvg.20258
7. Nilsson EE, Skinner MK. Progesterone regulation of primordial follicle assembly in bovine fetal ovaries. *Mol Cell Endocrinol*. (2009) 313:9–16. doi: 10.1016/j.mce.2009.09.004
8. Erickson BH. Development and senescence of the postnatal bovine ovary. *J Anim Sci*. (1966) 25:800–5. doi: 10.2527/jas1966.253800x
9. Byskov AG, Skakkebaek NE, Stafanger G, Peters H. Influence of ovarian surface epithelium and rete ovarii on follicle formation. *J Anat*. (1977) 123(Pt 1):77–86.
10. Smitz JE, Cortvrindt RG. The earliest stages of folliculogenesis *in vitro*. *Reproduction*. (2002) 123:185–202. doi: 10.1530/rep.0.1230185
11. Russe I. Oogenesis in cattle and sheep. *Bibl Anat*. (1983) 24:77–92.
12. Padmanabhan V, Veiga-Lopez A. Reproduction symposium: developmental programming of reproductive and metabolic health. *J Anim Sci*. (2014) 92:3199–210. doi: 10.2527/jas.2014-7637
13. Pepling ME. Follicular assembly: mechanisms of action. *Reproduction*. (2012) 143:139–49. doi: 10.1530/REP-11-0299
14. Hirshfield AN. Development of follicles in the mammalian ovary. *Int Rev Cytol*. (1991) 124:43–101. doi: 10.1016/S0074-7696(08)61524-7
15. Abbott DH, Dumesic DA, Franks S. Developmental origin of polycystic ovary syndrome - a hypothesis. *J Endocrinol*. (2002) 174:1–5. doi: 10.1677/joe.0.1740001
16. Braw-Tal R, Yossefi S. Studies *in vivo* and *in vitro* on the initiation of follicle growth in the bovine ovary. *J Reprod Fertil*. (1997) 109:165–71. doi: 10.1530/jrf.0.1090165
17. Picton HM. Activation of follicle development: the primordial follicle. *Theriogenology*. (2001) 55:1193–210. doi: 10.1016/S0093-691X(01)00478-2
18. Edson MA, Nagaraja AK, Matzuk MM. The mammalian ovary from genesis to revelation. *Endocr Rev*. (2009) 30:624–712. doi: 10.1210/er.2009-0012
19. Senger PL. *Pathways to Pregnancy and Parturition*. Ephrata, PA: Cadmus Professional Communications (2012).
20. Magoffin DA. Ovarian theca cell. *Int J Biochem Cell Biol*. (2005) 37:1344–9. doi: 10.1016/j.biocel.2005.01.016
21. Cushman RA, Allan MF, Kuehn LA, Snelling WM, Cupp AS, Freetly HC. Evaluation of antral follicle count and ovarian morphology in crossbred beef cows: investigation of influence of stage of the estrous cycle, age, and birth weight. *J Anim Sci*. (2009) 87:1971–80. doi: 10.2527/jas.2008-1728
22. Skinner MK, Schmidt M, Savenkova MI, Sadler-Riggleman I, Nilsson EE. Regulation of granulosa and theca cell transcriptomes during ovarian antral follicle development. *Mol Reprod Dev*. (2008) 75:1457–72. doi: 10.1002/mrd.20883
23. Adams GP, Jaiswal R, Singh J, Malhi P. Progress in understanding ovarian follicular dynamics in cattle. *Theriogenology*. (2008) 69:72–80. doi: 10.1016/j.theriogenology.2007.09.026
24. Conley AJ, Bird IM. The role of cytochrome P450 17 alpha-hydroxylase and 3 beta-hydroxysteroid dehydrogenase in the integration of gonadal and adrenal steroidogenesis via the delta 5 and delta 4 pathways of steroidogenesis in mammals. *Biol Reprod*. (1997) 56:789–99. doi: 10.1095/biolreprod56.4.789
25. Evans AC. Characteristics of ovarian follicle development in domestic animals. *Reprod Domest Anim*. (2003) 38:240–6. doi: 10.1046/j.1439-0531.2003.00439.x
26. Ireland JJ, Zielak-Steciwko AE, Jimenez-Krassel F, Folger J, Bettegowda A, Scheetz D, et al. Variation in the ovarian reserve is linked to alterations in intrafollicular estradiol production and ovarian biomarkers of follicular differentiation and oocyte quality in cattle. *Biol Reprod*. (2009) 80:954–64. doi: 10.1095/biolreprod.108.073791
27. Doshi SB, Agarwal A. The role of oxidative stress in menopause. *J Midlife Health*. (2013) 4:140–6. doi: 10.4103/0976-7800.118990
28. Roche JF. Control and regulation of folliculogenesis–a symposium in perspective. *Rev Reprod*. (1996) 1:19–27. doi: 10.1530/revreprod/1.1.19
29. Smith MF, McIntush EW, Smith GW. Mechanisms associated with corpus luteum development. *J Anim Sci*. (1994) 72:1857–72. doi: 10.2527/1994.7271857x
30. Wiltbank MC, Salih SM, Atli MO, Luo W, Bormann CL, Ottobre JS, et al. Comparison of endocrine and cellular mechanisms regulating the corpus luteum of primates and ruminants. *Anim Reprod*. (2012) 9:242–59.
31. Davis JS, Rueda BR. The corpus luteum: an ovarian structure with maternal instincts and suicidal tendencies. *Front Biosci*. (2002) 7:d1949–78. doi: 10.2741/A891
32. Davis JS, LaVoie HA. Molecular regulation of progesterone production in the corpus luteum. In: Leung PCK, Adashi EY, editors. *The Ovary*. Academic Press (2019). p. 237–53.
33. Talbott H, Davis JS. Lipid droplets and metabolic pathways regulate steroidogenesis in the corpus luteum. In: Meidan R, editor. *The Life Cycle of the Corpus Luteum*. Cham: Springer (2017). p. 57–78.
34. Khanthusaeng V, Thammasiri J, Bass CS, Navanukraw C, Borowicz P, Redmer DA, et al. Lipid droplets in cultured luteal cells in non-pregnant sheep fed different planes of nutrition. *Acta Histochem*. (2016) 118:553–9. doi: 10.1016/j.acthis.2016.05.007
35. Meidan R, Girsh E, Blum O, Aberdam E. *In vitro* differentiation of bovine theca and granulosa cells into small and large luteal-like cells:

morphological and functional characteristics. *Biol Reprod*. (1990) 43:913–21. doi: 10.1095/biolreprod43.6.913
36. Romereim SM, Summers AF, Pohlmeier WE, Zhang P, Hou X, Talbott HA, et al. Gene expression profiling of bovine ovarian follicular and luteal cells provides insight into cellular identities and functions. *Mol Cell Endocrinol*. (2017) 439:379–94. doi: 10.1016/j.mce.2016.09.029
37. Hild-Petito S, West NB, Brenner RM, Stouffer RL. Localization of androgen receptor in the follicle and corpus luteum of the primate ovary during the menstrual cycle. *Biol Reprod*. (1991) 44:561–8. doi: 10.1095/biolreprod44.3.561
38. Lavranos TC, Rodgers HF, Bertoncello I, Rodgers RJ. Anchorage-independent culture of bovine granulosa cells: the effects of basic fibroblast growth factor and dibutyryl cAMP on cell division and differentiation. *Exp Cell Res*. (1994) 211:245–51. doi: 10.1006/excr.1994.1084
39. Rodgers RJ, Lavranos TC, van Wezel IL, Irving-Rodgers HF. Development of the ovarian follicular epithelium. *Mol Cell Endocrinol*. (1999) 151:171–9. doi: 10.1016/S0303-7207(99)00087-8
40. Davis JS, Rueda BR, Spanel-Borowski K. Microvascular endothelial cells of the corpus luteum. *Reprod Biol Endocrinol*. (2003) 1:89. doi: 10.1186/1477-7827-1-89
41. Hummitzsch K, Irving-Rodgers HF, Hatzirodos N, Bonner W, Sabatier L, Reinhardt DP, et al. A new model of development of the mammalian ovary and follicles. *PLoS ONE*. (2013) 8:e55578. doi: 10.1371/journal.pone.0055578
42. Rotgers E, Jorgensen A, Yao HH. At the crossroads of fate-somatic cell lineage specification in the fetal gonad. *Endocr Rev*. (2018) 39:739–59. doi: 10.1210/er.2018-00010
43. Byskov AG. The role of the rete ovarii in meiosis and follicle formation in the cat, mink and ferret. *J Reprod Fertil*. (1975) 45:201–9. doi: 10.1530/jrf.0.0450201
44. Hirshfield AN. Heterogeneity of cell populations that contribute to the formation of primordial follicles in rats. *Biol Reprod*. (1992) 47:466–72. doi: 10.1095/biolreprod47.3.466
45. Hirshfield AN, DeSanti AM. Patterns of ovarian cell proliferation in rats during the embryonic period and the first three weeks postpartum. *Biol Reprod*. (1995) 53:1208–21. doi: 10.1095/biolreprod53.5.1208
46. McLaren A. Germ and somatic cell lineages in the developing gonad. *Mol Cell Endocrinol*. (2000) 163:3–9. doi: 10.1016/S0303-7207(99)00234-8
47. Liu Z, Ren YA, Pangas SA, Adams J, Zhou W, Castrillon DH, et al. FOXO1/3 and PTEN depletion in granulosa cells promotes ovarian granulosa cell tumor development. *Mol Endocrinol*. (2015) 29:1006–24. doi: 10.1210/me.2015-1103
48. Young JM, McNeilly AS. Theca: the forgotten cell of the ovarian follicle. *Reproduction*. (2010) 140:489–504. doi: 10.1530/REP-10-0094
49. Honda A, Hirose M, Hara K, Matoba S, Inoue K, Miki H, et al. Isolation, characterization, and *in vitro* and *in vivo* differentiation of putative thecal stem cells. *Proc Natl Acad Sci USA*. (2007) 104:12389–94. doi: 10.1073/pnas.0703787104
50. Liu CF, Liu C, Yao HH. Building pathways for ovary organogenesis in the mouse embryo. *Curr Top Dev Biol*. (2010) 90:263–90. doi: 10.1016/S0070-2153(10)90007-0
51. Swain A, Lovell-Badge R. Mammalian sex determination: a molecular drama. *Genes Dev*. (1999) 13:755–67. doi: 10.1101/gad.13.7.755
52. Hatzirodos N, Nigro J, Irving-Rodgers HF, Vashi AV, Hummitzsch K, Caterson B, et al. Glycomic analyses of ovarian follicles during development and atresia. *Matrix Biol*. (2012) 31:45–56. doi: 10.1016/j.matbio.2011.10.002
53. Fortune JE, Armstrong DT. Hormonal control of 17 beta-estradiol biosynthesis in proestrous rat follicles: estradiol production by isolated theca versus granulosa. *Endocrinology*. (1978) 102:227–35. doi: 10.1210/endo-102-1-227
54. Devoto L, Vega M, Kohen P, Castro A, Castro O, Christenson LK, et al. Endocrine and paracrine-autocrine regulation of the human corpus luteum during the mid-luteal phase. *J Reprod Fertil Suppl*. (2000) 55:13–20.
55. Miller WL. Disorders in the initial steps of steroid hormone synthesis. *J Steroid Biochem Mol Biol*. (2017) 165(Pt A):18–37. doi: 10.1016/j.jsbmb.2016.03.009
56. Falck B. Site of production of oestrogen in rat ovary as studied in micro-transplants. *Acta Physiol Scand Suppl*. (1959) 47:1–101. doi: 10.1111/j.1748-1716.1960.tb01823.x
57. Jamnongjit M, Hammes SR. Ovarian steroids: the good, the bad, and the signals that raise them. *Cell Cycle*. (2006) 5:1178–83. doi: 10.4161/cc.5.11.2803
58. Patel SS, Beshay VE, Escobar JC, Suzuki T, Carr BR. Molecular mechanism for repression of 17alpha-hydroxylase expression and androstenedione production in granulosa cells. *J Clin Endocrinol Metab*. (2009) 94:5163–8. doi: 10.1210/jc.2009-1341
59. Patel SS, Beshay VE, Escobar JC, Carr BR. 17alpha-Hydroxylase (CYP17) expression and subsequent androstenedione production in the human ovary. *Reprod Sci*. (2010) 17:978–86. doi: 10.1177/1933719110379055
60. Shemesh M. Estradiol-17 beta biosynthesis by the early bovine fetal ovary during the active and refractory phases. *Biol Reprod*. (1980) 23:577–82. doi: 10.1095/biolreprod23.3.577
61. Dominguez MM, Liptrap RM, Basrur PK. Steroidogenesis in fetal bovine gonads. *Can J Vet Res*. (1988) 52:401–6.
62. Quirke LD, Juengel JL, Tisdall DJ, Lun S, Heath DA, McNatty KP. Ontogeny of steroidogenesis in the fetal sheep gonad. *Biol Reprod*. (2001) 65:216–28. doi: 10.1095/biolreprod65.1.216
63. Yang MY, Fortune JE. The capacity of primordial follicles in fetal bovine ovaries to initiate growth *in vitro* develops during mid-gestation and is associated with meiotic arrest of oocytes. *Biol Reprod*. (2008) 78:1153–61. doi: 10.1095/biolreprod.107.066688
64. Burkhart MN, Juengel JL, Smith PR, Heath DA, Perry GA, Smith MF, et al. Morphological development and characterization of aromatase and estrogen receptors alpha and beta in fetal ovaries of cattle from days 110 to 250. *Anim Reprod Sci*. (2010) 117:43–54. doi: 10.1016/j.anireprosci.2009.02.010
65. Garverick HA, Juengel JL, Smith P, Heath DA, Burkhart MN, Perry GA, et al. Development of the ovary and ontongeny of mRNA and protein for P450 aromatase (arom) and estrogen receptors (ER) alpha and beta during early fetal life in cattle. *Anim Reprod Sci*. (2010) 117:24–33. doi: 10.1016/j.anireprosci.2009.05.004
66. Chen Y, Jefferson WN, Newbold RR, Padilla-Banks E, Pepling ME. Estradiol, progesterone, and genistein inhibit oocyte nest breakdown and primordial follicle assembly in the neonatal mouse ovary *in vitro* and *in vivo*. *Endocrinology*. (2007) 148:3580–90. doi: 10.1210/en.2007-0088
67. Fortune JE, Yang MY, Allen JJ, Herrick SL. Triennial Reproduction Symposium: the ovarian follicular reserve in cattle: what regulates its formation and size? *J Anim Sci*. (2013) 91:3041–50. doi: 10.2527/jas.2013-6233
68. Juengel JL, Sawyer HR, Smith PR, Quirke LD, Heath DA, Lun S, et al. Origins of follicular cells and ontogeny of steroidogenesis in ovine fetal ovaries. *Mol Cell Endocrinol*. (2002) 191:1–10. doi: 10.1016/S0303-7207(02)00045-X
69. da Silva RB, Yang MY, Caixeta ES, Castilho AC, Amorim RL, Price CA, et al. Fibroblast growth factor 18 regulates steroidogenesis in fetal bovine ovarian tissue *in vitro*. *Mol Reprod Dev*. (2019) 86:166–74. doi: 10.1002/mrd.23091
70. Magoffin DA, Weitsman SR. Insulin-like growth factor-I regulation of luteinizing hormone (LH) receptor messenger ribonucleic acid expression and LH-stimulated signal transduction in rat ovarian theca-interstitial cells. *Biol Reprod*. (1994) 51:766–75. doi: 10.1095/biolreprod51.4.766
71. Wood JR, Strauss JF III. Multiple signal transduction pathways regulate ovarian steroidogenesis. *Rev Endocr Metab Disord*. (2002) 3:33–46. doi: 10.1023/A:1012748718150
72. Stocco DM, Clark BJ. Regulation of the acute production of steroids in steroidogenic cells. *Endocr Rev*. (1996) 17:221–44. doi: 10.1210/er.17.3.221
73. Elustondo P, Martin LA, Karten B. Mitochondrial cholesterol import. *Biochim Biophys Acta Mol Cell Biol Lipids*. (2017) 1862:90–101. doi: 10.1016/j.bbalip.2016.08.012
74. Hunzicker-Dunn ME, Lopez-Biladeau B, Law NC, Fiedler SE, Carr DW, Maizels ET. PKA and GAB2 play central roles in the FSH signaling pathway to PI3K and AKT in ovarian granulosa cells. *Proc Natl Acad Sci USA*. (2012) 109:E2979–88. doi: 10.1073/pnas.1205661109
75. Fu D, Lv X, Hua G, He C, Dong J, Lele SM, et al. YAP regulates cell proliferation, migration, and steroidogenesis in adult granulosa cell tumors. *Endocr Relat Cancer*. (2014) 21:297–310. doi: 10.1530/ERC-13-0339
76. Puri P, Little-Ihrig L, Chandran U, Law NC, Hunzicker-Dunn M, Zeleznik AJ. Protein kinase a: a master kinase of granulosa cell differentiation. *Sci Rep*. (2016) 6:28132. doi: 10.1038/srep28132

77. Law NC, Donaubauer EM, Zeleznik AJ, Hunzicker-Dunn M. How protein kinase A activates canonical tyrosine kinase signaling pathways to promote granulosa cell differentiation. *Endocrinology*. (2017) 158:2043–51. doi: 10.1210/en.2017-00163
78. Lv X, He C, Huang C, Wang H, Hua G, Wang Z, et al. Timely expression and activation of YAP1 in granulosa cells is essential for ovarian follicle development. *FASEB J*. (2019) 33:10049–64. doi: 10.1096/fj.201900179RR
79. Plewes MR, Hou X, Zhang P, Liang A, Hua G, Wood JR, et al. Yes-associated protein (YAP1) is required for proliferation and function of bovine granulosa cells *in vitro*. *Biol Reprod*. (2019). doi: 10.1093/biolre/ioz139
80. Bao B, Garverick HA, Smith GW, Smith MF, Salfen BE, Youngquist RS. Changes in messenger ribonucleic acid encoding luteinizing hormone receptor, cytochrome P450-side chain cleavage, and aromatase are associated with recruitment and selection of bovine ovarian follicles. *Biol Reprod*. (1997) 56:1158–68. doi: 10.1095/biolreprod56.5.1158
81. Logan KA, Juengel JL, McNatty KP. Onset of steroidogenic enzyme gene expression during ovarian follicular development in sheep. *Biol Reprod*. (2002) 66:906–16. doi: 10.1095/biolreprod66.4.906
82. Hatzirodos N, Hummitzsch K, Irving-Rodgers HF, Rodgers RJ. Transcriptome comparisons identify new cell markers for theca interna and granulosa cells from small and large antral ovarian follicles. *PLoS ONE*. (2015) 10:e0119800. doi: 10.1371/journal.pone.0119800
83. Raja-Khan N, Urbanek M, Rodgers RJ, Legro RS. The role of TGF-beta in polycystic ovary syndrome. *Reprod Sci*. (2014) 21:20–31. doi: 10.1177/1933719113485294
84. Yalamanchi SK, Sam S, Cardenas MO, Holaday LW, Urbanek M, Dunaif A. Association of fibrillin-3 and transcription factor-7-like 2 gene variants with metabolic phenotypes in PCOS. *Obesity*. (2012) 20:1273–8. doi: 10.1038/oby.2011.400
85. Jeppesen JV, Nielsen ME, Kristensen SG, Yding Andersen C. Concentration of activin A and follistatin in follicular fluid from human small antral follicles associated to gene expression of the corresponding granulosa cells. *Mol Cell Endocrinol*. (2012) 356:48–54. doi: 10.1016/j.mce.2011.07.051
86. Forde N, Beltman ME, Lonergan P, Diskin M, Roche JF, Crowe MA. Oestrous cycles in Bos taurus cattle. *Anim Reprod Sci*. (2011) 124:163–9. doi: 10.1016/j.anireprosci.2010.08.025
87. Miyamoto A, Shirasuna K, Shimizu T, Bollwein H, Schams D. Regulation of corpus luteum development and maintenance: specific roles of angiogenesis and action of prostaglandin F2alpha. *Soc Reprod Fertil Suppl*. (2010) 67:289–304. doi: 10.7313/UPO9781907284991.024
88. Schams D, Berisha B. Regulation of corpus luteum function in cattle–an overview. *Reprod Domest Anim*. (2004) 39:241–51. doi: 10.1111/j.1439-0531.2004.00509.x
89. Berisha B, Schams D. Ovarian function in ruminants. *Domest Anim Endocrinol*. (2005) 29:305–17. doi: 10.1016/j.domaniend.2005.02.035
90. Baddela VS, Koczan D, Viergutz T, Vernunft A, Vanselow J. Global gene expression analysis indicates that small luteal cells are involved in extracellular matrix modulation and immune cell recruitment in the bovine corpus luteum. *Mol Cell Endocrinol*. (2018) 474:201–13. doi: 10.1016/j.mce.2018.03.011
91. Niswender GD, Schwall RH, Fitz TA, Farin CE, Sawyer HR. Regulation of luteal function in domestic ruminants: new concepts. *Recent Prog Horm Res*. (1985) 41:101–51. doi: 10.1016/B978-0-12-571141-8.50007-X
92. White LM, Keisler DH, Dailey RA, Inskeep EK. Characterization of ovine follicles destined to form subfunctional corpora lutea. *J Anim Sci*. (1987) 65:1595–601. doi: 10.2527/jas1987.6561595x
93. Rueda BR, Hendry IR, Hendry IW, Stormshak F, Slayden OD, Davis JS. Decreased progesterone levels and progesterone receptor antagonists promote apoptotic cell death in bovine luteal cells. *Biol Reprod*. (2000) 62:269–76. doi: 10.1095/biolreprod62.2.269
94. Odde KG. A review of synchronization of estrus in postpartum cattle. *J Anim Sci*. (1990) 68:817–30. doi: 10.2527/1990.683817x
95. Hansen TR, Bott R, Romero J, Antoniazzi A, Davis JS. Corpus luteum and early pregnancy in ruminants. In: Meidan R, editor. *The Life Cycle of the Corpus Luteum*. Cham: Springer (2017). p. 205–25.
96. Romero JJ, Antoniazzi AQ, Smirnova NP, Webb BT, Yu F, Davis JS, et al. Pregnancy-associated genes contribute to antiluteolytic mechanisms in ovine corpus luteum. *Physiol Genomics*. (2013) 45:1095–108. doi: 10.1152/physiolgenomics.00082.2013
97. Christenson LK, Gunewardena S, Hong X, Spitschak M, Baufeld A, Vanselow J. Research resource: preovulatory LH surge effects on follicular theca and granulosa transcriptomes. *Mol Endocrinol*. (2013) 27:1153–71. doi: 10.1210/me.2013-1093
98. Koos RD, Hansel W. The large and small cells of the bovine corpus luteum: ultrastructural and functional differences. In Schwartz NB, Hunzicker-Dunn M. *In Dynamics of Ovarian Function*. New York, NY: Raven Press (1981). p. 197–203.
99. Espey LL. Ovulation as an inflammatory reaction–a hypothesis. *Biol Reprod*. (1980) 22:73–106. doi: 10.1095/biolreprod22.1.73
100. Duffy DM, Ko C, Jo M, Brannstrom M, Curry TE. Ovulation: parallels with inflammatory processes. *Endocr Rev*. (2019) 40:369–416. doi: 10.1210/er.2018-00075
101. Stassi AF, Baravalle ME, Belotti EM, Amweg AN, Angeli E, Velazquez MML, et al. Altered expression of IL-1beta, IL-1RI, IL-1RII, IL-1RA and IL-4 could contribute to anovulation and follicular persistence in cattle. *Theriogenology*. (2018) 110:61–73. doi: 10.1016/j.theriogenology.2017.12.048
102. Poulsen LC, Englund ALM, Wissing MLM, Yding Andersen C, Borup R, Grondahl ML. Human granulosa cells function as innate immune cells executing an inflammatory reaction during ovulation: a microarray analysis. *Mol Cell Endocrinol*. (2019) 486:34–46. doi: 10.1016/j.mce.2019.02.014
103. Richards JS, Liu Z, Shimada M. Immune-like mechanisms in ovulation. *Trends Endocrinol Metab*. (2008) 19:191–6. doi: 10.1016/j.tem.2008.03.001
104. Liu Z, Shimada M, Richards JS. The involvement of the Toll-like receptor family in ovulation. *J Assist Reprod Genet*. (2008) 25:223–8. doi: 10.1007/s10815-008-9219-0
105. Spanel-Borowski K. Ovulation as danger signaling event of innate immunity. *Mol Cell Endocrinol*. (2011) 333:1–7. doi: 10.1016/j.mce.2010.12.008
106. Orostica L, Astorga I, Plaza-Parrochia F, Vera C, Garcia V, Carvajal R, et al. Proinflammatory environment and role of TNF-alpha in endometrial function of obese women having polycystic ovarian syndrome. *Int J Obes*. (2016) 40:1715–22. doi: 10.1038/ijo.2016.154
107. Lee JY, Tae JC, Kim CH, Hwang D, Kim KC, Suh CS, et al. Expression of the genes for peroxisome proliferator-activated receptor-gamma, cyclooxygenase-2, and proinflammatory cytokines in granulosa cells from women with polycystic ovary syndrome. *Clin Exp Reprod Med*. (2017) 44:146–51. doi: 10.5653/cerm.2017.44.3.146
108. Adams J, Liu Z, Ren YA, Wun WS, Zhou W, Kenigsberg S, et al. Enhanced inflammatory transcriptome in the granulosa cells of women with polycystic ovarian syndrome. *J Clin Endocrinol Metab*. (2016) 101:3459–68. doi: 10.1210/jc.2015-4275
109. Hernandez-Gonzalez I, Gonzalez-Robayna I, Shimada M, Wayne CM, Ochsner SA, White L, et al. Gene expression profiles of cumulus cell oocyte complexes during ovulation reveal cumulus cells express neuronal and immune-related genes: does this expand their role in the ovulation process? *Mol Endocrinol*. (2006) 20:1300–21. doi: 10.1210/me.2005-0420
110. Brannstrom M, Giesecke L, Moore IC, van den Heuvel CJ, Robertson SA. Leukocyte subpopulations in the rat corpus luteum during pregnancy and pseudopregnancy. *Biol Reprod*. (1994) 50:1161–7. doi: 10.1095/biolreprod50.5.1161
111. Best CL, Pudney J, Welch WR, Burger N, Hill JA. Localization and characterization of white blood cell populations within the human ovary throughout the menstrual cycle and menopause. *Hum Reprod*. (1996) 11:790–7. doi: 10.1093/oxfordjournals.humrep.a019256
112. Jiemtaweeboon S, Shirasuna K, Nitta A, Kobayashi A, Schuberth HJ, Shimizu T, et al. Evidence that polymorphonuclear neutrophils infiltrate into the developing corpus luteum and promote angiogenesis with interleukin-8 in the cow. *Reprod Biol Endocrinol*. (2011) 9:79. doi: 10.1186/1477-7827-9-79
113. Shirasuna K, Jiemtaweeboon S, Raddatz S, Nitta A, Schuberth HJ, Bollwein H, et al. Rapid accumulation of polymorphonuclear neutrophils in the corpus luteum during prostaglandin F(2alpha)-induced luteolysis in the cow. *PLoS ONE*. (2012) 7:e29054. doi: 10.1371/journal.pone.0029054
114. Gaytan F, Morales C, Garcia-Pardo L, Reymundo C, Bellido C, Sanchez-Criado JE. Macrophages, cell proliferation, and cell death in the human menstrual corpus luteum. *Biol Reprod*. (1998) 59:417–25. doi: 10.1095/biolreprod59.2.417

115. Penny LA, Armstrong D, Bramley TA, Webb R, Collins RA, Watson ED. Immune cells and cytokine production in the bovine corpus luteum throughout the oestrous cycle and after induced luteolysis. *J Reprod Fertil*. (1999) 115:87–96. doi: 10.1530/jrf.0.1150087
116. Bauer M, Reibiger I, Spanel-Borowski K. Leucocyte proliferation in the bovine corpus luteum. *Reproduction*. (2001) 121:297–305. doi: 10.1530/rep.0.1210297
117. Wu J, Groh V, Spies T. T cell antigen receptor engagement and specificity in the recognition of stress-inducible MHC class I-related chains by human epithelial gamma delta T cells. *J Immunol*. (2002) 169:1236–40. doi: 10.4049/jimmunol.169.3.1236
118. Townson DH, Liptak AR. Chemokines in the corpus luteum: implications of leukocyte chemotaxis. *Reprod Biol Endocrinol*. (2003) 1:94. doi: 10.1186/1477-7827-1-94
119. Pate JL, Toyokawa K, Walusimbi S, Brzezicka E. The interface of the immune and reproductive systems in the ovary: lessons learned from the corpus luteum of domestic animal models. *Am J Reprod Immunol*. (2010) 64:275–86. doi: 10.1111/j.1600-0897.2010.00906.x
120. Shirasuna K, Akabane Y, Beindorff N, Nagai K, Sasaki M, Shimizu T, et al. Expression of prostaglandin F2alpha (PGF2alpha) receptor and its isoforms in the bovine corpus luteum during the estrous cycle and PGF2alpha-induced luteolysis. *Domest Anim Endocrinol*. (2012) 43:227–38. doi: 10.1016/j.domaniend.2012.03.003
121. Talbott H, Hou X, Qiu F, Zhang P, Guda C, Yu F, et al. Early transcriptome responses of the bovine midcycle corpus luteum to prostaglandin F2alpha includes cytokine signaling. *Mol Cell Endocrinol*. (2017) 452:93–109. doi: 10.1016/j.mce.2017.05.018
122. Neuvians TP, Schams D, Berisha B, Pfaffl MW. Involvement of pro-inflammatory cytokines, mediators of inflammation, and basic fibroblast growth factor in prostaglandin F2alpha-induced luteolysis in bovine corpus luteum. *Biol Reprod*. (2004) 70:473–80. doi: 10.1095/biolreprod.103.016154
123. Shah KB, Tripathy S, Suganthi H, Rudraiah M. Profiling of luteal transcriptome during prostaglandin F2-alpha treatment in buffalo cows: analysis of signaling pathways associated with luteolysis. *PLoS ONE*. (2014) 9:e104127. doi: 10.1371/journal.pone.0104127
124. Hou X, Arvisais EW, Jiang C, Chen DB, Roy SK, Pate JL, et al. Prostaglandin F2alpha stimulates the expression and secretion of transforming growth factor B1 via induction of the early growth response 1 gene (EGR1) in the bovine corpus luteum. *Mol Endocrinol*. (2008) 22:403–14. doi: 10.1210/me.2007-0272
125. Mondal M, Schilling B, Folger J, Steibel JP, Buchnick H, Zalman Y, et al. Deciphering the luteal transcriptome: potential mechanisms mediating stage-specific luteolytic response of the corpus luteum to prostaglandin F(2)alpha. *Physiol Genomics*. (2011) 43:447–56. doi: 10.1152/physiolgenomics.00155.2010
126. Atli MO, Bender RW, Mehta V, Bastos MR, Luo W, Vezina CM, et al. Patterns of gene expression in the bovine corpus luteum following repeated intrauterine infusions of low doses of prostaglandin F2alpha. *Biol Reprod*. (2012) 86:130. doi: 10.1095/biolreprod.111.094870
127. Penny LA, Armstrong DG, Baxter G, Hogg C, Kindahl H, Bramley T, et al. Expression of monocyte chemoattractant protein-1 in the bovine corpus luteum around the time of natural luteolysis. *Biol Reprod*. (1998) 59:1464–9. doi: 10.1095/biolreprod59.6.1464
128. Talbott H, Delaney A, Zhang P, Yu Y, Cushman RA, Cupp AS, et al. Effects of IL8 and immune cells on the regulation of luteal progesterone secretion. *Reproduction*. (2014) 148:21–31. doi: 10.1530/REP-13-0602
129. Fairchild DL, Pate JL. Modulation of bovine luteal cell synthetic capacity by interferon-gamma. *Biol Reprod*. (1991) 44:357–63. doi: 10.1095/biolreprod44.2.357
130. Benyo DF, Pate JL. Tumor necrosis factor-alpha alters bovine luteal cell synthetic capacity and viability. *Endocrinology*. (1992) 130:854–60. doi: 10.1210/en.130.2.854
131. Wuttke W, Pitzel L, Knoke I, Theiling K, Jarry H. Immune-endocrine interactions affecting luteal function in pigs. *J Reprod Fertil Suppl*. (1997) 52:19–29.
132. Estevez A, Tognetti T, Luchetti CG, Sander V, Motta AB. Sequence of interleukin 1beta actions on corpus luteum regression: relationship with inducible cyclooxygenase and nitric oxide synthase expression. *Reproduction*. (2003) 126:639–45. doi: 10.1530/rep.0.1260639
133. Taniguchi H, Yokomizo Y, Okuda K. Fas-Fas ligand system mediates luteal cell death in bovine corpus luteum. *Biol Reprod*. (2002) 66:754–9. doi: 10.1095/biolreprod66.3.754
134. Nishimura R, Komiyama J, Tasaki Y, Acosta TJ, Okuda K. Hypoxia promotes luteal cell death in bovine corpus luteum. *Biol Reprod*. (2008) 78:529–36. doi: 10.1095/biolreprod.107.063370
135. Nishimura R, Okuda K. Multiple roles of hypoxia in ovarian function: roles of hypoxia-inducible factor-related and -unrelated signals during the luteal phase. *Reprod Fertil Dev*. (2015) 28:1479–86. doi: 10.1071/RD15010
136. Poole DH, Pate JL. Luteal microenvironment directs resident T lymphocyte function in cows. *Biol Reprod*. (2012) 86:29. doi: 10.1095/biolreprod.111.092296
137. Richards JS, Ren YA, Candelaria N, Adams JE, Rajkovic A. Ovarian follicular theca cell recruitment, differentiation, and impact on fertility: 2017 update. *Endocr Rev*. (2018) 39:1–20. doi: 10.1210/er.2017-00164
138. Da Silva-Buttkus P, Jayasooriya GS, Mora JM, Mobberley M, Ryder TA, Baithun M, et al. Effect of cell shape and packing density on granulosa cell proliferation and formation of multiple layers during early follicle development in the ovary. *J Cell Sci*. (2008) 121(Pt 23):3890–900. doi: 10.1242/jcs.036400
139. Yang MY, Fortune JE. Testosterone stimulates the primary to secondary follicle transition in bovine follicles *in vitro*. *Biol Reprod*. (2006) 75:924–32. doi: 10.1095/biolreprod.106.051813
140. Kayampilly PP, Menon KM. AMPK activation by dihydrotestosterone reduces FSH-stimulated cell proliferation in rat granulosa cells by inhibiting ERK signaling pathway. *Endocrinology*. (2012) 153:2831–8. doi: 10.1210/en.2011-1967
141. Pradeep PK, Li X, Peegel H, Menon KM. Dihydrotestosterone inhibits granulosa cell proliferation by decreasing the cyclin D2 mRNA expression and cell cycle arrest at G1 phase. *Endocrinology*. (2002) 143:2930–5. doi: 10.1210/endo.143.8.8961
142. Chen MJ, Chou CH, Chen SU, Yang WS, Yang YS, Ho HN. The effect of androgens on ovarian follicle maturation: dihydrotestosterone suppress FSH-stimulated granulosa cell proliferation by upregulating PPARgamma-dependent PTEN expression. *Sci Rep*. (2015) 5:18319. doi: 10.1038/srep18319
143. Azziz R. Androgen excess is the key element in polycystic ovary syndrome. *Fertil Steril*. (2003) 80:252–4. doi: 10.1016/S0015-0282(03)00735-0
144. Wood JR, Ho CK, Nelson-Degrave VL, McAllister JM, Strauss JF III. The molecular signature of polycystic ovary syndrome (PCOS) theca cells defined by gene expression profiling. *J Reprod Immunol*. (2004) 63:51–60. doi: 10.1016/j.jri.2004.01.010
145. Osuka S, Nakanishi N, Murase T, Nakamura T, Goto M, Iwase A, et al. Animal models of polycystic ovary syndrome: a review of hormone-induced rodent models focused on hypothalamus-pituitary-ovary axis and neuropeptides. *Reprod Med Biol*. (2019) 18:151–60. doi: 10.1002/rmb2.12262
146. Mossa F, Jimenez-Krassel F, Folger JK, Ireland JL, Smith GW, Lonergan P, et al. Evidence that high variation in antral follicle count during follicular waves is linked to alterations in ovarian androgen production in cattle. *Reproduction*. (2010) 140:713–20. doi: 10.1530/REP-10-0214
147. Knight PG, Glister C. TGF-beta superfamily members and ovarian follicle development. *Reproduction*. (2006) 132:191–206. doi: 10.1530/rep.1.01074
148. Teede H, Ng S, Hedger M, Moran L. Follistatin and activins in polycystic ovary syndrome: relationship to metabolic and hormonal markers. *Metabolism*. (2013) 62:1394–400. doi: 10.1016/j.metabol.2013.05.003
149. Gorsic LK, Dapas M, Legro RS, Hayes MG, Urbanek M. Functional genetic variation in the anti-mullerian hormone pathway in women with polycystic ovary syndrome. *J Clin Endocrinol Metab*. (2019) 104:2855–74. doi: 10.1210/jc.2018-02178
150. Roy S, Gandra D, Seger C, Biswas A, Kushnir VA, Gleicher N, et al. Oocyte-derived factors (GDF9 and BMP15) and FSH regulate AMH expression via modulation of H3K27AC in granulosa cells. *Endocrinology*. (2018) 159:3433–45. doi: 10.1210/en.2018-00609
151. Dumont A, Robin G, Dewailly D. Anti-mullerian hormone in the pathophysiology and diagnosis of polycystic ovarian

syndrome. *Curr Opin Endocrinol Diabetes Obes*. (2018) 25:377–84. doi: 10.1097/MED.0000000000000445

152. Bozdag G, Mumusoglu S, Coskun ZY, Yarali H, Yildiz BO. Anti-Mullerian hormone as a diagnostic tool for PCOS under different diagnostic criteria in an unselected population. *Reprod Biomed Online*. (2019) 39:522–9. doi: 10.1016/j.rbmo.2019.04.002
153. Lunn SF, Fraser HM, Mason HD. Structure of the corpus luteum in the ovulatory polycystic ovary. *Hum Reprod*. (2002) 17:111–7. doi: 10.1093/humrep/17.1.111
154. Hambridge HL, Mumford SL, Mattison DR, Ye A, Pollack AZ, Bloom MS, et al. The influence of sporadic anovulation on hormone levels in ovulatory cycles. *Hum Reprod*. (2013) 28:1687–94. doi: 10.1093/humrep/det090
155. Boutzios G, Karalaki M, Zapanti E. Common pathophysiological mechanisms involved in luteal phase deficiency and polycystic ovary syndrome. *Impact on fertility Endocrine*. (2013) 43:314–7. doi: 10.1007/s12020-012-9778-9
156. Kinder JE, Kojima FN, Bergfeld EG, Wehrman ME, Fike KE. Progestin and estrogen regulation of pulsatile LH release and development of persistent ovarian follicles in cattle. *J Anim Sci*. (1996) 74:1424–40. doi: 10.2527/1996.7461424x

Conflict of Interest: The authors declare that the research was conducted in the absence of any commercial or financial relationships that could be construed as a potential conflict of interest.

Advantages of publishing in Frontiers

OPEN ACCESS
Articles are free to read for greatest visibility and readership

FAST PUBLICATION
Around 90 days from submission to decision

HIGH QUALITY PEER-REVIEW
Rigorous, collaborative, and constructive peer-review

TRANSPARENT PEER-REVIEW
Editors and reviewers acknowledged by name on published articles

Frontiers
Avenue du Tribunal-Fédéral 34
1005 Lausanne | Switzerland

Visit us: www.frontiersin.org
Contact us: info@frontiersin.org | +41 21 510 17 00

REPRODUCIBILITY OF RESEARCH
Support open data and methods to enhance research reproducibility

DIGITAL PUBLISHING
Articles designed for optimal readership across devices

FOLLOW US
@frontiersin

IMPACT METRICS
Advanced article metrics track visibility across digital media

EXTENSIVE PROMOTION
Marketing and promotion of impactful research

LOOP RESEARCH NETWORK
Our network increases your article's readership